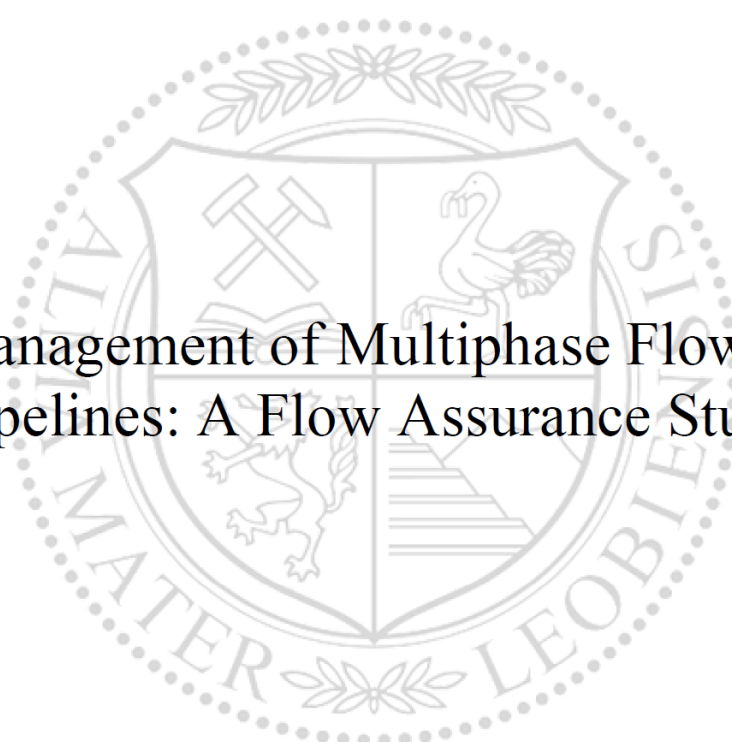




Chair of Petroleum and Geothermal Energy Recovery

Master's Thesis



Management of Multiphase Flow in  
Pipelines: A Flow Assurance Study

Ahmed Hussein Mahmoud Ali Ali

May 2020



## Master's Thesis

# Management of Multiphase Flow in Pipelines: A Flow Assurance Study

In collaboration with PM Lucas Enterprises



**Written by:**

Ahmed H. Ali  
11723201

**Advisors, MUL:**

Univ.-Prof. Dipl.-Ing. Dr.mont. Herbert Hofstätter  
Dipl.-Ing. Dipl.-Ing. Dr.mont. Clemens Langbauer

**Advisors, PML:**

Dipl.-Ing. Georg Zangl  
Dipl.-Ing. Dr.mont. Georg Mittermeir

**Leoben, on 27 May 2020**



## AFFIDAVIT

I declare on oath that I wrote this thesis independently, did not use other than the specified sources and aids, and did not otherwise use any unauthorized aids.

I declare that I have read, understood, and complied with the guidelines of the senate of the Montanuniversität Leoben for "Good Scientific Practice".

Furthermore, I declare that the electronic and printed version of the submitted thesis are identical, both, formally and with regard to content.

Date 27.05.2020



---

Signature Author  
Ahmed Hussein Mahmoud Ali, Ali



## Acknowledgement

First, I would like to thank my supervisor, Prof. Herbert Hofstätter, for giving me the opportunity to work on this thesis, and my co-supervisor, Dr. Clemens Langbauer, for his valued support and feedback.

I also would like to thank Dr. Pavle Matijevic, PM Lucas, for sponsoring me during my work on the thesis. Special thanks go to Mr. Georg Zangl for his immense support to me at the kick-off of my thesis, and to Dr. Georg Mittermeir for his follow-up and feedback. I sincerely thank Mr. Donald Yee for helping me find a project that I am interested in, and the rest of the PM Lucas team in the technology center in Kać, Serbia, for their kind and prompt responses to my inquiries during the 10 weeks I spent there.

Last but not least, I would like to thank my good friends, Sherif Hamdy, Mostafa Selmy, and Ayman Henawy, NOSPCO, Egypt, for their encouragement and insightful discussions.





---

## Kurzfassung

Diese Arbeit handelt von einer Flow-Assurance-Studie (FA-Studie) eines Gaskondensat-Rohrleitungsnetzes, das an Land in einem kontinentalen Klima mit extrem kalten Wintern und heißen Sommern gebaut werden soll. Das Rohrleitungsnetz ist insgesamt 33 km lang und besteht aus fünf Zweige, die an eine Hauptleitung angeschlossen sind.

Das gesamte Rohrleitungs-Netzwerk wird unter Ziel-, Turndown- und Rampup-bedingungen sowie unter Abschaltungen analysiert. OLGA [Version 2018.1.0], eine spezielle Software, die zur Simulation der dynamischen Mehrphasenströmung verwendet wird, um das stationäre und transiente Verhalten des Systems unter hydraulischen und thermischen Standpunkten zu untersuchen. Multiflash [Version 7.0], eine Software für PVT und physikalische Eigenschaften, wird verwendet, um PVT-Tabellen und Hydratkurven als Eingabe für OLGA zu erstellen.

Die im Basis-of-Design angegebenen Rohrleitungsgrößen werden bestätigt und weitere mögliche Größen, basierend auf dem Auslegungsdruck der Pipeline, werden untersucht. Druck-, Temperatur- und Geschwindigkeitsprofile werden basierend auf den Produktionsprofilen zusammen mit den Strömungsregimen und Flüssigkeits-Holdups bestimmt. Die vorherrschenden Strömungsregime in den Netzwerkzweigen und die minimale stabile Fließrate in den Flüssigkeitsabscheider (slug catcher) werden unter Turndown-bedingungen bestimmt. Die Eigenschaften der Schwallströmung in der Pipeline und die Flüssigkeitshandhabungsfähigkeiten des Flüssigkeitsabscheiders werden untersucht, wenn die Fließraten wieder erhöht werden. Die erforderlichen Fließraten der Methanol-Injektionen werden abgeschätzt, und die richtige Isolierung für die Zweige wird bestimmt, um die Hydratbildung und/oder Wachsbildung während der Produktion zu verhindern und die vom Betreiber festgelegte, erforderliche No-Touch-Time zu berücksichtigen. Molchsimulationen werden durchgeführt, um angemessene Molchgeschwindigkeiten zu bestimmen, die den Flüssigkeitsabscheider nicht überflutet, und Pipeline-Füllung (pipeline-packing) wird simuliert, um die erforderliche Zeit zum Erreichen des Auslegungsdrucks der Pipeline während einer Prozessstörung zu bestimmen.

Die Arbeit dient auch als Leitfaden für die Durchführung von FA-Studien: Der Aufbau des Simulationsmodells und die Einrichtung der Simulationsfälle werden diskutiert, und verschiedene Methoden zur Ausführung der Simulationsfälle werden verglichen. Quellenmodelle und IPRs werden verwendet, um die Quellen des Gaskondensats anstelle der typischen Massenquellen zu modellieren, und alle Netzwerkzweige werden gleichzeitig und nicht isoliert simuliert, um den dynamischen Effekt der verschiedenen Zweige aufeinander zu erfassen.



---

## Abstract

This thesis provides a Flow Assurance (FA) study of a gas condensate pipeline network that is planned to be constructed onshore in a continental climate with extremely cold winters and hot summers. The pipeline network is 33 km long in total and consists of five flowlines tied into a main trunk-line.

A range of operating conditions is considered, where the analysis of the whole pipeline network is performed at target gas flowrate, as well as turndown, ramp-up, and shutdown conditions. OLGA [version 2018.1.0], a specialized dynamic multiphase flow simulator, is used to study the steady-state and transient behaviors of the system from a hydraulic standpoint and a thermal standpoint. Multiflash [version 7.0], a PVT and physical properties package, is used to create PVT tables and hydrate curves as input for OLGA.

Line sizes, as reported in the Basis-of-Design, are confirmed, and more possible sizes, based on the given pressure rating, are examined. Pressure, temperature, velocity profiles are determined based on production profiles, along with flow regimes and liquid hold-ups. The predominant flow regimes in the network branches are determined under turndown flowrates, in addition to the minimum stable flowrate (MSFR) into the slug catcher, then the slugging characteristics in the pipeline and the liquid handling capabilities of the slug catcher are examined as flowrates are ramped up again. The required methanol injection flowrates are estimated, and the right insulations for flowlines are determined to prevent hydrate formation and/or wax deposition during production, and to allow for the required no-touch time set by the operator. Pigging simulations are performed to determine proper pigging velocities that avoid surging the slug catcher at the pipeline outlet, and pipeline packing is simulated to determine the time required to reach the pipeline design pressure during a process shutdown.

The thesis also serves as a guide for carrying out FA studies: It elaborates on building the simulation model, setting up the simulation cases, and compares different methods of running the cases. Well models and IPRs are used to simulate the sources of the gas condensate instead of the typical mass sources, and all network branches are simulated simultaneously, rather than in isolation, to capture the dynamic effect of the different branches on one-another.



## Table of Content

	<b>Page</b>
<b>1 INTRODUCTION.....</b>	<b>1</b>
<b>2 LITERATURE REVIEW .....</b>	<b>3</b>
2.1 Modelling of Multiphase Flow in Pipes .....	3
2.2 Flow Assurance .....	11
<b>3 CASE STUDY: BASIS OF DESIGN .....</b>	<b>19</b>
3.1 Field Data .....	19
3.2 Pipeline Network.....	23
3.3 Ambient Conditions.....	25
<b>4 BUILDING THE SIMULATION MODEL .....</b>	<b>27</b>
4.1 Defining the fluid .....	27
4.2 Building the Network Components.....	40
4.3 Setting up the Heat Transfer.....	48
<b>5 SIMULATION WORK .....</b>	<b>55</b>
5.1 Confirm Pipeline Sizes.....	57
5.2 Pipeline Parameters Based on Production Profiles .....	62
5.3 Turndown Rates .....	71
5.4 Methanol Injection under Flowing Conditions .....	79
5.5 Methanol Injection under Shut-in Conditions .....	84
5.6 Insulation Thickness under Flowing Conditions .....	87
5.7 Insulation Thickness under Shut-in Conditions.....	92
5.8 Ramp-up Rates.....	95
5.9 Pigging.....	99
5.10 Pipeline Packing .....	104
<b>6 CONCLUSION .....</b>	<b>107</b>
6.1 Summary .....	107
6.2 Building the Model .....	107
6.3 Results.....	107
6.4 Remarks .....	109
<b>REFERENCES.....</b>	<b>111</b>

---

<b>LIST OF TABLES</b> .....	<b>114</b>
<b>LIST OF FIGURES</b> .....	<b>116</b>
<b>ABBREVIATIONS</b> .....	<b>118</b>
<b>NOMENCLATURE</b> .....	<b>120</b>
<b>APPENDICES</b> .....	<b>122</b>
A. Keyword-based PVT Table .....	122
B. Composition of Produced Fluid over Time .....	125
C. Hydrate Formation Curves .....	129
D. Pipeline Profiles .....	130
E. Pipeline Walls.....	131
F. Production Profiles .....	133
G. Variables .....	134
H. Simulation Results .....	136
I. Surge Volume during Ramp-up.....	175
J. Surge Volume during Pigging.....	177
K. Cases Runtime.....	181

# 1 Introduction

Flow assurance (FA) is a term that has gained great popularity in the oil and gas industry. Originated from the Portuguese “*Garantia do escoamento*” in the 1990s [1], the term literally translates to “*Guarantee of flow.*” That is ensuring that produced fluids will continue to flow consistently from reservoir to separator over the whole life of the field. FA tackles those phenomena that are related to the fluid properties or the pipeline hydraulics, e.g. hydrate formation, wax formation, slugging, liquid loading, and it depends on the analysis of multiphase flow in wells, risers, flowlines, pipelines, and process equipment, from both thermal and hydraulic standpoints.

This thesis provides an FA study of a gas condensate pipeline network that is planned to be constructed onshore in a continental climate with extreme ambient conditions. The FA study aims at achieving the following objectives:

- Confirming the line sizes estimated in the Basis of Design and determining other possible line sizes based on the pipeline pressure rating.
- Determining the pressures, temperatures, velocities, liquid hold-up, and flow regimes in the pipeline branches based on the production profiles.
- Defining the predominant flow regimes and the liquid hold-ups in the flowlines and the trunk-line at different turndown rates and determining the minimum stable flowrate (MSFR) into the slug catcher.
- Estimating the methanol injection rates that are required to avoid hydrate formation in the pipeline network during production (active inhibition).
- Estimating the methanol injection rates that would allow for the required no-touch time of 6 hours that is set by the operator (shut-in scenario).
- Determining the required flowline insulation thickness that could prevent hydrate and/or wax formation during production (passive inhibition).
- Determining the flowline insulation thickness that would allow for the required no-touch time of 6 hours that is set by the operator (shut-in scenario).
- Determining the proper flowrate ramp-up from turndown rates to the design rate and examining the related slugging characteristics and liquid handling capabilities.
- Determining proper pigging velocities for the flowlines and the trunk-line that would avoid surging the slug catcher at the network outlet and examining the related slugging characteristics and liquid handling capabilities.
- Estimating the time required to reach the pipeline and equipment design pressure during a process shutdown at the slug catcher (packing analysis).

The thesis also presents a number of tasks that can help understand how different ways of setting up the simulation cases can affect their results, and consequently, the system design and flow assurance strategies that need to be implemented in the field development. These tasks aim to:

- Compare mass sources to well models as the sources of the gas condensate inflow to the system in cases where both are applicable.

- Compare the solution of the network using black-oil versus compositional model for the calculation of fluid properties.
- Compare the effect of considering pure versus saline produced water for estimating the hydrate prevention requirements.
- Compare the results of steady-state and transient simulations in cases where both are expected to be applicable.
- Examine the value of using 2D heat transfer to set up the temperature calculations for the buried pipeline network under the extreme design ambient conditions compared to the typical 1D heat transfer.

The thesis is divided into six chapters. Chapter 2 provides a literature review about multiphase flow modelling and flow assurance. It presents some of the main concepts encountered in multiphase flow modelling, a historical review about the development of research in this field, and a description of the flow assurance phenomena that will be tackled in the next chapters. A background about OLGA, the multiphase flow simulator that will be used in the case study, is also provided in this chapter.

Chapter 3 presents the basis-of-design of the field development, which provides the essential information on which the case study will be built. It gives a short description of the gas condensate reservoir and the wells that were drilled to develop it, the produced fluid composition, the conceptual design of the pipeline and surface facilities, and the ambient design conditions in the region where the gas condensate field is located.

Chapter 4 discusses the process of building a preliminary simulation model in OLGA for the case study. The chapter discusses creating the required PVT tables and hydrate curves in Multiflash, taking into account the effects of the changing composition of the produced gas condensate with time, the maximum expected water production, and the salinity of the produced water. The chapter then covers building the production network components. This includes selecting different pipe sizes for the pipeline network, selecting different insulation thicknesses for the flowlines, generating representative IPRs and well completions for the well models to simulate the inflow of the gas condensate from the reservoir to the wellhead, creating a choke model to accurately predict the flow conditions of the gas condensate entering the pipeline network, and setting up the heat transfer for the pipelines and the well models.

Chapter 5 discusses the simulation tasks of the FA study that were mentioned earlier. For each task, the objective of the task, the setup of the simulation cases, and the results of the cases are presented.

Chapter 6 summarizes the work that has been presented in the thesis, starting from building the simulation model, going through the simulation results, and ending with a brief record of remarks about the study results.



## 2 Literature Review

To perform the case study of this thesis, an understanding of the concepts of multiphase flow modelling and flow assurance is required, as well as of the simulation tool chosen to perform the study (OLGA). This chapter provides a literature review of the aforementioned topics. It is intentionally principle-based in order to cover as many ideas as possible, and it does not aim to provide any mathematical formulas as long as they will not be exclusively presented as part of the case study in the coming chapters.

### 2.1 Modelling of Multiphase Flow in Pipes

#### 2.1.1 Concepts and Definitions

##### 2.1.1.1 Multiphase Flow

**Multiphase Flow:** Multiphase flow is the simultaneous flow of two or more immiscible phases of matter. It occurs in almost all oil and gas producing wells and surface flowlines, as well as in many reservoirs. The differences in densities and viscosities of the produced fluids and the mass transfer between the different phases along the production system significantly complicate the prediction of multiphase flow behavior compared to single-phase flow.

In their book, “Applied Multiphase Flow in Pipes and Flow Assurance,” [2] Brill and Al-Safran describe the central idea of the book and explain that the design and operation of a multiphase flow piping system require the determination of the following variables: flow patterns, liquid holdups, and pressure gradients along the pipes; and that the determination of those variables requires the knowledge of the in-situ fluid properties, and the in-situ flowrates. This section 2.1 presents the concepts required to understand multiphase flow modelling.

**Homogenous Multiphase Flow:** A homogenous multiphase flow is a flow condition in which the phases are flowing at the same in-situ velocities. This assumes that no “slippage” exists between the phases, where one phase would be travelling at a higher velocity than the other phase. The geometrical distribution of the phases across and along a pipe is uniform or homogenous. This is true for high-velocity conditions where phase dispersion takes place and the difference in phase densities is not significant (ratio of liquid to gas density is less than 10), as in the cases of dispersed bubble flow, mist flow, steam flow, and non-settling solid/liquid flow, where fine sands are being carried by high-velocity liquid flow. Homogenous multiphase or two-phase flow is also referred to as no-slip two-phase flow.

**Non-homogenous Multiphase Flow:** A non-homogenous multiphase flow is that where the geometrical distribution of the phases across a pipe is not uniform. This happens due to the velocity difference, or slippage, between the phases flowing in the pipe, which leads to the accumulation of the heavier phase along the pipe. Gas, which has a lower density and viscosity than the liquid, slips past the liquid in horizontal and slightly-inclined two-phase pipes, leading to the accumulation of the liquid phase. The resulting non-uniform distribution

of the two phases due to slippage takes the form of different flow regimes, such as annular flow, stratified flow, and intermittent flow.

**Pressure Gradient:** The pressure gradient of a fluid flowing in a pipe is the change in fluid pressure per unit length of pipe. It is used to calculate pressure at any point along the pipe after flow patterns and liquid holdups had been determined.

The procedure for calculating the pressure gradient starts with calculating the in-situ physical properties and the in-situ flowrates of the phases with the help of a proper PVT model, and from that, two-phase flow variables, such as superficial and mixture velocities, are calculated. The flow pattern is determined using the flow variables and is used to calculate liquid holdup. Knowing the liquid holdup and the physical properties of the phases, the mixture physical properties can now be calculated and used to calculate the pressure gradient. Fig. 1 shows the calculation process of pressure gradient.

If slippage is not accounted for and the fluid is already assumed to be homogenous, no flow pattern prediction is performed, and a no-slip liquid holdup can be readily calculated from the flow variables.

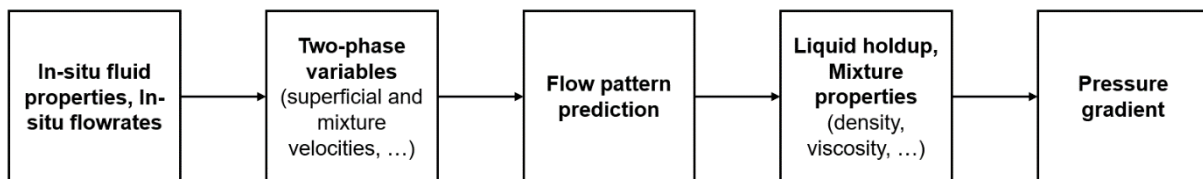


Fig. 1 – Calculation process of pressure gradient. A modification of the figure in [2, p. 47]

**Superficial Velocity:** Superficial velocity of a phase flowing in a pipe segment is the velocity of that phase if it would occupy the whole cross section of the pipe. It is also referred to as phase velocity.

**Liquid Holdup:** Liquid holdup is the fraction of a pipe volume or a pipe cross-sectional area that is occupied by liquid. It is used to calculate mixture fluid properties (density, viscosity, surface tension, etc.). The way of calculating liquid holdup in a pipe segment depends on the existing flow regime in that segment.

**Flow Pattern:** A flow pattern is a description of how gas and liquid are geometrically distributed across and along a pipe segment (in the radial and axial directions). A number of flow patterns can be observed in pipelines; each of which has its own characteristics. Fig. 2 shows the different flow patterns in horizontal and slightly-inclined pipes. Note that the direction of increased gas flowrate in the figure is meant to be compared to some liquid flowrate, and it does not mean that the total flowrate of the fluid is increasing in this direction.

A number of forces in different magnitudes acts on each phase and the relative amount of these forces results in the observed flow patterns that the flow exhibits. In the following discussion, only inertia (or momentum) force and gravity force are considered, for simplicity. Fig. 3 is an inertia versus gravity matrix that shows which multiphase flow pattern is most

likely to exist based on the relative amount of the two forces. It shows that as the relative effect of inertia increases, dispersion is promoted, while as the gravity effect increases, phase separation is promoted.

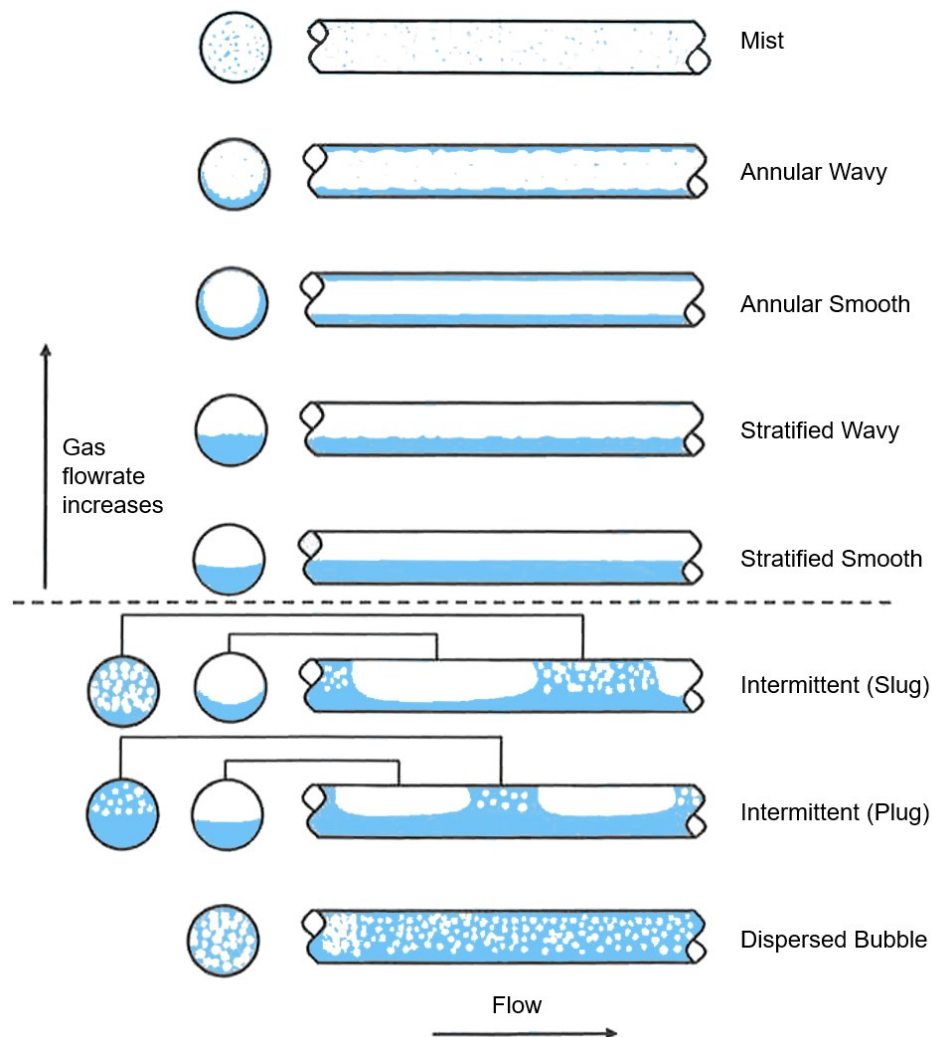


Fig. 2 – Flow patterns in horizontal and slightly-inclined pipes [2, p. 48]

The change in flow conditions in the pipe affects the balance between these forces and leads to the transition from one flow pattern to another. This can be a change in the volumetric flowrates, the pipe geometry (diameter and inclination), or the fluid's physical properties (phase density, viscosity, and gas-liquid surface tension).

At high flowrates, the inertia of the phases is high, and the relative effect of gravity is, therefore, low. This fosters the dispersion between the phases and results in an inertia-dominated flow pattern. If the flowrate is decreased, the relative gravity effect increases and starts to promote separation between the phases.

For a fluid flowing at some flowrate, the local velocity of the fluid in a small pipe is higher than that in a larger pipe, hence the inertia force; and the relative gravity effect is smaller. This means that smaller pipe diameters promote phase dispersion, while larger diameters promote phase separation. The effect of pipe inclination is more complicated and depends

on the flow direction. When the fluid flows uphill, the liquid phase is pulled backwards increasing the gravity effect in the opposite direction. The liquid holdup increases and allows for a smaller area for the gas to flow, thus increasing its velocity and leading to the formation of waves at the gas-liquid interface (stratified wavy flow) that can develop into slugs (intermittent slug flow). On the other hand, as the fluid flows downhill, the liquid phase is pulled downwards in the direction of the flow. The liquid holdup decreases, and the gas velocity decreases as well, promoting a stratified flow.

High phase densities increase the relative gravity effect and lead to flow stratification, and high phase viscosities lead to high shear forces between the phases and the pipe wall and at the gas-liquid interface, which leads to a low inertia effect and promotes intermittent flow patterns.

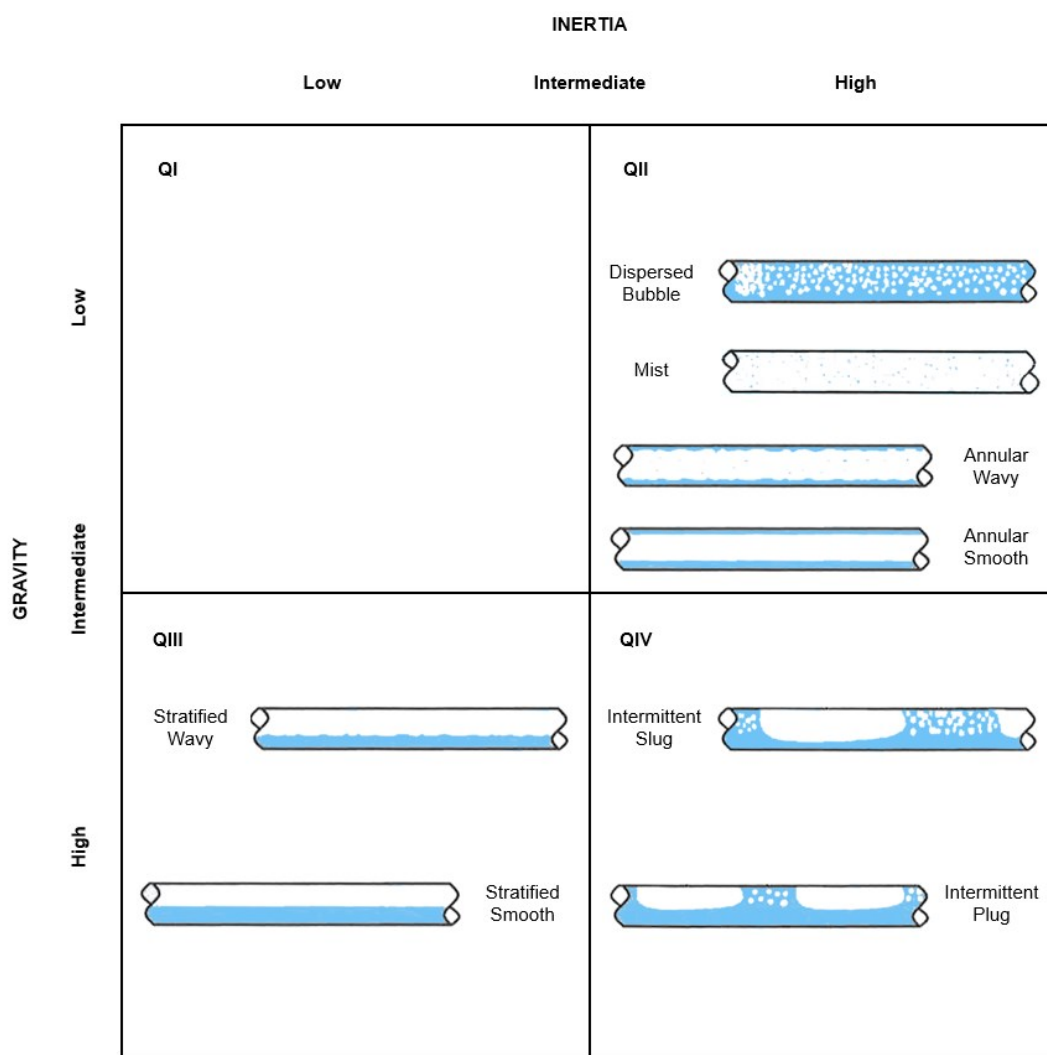


Fig. 3 – Inertia vs Gravity matrix of flow patterns [2, p. 50]

Both empirical and mechanistic models exist that predict the flow pattern of a multiphase flow. So-called “flow pattern maps” were created that show the transition between the different flow patterns as a function of some dimensionless parameters. Predicting the flow pattern is a prerequisite for calculating the liquid holdup and the pressure gradient in pipes.

### 2.1.1.2 Empirical Correlations and Mechanistic Modelling

**Empirical Correlation:** The empirical correlation approach for modelling a physical phenomenon is an experimental approach in which the data that describe the phenomenon are correlated as a relationship among dimensionless groups of parameters (data fitting). These parameters are typically chosen based on intuition or some statistical criteria. Empirical correlations are widely used in the oil & gas industry. However, they do not provide an explanation of the physics behind the correlated relationship, and their use should only be constrained to the range of the data in the underlying experiments.

**Mechanistic Modelling:** The mechanistic modelling approach aims to describe a physical phenomenon using mathematical models that are based on conservation laws and require a simple numerical solution. It is often based on laboratory studies, field experiments and physical models. It tries to simplify the actual relationships between the system's parameters by focusing on the dominant ones and ignoring the less important ones. The mechanistic modelling approach is more accurate than the empirical correlation approach and can be extrapolated outside the range of the experimental data and upscaled to field conditions.

**Closure relationships:** Mechanistic models used to describe multiphase flow still require some empiricism to close the models. That is to equate the number of equations to the number of unknowns. This is required because the number of conservation laws used in those models is lower than the number of unknown parameters. The empirical correlations used to close the mechanistic models are, therefore, referred to as closure relationships.

### 2.1.1.3 Steady-state and Transient Flows

**Steady-state Flow:** Steady-state flow is a flowing condition in which the flowrates of mass, linear momentum, and energy into a pipe segment (control volume) are equal to their flowrates out of the segment. That is, their rate of change along the control volume is zero. For a fluid flowing in a pipeline under steady-state conditions, the fluid pressure, temperature, and velocity at any specific location in the pipeline do not change with time. Steady-state flow is also referred to as developed flow.

**Transient Flow:** As opposed to steady-state flow, transient flow is a flowing condition where flow variables such as pressure, velocity, and mass flowrate vary with time at the same location. It occurs as a response to changes in the system, such as flowrate turndown, ramp-up, start-up, shutdown, pipeline blowdown, etc., or due to changes in pipeline inclination that might induce liquid accumulation and slug flow. Variations in the flow variables can be slow and gradual or rapid and abrupt. Transient flow is also referred to as developing flow or unsteady flow.

### 2.1.1.4 Black-oil and Compositional Models

As mentioned in 2.1.1.1, the design and operation of a multiphase flow piping system require the determination of parameters that depend on the in-situ fluid properties and the in-situ flowrates. In order to accurately predict the fluid properties, fluid characterization by lab tests is carried out based on fluid samples that can be taken at different points in the production

system, such as downhole, at wellhead, or at the separator. A pressure-volume-temperature (PVT) model can be built based on the characterized fluid to help predict the fluid properties as pressure and temperature vary along the production system. PVT modelling can be carried out by two models: the black-oil model, and the compositional model.

**Black-oil Model:** The black-oil model is a simple, yet reliable empirical approach for fluid characterization. The model treats oil and gas as two separate substances whose properties are calculated based on empirical correlations, and if water is present, then its properties are also introduced into the model [3].

The black-oil model assumes that the oil and the gas have constant compositions that do not change with pressure and temperature. While this might be valid to some extent for the oil phase, it leads to errors in predicting the gas phase properties, and it cannot capture a phenomenon like retrograde condensation. That is why the black-oil model should not be used to predict the fluid properties of volatile oils and gas condensates. As the case with other empirical approaches, the application of a black-oil model correlation should only be constrained to the range of the data that are believed to be representative of the given model. Fig. 4 shows the basic inputs and outputs of the black-oil model. A description of the variables can be found in the attached Nomenclature.

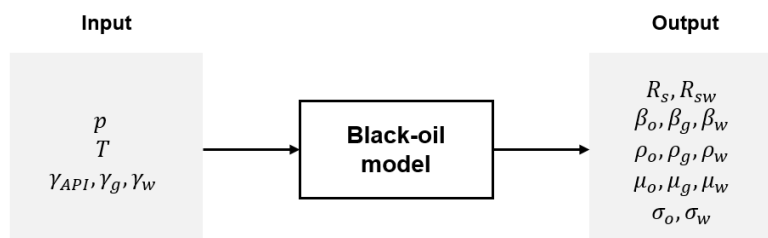


Fig. 4 – Black-oil model. A modification of the figure in [2, p. 282]

**Compositional Model:** The compositional model is a model that is described by Equations of State (EoS) that relate the pressure, volume, and temperature of a given amount of substance and serve as the basis to calculate the phase behavior of fluids [3].

The model considers the total composition of the produced fluid and calculates phase properties (vapor and liquid properties for two-phase flow) and in-situ flowrates. Flash calculations, or Vapor-Liquid-Equilibrium (VLE) calculations, are the heart of the compositional model, and they are based on the concept of equilibrium constants, which are also referred to as K-values [2]. As the pressure and temperature change along a production system, the compositions of the vapor and liquid phases change as a result of the new equilibrium state. The compositional model is therefore the recommended model to predict the fluid properties of volatile oils and gas condensates. Fig. 5 shows the basic inputs and output of the compositional model. A description of the variables can be found in the attached Nomenclature.

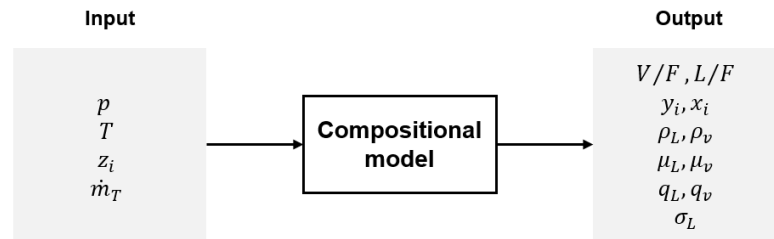


Fig. 5 – Compositional model [2, p. 314]

### 2.1.2 Evolution of Multiphase Flow Modelling

In their paper published in 2012 [4], Shippen and Bailey presented a review of the history of multiphase flow modelling that shows the amount of research and development that has been invested in this field. Reviewing the history of multiphase flow modelling gives a perspective on why so many models exist. In Fig. 6, which is present in their paper, Shippen and Bailey adopted a classification of the axes in the figure that Brill and Arirachakaran had originally come up with in 1992 [5], where they divided the timeline since the beginning of multiphase flow research into three periods or eras, and classified the multiphase flow models according to the level of the physics behind them.

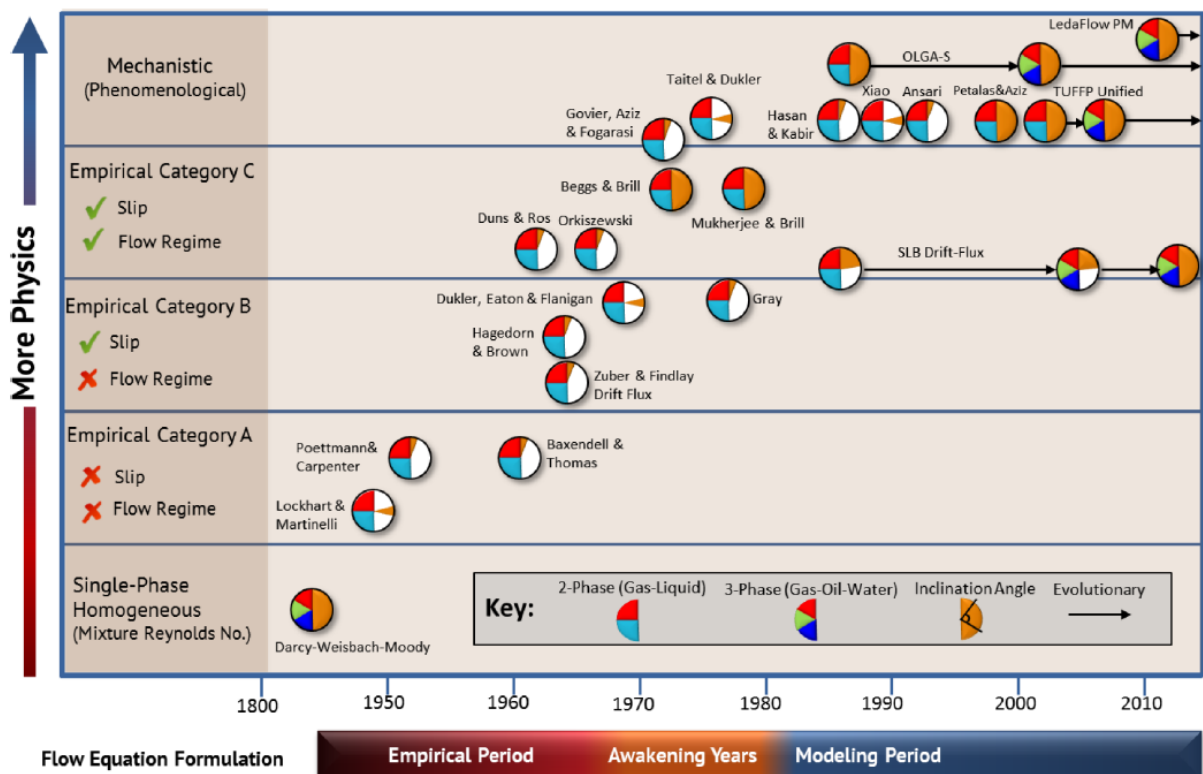


Fig. 6 – Evolution of Multiphase flow modelling [4, p. 4147]

**The Empirical Period (1950–1975):** As can be deduced from the title, the models that emerged in this period were empirical correlations from experimental or field data. They treated fluids as homogenous mixtures, but accounted for slippage effects, and used empirical flow pattern maps. Pressure gradient equations for steady-state flow were

developed based on applying the conservation laws to homogenous mixtures. The empirical correlations created in this period had a limited accuracy due to the lack of physics behind them.

**The Awakening Years (1975–1985):** In this period, the need for introducing physical mechanisms to improve the accuracy of the predictions and overcome the limitations of the empirical approach was realized, and the application of mechanistic modelling was witnessed. The introduction of the personal computer (PC) and the concept of nodal analysis in this period helped with the progress in multiphase flow modelling.

**The Modeling Years (1980–present):** The technological advancement in this period helped arrive at mechanistic models that better capture the physical phenomena taking place in multiphase flow. Test facilities with new measurement instrumentations and high-speed data acquisition were built to study multiphase flow. Improved theoretical methods, steady-state models, and state-of-the-art transient simulators were developed. A unified approach of steady-state mechanistic modelling was developed that predicts flow pattern transitions and flow behavior for all inclination angles. Many closure relationships in place are still empirical; however, improved correlations have been developed as a result of experimental research.

### 2.1.3 OLGA

OLGA is the oil & gas industry-standard software for transient simulation of multiphase flow in networks of wells, risers, flowlines, pipelines, and process equipment, with a focus on flow assurance. OLGA includes a steady-state pre-processor that calculates initial values for transient simulations and can also be used independently for steady-state simulations [6]. OLGA is widely used in the oil & gas industry for feasibility studies, Front-End Engineering Design (FEED), establishing operational procedures, mitigating flow assurance risks, and evaluating the consequences of operational failures.

The OLGA project started in 1980, when the Institute for Energy Technology (IFE) in Norway converted a steam/water nuclear transient simulator into an oil/gas transient simulator [2]. The development of OLGA was, for the most part, based on data from the SINTEF large-scale multiphase test facility (flow loop) that was built in 1982 near Trondheim, Norway. The software was commercialized by Scandpower Petroleum Technology (SPT Group), which was acquired by Schlumberger in 2012 [4].

OLGA is a 1D, three-fluid model, where separate continuity equations are solved for the gas phase, the continuous oil and water phases, and the entrained oil and water droplets in the gas. OLGA solves five conservation of mass equations, three conservation of momentum equations, and one conservation of energy equation. The five conservation of mass equations are for: the mass of gas phase, the mass of continuous oil phase, the mass of continuous water phase, the mass of oil droplets in the gas, and the mass of water droplets in the gas. The three conservation of momentum equations are for: the continuous oil phase, the continuous water phase, and the combination of gas and liquid droplets. One conservation of energy equation is applied for the whole mixture, assuming that all the



phases are at the same temperature. Fluid properties, boundary conditions, and initial conditions are required to close the system of equations.

## 2.2 Flow Assurance

Flow assurance has various definitions in the literature. According to Brill and Al-Safran, flow assurance is:

*“the ability to produce hydrocarbon mixtures from reservoir to sales point reliably, economically, and safely over the life of a field and in any environment”* [2, p. 169]

While according to Makogon, it is:

*“the analysis of thermal, hydraulic and fluid-related threats to flow and product quality and their mitigation using equipment, chemicals and procedure”* [1, p. 2]

However, whether the term is referring to the target of “producing hydrocarbons reliably” or the means to achieve the target; “analyzing and mitigating threats to flow,” flow assurance is special in that it covers the whole production system and requires knowledge in several scientific and engineering subjects. Flow assurance tackles those phenomena that can cause flow restrictions, such as gas hydrates, wax, asphaltene, and scale; pipe damage, such as erosion, and corrosion; flow instabilities, such as slugging, and gas well liquid-loading; and fluid rheology; such as emulsions and heavy oil [2].

The following parts will briefly describe those flow assurance phenomena that will be considered in the case study in this thesis, namely gas hydrates, wax, slugging, and pipe erosion; and will present a workflow for the main steps of flow assurance.

### 2.2.1 Flow Assurance Phenomena

#### 2.2.1.1 Gas Hydrates

Gas hydrate is a solid substance that is formed when water and gases such as methane, carbon dioxide, and propane come into contact at high pressures and low temperatures. The water molecules (the host) form cages where gas molecules (the guest) are confined [7]. The smaller the gas molecules confined in the water cages, the more stable the hydrate phase is. Being composed of about 85 mol% water, many of the hydrate properties resemble those of ice, such as physical appearance and density, yet they still differ in other properties. When allowed to form in a pipeline, gas hydrate can deposit and grow in size until it blocks the whole cross-sectional area of the pipe and stops the flow.

The crystal structure of the gas hydrates have three main types, depending essentially on the size of the guest molecules: structure I, structure II, and structure H, as can be seen in Fig. 7. The water cages in these structures are also of different types/sizes, and each structure contains more than one type of cages. Structure I forms with light gas molecules such as methane, ethane, and carbon dioxide that are confined in relatively small water cages. Structure II can confine heavier gas molecules such as propane and iso-butane in its cages,

and it is the most common type of hydrate in oil and gas pipelines, which contain high amounts of methane to iso-butane. Structure H is produced synthetically and does not form naturally.

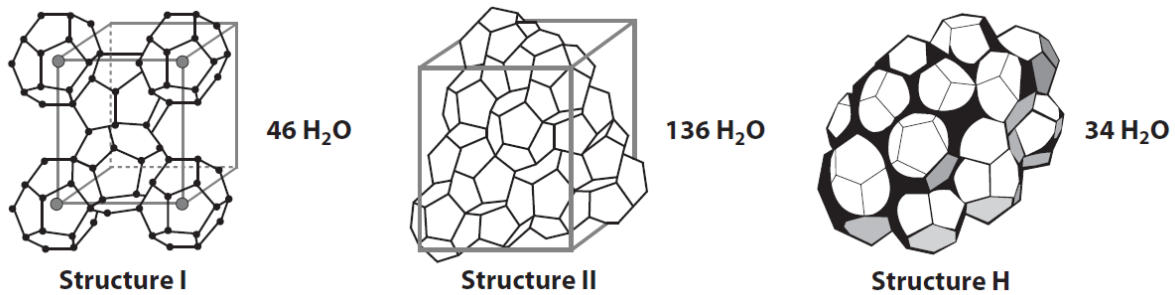


Fig. 7 – Gas Hydrate Structures, from [7, p. 242]

Fig. 8 shows the pressure-temperature profile of a hydrocarbon as it flows in a subsea pipeline from a well then to a production platform and a central processing facility (grey curve). The shaded area (in blue) is referred to as the hydrate-forming region or the hydrate-stability region and represents the conditions at which hydrate can form for the composition of the fluid in question, leading to the risk of blockage in the pipeline. The figure also shows that if methanol, which is a thermodynamic hydrate inhibitor as will be discussed later, is added to the transported fluid, the hydrate-forming region is shifted to lower temperatures and higher pressures which can help prevent hydrate formation in the pipeline.

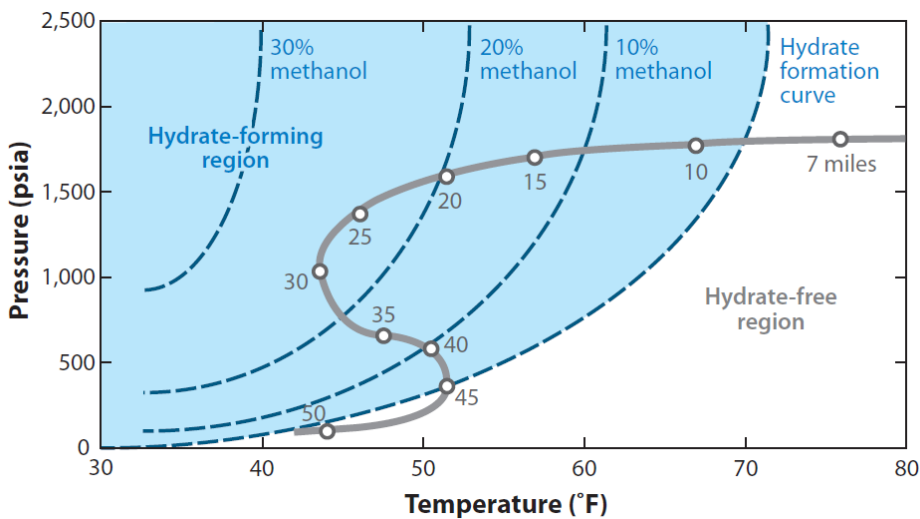


Fig. 8 – Methane hydrate curves for a multiphase flow in a subsea pipeline [7, p. 244]

As already stated, gas hydrates form in the presence of a mixture of hydrocarbons and liquid water under a range of high pressures and low temperatures. Therefore, the exclusion of any of these factors can help prevent hydrate formation. Although operating a pipeline under low pressure would theoretically help stay away from the hydrate region, it is not a practical solution since very low pressures would be required to stay away from the hydrate region that would not be enough to drive the required flowrates to their destination. To keep the fluid temperature at a high value, heat can be added to the fluid through hot-fluid circulation in a

pipeline bundle and electrical heating of the pipeline (active heating), or the heat of the fluid can be preserved through pipeline insulation and burial (passive insulation). Dehydration of gas to remove its water content is a very effective way of preventing hydrate formation. However, it requires a processing facility where dehydration can be performed, and therefore it is applicable for downstream pipelines, not for well flowlines.

Hydrate formation can also be prevented by injecting a chemical inhibitor into the hydrocarbon/water mixture that pushes the hydrate formation conditions to lower temperatures and higher pressures. This inhibitor is referred to as a thermodynamic hydrate inhibitor (THI). The THI bonds to water molecules, preventing them from participating in hydrate formation. The two most common THIs are methanol (MeOH) and mono-ethylene glycol (MEG). The effect of methanol injection on hydrate formation conditions was shown in Fig. 8.

Another approach of mitigating the problem of gas hydrate is to allow the hydrate to form and manage the formed hydrate by preventing its agglomeration and growth. Two types of chemicals can be used to achieve this: kinetic inhibitors and antiagglomerants. Kinetic inhibitors prevent hydrate from growing into stable nuclei that can form large crystals, while antiagglomerants prevent hydrate particles from agglomerating, thus preventing the risk of hydrate blockage.

Some of the aforementioned techniques can be utilized to remove a hydrate blockage after it had already formed, such as depressurization, active heating, chemical injection, in addition to removing the blockage mechanically by a pigging operation if the hydrate is not completely blocking the pipeline. In pipeline pigging, an object called a “pig” is inserted into the pipeline where it travels freely, driven by the production fluids [8]. As it travels through the pipeline, the pig removes accumulated liquids and deposited solids, among other applications for which different types of pigs are used. Fig. 9 shows an example of cleaning pigs with polyurethane cups/discs and steel brushes.



Fig. 9 – Cleaning pigs [9]

### 2.2.1.2 Wax

Wax is not a single component, but rather a large number of high-molecular-weight paraffinic compounds that are soluble in black oils and condensates [10]. Wax components, which range from  $C_{20}$  to  $C_{90}$ , are typically dissolved in oil at high temperatures. As the oil temperature drops, higher molecular weight components start to solidify at a specific temperature that is known as the wax appearance temperature (WAT), and as the temperature continues to drop, lighter components start to solidify as well, increasing the volume of the solid wax. Wax deposition in pipelines is a slow process, but it increases the flow resistance by decreasing the area available for the fluid to flow, which increases the pressure drop in the pipeline and reduces the flowrate.

Wax deposition in pipelines can be prevented by thermal management (active heating and passive insulation) as in the case of hydrate prevention, or by injecting wax inhibitors, which do not prevent wax from crystallizing, but rather reduce the deposition rate of crystalline wax onto surfaces. Typically, WAT is higher than hydrate formation temperature, and wax deposition cannot be easily avoided in the field. Also, even though crystalline wax can re-dissolve if the temperature is raised above WAT, if resins and asphaltenes; which do not have specific melting points, are also deposited with the wax, the wax cannot be re-dissolved by heating [2]. It is more economical to remove the wax after deposition by injecting solvents or performing pipeline pigging.

### 2.2.1.3 Slugging

Slugging, or slug flow, is one of the phenomena that most multiphase production systems experience. It is especially observed in long and large-diameter pipelines where very large slugs can form and grow as they progress along the pipeline. Slugging can adversely affect the downstream process, cause pressure fluctuation, mechanical damage, and may lead to facility shutdown and loss of production if the downstream terminal was not properly designed to handle the volume of the slugs.

Pipe geometry plays a great role in inducing slugs. Terrain slugging is induced by the topography of the pipeline, where liquids are repeatedly accumulated at low points along the pipeline due to gravity until they are pushed by the gas, generating slugs. Severe slugging is similar to terrain slugging, but it is related to a certain pipe configuration that is mostly seen in risers, and it has a more “severe” nature with higher pressure fluctuations and flowrates. Fig. 10 shows the two common configurations where severe and terrain slugging tend to be generated, with a snapshot of slugging in the pipes. Changes in the operating conditions of a multiphase pipeline that are caused by shutdowns, start-ups, flow ramp-ups, or pigging are also drivers for slugging.

The fact that terrain and severe slugging are induced by topography and pipe configuration makes them very difficult to prevent. Trying to avoid unfavorable terrains by routing a pipeline around them or by trenching might not be an economical decision, and using a small-diameter pipeline to achieve a high flow velocity that promotes dispersion might not be practical. Therefore, slugging is typically allowed to occur while trying to mitigate it.

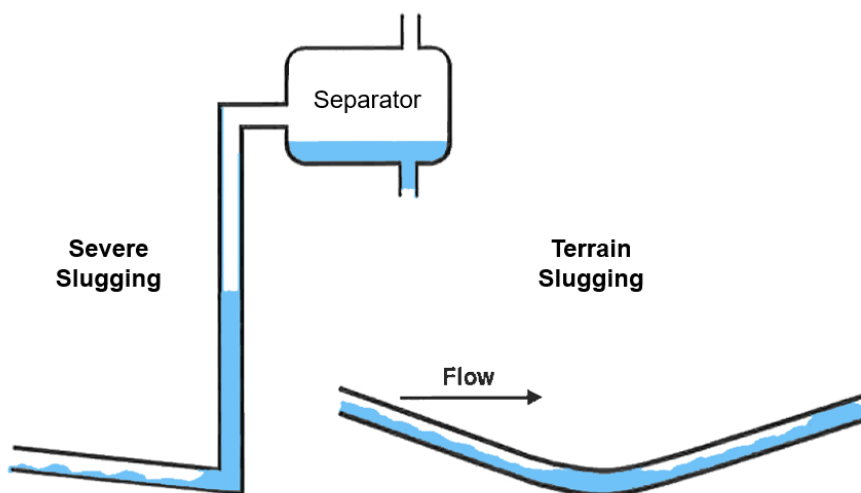


Fig. 10 – Severe and terrain slugging [2, p. 194]

Pipeline pigging is performed to clean the line from accumulated liquids, and slug catchers are installed at the pipeline outlet to handle the volume of slugs and move the flow regime into stratified flow before continuing to the rest of the separation/processing equipment. Other techniques can be used to mitigate severe slugging if deemed economical, such as subsea separation, gas lifting at the riser base, and foaming.

#### 2.2.1.4 Pipe Erosion

Erosion is the removal of material by mechanical action, such as solid particle or liquid droplet impingement, for example, where the energy for cutting the material comes from the velocity of the particles or liquid droplets [11]. This should be distinguished from corrosion, which is the removal of material by chemical action, such as the dissolution of iron in aqueous solutions, which can be enhanced by turbulent flow [12]. The removal of material by a combined mechanical-chemical action, such as the removal of a protective corrosion film by solid or liquid impingement, followed by attacking the unprotected material by a corrosive environment, is therefore referred to as erosion-corrosion.

Pipe erosion occurs due to cavitation, particle impingement, or abrasion [2]. Cavitation takes place when vapor bubbles form at some point where the local pressure of a liquid drops below the vapor pressure, then when subjected to a higher pressure, these bubbles (cavities) implode generating a shock wave that hits the inner surface of the pipe causing mechanical damage as this process is repeated. This most commonly happens to pump impellers, but it also takes place at chokes and elbows.

Fig. 11 illustrates the process of cavitation erosion, showing the possibility of a secondary evaporation/implosion of smaller bubbles. Particle impingement occurs when high-velocity liquid droplets carried in gas or solid particles carried in liquid and/or gas hit the inner surface of a pipe and erode it, while abrasion damage occurs due to the frictional forces between the pipe inner surface and the flowing fluids.

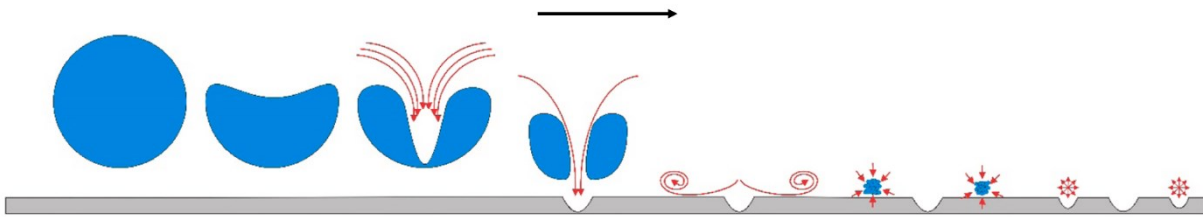


Fig. 11 – Cavitation erosion [13, p. 14]

A few measures can be considered to prevent or mitigate pipe erosion. Reducing the flowrate reduces the flow velocity and can reduce sand production, regardless of its effect on cash flow. Sand production should be monitored to make sure it is kept at acceptable limits, and the most exposed components should be routinely inspected for erosion damage. Proper dimensioning of pipes is recommended by increasing the pipe wall thickness at locations that are expected to be most exposed to erosion and also by increasing the radius of curvature. Erosion resistant materials such as ceramics can be used in those locations that are most exposed to erosion as internal coatings or inserts. Another approach is to try to exclude sand production by the installation of gravel packs and sand screens in well completions or by chemical consolidation treatments of the reservoir [14].

## 2.2.2 Flow Assurance Workflow

Brill and Al-Safran [2] presented a workflow for flow assurance that should start at an early stage of field development, as shown in Fig. 12.

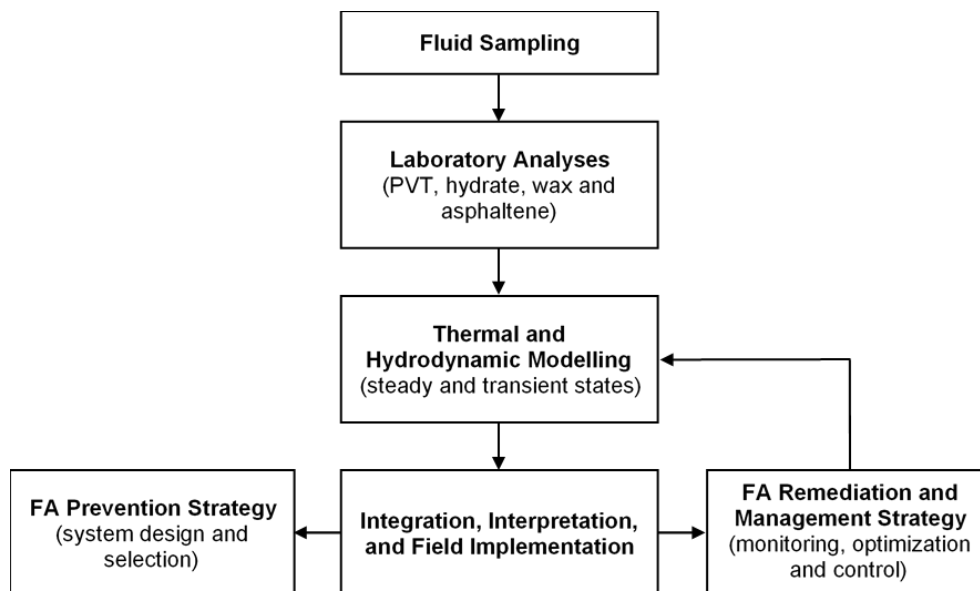


Fig. 12 – Flow assurance (FA) workflow [2, p. 210]

It begins with collecting representative reservoir fluid samples, which is the cornerstone for all the subsequent steps. Fluid samples are analyzed in the laboratory, where PVT analysis is performed to determine the fluid properties, and more tests could be conducted for the characterization of wax, asphaltene, hydrate, and scale. The hydrodynamic and thermal behaviors of the production system are then modelled under the steady-state and transient conditions of the different expected operating scenarios. The simulation results are

interpreted and used to create the system design and flow assurance strategies to be implemented in the field. After the system is implemented and the production operations are in place, the production system is monitored, and the feedback from the system shall be used to optimize the way in which the system is operated and the flow assurance risks are managed.





### 3 Case Study: Basis of Design

The subject of the case study in this thesis is a gas condensate field (will be referred to here as the GCF instead of its real name for confidentiality reasons) that is located onshore in a continental climate zone with significant annual variations in temperature. All the wells drilled in the GCF during the appraisal phase were productive from a gas condensate reservoir that will be referred to as the GCR.

The initial field development plan includes producing from the GCR through five wells (Well\_01 to Well\_05) at a production plateau of 53 MMscfd of gas and, according to well tests, an initial condensate gas ratio (CGR) of around 200 STB/MMscf. The produced fluids will be transferred to a neighboring processing facility 20 km away, where the gas and the condensate will be treated to sales specifications.

This chapter summarizes the design basis of the initial development plan of the GCF. It is not intended to discuss all the data required for the execution of the plan, but rather to cover those details that will be used as input to the flow assurance (FA) study.

#### 3.1 Field Data

##### 3.1.1 Reservoir and Wells

The GCR is a near-critical retrograde condensate reservoir. The initial reservoir pressure is 495.5 barg, and the reservoir temperature is 94.5 °C. All the five wells drilled to develop the GCR are vertical wells. They encounter the top of the GCR at depths that range from 4340-4380 m.

A GAP model<sup>1</sup> was created by the operator for the GCF and a mid-case was chosen for the design of the daily capacity of the project. The normal daily capacity is 53 MMscfd of raw gas<sup>2</sup>, and can only go up to 56.5 MMscfd due to restrictions set by the neighboring processing facility that is going to receive the produced fluids from the GCF. This processing facility belongs to a different operator than that of the GCF. Table 1 gives the expected range of gas flowrate for all the wells.

Table 1 – Expected range of gas flowrate for each well

Well	Minimum flowrate [MMscfd]	Maximum flowrate [MMscfd]
Well_01	4	12
Well_02	4	12

<sup>1</sup> GAP is a steady-state network modelling and optimization software that is typically used for long-term forecasting and production optimization [15].

<sup>2</sup> Raw gas is unprocessed natural gas which still contains hydrocarbon liquids, water, and other impurities [16].

Well	Minimum flowrate [MMscfd]	Maximum flowrate [MMscfd]
Well_03	10	25
Well_04	10	40
Well_05	10	25

The production profile of the GCF is shown in Fig. 13 for 20 years (240 months), as well as the expected decline in reservoir pressure. The figure also shows when the wells are no longer able to sustain the plateau of 53 MMscfd, and when Well\_01 and Well\_02 are expected to stop producing.

No significant water production is expected from the wells during the initial development plan. However, any produced water will also be treated at the neighboring processing facility according to the agreement between the two operators. The facilities will be designed for a maximum water flowrate of 500 Sm<sup>3</sup>/day. In case of significant water production, affected wells will need to be choked in order to reduce water production.

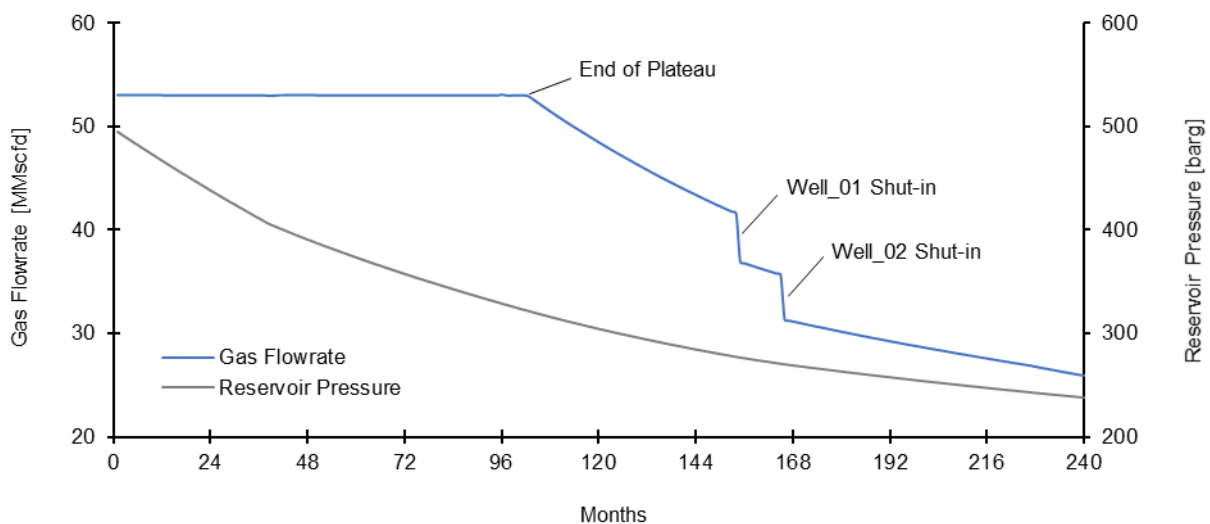


Fig. 13 – Production profile of the GCF's initial development plan

### 3.1.2 Produced Fluids

A number of fluid samples were taken during the drill stem test (DST) of Well\_01, and a PVT study was conducted. Table 2 shows the fluid composition based on a representative sample of the reservoir fluid from the DST, and Table 3 shows the parameters of the pseudo-components.

Table 2 – Reservoir fluid composition

Component	Mole Fraction
Nitrogen	0.0287
CO <sub>2</sub>	0.0135
H <sub>2</sub> S	0.0090
H <sub>2</sub> O	0.0050
Methane	0.6659

<b>Component</b>	<b>Mole Fraction</b>
Ethane	0.0810
Propane	0.0463
i-Butane	0.0107
n-Butane	0.0207
i-Pentane	0.0075
n-Pentane	0.0080
n-Hexane	0.0115
n-Heptane	0.0132
C <sub>8</sub> -C <sub>9</sub>	0.0265
C <sub>10</sub> -C <sub>12</sub>	0.0203
C <sub>13</sub> -C <sub>15</sub>	0.0119
C <sub>16</sub> -C <sub>19</sub>	0.0087
C <sub>20</sub> -C <sub>25</sub>	0.0066
C <sub>26</sub> -C <sub>31</sub>	0.0031
C <sub>32+</sub>	0.0019
<b>Total</b>	<b>1.0000</b>

Table 3 – Parameters of pseudo-components

	<b>C<sub>8-9</sub></b>	<b>C<sub>10-12</sub></b>	<b>C<sub>13-15</sub></b>	<b>C<sub>16-19</sub></b>	<b>C<sub>20-25</sub></b>	<b>C<sub>26-31</sub></b>	<b>C<sub>32+</sub></b>
<b>Molecular Weight [g/mol]</b>	112.8	147.0	188.8	241.4	277.6	390.4	504.7
<b>Specific Gravity [-]</b>	0.7424	0.7762	0.8035	0.8280	0.8414	0.8732	0.8967
<b>Boiling Point [°C]</b>	127.5	184.3	243.6	306.0	342.9	435.1	503.9
<b>Critical Temperature [°C]</b>	308.8	367.7	424.7	481.0	513.0	590.3	647.2
<b>Critical Pressure [barg]</b>	26.82	22.37	18.41	15.00	13.31	9.99	8.20
<b>Critical Volume [m<sup>3</sup>/kmol]</b>	0.5355	0.6823	0.8676	1.0970	1.2476	1.6598	1.9805
<b>Critical Z Factor [-]</b>	0.307	0.307	0.307	0.307	0.307	0.307	0.307
<b>Acentric Factor [-]</b>	0.348	0.436	0.540	0.660	0.736	0.943	1.110
<b>Parachor</b> <b>[(dyne/cm)<sup>1/4</sup>·cm<sup>3</sup>/mol]</b>	346.5	432.7	526.5	632.2	700.5	917.7	1200.9

Laboratory tests were performed on the samples collected from Well\_01. They showed a dewpoint pressure ( $P_d$ ) of 403 barg, a wax appearance temperature (WAT) of 17.5 °C, and a pour point between -22 °C and -25 °C. A hydrate curve was created by a third party, and can be seen in Fig. 14, along with one possible path for flowing operating conditions. The shaded area covers the pipeline operating pressure during steady-state production. This ranges from the pipeline design pressure of 100 barg (not to be reached) to the slug catcher pressure of 45 barg.

Chemical analysis of formation water was conducted, and the results are listed in Table 4 for two samples that were collected from the same well. It should be noted though that the well from which these water samples were collected is not one of the five wells considered in the initial development plan of the GCF, and it has no other mention in the resources available for this thesis. Probably, it is one of the wells that were drilled during the appraisal phase.

The PVT study report, which details the behavior of the GCR's gas condensate, was not available as a resource for this thesis. Therefore, the data reported so far in 3.1 will be the basis on which the fluid characterization will be done later in Multiflash.

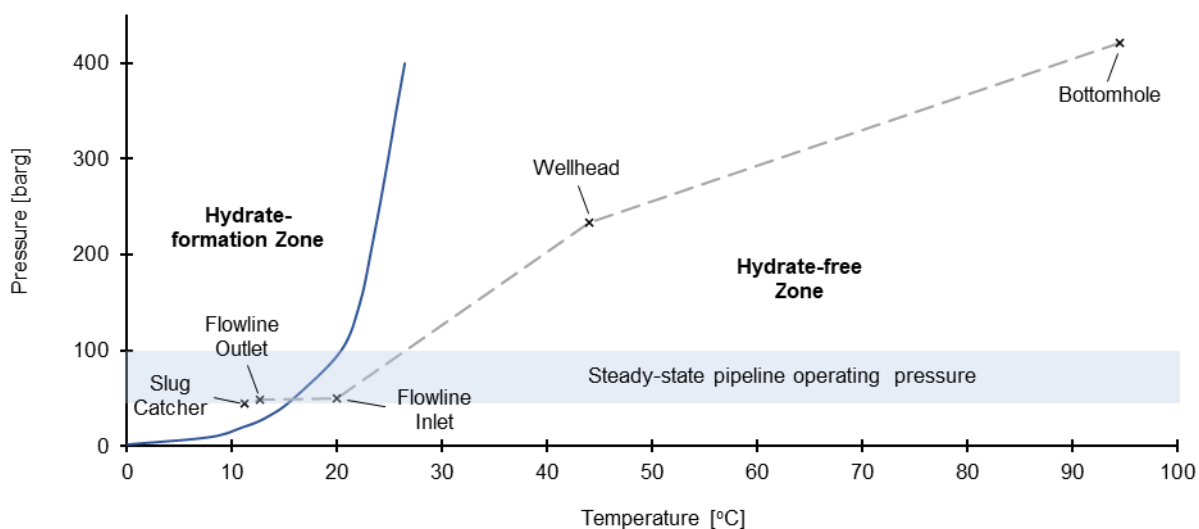


Fig. 14 – Hydrate formation curve and possible flowing operating conditions

Table 4 – Chemical analysis of formation water

Parameter	Unit	Value (sample #1)	Value (sample #2)
pH	-	6.25	6.23
Density	gm/cc	1.17	1.17
Na <sup>+</sup>	mg/L (meq/L)	67,350 (2,928)	68,575 (2,982)
K <sup>+</sup>	mg/L (meq/L)	15,000 (384)	15,000 (384)
Ca <sup>2+</sup>	mg/L (meq/L)	11,623 (580)	11,423 (570)
Mg <sup>2+</sup>	mg/L (meq/L)	2,310 (190)	2,310 (190)
Cl <sup>-</sup>	mg/L (meq/L)	144,563 (4,077)	146,300 (4,126)
F <sup>-</sup>	mg/L (meq/L)	0.4 (0.0)	0.4 (0.0)
SO <sub>4</sub> <sup>2-</sup>	mg/L (meq/L)	1,161 (24)	1,162 (24)
HCO <sub>3</sub> <sup>-</sup>	mg/L (meq/L)	707.6 (11.6)	488.0 (8.0)
CO <sub>3</sub> <sup>2-</sup>	mg/L (meq/L)	None	None
H <sub>2</sub> S	mg/L (meq/L)	27.4 (1.6)	41.7 (2.5)
HS <sup>-</sup>	mg/L (meq/L)	3.3 (0.1)	4.0 (0.1)
B <sup>3+</sup>	mg/L (meq/L)	56.3 (15.6)	53.7 (14.9)
Fe <sup>3+</sup>	mg/L	Traces	Traces
Li	mg/L	7.5	7.5
Rb	mg/L	0.2	0.2
Cd	mg/L	1.1	1.1
Ag	mg/L	0.4	0.4
Pb	mg/L	8.1	8.1
Sr	mg/L	178	178
Zn	mg/L	0.8	0.8
Cu	mg/L	1.1	1.1

## 3.2 Pipeline Network

Four of the five wells (Well\_01, Well\_02, Well\_03, and Well\_05) will be connected to a gathering station (manifold) through individual flowlines. These wells and their gathering station lie to the west of a river that crosses the GCF. The produced fluids from these wells will then be transferred through a single trunk-line that goes below the river and continues until it reaches the transfer station. Well\_04, which lies to the east of the river along with the transfer station, will be tied directly to the trunk-line as it passes near the well. A simplified layout of the GCF's pipeline network is shown in Fig. 15.

### 3.2.1 Well Pads

Each well pad consists of a single well. The X-tree on each of the wellheads has a pressure rating of 10K psi and is connected to 3-1/16" wing and choke valves with the same rating. Methanol injection pumps and storage tanks are available at all the well pads for methanol injection upstream of the choke valves. Wax inhibition is not foreseen, yet provisions for wax inhibitor injection shall be considered for utilization later in the life of the field.

All the well pads, except that of Well\_04, will have connections for mobile pig launchers. The flowline of Well\_04 will be flushed with hot fluids instead of being pigged. Another difference is that unlike the rest of the wells, the well pad of Well\_04 will contain a fixed three-phase test separator that will be equipped with single-phase flowmeters on its outlets.

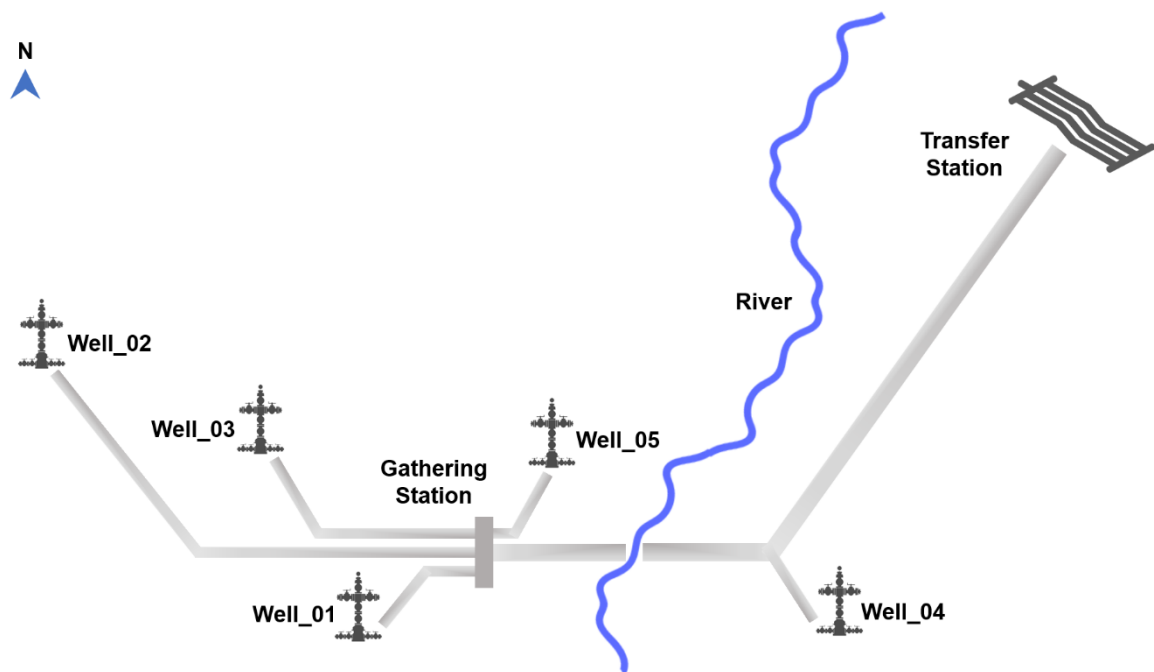


Fig. 15 – Simplified layout of the GCF's pipeline network

### 3.2.2 Flowlines and Trunk-line

The operator's preference after the conceptual design is to install 6" flowlines made of glass reinforced epoxy (GRE), and a seamless 10 3/4" carbon steel trunk-line. The flowlines and the

trunk-line are going to be insulated and buried at a depth of 1.8 m to bottom of pipe. Fig. 16 shows the lengths of the trunk-line and the flowlines of Well\_01 to Well\_05 (FL\_01 to FL\_05).

The flowlines and the rest of the network including the transfer station are designed for a pressure of 100 barg. The pipeline network is to be protected from overpressure using a high-integrity pressure protection system (HIPPS) at each of the well pads.

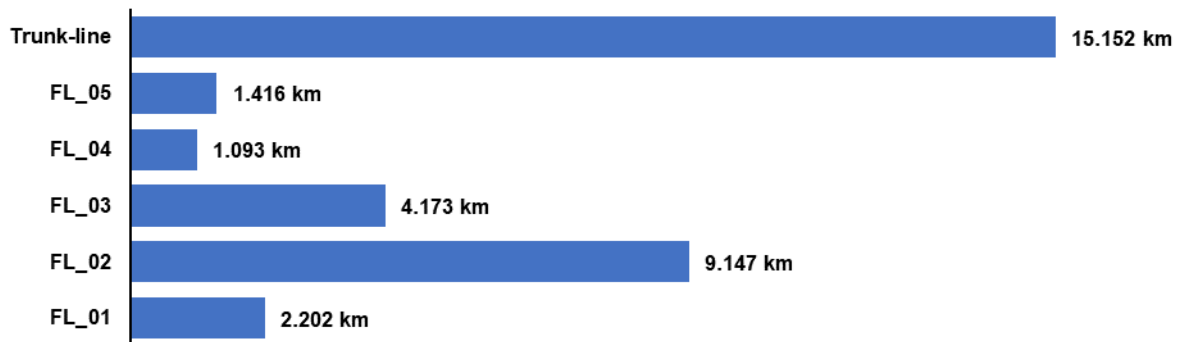


Fig. 16 – Flowlines and trunk-line lengths in kilometers

### 3.2.3 Gathering Station

The gathering station contains separate production and test manifolds with slots for individual wells. The test manifold includes a three-phase test separator that is equipped with single-phase flowmeters at its outlets.

Connections for mobile pig receivers will be provided for all the flowlines arriving at the gathering station, and a permanent pig launcher will be installed to allow the pigging of the trunk-line until the transfer station.

### 3.2.4 Transfer Station

Produced fluids flowing in the trunk-line will eventually arrive at the transfer station, which consists of an inlet slug catcher with a surge capacity of 50 m<sup>3</sup>, a heater that brings the produced fluids to the required export temperature, and a three-phase separator. The flowrates of the separated gas, condensate and water leaving the separator are measured before they are exported to the nearby processing facility.

A permanent pig receiver will be installed at the trunk-line as it arrives to the transfer station to receive any pigs coming from the gathering station. Electric heat tracing will be applied to the well pads, gathering station, and transfer station to prevent freezing and hydrate formation.

### 3.2.5 Valve Stations

Valve stations are distributed along the pipeline network at pipeline junctions and river crossings, and provisions are prepared for the installation of valves at 5-km intervals given the presence of H<sub>2</sub>S in the produced fluids.

### 3.3 Ambient Conditions

The GCF is located in a continental climate with sharp temperature contrast between winter and summer, and between day and night. The winters are extremely cold, and the summers are hot and dry, with strong winds in both winter and summer.

The soil at the location of the field, where the pipeline will be buried, is sandy loam<sup>1</sup>, and the maximum frost penetration depth in the region is 2.28 m. Fig. 17 shows the average high temperature and the average low temperature of the ambient air around the year in that region, in addition to the soil temperature at depths of 2.28 m and 25 m.

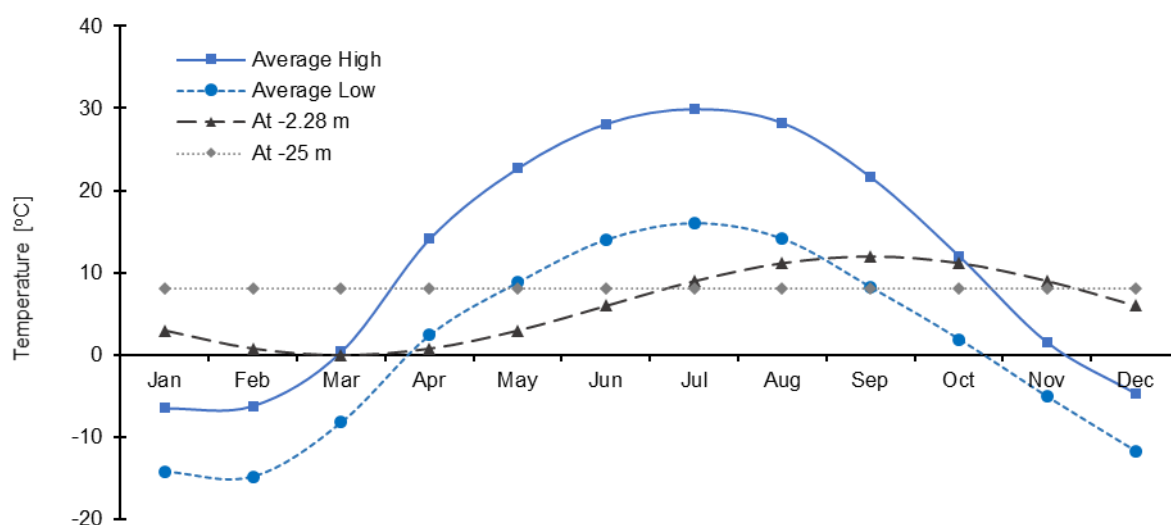


Fig. 17 – Air and soil temperatures around the year

The figure shows that at the depth of 25 m, the soil temperature is not affected by the ambient air temperature anymore, and it records a constant value of 8 °C throughout the year. The design ambient conditions at the GCF based on the region's climate are listed in Table 5.

Table 5 – Design ambient parameters

Design parameter	Value
Maximum ambient temperature [°C]	+45
Minimum ambient temperature [°C]	-43
Wind velocity [km/hr]	90 (25 m/s)
Frost penetration [m]	≤ 2.28

<sup>1</sup> Sandy loam soils are those which are made up dominantly by sand particles, in addition to clays and sediments that provide structure and fertility [17].





## 4 Building the Simulation Model

This chapter discusses building a preliminary simulation model in OLGA [version 2018.1] to be used later to set up and run the different simulation cases that will be discussed in chapter 5. The model is preliminary because more components will be added to it, depending on the objective of running the simulation task in question, and it will be set up in different ways for the same reason. The chapter will cover creating the PVT tables and hydrate curves using Multiflash as input to OLGA, building the pipeline network, and setting up the heat transfer between the network and its surroundings.

Fluid characterization was performed using Multiflash [version 7.0]. This was mainly done for the initial gas condensate composition. An attempt was made to capture the effect of condensate drop-out in the reservoir on the composition of the gas condensate flowing into the network. This was done to be able to simulate the pipeline network in different points in time over the life of the field. Different hydrate tables were created for the gas condensate at varying concentrations of hydrate inhibitor. The effects of water production, the salinity of produced water, and the different gas condensate compositions on the hydrate formation conditions were examined.

Building the network components was then covered. More line sizes were selected according to API Spec 5L to check their applicability in place of the ones from the conceptual design, and different insulation thicknesses were chosen in accordance with the requirements of the European standard EN253:2009 to study their effect on hydrate and wax formation. Well models were built to simulate the inflow to the simulation model. For that, well IPRs were generated that could match the production profiles from the GAP model. A choke model was created with the help of MFSizing<sup>1</sup> [version 7.1] for the prediction of pressure drop across the valves and, as importantly for the FA study, the flowlines inlet temperatures.

Finally, the chapter covered setting up the heat transfer for the pipelines and the well models. Two-dimensional temperature field calculations for the pipelines were set up in OLGA using the FEMTherm module with optimized spatial and temporal discretization, and one-dimensional heat transfer was set up for the well models. The effect of well path discretization on the geothermal gradient near the surface was also examined.

### 4.1 Defining the fluid

#### 4.1.1 PVT Models in OLGA

Fluid properties can be defined in OLGA using four different methods [6]. These are:

1. **Lookup tables:** Fluid properties are read at given pressures and temperatures from a PVT table file.

---

<sup>1</sup> MFSizing is a choke valve sizing software by Master Flo™. It calculates choke valve capacity, pressure drop across the valve, flow rate, and sizing of choke actuators [18].

2. **Compositional tracking:** Fluid properties are calculated using a full compositional approach.
3. **Black-oil:** Fluid properties are calculated based on black-oil correlations.
4. **Single component:** Fluid properties are calculated for single-component fluids.

Lookup tables can be created by Multiflash or other PVT packages with OLGA table file generator. The PVT package calculates phase equilibrium and fluid properties for a given composition at user-defined pressures and temperatures, then it is used to export the calculated properties into a PVT table file (\*.tab). OLGA imports the table and calculates the fluid properties at certain pressures and temperatures as required for the simulations by interpolation in the PVT tables. This method is the least computationally demanding method. It is suitable for those cases where fluid composition isn't expected to change significantly along the flow paths, or at the same point over time.

Compositional tracking is considered when significant changes in the fluid composition are expected to take place along the same flow path, or at the same point in space over time. Typical scenarios where this happens are during start-ups, shutdowns, and restarts; where gas and liquid phases redistribute, blowdowns; where continuous change in composition occurs between the depressurized and the remaining fluids, and during gas lift at varying flow rates [19].

Fluid characterization is carried out using the PVT package Multiflash, which is then used to create a feed file (\*.mfl) that includes all the compositional data of the fluid. OLGA imports the feed file to the simulation case, and Multiflash is used to perform the thermodynamic equilibrium calculations. Mass equations are solved for each component, and consequently each of the fluid components is tracked, resulting in a more accurate description of the fluid compared to the lookup tables method. This level of accuracy makes compositional tracking the most computationally demanding PVT method.

Black-oil method is useful when little information is available about the fluid. Even though more information could be input, it only requires the specific gravities of oil and gas and the gas-oil-ratio (GOR) at standard conditions. If water exists, then it also requires the specific gravity of water and the water cut (WC). These are directly input to the OLGA simulation case to define one or more so-called black-oil feeds, and the fluid properties are calculated using available black-oil correlations. A black-oil feed can consist of one oil, one gas, and one water component. Due to the assumptions and limitations of the black-oil model that were mentioned in 2.1.1.4, this method is not suitable for modelling gas condensate or volatile oils.

Single component method handles single component fluids crossing the saturation line along a flow path, or at the same point over time. The method should be used for fluids consisting of only one component.

In addition to modelling a typical reservoir fluid<sup>1</sup>, OLGA offers different models to account for other types of fluids and solids. Table 6 lists these different types of fluids and solids in combination with the PVT methods with which they can be used.

Table 6 – Compatibility between fluid/solid models and PVT methods [6, p. 58]

	PVT method			
	Lookup table	Compositional tracking	Black-oil	Single component
<b>Reservoir fluid</b>	x	x	x	
<b>Mud</b>	x	x		
<b>Particles</b>	x	x		
<b>Inhibitor</b>	x	x		
<b>Hydrates</b>	x			
<b>Wax</b>	x			
<b>Steam</b>	x			x
<b>CO<sub>2</sub>, H<sub>2</sub>O, ...</b>				x
<b>Tracer</b>	x	x	x	x

#### 4.1.2 Defining the Fluid in Multiflash

The lookup tables method is chosen here as the base case of setting up the PVT modelling in all the FA simulations in OLGA. It is the least computationally demanding PVT method, which is a great advantage considering that all the network branches will be simulated simultaneously; not in isolation, which is already computationally intensive. The black-oil method, even though it is not suitable for modelling gas condensate, will be used in one case just to see how much its results could deviate from those obtained by the look-up tables.

Multiflash was used to create PVT lookup tables for OLGA based on the composition of the gas condensate and the properties of the pseudo-components in 3.1.2. The Advanced Peng-Robinson 1978 equation of state (PR78A) was selected for thermodynamic equilibrium calculations. By default, using PR78A as the thermodynamic model, Multiflash identifies a gaseous phase, a liquid phase, and an aqueous phase; and uses the SuperTRAP model for viscosity and thermal conductivity calculations, and the Linear Gradient Theory Model (LGTM) for surface tension calculations. The default options were left unchanged.

A Multiflash model file (\*.mfl) is saved and used to generate the PVT tables for OLGA, and a PVT table file (\*.tab) is created containing all the physical properties required by OLGA. These are the results of flash calculations carried out at a series of user-defined pressures and temperatures. The file uses a keyword-based format, which is the same format that OLGA uses for its input. It has the form:

<sup>1</sup> Typical reservoir fluids in OLGA are gas/oil/water fluids with Newtonian rheology. These are modeled using any of the PVT methods except *Single component* [6].

KEYWORD KEY = Parameters list, ...

A keyword identifies some input statement that has a set of variables (keys). A key has one or more parameters to which some values are assigned. The different keys and parameters of the keyword-based PVT table as reported in OLGA user manual [6, pp. 540-542] are described in Appendix A.

### 4.1.3 Composition Change over Time

One of the first steps of the planned FA study is to determine the profiles of pressure, temperature, liquid hold-up and some other variables along the pipeline based on production profiles and ranges of possible flowrates, pressures, and temperatures from each well. The production profiles on which this step is based are those of the mid-case of the GAP model mentioned in 3.1.1.

The GAP model itself is not an available resource for this thesis, neither are the reservoir or well data that were input to the model beyond what was already mentioned in chapter 3. However, the results of the mid-case were reported and available for all the wells on a monthly basis for a total of 241 months. The most important reported variables are reservoir pressure ( $P_{res}$ ), bottom-hole pressure (BHP), wellhead pressure (WHP), wellhead temperature (WHT), gas rate, oil rate, water rate, gas-oil-ratio (GOR), water cut (WC), choke size, flowline pressure (FLP), and flowline temperature (FLT).

A number of points (dates) in the life of the field are therefore chosen for this task. Reported in Table 7 in the format of “yy/mm,”<sup>1</sup> these are:

Table 7 – Important dates in the GCF life

Date	Description
01/01	The start of the GCF production. At this point, only Well_01 to Well_04 will be put to production to achieve the plateau of 53 MMscfd of gas with its associated condensate.
02/01	Well_05 starts producing. The production of the other wells will be reduced to continue following the production plateau.
09/04	The end of the production plateau. After this point, wells will not be able to sustain the plateau of 53 MMscfd at the given slug catcher pressure of 45 barg.
13/10	Production of Well_01 stops, causing a step drop in the total production of the GCF in the next month.
14/09	Production of Well_02 stops, causing a step drop in the total production of the GCF in the next month.
21/01	The end of production of the GCF initial development plan.

The point 02/01 will be chosen as the base case, where almost all the FA simulations will be done. This is due to the following reasons:

<sup>1</sup> The numbers here do not represent specific dates; they represent order. For example, “02/01” means “the second year of production, and the first month of the year,” etc.

- At this point, all the wells will have been put to production. An ideal case would be to conduct an FA study for the period where only four wells are in production as well, but this is not going to be part of the scope of work discussed in this thesis.
- The reservoir pressure at this point (474.3 barg) is still above the dewpoint pressure (403 barg), and the producing GOR is still the initial dissolved GOR (5119 scf/STB). This means that the composition of the produced fluids can be still accurately represented by the composition in Table 2.
- Compared to the rest of the points where all the wells are still producing the target flowrates above the dewpoint pressure, this point corresponds to the highest WHPs, and therefore to the smallest choke openings that will achieve just the required flowline pressures to transfer the target flowrates at the given slug catcher pressure. The pressure drops across the choke valves at this point will be the highest, and consequently the temperature drops as well, according to the Joule–Thomson effect. This will bring the flow conditions in the flowlines closer to the hydrate formation zone and the wax appearance temperature, which makes 02/01 a good point in time to perform the FA study.

After the reservoir pressure falls below the dewpoint, liquid condensate will start to form in the reservoir, especially near the wellbore, and may form banks that can impair the well's deliverability and reduce the amount of heavy components flowing into the well [20]. The deliverability impairment is beyond the scope of this thesis. However, the loss of heavy components in the fluid going into the wells will be elaborated on.

The composition of the fluid flowing into the wellbore and in the part of the reservoir present below the dewpoint pressure will continue to change with time during production. This will be accompanied by an increase in the producing GOR. Going back to the six dates in Table 7, the last four points from 09/04 to 21/01 correspond to reservoir pressures that are below the dewpoint, and therefore the produced fluid in these cases will not be accurately represented by the initial composition in Table 2. The predicted reservoir pressures and producing GORs over time are listed in Table 8.

Table 8 – Reservoir pressure and GOR over time

<b>Date</b>	<b>P<sub>res</sub> [barg]</b>	<b>GOR [scf/STB]</b>
01/01	494.5	5,119
02/01	464.3	5,119
09/04	324.3	11,296
13/10	277.2	16,101
14/09	270.5	17,031
21/01	237.8	22,680

Although the task of simulating the pipeline profiles to a great accuracy after +9 years is not as critical as the rest of the FA study, it is still preferred to arrive to a better approximation of the produced fluid composition at this time compared to using the initial composition as it is or with only modifying the producing GORs in OLGA. An attempt was made to arrive at such compositions with the help of the results of the GAP model.

The target here, considering the points from 09/04 to 21/01, is to reach to a fluid composition at each of the points that contains reduced amounts of heavy components and results in a produced GOR that matches the one in the production profiles. It is not meant to simulate how condensate drop-out actually happens in the reservoir.

An amount of the gas condensate, say 100 moles, at its initial composition is taken as a starting point in Multiflash. The gas condensate is flashed to the new reservoir pressure that corresponds to one of the dates at which we want to calculate the fluid composition. Since this new reservoir pressure is below the dewpoint, the flashed fluid exists in two phases (vapor and liquid). The composition of the vapor phase is used to represent that of the gas that is going to be produced ( $Gas_{prod}$ ), while the liquid phase represents the condensate drop-out ( $Cond_{drop}$ ). Only a part of this condensate ( $Cond_{prod}$ ) will be combined with the gas to represent the gas condensate that is going to be produced ( $GC_{prod}$ ).

To find out how much condensate should be added to the gas in order to get a producing GOR that matches the one from the production profiles, the liquid condensate is initially split into two parts using a random split ratio (SR), where:

$$SR = Cond_{prod}/Cond_{drop} \dots\dots\dots (1)$$

Where SR is the split ratio [-],  $Cond_{prod}$  is the condensate produced [moles], and  $Cond_{drop}$  is the condensate drop-out [moles]. The amount of each component of  $Cond_{prod}$  is calculated by multiplying SR by the amount of each component in  $Cond_{drop}$ , where:

$$[X_i]_{prod} = SR \times [X_i]_{drop} \dots\dots\dots (2)$$

Where  $[X_i]_{prod}$  is component  $i$ 's liquid produced amount [moles],  $[X_i]_{drop}$  is component  $i$ 's liquid drop-out amount [moles], and SR is the split ratio [-].  $Gas_{prod}$  and  $Cond_{prod}$  are then combined by adding the amounts of each component in both fluids;  $[Y_i]_{prod}$  and  $[X_i]_{prod}$ , to form a new composition that represents the produced gas condensate ( $GC_{prod}$ ), where:

$$[Z_i]_{prod} = [Y_i]_{prod} + [X_i]_{prod} \dots\dots\dots (3)$$

Where  $[Z_i]_{prod}$  is component  $i$ 's overall produced amount [moles],  $[X_i]_{prod}$  is component  $i$ 's liquid produced amount [moles], and  $[Y_i]_{prod}$  is component  $i$ 's vapor produced amount [moles]. A separator test simulation is run in Multiflash where  $GC_{prod}$  is flashed to standard conditions and the producing GOR from the test is checked and compared to the one from the production profiles. If the GORs do not match, a different SR is chosen, and the rest of the steps are repeated until a match is achieved.

This is done for the four points from 09/04 to 21/01 using the corresponding reservoir pressures at these points. The composition of  $GC_{prod}$  can then be used to represent the composition of the produced fluid at these points. A flow chart summarizing the calculation procedure is shown in Fig. 18.

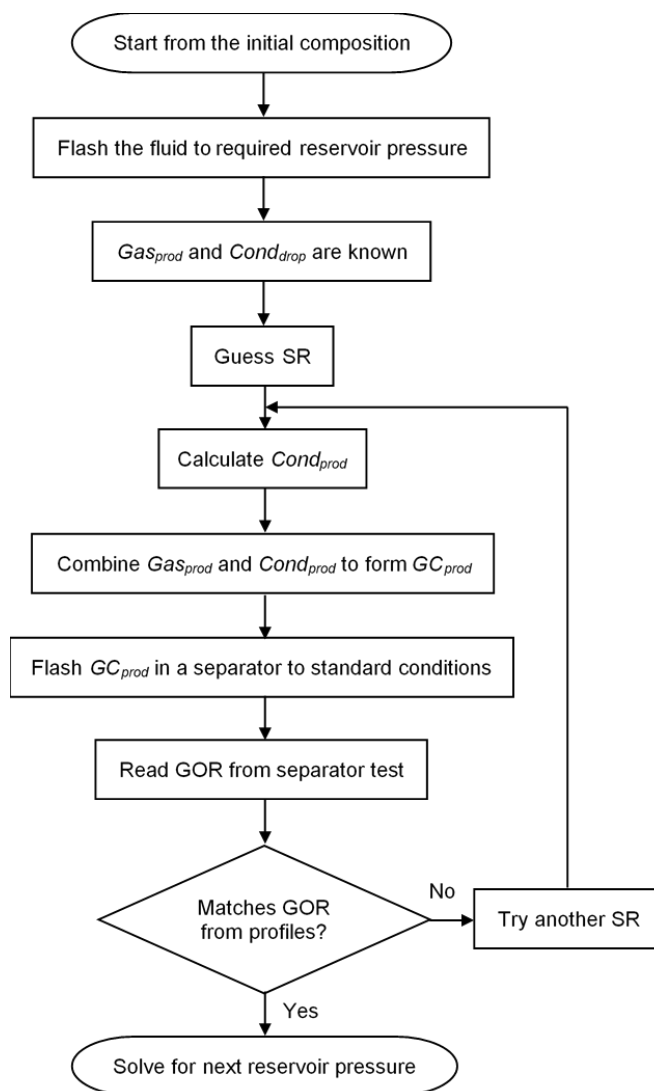


Fig. 18 – Procedure of calculating new fluid compositions

It is more convenient to report the composition in this task in amounts (moles) rather than in mole fractions to clearly capture the splitting procedure, then convert it later to mole fractions for the sake of comparison between the different compositions. The calculated compositions are normalized to be reported in mole fractions and compared together, and the different fluid compositions over time are shown in Fig. 19, where:

$$[z_i]_{prod} = [Z_i]_{prod} / \sum [Z_i]_{prod} \dots\dots\dots (4)$$

Where  $[z_i]_{prod}$  is component  $i$ 's overall produced mole fraction [-], and  $[Z_i]_{prod}$  is component  $i$ 's overall produced amount [moles]. The desired effect of the condensate drop-out on the composition of the heavier components is achieved as their mole fractions keep decreasing with time, starting from propane (C<sub>3</sub>), in addition to hydrogen sulfide (H<sub>2</sub>S). This is accompanied by an increase in the mole fractions of the rest of the components, especially methane (C<sub>1</sub>). The values of the split ratios, the calculated amounts and mole fractions are listed in Appendix B. In addition to the PVT table file that was created for the original composition, more files were created for the different compositions to be used as input for OLGA.

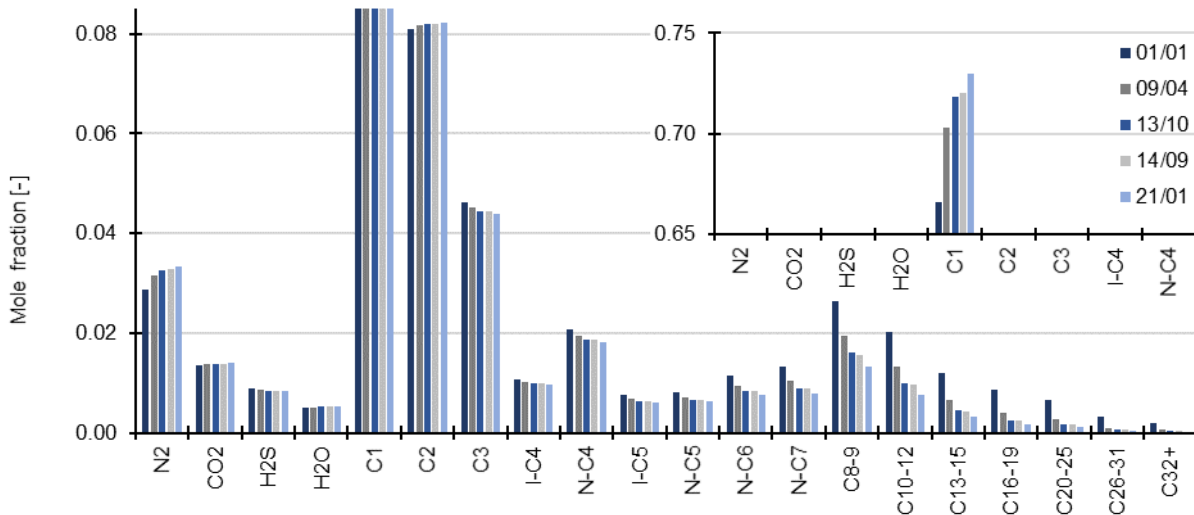


Fig. 19 – Composition of produced fluid over time

### 4.1.4 Creating the Hydrate Curves

Multiflash was used to create hydrate curves based on the composition of the gas condensate and the properties of the pseudo-components in 3.1.2. The hydrate model used was CPA Infochem, and its default options were left unchanged. A hydrate phase boundary (hydrate curve) was generated that shows the areas of pressure and temperature where hydrate is likely to form. Fig. 20 shows the hydrate curve generated by Multiflash, and the given hydrate curve that was created by a third-party and displayed in Fig. 14. The two curves are similar, even though they start to diverge at pressures higher than 100 barg. The difference in the hydrate formation temperature of the two curves at 400 barg is only 1.3 °C.

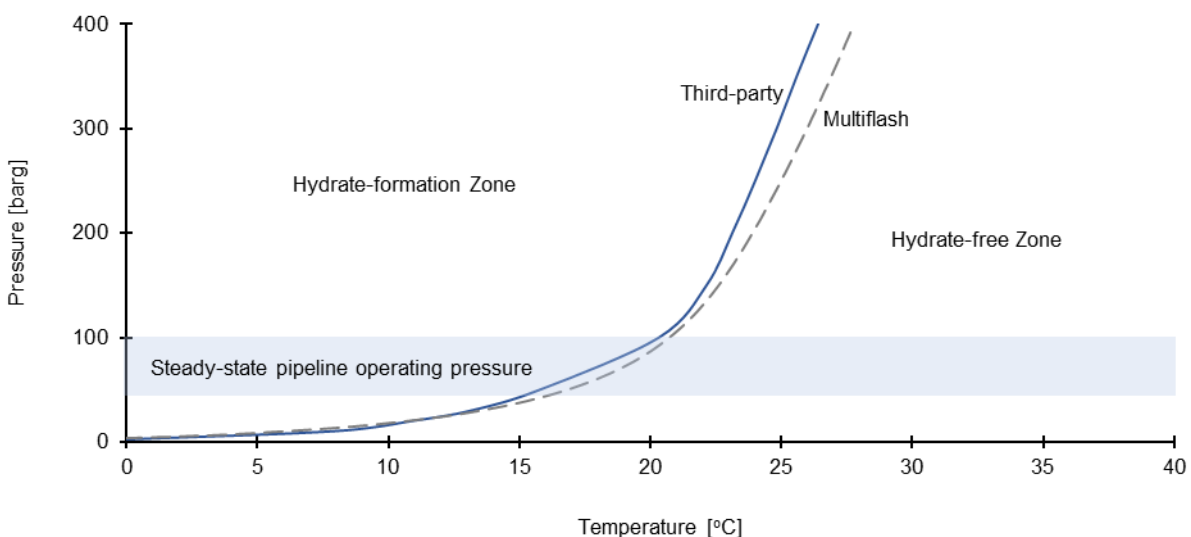


Fig. 20 – Hydrate curves (Multiflash vs Third-party)

#### 4.1.4.1 Effect of Methanol

The hydrate mitigation strategy, as can be deduced from the basis of design in chapter 3, includes pipeline insulation and methanol injection at the well pads. The estimation of the



pipeline insulation thickness and the methanol injection rates required to avoid hydrate formation are two of the main objectives of the FA study.

To be able to estimate the injection rates of methanol required to avoid hydrate formation at the different conditions that will be met during the simulation work, more hydrate curves are needed at different concentrations of methanol in the water present in the characterized fluid. Multiflash can specify this concentration in mass, molar or volume units [21]. However, to comply with OLGA’s convention for inhibitor concentration calculations, mass units were used for the calculation of the hydrate curves, where:

$$\text{Methanol wt\%} = \frac{\text{mass of methanol}}{\text{mass of methanol} + \text{mass of water}} \times 100\% \dots\dots\dots (5)$$

Fig. 21 shows the created hydrate curves at different concentrations of methanol in weight percent (wt%). The data points from each curve were copied into separate text files (\*.txt) to be imported later by OLGA as hydrate tables, or into Excel, as will be discussed in chapter 5.

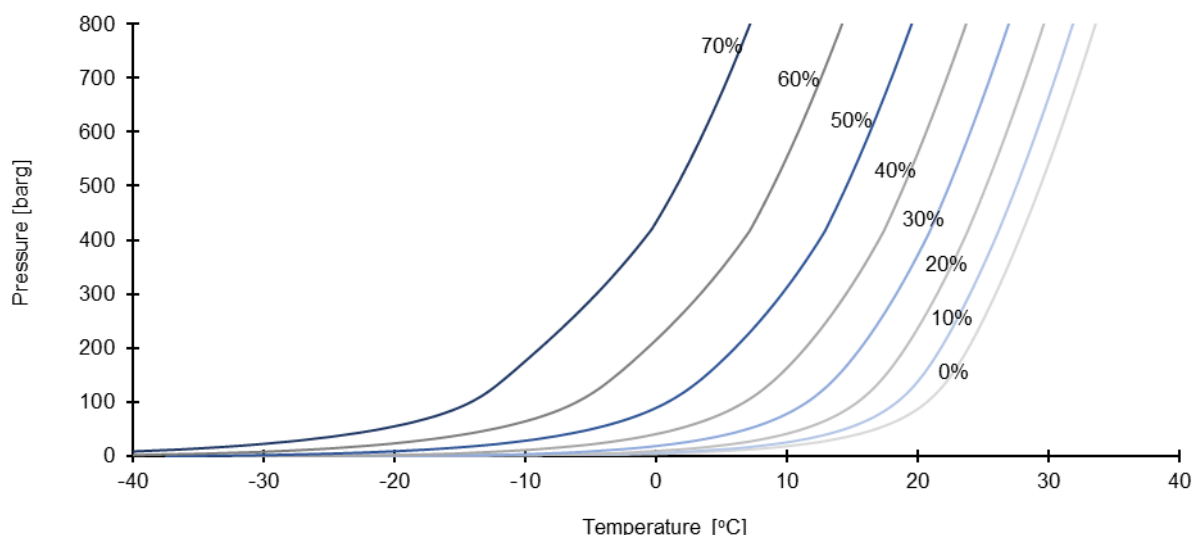


Fig. 21 – Hydrate curves at different methanol wt%

#### 4.1.4.2 Effect of Water Production

It should be noted that the hydrate formation calculations are sensitive to the amount of water in the fluid composition, especially if the fluid is undersaturated with water, or in the presence of inhibitors and water-soluble gases. If the amount of water in the fluid composition is less than what it actually is, water might be modelled to be distributed among the fluid phases rather than forming a hydrate phase. On the other hand, if the amount of water in the fluid composition is higher than in reality, hydrate might be predicted to form at conditions where no hydrate should be found [21].

The hydrate curves in Fig. 21 were calculated using the initial composition in 3.1.2. At that point, the GCR is not producing any water, and the water flowing in the system is the water of condensation, which only represents around 0.22-0.25% WC based on the production profiles at the initial GOR, where the reservoir pressure is higher than the dewpoint pressure, and it increases to only 1.5% WC at the end of field life. In case of water production, these

hydrate curves cannot be used to predict hydrate formation accurately, especially in the presence of methanol.

In order to study the effect of formation water production as part of the FA study, the simulation work in chapter 5 will consider two scenarios for running the different cases: no water production, and the maximum water production of 500 Sm<sup>3</sup>/day at which the facilities will be designed, as mentioned in 3.1.1. This figure (500 Sm<sup>3</sup>/day) corresponds to a WC of around 26% at the point 02/01 that was chosen to conduct the FA study at, as mentioned in 4.1.3. This is not a significant amount of water; therefore, no intermediate cases for expected water production were considered.

The fluid composition was edited to account for the water production of 500 Sm<sup>3</sup>/day at the target flowrate of 53 MMscfd of gas, and more hydrate curves were created as shown in Fig. 22.

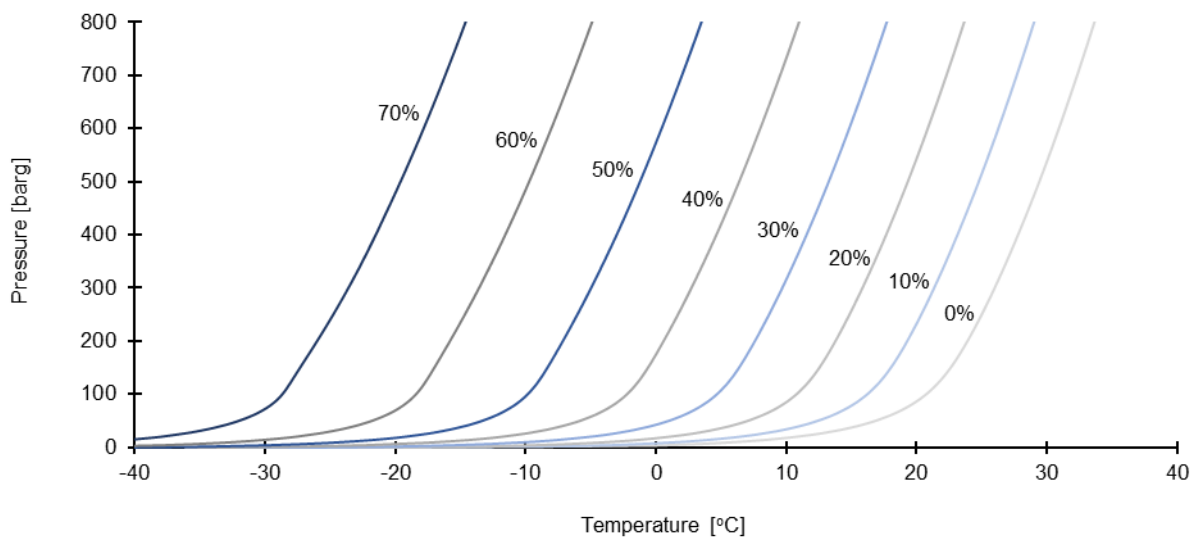


Fig. 22 – Hydrate curves at different methanol wt% during formation water production

Although it virtually looks like adding more water to the initial composition has pushed the hydrate formation conditions (the curves) to lower temperatures, which is counter-intuitive, this is actually related to higher methanol concentrations in the aqueous phase compared to the case with no added water.

Note that the injected inhibitor distributes into the different phases of the fluid at equilibrium. It partitions into the vapor phase, the liquid hydrocarbon phase, and into the aqueous phase in which hydrate inhibition occurs and the concentration of the inhibitor matters the most [22]. The amount of the inhibitor in each of the phases depends on the amounts of the other components and at which conditions the fluid exists [21].

To have a closer look at this, a side task was performed. Methanol was added to the two fluids (with and without added water) to get the same mass fraction of methanol in water, then the fluids were flashed to the same conditions and the amount of methanol in each phase was checked. Both fluids with 50 wt% methanol in water (the weight of methanol is

equal to the weight of water) were flashed to 2000 psig (137.9 barg) and 10 °C, and the results are listed in Table 9.

Table 9 – wt% of methanol in different phases

Case	Overall	Vapor phase	Liquid phase	Aqueous phase
No added water	0.25	0.09	0.16	31.53
With added water	14.29	0.16	0.54	48.76

So, even though the methanol mass fraction in the total water composition (liquid + vapor) is the same in both cases, there is more methanol in the aqueous (liquid) phase in the case with the added water, and therefore the hydrate formation conditions are pushed to lower temperatures compared to the case with no added water as can be seen by comparing Fig. 22 with Fig. 21. However, this comes at the price of higher methanol injection requirements.

Another observation is that the hydrate curves at 0 wt% methanol are the same in both cases; with and without added water. It becomes interesting to check the amount of water in the composition beyond which the hydrate formation conditions do not change in the absence of methanol.

To have a look at this, another side task was performed. The fluid composition with the added water was considered as a starting point. The amount of water in the composition was reduced in steps, and a hydrate curve was calculated at each step. Fig. 23 shows the calculated hydrate curves, and Table 10 lists the mass fraction of water at each step.

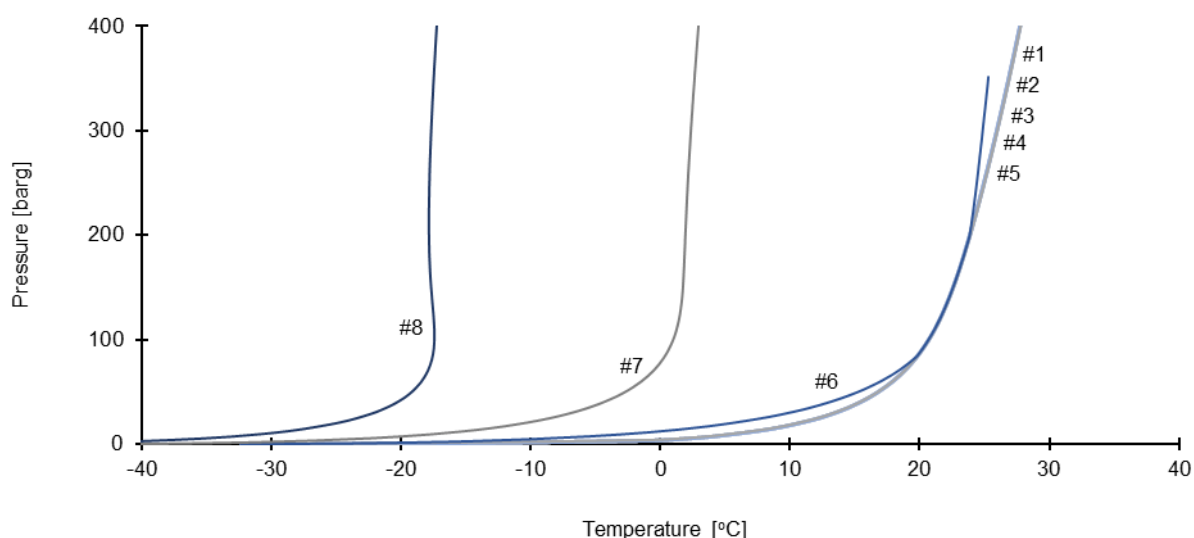


Fig. 23 – Hydrates curves at different water mass fractions

Table 10 – Water mass fraction at different water production rates

Step #	Water production* [m <sup>3</sup> /day]	Water mass fraction [%]
1	500.00	16.670
2	125.00	4.763

Step #	Water production* [m <sup>3</sup> /day]	Water mass fraction [%]
3	31.25	1.235
4	7.81	0.312
5	1.95	0.078
6	0.49	0.020
7	0.12	0.005
8	0.03	0.001

\*accompanying 53 MMscfd of gas and its associated condensate

It is only below a water mass fraction between 0.020% and 0.078% that the hydrate formation conditions are affected by the amount of water in the fluid. The initial composition of the gas condensate with no added water already contained 0.25% water mass fraction.

#### 4.1.4.3 Effect of Produced Water Salinity

The hydrate curves created so far in 4.1.4.1 and 4.1.4.2 were calculated considering hydrate formation in pure water. However, while this assumption could be valid for the case where water comes only from condensation in the network, the produced formation water will always carry a considerable concentration of salts.

In practice, salts dissolved in water act to inhibit hydrate formation. Water becomes attracted to salt ions more than to hydrate structure, which in turn requires more subcooling to cause hydrate to form [23]. In this manner, salts are similar to other thermodynamic hydrate inhibitors except that they do not enter the vapor phase or the hydrocarbon liquid phase; they remain in the aqueous phase or else precipitate [24].

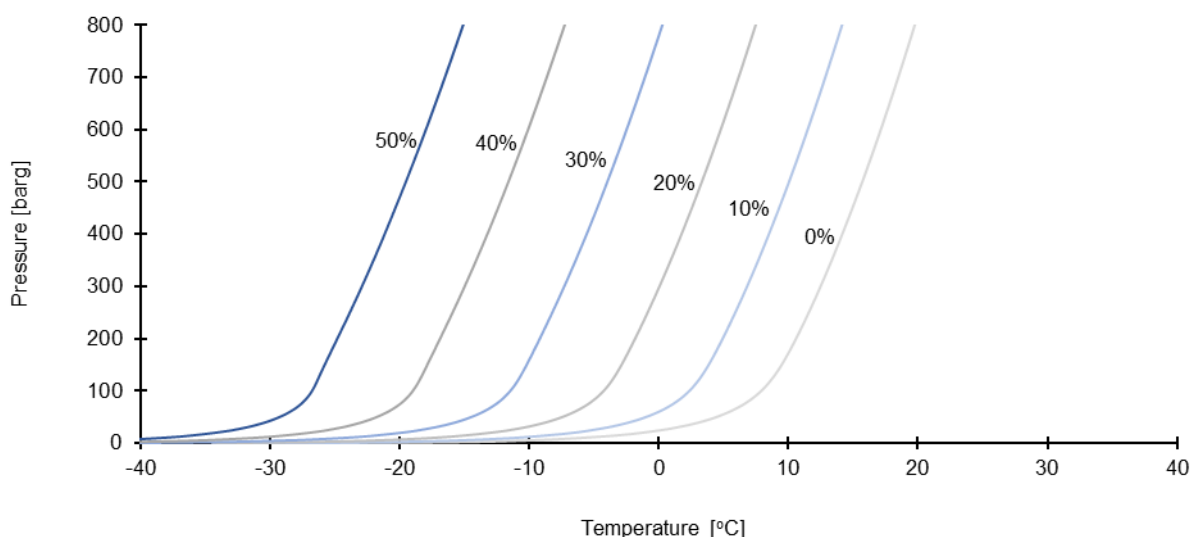


Fig. 24 – Hydrate curves at different methanol wt% during formation water production and considering water salinity

To account for the effect of water salinity in the calculation of the hydrate curves, the concentration of the various salts in water is specified in Multiflash using the produced water analysis in Table 4. In the case where salts are present, the thermodynamic model used in Multiflash needs to be CPA + Electrolytes [21]. Hydrate curves were calculated for the case

with formation water production considering the effect of water salinity, and the results are shown in Fig. 24. Multiflash could not calculate the hydrate phase boundary at 60 wt% and 70 wt% methanol.

The reason why the hydrate formation calculations when water production is assumed were performed twice; with and without taking salts into account, is to compare the methanol requirements for both cases, and assess how much it would be advisable to assume some value for produced water salinity even if no water analysis is available. The data points of the hydrate curves in Fig. 22 and Fig. 24 were also copied into separate text files (\*.txt) to be imported by OLGA or into Excel.

#### 4.1.4.4 Effect of Changing Composition

All the hydrate curves mentioned earlier were calculated based on the initial composition of the produced gas condensate. This composition was edited to account for water production, methanol injection, and produced water salinity, but the rest of the gas condensate components were not manipulated. However, the composition of the produced gas condensate will change over time due to condensate drop-out in the reservoir at reservoir pressures below the dewpoint, which shall affect the hydrate formation conditions, especially in the presence of methanol. This changing composition was roughly approximated at different points in the life of the field as discussed in 4.1.3.

For the simulation of the points in time from 09/04 to 21/01, it is part of the scope of work to calculate how much methanol is needed to avoid hydrate formation, but only to know if hydrate is going to form or not without methanol injection. Therefore, hydrate curves were calculated for the different compositions only at 0 wt% methanol. No water production was assumed, but the effect of water salinity was still considered as an attempt to account for when water condensation takes place in the formation and water starts to “pick up” salts from the reservoir, even though the concentration of salts in this case is probably not going to be the same as in Table 4.

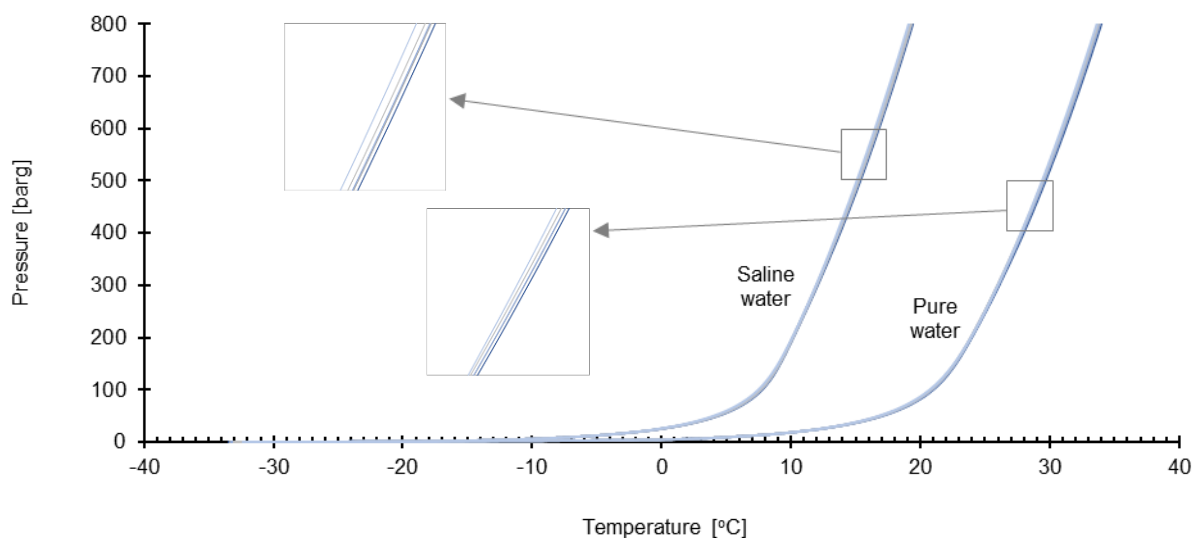


Fig. 25 – Hydrate curves at different compositions considering pure and saline water content

Fig. 25 shows the calculated hydrate curves for the different compositions considering both pure and saline water. The hydrate curves for the initial composition is also included in the graph for comparison. The figure shows that the change in composition, as depicted in Fig. 19, had a very little effect on the hydrate formation conditions in the absence of methanol. The hydrate curves are almost the same for the different compositions, considering pure and saline water.

However, in the presence of methanol, these hydrate curves would be more visibly distinct from one another at the same methanol wt%. For demonstration only, the hydrate curves were calculated for the different compositions at 50 wt% methanol in pure water and the results are shown in Fig. 26.

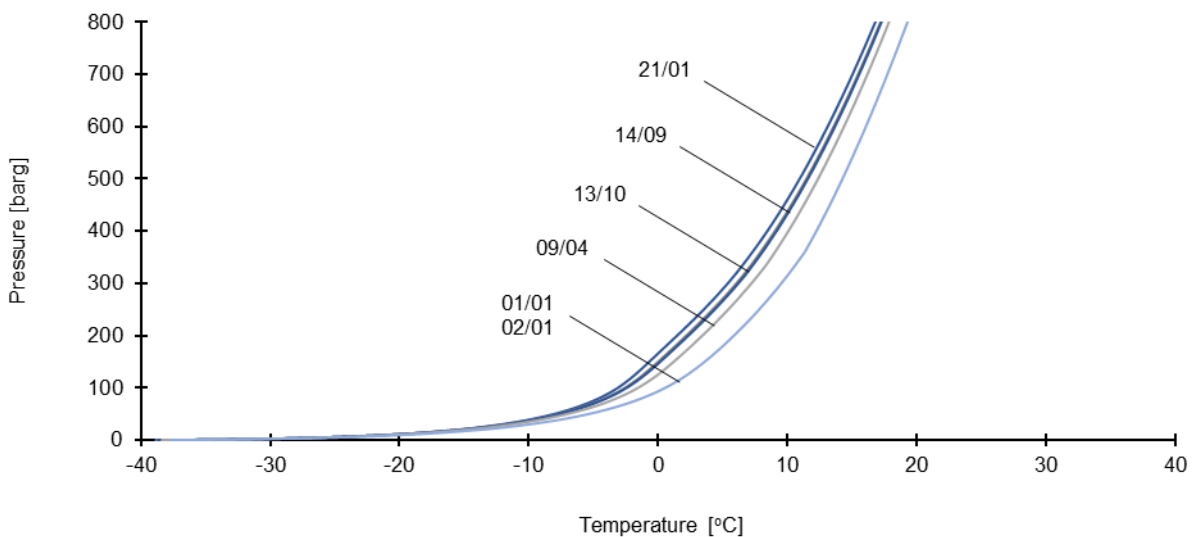


Fig. 26 – Hydrate curves at different compositions and 50 wt% methanol in pure water

Since the required hydrate curves at 0 wt% methanol were almost the same, no hydrate tables (\*.txt) were created for the different compositions from 09/04 to 21/01, and the hydrate curve of the initial composition will be used for these dates as well. All the hydrate formation curves that will be used for the FA study are shown in a panel plot in Appendix C.

## 4.2 Building the Network Components

A simulation model in OLGA consists of several simulation objects that are the building blocks of the simulation network. These simulation objects can be of different types [6]:

- **Branch (flow path):** A pipeline through which the fluids flow.
- **Node:** A boundary condition for a flow path, or a coupling point for two or more paths.
- **Separator:** A special type of node that separates a fluid into different phases.
- **Controller:** Objects that perform supervision and automatic adjustments of other parts of the simulation network.
- **Thermal:** Objects for ambient heat conditions.

The branch is the main component in the simulation network. It represents a pipeline connecting two points in space. Each branch consists of one or several pipes, which in turn

are divided into several sections. The sections represent the control volumes where the transport equations are solved.

A pipe represents one segment of a branch or a flow path. It can be defined by length and elevation, or by coordinates. Pipes of one branch can have different lengths and elevations. Each pipe has a set of constant properties: inner diameter, pipe wall, and wall surface roughness; but the different pipes of a branch can have different properties. The pipe wall itself may consist of a number of layers of different materials, each having its own thickness and thermal properties, as in the case of insulated pipes, for example.

Each branch must start and end at a node. Some nodes are used to define boundary conditions for a flow path: closed nodes, mass nodes, and pressure nodes; while others are used to merge or split flow paths: internal nodes, junction nodes, and phase split nodes.

A source is an object that can also be used to define boundary conditions for a flow path by modelling fluid flow into or out of the flow path, similar to a mass node to some extent. Sources can be divided into mass sources, with a given mass flowrate; and pressure-driven sources, where the source's mass flowrate is controlled by upstream or downstream pressure. However, unlike nodes, a source does not have to be located at the start or the end of a flow path. The input flowrate to sources can either be defined as mass flow or as volumetric flow at standard conditions, but in either case, OPGA will perform its calculations using mass flowrate.

A reservoir contact is yet another object that can be used to define a boundary condition for a flow path; in this case, a wellbore. It represents the contact region between the reservoir and the wellbore, and it uses inflow performance relationships (IPRs) to calculate the flow out of or into the reservoir.

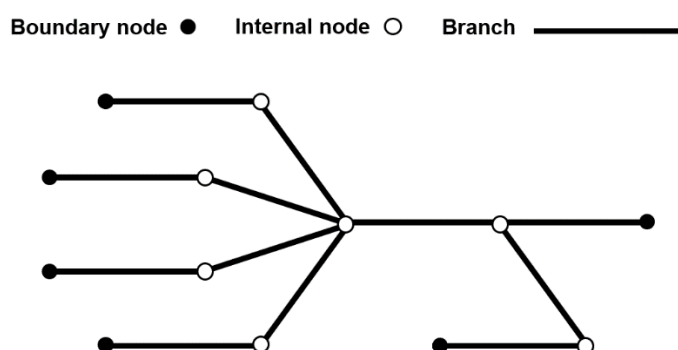


Fig. 27 – Simulation network sketch

This section is going to cover creating the objects required to build the simulation network in OPGA. Five closed nodes at the inlet side are connected to wellbores, where reservoir contacts are defined. Internal nodes representing the wellheads are used to connect the wellbores to several branches that will converge until reaching a single pressure node that

represents the slug catcher at the outlet side. Fig. 27 shows a simple sketch of the network based on the layout in Fig. 15.

#### 4.2.1 Selecting Line Sizes and Insulation Thicknesses

As mentioned in 3.2, the operator's preference is to install 6" GRE flowlines, and a 10 ¾" carbon steel (CS) trunk-line. All the lines are planned to be buried at a depth of 1.8 m to bottom of pipe. A pipeline survey was provided for the different lines. The provided survey does not account for the geometry of the pipeline at the well pads, the gathering station, or the transfer station. It also does not take into account the river crossing, where the pipeline will be buried below the river at a depth higher than 1.8 m. The survey was edited considering the mentioned points to achieve a more realistic representation of the pipeline network, and the pipeline model in OLGA was built accordingly. The profiles of both the given and the edited pipeline profiles can be seen in Appendix D.

Although all the flowlines were initially planned to be insulated, it was reported internally that the GRE pipe manufacturer does not provide the pipes with insulation. Therefore, the flowlines will not be insulated in the base case of the pipeline model that will be used for all the FA simulations. However, the effect of varying the insulation thickness on hydrate and wax formation is considered as part of the FA study. The operator might eventually decide to consider another GRE pipeline manufacturer that produces readily insulated pipes. On the other hand, the foreseen insulation of the carbon steel trunk-line was reported to be 2" polyurethane. Therefore, the trunk-line will always be modelled accordingly in the base case.

The first step of the FA study in chapter 5 will be to confirm the line sizes as per the basis of design, and to determine other possible line sizes based on the given pressure rating of the pipeline, which is 100 barg. In addition to line sizes chosen for the base case, a number of different sizes were chosen to check their applicability according to API Spec 5L (Specification for Line Pipe) [25].

All chosen pipes are of Grade X52. Size 8 5/8" was chosen for the trunk-line in addition to the 10 ¾"; and sizes 6 5/8", 5 9/16", and 4 ½" were chosen for the flowlines in addition to the 6" GRE pipe. The next smaller size of GRE pipes that has the same rating as that of the base case is 3" [26], which is too small to consider, and therefore only CS pipes were considered to check if they can be applicable as flowlines. The minimum thickness of each of the lines was calculated as per ASME B31.3 standard using a corrosion allowance of 6 mm that was set by the operator, then the inner diameter was determined accordingly. The dimensions of the selected pipes are listed in Table 11.

Table 11 – Trunk-line and flowline dimensions for 100 barg rating pressure

Application	Size [in]	OD [in]	Thickness [in]	ID [in]	Material	Notes
Trunk-line	10 ¾	10.750	0.625	9.500	CS	Base case
Trunk-line	8 5/8	8.625	0.562	7.501	CS	Check applicability
Flowline	6	7.230	0.690	5.850	GRE	Base case
Flowline	6 5/8	6.625	0.500	5.625	CS	Check applicability



Application	Size [in]	OD [in]	Thickness [in]	ID [in]	Material	Notes
Flowline	5 9/16	5.563	0.500	4.563	CS	Check applicability
Flowline	4 1/2	4.500	0.438	3.624	CS	Check applicability

Since the effect of flowline insulation thickness is going to be studied in the FA study, some values for insulation thickness needed to be chosen. Instead of assuming some hypothetical values, thicknesses were chosen in accordance with the requirements of the European standard EN253:2009 as an attempt to reach a design that is close to that of commercially available pipes. The standard specifies requirement and test methods for district heating pipes with polyurethane (PUR) foam thermal insulation and polyethylene (PE) outer casing [27]. The chosen thicknesses for the flowline insulation and outer casing are listed in Table 12, in addition to the sole case of the trunk-line. The effect of different insulations will be studied for the base case of the flowline only (6" GRE) and not for any of the other CS pipes.

Table 12 – Line dimensions including PUR-foam insulation and PE outer casing

Line	PUR-foam thickness [in]	PE thickness [in]	OD [in]
10 3/4" CS	2.00	0.19	15.13
	none	none	7.23
6" GRE	1.17	0.14	9.85
	1.75	0.15	11.03
	2.43	0.16	12.41
	3.19	0.18	13.97

The default pipe roughness in OLGA for the CS (0.05 mm) was used, while that of the GRE was taken as 0.00533 mm as per the pipe datasheet [26].

#### 4.2.2 Defining Pipe Walls

As preparation for the simulation work, several pipe walls were defined in OLGA to choose from according to the simulation case. A wall is defined by the thicknesses and thermal properties of its layers. The inner diameter and the surface roughness are input to each of the pipe segments of a branch; not to the wall itself.

The different pipe and insulation thicknesses of the base case were listed in 4.2.1, and the thermal properties of the different materials are shown in Table 13. The properties of the steel are according to OLGA library. The density and the conductivity of the GRE come from the pipe manufacturer's datasheet [26], while the heat capacity is taken from [28]. The properties of polyurethane come from [29], and those of high-density polyethylene (HDPE) are from [30]. The density and the heat capacity of the soil are taken as average values of sand and clay as reported in [31], and the conductivity as an average value for sand and clay (dry, moist, and wet) as per Aspen HYSYS library.

When defining a layer thickness for a wall, sometimes it is necessary to discretize the layer into sublayers with smaller thicknesses. This discretization is not required for steady-state simulations, but it might be required for transient simulations, where heat storage in the walls

is important, as in the case of cool-down, for example. This is because the layer discretization affects the numerical solution for the temperature in the wall layers.

Table 13 – Thermal properties of wall layers

Material	Density [kg/m <sup>3</sup> ]	Conductivity [W/m·K]	Heat capacity [J/kg·K]
CS	7850	50.000	500
GRE	2000	0.400	900
PUR	30	0.025	1500
HDPE	940	0.440	2400
Soil	1850	1.047	800

OLGA advises that a wall layer should not be thicker than 30% of the layer's outer radius, and that the change in thickness between two adjacent layers should be kept between 0.2-5 [6]. This rule was considered for defining the walls in the simulation model. A list of all the walls including the materials of the layers and the discretization of the thicknesses is attached in Appendix E.

### 4.2.3 Creating Valve Models

The main application of the valve model in OLGA is to calculate the pressure drop and the critical flow constraints across different types of valves, e.g. orifices, and chokes. There are two main valve models in OLGA: the choke model, and the valve sizing equation. In the choke model, the valve diameter and discharge coefficient ( $C_D$ ) are required as input to the model; while in the valve sizing equation, the valve sizing coefficients, namely the liquid and the gas flow coefficients ( $C_v$  and  $C_g$ ), are used instead.

Two valve models needed to be defined: one for the choke valves, and another for the shutdown valve (SDV) upstream the transfer station. The rest of the valves in the pipeline network will not be simulated. Two commercially available valves were chosen to simulate, and the valve sizing equation model was used to define the valves. In this case, the valve model requires a table that contains a valve sizing coefficient ( $C_v$  or  $C_g$ ) versus the relative valve opening as a fraction or a percentage. For the 3-1/16" choke valves, the Master Flo™ P3E choke valve with a maximum bean size of 137/64 in. and a maximum  $C_v$  of 83 gpm/psi<sup>1/2</sup> was selected [32]. For the SDV, the KLINGER Ballostar® full-bore ball-valve with a nominal diameter of 250 mm was chosen to be installed on the main trunk-line. The valve has a flow factor ( $K_v$ ) of 13,630 m<sup>3</sup>/hr·bar<sup>1/2</sup> [33], which corresponds to a  $C_v$  value of 15,757 gpm/psi<sup>1/2</sup>.

In practice, only the maximum  $C_v$  value is sufficient to build a valid  $C_v$  table. In this case, OLGA would linearly interpolate between 0, when the valve is closed, and the maximum  $C_v$  value, when the valve is fully open. However, this assumes a linear relationship between the flow coefficient and the relative opening, which is not necessarily true.

For the case of the choke valve, it is better to use a detailed  $C_v$  table or curve in order to simulate the actual opening of the valve at the different in-situ conditions of flowrate, pressure, and temperature. Since no readily available  $C_v$  curve was found for the chosen

valve model, the software MFSizing [version 7.1] by Master Flo™ was used to calculate one as input to OLGA. Several  $C_v$  values were entered in the software for the choke model P3, and the corresponding stem travel values were calculated. Fig. 28 shows the  $C_v$  curve versus the relative valve opening as a percentage of the maximum stem travel.

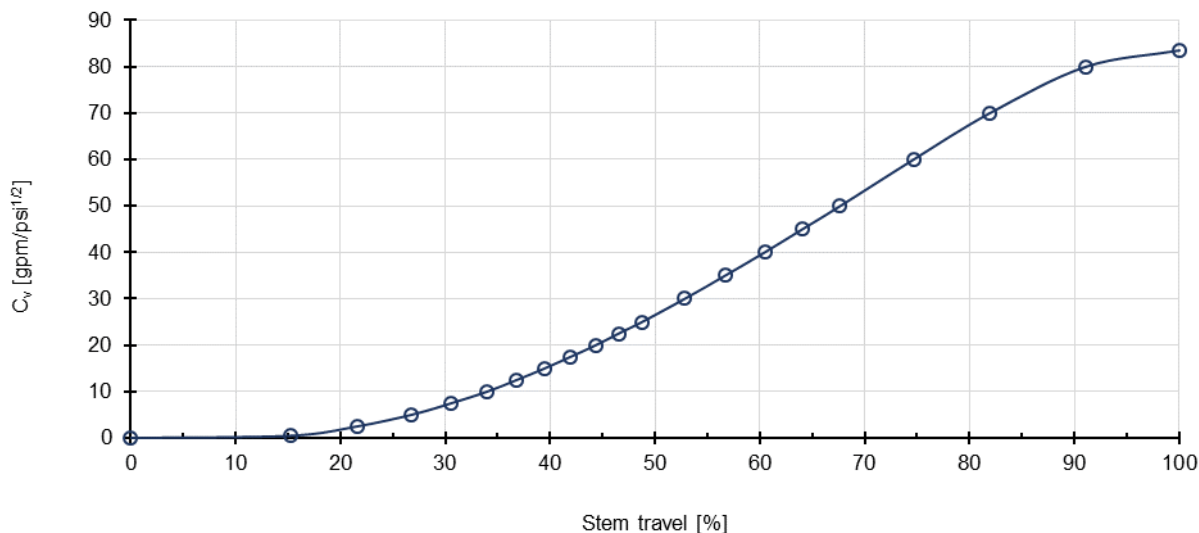


Fig. 28 –  $C_v$  curve for choke valve model P3

For the case of the SDV, the relationship between the  $C_v$  and the relative opening holds no useful information since the valve is not used for throttling; it is operated either fully open or fully closed. Therefore, it is ideal to build the  $C_v$  table from two points only: (zero opening, zero  $C_v$ ) and (full opening, maximum  $C_v$ ). OLGA will still interpolate linearly between the two points during the time it takes the valve to open or close, which is another parameter set by the user.

#### 4.2.4 Creating Well Models

Two main tasks were performed to create the well models in OLGA. The first one was to build the wellbore (branch) by the Well Editor tool in OLGA based on an existing completion schematic, and the second one was to define the reservoir contact and the inflow relationships based on the provided production profiles.

No well completion schematics were provided for the GCF; however, a schematic was available for a well that is also producing from the GCR in an adjacent field. This schematic was used as a reference for casing sizes and casing setting depths. The production casing setting depth, the tubing setting depth, and the reservoir contact depth were input based on the average depth of the top of the GCR as encountered in the five wells in the GCF as was mentioned in 3.1.1. The chosen tubing size 3 1/2" was validated against the flowrate and the pressure values in the production profiles after the model was built.

All top-of-cement depths were assumed to be the surface level. Flow in annulus was not activated in OLGA; therefore, no production packer was modelled. Still, a completion fluid was assumed to be present behind the tubing. The default values of the thermal properties of

the steel, the cement, and the completion fluid in OLGA were left unchanged. Fig. 29 shows the completion schematic of the well model as displayed in the well editor.

The attempt to arrive to a detailed well schematic that is thought to be as close as possible to the real completions used in the GCF; not just a valid tubing size, was to establish a basis for accurate heat transfer calculations between the gas condensate flowing inside the tubing and the surrounding formations.

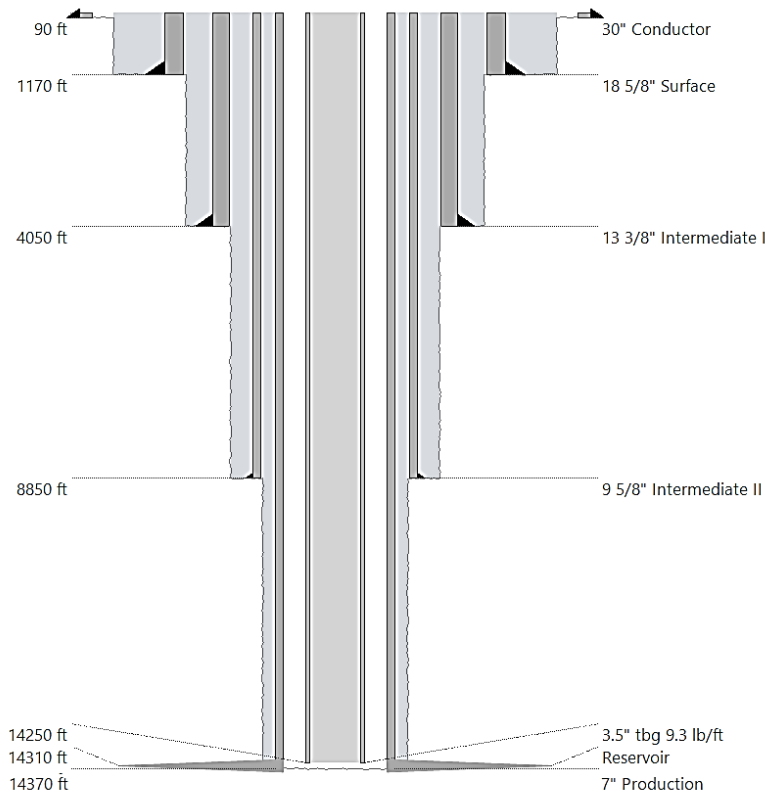


Fig. 29 – Completion schematic of the well model

The second task in building the well model was to model the inflow performance of the GCR in the different wells. The values of the reservoir pressure, bottom-hole flowing pressure, and gas flowrate as reported in the provided production profiles were used to define IPR models for the wells using the backpressure equation, where:

$$q_g = C(P_{res}^2 - P_{wf}^2)^n \dots\dots\dots (6)$$

Where  $q_g$  is the gas flowrate [MMscfd],  $P_{res}$  is the reservoir pressure [psi],  $P_{wf}$  is the bottom-hole flowing pressure [psi],  $C$  is the flow coefficient [MMscfd/psi<sup>2</sup>], and  $n$  is the deliverability exponent [-].

All the production points were used to arrive to values of  $C$  and  $n$  for each of the wells that can produce a production profile that matches the one from the GAP model's results. A two-step procedure was found to produce good matching between the profiles. The first step was to visually match the production profiles after iteration in  $n$  and calculating the corresponding

C value. The second step was to analytically fine-tune the C and n values from the first step by minimizing the standard deviation of the calculated C values at the different production points. Instead of discussing the matching procedure here step-by-step, a flow chart summarizing the procedure is shown in Fig. 30.

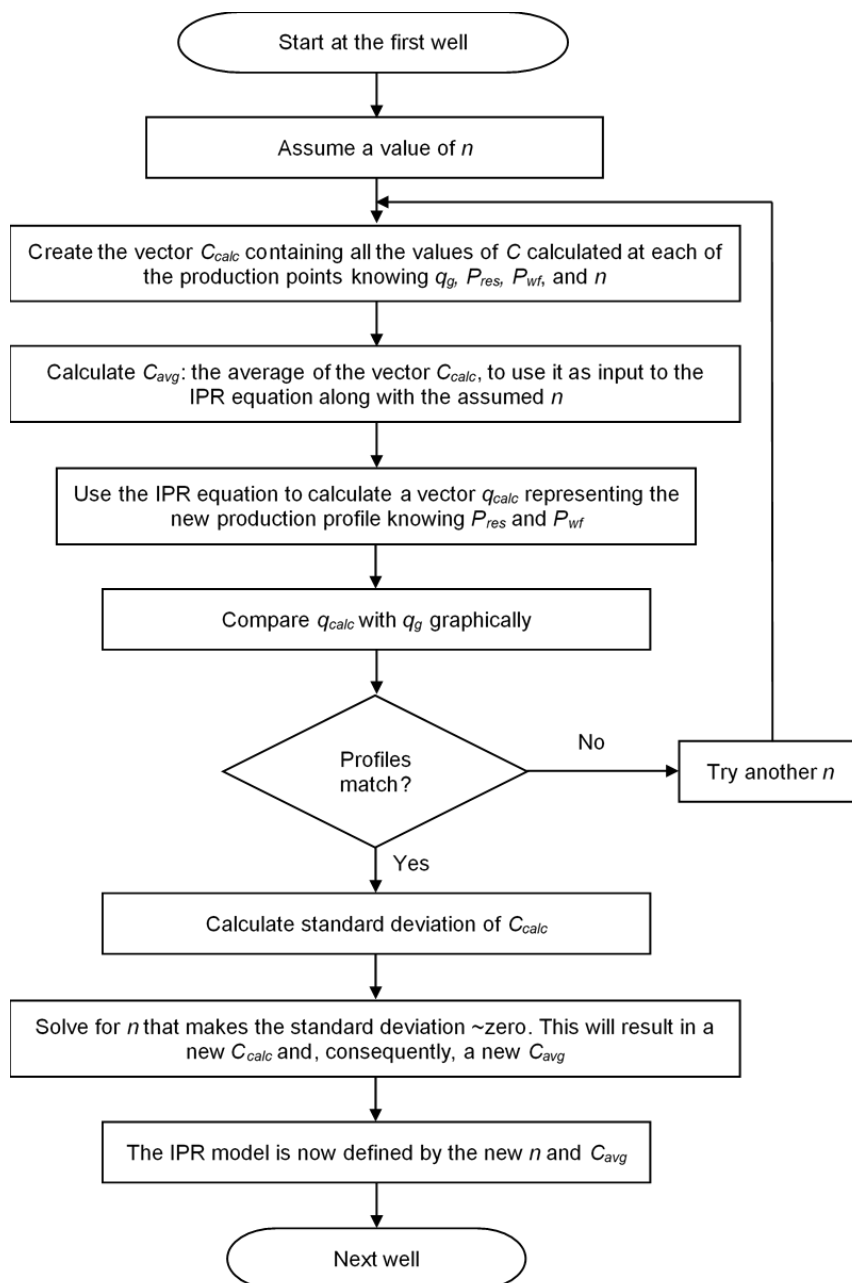


Fig. 30 – Procedure of matching the IPR models

Matching was successfully achieved for all the wells from Well\_01 to Well\_04 by finding the pairs of C and n that could produce production profiles that match those from the GAP model's results. However, no pair of C and n could match all the production points of Well\_05 simultaneously, and therefore different IPR models had to be calculated only for those points in time that are going to be considered in the FA study: n was given a value of 1, and the corresponding C values for each of the points were calculated independently.

The constants of the created backpressure IPR models for all the wells are listed in Table 14, and the production profiles from the GAP model and created IPR models are plotted and attached in Appendix F.

Table 14 – Constants of backpressure inflow equation

Well	Date	C [scfd·psi <sup>2</sup> ]	n
Well_01	All dates	1.23	0.94
Well_02	All dates	0.39	1.00
Well_03	All dates	3.54	0.92
Well_04	All dates	8.00	0.95
Well_05	02/01	0.26	1.00
Well_05	09/04	0.38	1.00
Well_05	13/10	0.45	1.00
Well_05	14/09	0.46	1.00
Well_05	21/01	0.52	1.00

The fact that the production profile of each of the wells from Well\_01 to Well\_04 was matched using the same pair of C and n means that no change in productivity was assumed for these wells while building and running the GAP model.

## 4.3 Setting up the Heat Transfer

### 4.3.1 Heat Transfer in OLGA

OLGA provides different settings for temperature calculations that can be selected in the simulation case options under the key TEMPERATURE, as listed in Table 15.

Table 15 – Temperature calculation settings in OLGA [6, p. 91]

Setting	Description
OFF	No temperature calculation – initial temperatures must be specified.
ADIABATIC	No heat transfer to surroundings.
UGIVEN	A user-defined overall heat transfer coefficient is used for the entire wall.
WALL	The heat flux through the pipe wall layers is calculated with user-defined thermal conductivities, specific heat capacities and densities for each wall layer.
FASTWALL	Similar to WALL but heat storage is neglected in the wall.

The heat transfer between a fluid flowing, or sitting, in a pipe segment and its surroundings can be modelled in OLGA in two ways:

- **One-dimensional heat transfer.**
- **Two-dimensional heat transfer.**

The one-dimensional heat transfer is the default method for heat transfer calculations in OLGA. Heat transfer takes place symmetrically in the radial direction through concentric wall layers. The wall layers here not only represent the pipe itself and its insulation, for example,

but can also include the surrounding medium, like the soil in which the pipe could be buried, until what a user would choose as the ambience.

The heat transfer coefficient between the outer wall and the ambience can either be given by the user or calculated based on some given value(s) for the ambient temperature.

If simulating heat storage in the walls is not required, OLGA can allow for applying steady-state heat transfer calculations in the walls during transient simulation of the fluid flow, or simply using an overall heat transfer coefficient (U-value) between the fluid and the ambient.

The two-dimensional heat transfer uses a two-dimensional temperature field around flow paths to simulate complex heat transfer configurations more accurately, as in the case of buried pipelines and complex risers. OLGA provides a module that models this explicitly called FEMTherm.

Using FEMTherm, a user can build a two-dimensional triangular mesh representing a cross section of the solid medium around a flow path- denoted in OLGA as a solid bundle-, and the temperature distribution in the cross section is calculated using a Finite Element Method (FEM) solver. However, the temperature of the fluid inside the flow path and the temperature of the pipe wall are still computed using OLGA's default model (finite difference method), so the fluid temperature would only vary in the axial direction along the flow path. In this manner, the pipe wall's outer surface represents the boundary between the two calculation models.

### 4.3.2 Defining the Heat Transfer for the Pipelines

Since the pipeline network in the case study is going to be buried, one way to perform the temperature calculations would be considering one-dimensional heat transfer, using concentric wall layers and letting the outer layer represent the sandy-loam soil. However, in reality, the heat flow inside the soil can be far from radial, especially if the ambient air temperature is extremely high or extremely low. This is true for the case study, where the maximum ambient air temperature is +45 °C and the minimum is -43 °C. This brings the need for the other way of temperature calculations: two-dimensional heat transfer using FEMTherm.

FEMTherm will be used as the base case for heat transfer calculations around the pipeline network in the FA study. This requires that the temperature calculation method selected is either WALL or FASTWALL. However, since FASTWALL neglects heat storage in the wall, it is not suitable for transient simulations. The one-dimensional method will be used in a few cases only for comparison with the results from FEMTherm. In this case, the WALL calculation method will also be used because of the large thermal mass of the soil.

A square solid bundle with a side length of 2.28 m was created to accommodate the grid. This length corresponds to a depth where temperature measurements are available on a monthly basis as shown in Fig. 17. The top side of the shape represents the soil surface level, and the pipeline is buried at a depth of 1.8 m to bottom of pipe. Fig. 31 shows the

created solid bundles around the trunk-line (left) and one of the flowlines (right) at their base case, as displayed in OLGA.

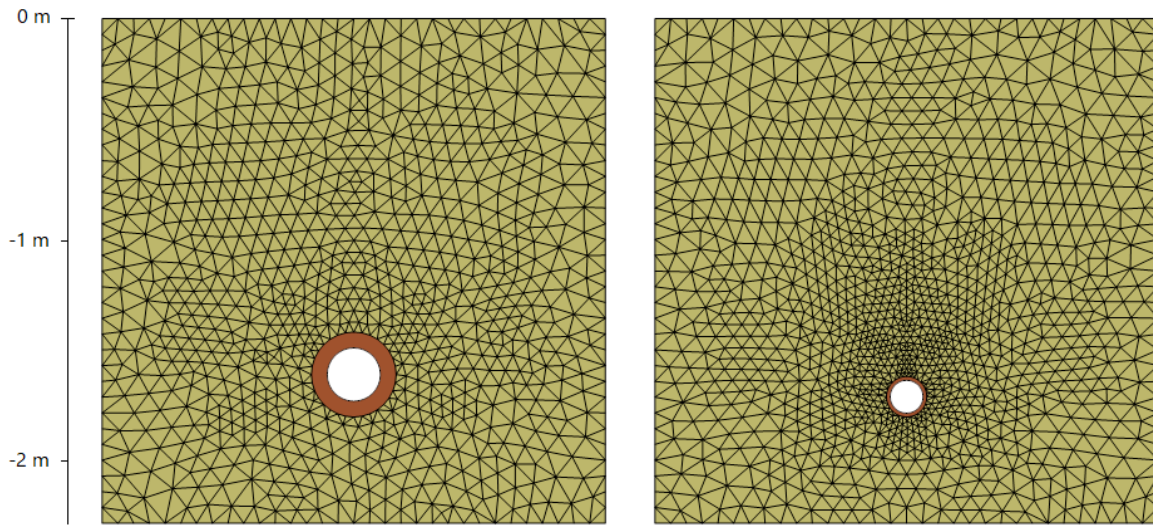


Fig. 31 – Solid bundles around the trunk-line (left) and a flowline (right)

The mesh fineness of the solid bundle is determined by the number of the nodes on the component of the largest circumference. OLGA states that the typical value of mesh fineness, rounded to multiples of 32, is between 128 and 640, and strongly advises that the number of internal nodes between external boundaries is not below 4 to assure numerical accuracy of the temperature distribution [6].

A mesh fineness of 128 was chosen, representing the number of nodes on the circumference of the square shape in this case. The corresponding number of internal nodes between the external boundary of the pipe wall and the closest solid bundle’s boundary (bottom boundary) is 5 in the case of the trunk-line and 9 in the case of the flowline, which satisfies the criteria for spatial discretization.

The temperature calculations with FEMTherm are CPU intensive, thus they are not performed at each time-step in OLGA. A fixed time-step is defined to solve for the temperature distribution in the solid bundle, unlike the temperature calculations for the fluid and the pipe wall, where time-step control can be applied to adjust the step-size according to different criteria.

OLGA recommends that the time-step in FEMTherm should be below the smallest characteristic time-constant in the simulation case [6]. This time constant (TC) is calculated for all the pipe wall layers in the case, and the time-step in FEMTherm should be set to a value below the smallest time-constant calculated, where:

$$TC = \frac{1}{2} \frac{\rho c_p}{\lambda} L^2 \dots\dots\dots (7)$$



Where TC is the time constant [s],  $\rho$  is the layer's density [ $\text{kg}/\text{m}^3$ ],  $C_p$  is the layer's specific heat capacity [ $\text{J}/\text{kg}\cdot\text{K}$ ],  $\lambda$  is the layer's thermal conductivity [ $\text{W}/\text{m}\cdot\text{K}$ ], and L is the layer's thickness [m].

This was done for all the possible layers in the case study and the results are listed in Table 16. A time-step of 5 seconds will be used in FEMTherm for simulating the base case of the pipeline network, which includes the layers 01, 06, 09, and 18; thus satisfying the criteria for temporal discretization.

Table 16 – FEMTherm time constant of different layers

#	Layer	$\rho$ [ $\text{kg}/\text{m}^3$ ]	$C_p$ [ $\text{J}/\text{kg}\cdot\text{K}$ ]	$\lambda$ [ $\text{W}/\text{m}\cdot\text{K}$ ]	L [m] (inch)	T [s]
01	CS (10 3/4" pipe)	7850	500	50.000	0.016 (0.625)	9.9
02	CS (8 5/8" pipe)	7850	500	50.000	0.014 (0.562)	8.0
03	CS (6 5/8" pipe)	7850	500	50.000	0.013 (0.500)	6.3
04	CS (5 9/16" pipe)	7850	500	50.000	0.013 (0.500)	6.3
05	CS (4 1/2" pipe)	7850	500	50.000	0.011 (0.438)	4.9
06	GRE (6" pipe)	2000	900	0.400	0.018 (0.690)	691.1
07	PUR (1.17" insulation)	30	1500	0.025	0.030 (1.170)	794.8
08	PUR (1.75" insulation)	30	1500	0.025	0.044 (1.750)	1778.2
09	PUR (2" insulation)	30	1500	0.025	0.051 (2.000)	2322.6
10	PUR (2.05" insulation)	30	1500	0.025	0.052 (2.050)	2440.2
11	PUR (2.43" insulation)	30	1500	0.025	0.062 (2.430)	3428.6
12	PUR (3.19" insulation)	30	1500	0.025	0.081 (3.190)	5908.7
13	HDPE (0.13" casing)	940	2400	0.440	0.003 (0.130)	28.0
14	HDPE (0.14" casing)	940	2400	0.440	0.004 (0.140)	32.4
15	HDPE (0.15" casing)	940	2400	0.440	0.004 (0.150)	37.2
16	HDPE (0.16" casing)	940	2400	0.440	0.004 (0.160)	42.3
17	HDPE (0.18" casing)	940	2400	0.440	0.005 (0.180)	53.6
18	HDPE (0.19" casing)	940	2400	0.440	0.005 (0.190)	59.7

For the definition of the ambient conditions in the case study, the heat transfer coefficient between the soil surface and the ambience is calculated by OLGA based on user-given values for the ambient temperature and air velocity. The temperature at the lower boundary of the solid bundle is also given, and below this level the temperature is assumed to be constant. No heat flux is assumed to take place across the vertical boundaries of the solid bundle.

Different ambient conditions are considered for running the FA study. Four different scenarios are defined: winter design conditions (WD), summer design conditions (SD), winter average conditions (WA), and summer average conditions (SA). Table 17 lists the ambient conditions for the four cases based on the data given in the basis of design in 3.3.

Most of the FA study cases will be run at the WD conditions, and only a few cases will be run using other ambient conditions. When one-dimensional heat transfer is considered for comparison with FEMTherm, the same ambient conditions will be used, except that the

temperature at the depth of 2.28 m will not be applicable for the definition of the heat transfer in this case.

Table 17 – FEMTherm ambient conditions

Parameter	WD	SD	WA	SA
Ambient temperature [°C]	-43.0	45.0	-14.8	29.9
Wind velocity [m/s]	25.0	25.0	4.0*	4.0*
Temperature at -2.28 m [°C]	0.8	9.0	0.8	9.0

\*OLGA's default value for ambient air velocity

### 4.3.3 Defining the Heat Transfer for the Wells

Considering the wells in the simulation model, where radially symmetrical heat transfer is expected to take place, it is sufficient to use OLGA's default one-dimensional heat transfer calculations. In this case, the formations surrounding the well represent the ambient environment, and the ambient temperature along the well path is represented by the local geothermal gradient.

Four geothermal gradients were created to examine the effect of the different ambient conditions at the surface as mentioned in Table 17 on the upper part of the geothermal gradient. The gradients would only differ above the depth of 25 m, where the temperature was measured to be 8 °C throughout the year, as mentioned in 3.3.

The geothermal gradients were created using the well editor as part of the well model that was described in 4.2.4. A series of temperature values versus depths were input, each case at a time, to define the ambient conditions as in Table 18. The top points can also be seen in the left part of Fig. 32.

Table 18 – Input to ambient conditions in the well editor

TVD [m]	Temperature [°C]			
	WD	WA	SD	SA
0.00	-43.0	-14.8	29.9	45.0
2.28	0.8	0.8	9.0	9.0
25.00	8.0	8.0	8.0	8.0
4361.69	94.5	94.5	94.5	94.5

After the rest of the well data are input to the well editor, and to finally generate the well model, OLGA discretizes the well path into different pipes, and the pipes into sections. The geothermal gradient on the boundaries of the well is then by default reported section-wise, where one value of temperature is assigned to the mid-point of a section. A mean heat transfer coefficient of 500 W/m<sup>2</sup>·K was introduced by OLGA upon the generation of the well model on the outer wall surface along the well path, and its value was kept unchanged.

The top part of the created geothermal gradients can be seen in the middle part of Fig. 32, where the effect of discretization can be examined. It is observed that the two gradients

representing the winter conditions are identical, even though the input temperatures at the surface are different. The same thing applies to the ones representing the summer conditions. This shows that OLGA, in this setting, did not account for the input temperature at the surface in calculating the geothermal gradient for the top section of the well path, which represents here the top ~12 m of the well.

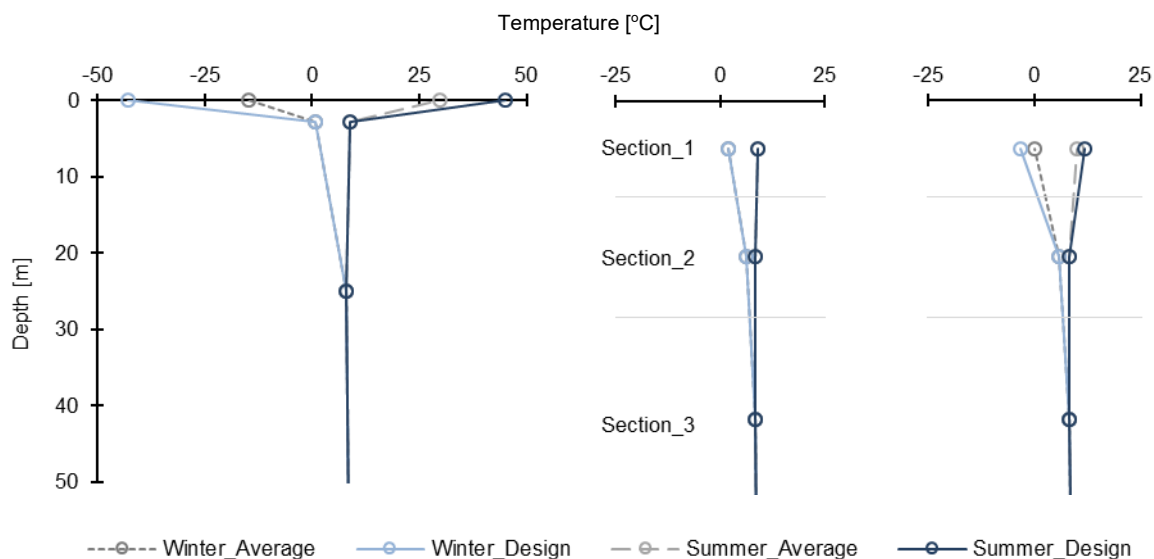


Fig. 32 – Geothermal gradients: before discretization (left), after discretization (middle), and after manual editing (right)

A side task was performed where the temperature at the surface was varied to even a higher extent compared to the lower points and the geothermal gradient was checked, but the output values were still the same. The temperature at the second top point at 2.28 m was then slightly changed, and the output values were found to have changed accordingly.

To overcome this, the temperature values for Section\_1 were manually edited by calculating a weighted average temperature at the section for each case that considers the two local gradients inside the section, and the result is shown in the right part of Fig. 32. It can be eventually seen that the variations in temperature at the top 2.28 meters did not affect the average temperature of the top section significantly. The largest shift took place for the WD case, where the manually edited temperature went down by 5 °C compared to the one from OLGA.

This difference in the geothermal gradients is not expected to have a noticeable effect on the temperature of the fluid flowing out of the well at relatively high flowrates. However, it will be still accounted for while running the cases in different ambient conditions, especially in the cases of cooldown and turndown at WD conditions.



## 5 Simulation Work

This chapter discusses the simulation of the different tasks of the FA study of the GCF. It presents the objective of each task, gives a description of the simulation setup, and presents the results of the simulation runs. The FA study aims at achieving the following objectives:

- Confirming the line sizes estimated in the Basis of Design and determining other possible line sizes based on the pipeline pressure rating of 100 barg. [5.1]
- Determining the pressures, temperatures, velocities, liquid hold-up, and flow regimes in the pipeline branches based on the production profiles. [5.2]
- Defining the predominant flow regimes and the liquid hold-ups in the flowlines and the trunk-line at different turndown rates and determining the minimum stable flowrate (MSFR) into the slug catcher. [5.3]
- Estimating the methanol injection rates that are required to avoid hydrate formation in the pipeline network during production (active inhibition). [5.4]
- Estimating the methanol injection rates that would allow for the required no-touch time of 6 hours that is set by the operator (shut-in scenario). [5.5]
- Determining the required flowline insulation thickness that could prevent hydrate and/or wax formation during production (passive inhibition). [5.6]
- Determining the flowline insulation thickness that would allow for the required no-touch time of 6 hours that is set by the operator (shut-in scenario). [5.7]
- Determining the proper flowrate ramp-up from turndown rates to the design rate and examining the related slugging characteristics and liquid handling capabilities. [5.8]
- Determining proper pigging velocities for the flowlines and the trunk-line that would avoid surging the slug catcher and examining the related slugging characteristics and liquid handling capabilities. [5.9]
- Estimating the time required to reach the pipeline and equipment design pressure of 100 barg during a process shutdown at the slug catcher (packing analysis). [5.10]

In addition to achieving the objectives of the FA study, a few points will be discussed that are related to the execution of the tasks. These are:

- Explaining why the erosional velocity ratio (EVR), as calculated in OLGA, was not chosen as a criterion for pipeline size selection. [5.1.4]
- Comparing mass sources to well models in cases where both are applicable as sources of the produced fluids. [5.2.4.2]
- Comparing the solution of the network using the black-oil model for fluid properties to that of the compositional model. [5.2.4.3]
- Examining the effect of considering produced water salinity on hydrate mitigation. [5.3.4.2, 5.4.3, 5.5.3]
- Comparing the results of steady-state simulation with transient simulation at different turndown flowrates. [5.3.4.3]
- Performing methanol injection rate calculations in Excel and validating the results in OLGA. [5.4.4]

- Examining the value of using 2D heat transfer for the buried pipeline network under the extreme design ambient conditions compared to the typical 1D heat transfer. [5.6.4]

The base case of the pipeline network, as described in chapter 4, will be used to carry out the FA study. The base case description can be summarized in the following points:

- Trunk-line: 10  $\frac{3}{4}$ " CS, with 2" PUR insulation.
- Flowlines: 6" GRE, without insulation.
- Heat transfer: 2D, using FEMTherm.
- PVT model: Compositional model using lookup tables.

Fig. 33 shows the simplest look for the pipeline network in OLGA considering only the components that were described in chapter 4. More components will be added to the network in the FA study, depending on the task that needs to be executed.

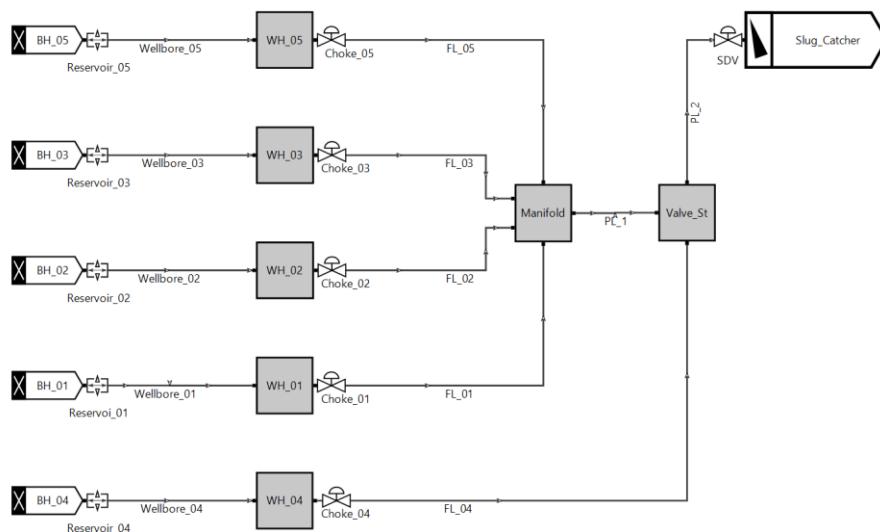


Fig. 33 – Network schematic in OLGA (base case)

## 5.1 Confirm Pipeline Sizes

### 5.1.1 Objective

The objective of this task is to confirm the line sizes estimated in the Basis of Design, and to determine other possible line sizes based on the pipeline pressure rating of 100 barg.

### 5.1.2 Setup

Different line sizes will be used to run the cases at the maximum expected flowrates from the wells as reported in Table 1. It should be noted here that the maximum values from the table were not encountered in the production profiles from the GAP model's mid-case as can be seen in Appendix F, which suggests that they might represent the flowrates from a high-case; not the maximum values of flowrates in the mid-case.

The trunk-line will be examined under two different sizes: 10 ¾" CS and 8 5/8" CS, and the flowlines will be examined under four different sizes: 6" GRE, 6 5/8" CS, 5 9/16" CS, and 4 ½" CS. The dimensions of the pipes were listed in Table 11.

Each branch will be simulated while being connected to the pipeline network, which terminates at the slug catcher, where the pressure is 45 barg and the temperature is taken as 30 °C. As mentioned in 3.1.1, due to restrictions set by the neighboring processing facility, the maximum allowable gas flowrate from the GCF is 56.5 MMscfd. Therefore, during simulating individual flowlines at their maximum flowrates, more gas condensate will be fed into the network, either at the gathering station (PL\_1 inlet) or at the tie-in of Well\_04 to the trunk-line (PL\_2 inlet), to bring the total gas flowing in the network to 56.5 MMscfd and exert more backpressure on the branch being examined. If the pressure at the inlet of the branch reaches or exceeds the design pressure of the pipeline (100 barg), the examined size shall be disregarded. The erosional velocity ratio (EVR) will also be examined even though it will not be considered as a criterion for design, as will be discussed in 5.1.4.

The cases will be run at 26% WC and at the summer design conditions to reach the highest possible pressure values at the inlet of the branches during steady-state production, and they will be run in steady-state mode. Mass sources will be used to represent the gas condensate feed at the inlet of the branches, and the temperature of the feed will be assumed to be 45 °C at the wellheads, 40 °C at the gathering station, and 35 °C at Well\_04 tie-in location. FEMTherm will be used for the temperature calculations around the pipeline network.

### 5.1.3 Results

Table 19 shows the results of the simulation runs. Inlet pressure values of 100 barg or higher are written in **bold** between parentheses and indicate that the line size in question shall not be used for the branch under which the value is found. EVR values of 1.0 or higher are formatted similarly, but only to indicate that the fluid velocity has reached or exceeded the erosional velocity as defined in API RP-14E. A short description of the reported variables can be found in Appendix G.

Table 19 – Pressure and EVR of different branch sizes at maximum gas flowrate

10 3/4" CS								
Branch	PL_1 size [in]	PL_2 size [in]	QGST [MMscfd]	QGST <sub>tot</sub> [MMscfd]	PT <sub>in</sub> [barg]	PT <sub>out</sub> [barg]	DP [barg]	EVR <sub>max</sub> [-]
PL_2	-	10 3/4	56.5	56.5	62.4	45.0	17.4	0.7
PL_1	10 3/4	10 3/4	56.5	56.5	71.3	62.7	8.5	0.6
8 5/8" CS								
Branch	PL_1 size [in]	PL_2 size [in]	QGST [MMscfd]	QGST <sub>tot</sub> [MMscfd]	PT <sub>in</sub> [barg]	PT <sub>out</sub> [barg]	DP [barg]	EVR <sub>max</sub> [-]
PL_2	-	8 5/8	56.5	56.5	91.5	45.0	46.5	(1.1)
PL_1	8 5/8	10 3/4	56.5	56.5	89.4	62.6	26.9	0.9
PL_1	8 5/8	8 5/8	56.5	56.5	(111.9)	92.0	19.9	0.7
6" GRE								
Branch	PL_1 size [in]	PL_2 size [in]	QGST [MMscfd]	QGST <sub>tot</sub> [MMscfd]	PT <sub>in</sub> [barg]	PT <sub>out</sub> [barg]	DP [barg]	EVR <sub>max</sub> [-]
FL_01	10 3/4	10 3/4	12.0	56.5	72.6	71.3	1.3	0.3
FL_01	8 5/8	10 3/4	12.0	56.5	90.5	89.4	1.1	0.3
FL_02	10 3/4	10 3/4	12.0	56.5	75.6	71.0	4.6	0.3
FL_02	8 5/8	10 3/4	12.0	56.5	92.7	89.0	3.6	0.3
FL_03	10 3/4	10 3/4	25.0	56.5	82.6	71.2	11.3	0.6
FL_03	8 5/8	10 3/4	25.0	56.5	98.2	89.4	8.8	0.6
FL_04	-	10 3/4	40.0	56.5	72.0	63.2	8.9	(1.1)
FL_05	10 3/4	10 3/4	25.0	56.5	75.6	71.4	4.2	0.6
FL_05	8 5/8	10 3/4	25.0	56.5	92.9	89.7	3.2	0.6
6 5/8" CS								
Branch	PL_1 size [in]	PL_2 size [in]	QGST [MMscfd]	QGST <sub>tot</sub> [MMscfd]	PT <sub>in</sub> [barg]	PT <sub>out</sub> [barg]	DP [barg]	EVR <sub>max</sub> [-]
FL_01	10 3/4	10 3/4	12.0	56.5	73.3	71.4	1.9	0.3
FL_01	8 5/8	10 3/4	12.0	56.5	91.1	89.6	1.5	0.3
FL_02	10 3/4	10 3/4	12.0	56.5	78.3	71.3	7.0	0.3
FL_02	8 5/8	10 3/4	12.0	56.5	95.0	89.5	5.5	0.3
FL_03	10 3/4	10 3/4	25.0	56.5	87.7	71.4	16.3	0.7
FL_03	8 5/8	10 3/4	25.0	56.5	(102.7)	89.7	13.1	0.6
FL_04	-	10 3/4	40.0	56.5	75.0	63.2	11.8	(1.2)
FL_05	10 3/4	10 3/4	25.0	56.5	77.6	71.5	6.1	0.7
FL_05	8 5/8	10 3/4	25.0	56.5	94.6	89.7	4.8	0.6
5 9/16" CS								
Branch	PL_1 size [in]	PL_2 size [in]	QGST [MMscfd]	QGST <sub>tot</sub> [MMscfd]	PT <sub>in</sub> [barg]	PT <sub>out</sub> [barg]	DP [barg]	EVR <sub>max</sub> [-]
FL_01	10 3/4	10 3/4	12.0	56.5	77.6	71.4	6.2	0.5
FL_02	10 3/4	10 3/4	12.0	56.5	93.1	71.3	21.8	0.5
FL_03	10 3/4	10 3/4	25.0	56.5	(111.2)	71.2	40.0	(1.0)
FL_04	-	10 3/4	40.0	56.5	89.6	63.4	26.2	(1.7)
FL_05	10 3/4	10 3/4	25.0	56.5	86.9	71.4	15.5	(1.0)



4 ½" CS								
Branch	PL_1 size [in]	PL_2 size [in]	QGST [MMscfd]	QGST <sub>tot</sub> [MMscfd]	PT <sub>in</sub> [barg]	PT <sub>out</sub> [barg]	DP [barg]	EVR <sub>max</sub> [-]
FL_01	10 ¾	10 ¾	12.0	56.5	90.1	71.3	18.8	0.8
FL_02	10 ¾	10 ¾	12.0	56.5	<b>(132.3)</b>	71.1	61.1	0.8
FL_04	-	10 ¾	40.0	56.5	<b>(122.7)</b>	63.8	58.9	<b>(2.7)</b>
FL_05	10 ¾	10 ¾	25.0	56.5	<b>(108.2)</b>	71.3	37.0	<b>(1.6)</b>

For the trunk-line, the 10 ¾" CS pipe results in inlet pressures considerably below 100 barg; 71 barg at the inlet of the first part (PL\_1) and 62 barg at the inlet of the second part (PL\_2), and therefore is confirmed as being a suitable choice. The smaller size of 8 5/8", on the other hand, cannot be used for the whole trunk-line because the inlet pressure in this case exceeds the design pressure as it reaches 112 barg. However, if it is only used for PL\_1 while PL\_2 is kept at 10 ¾", the inlet pressure becomes 89 barg and it can be considered for further analysis while running the rest of the cases.

For the flowlines, the 6" GRE is confirmed to be a suitable size, especially while considering 10 ¾" CS for the whole trunk-line. When PL\_1 is taken as 8 5/8" CS, the inlet pressure at the flowlines ranges from 91 barg in FL\_01 to 98 barg in FL\_03, which is close to design pressure. The same applies to the 6 5/8" CS pipe, except that the inlet pressure of FL\_3 exceeds the design pressure when the 8 5/8" CS pipe is chosen for PL\_1. This eliminates the 8 5/8" CS for PL\_1 from further analysis as smaller sizes are considered for the flowlines.

Now, considering a trunk-line that is totally 10 ¾" CS, the 5 9/16" CS works for all the flowlines except for FL\_03, where the expected inlet pressure is 111 barg, while the 4 ½" CS works only for FL\_01.

Table 20 lists the different combinations of line sizes that can be used for the network branches. If consistency within the trunk-line parts and the flowlines is required, 10 ¾" CS would be chosen for the trunk-line, and either 6" GRE or 6 5/8" CS would be chosen for the flowlines.

Table 20 – Possible combinations of network line sizes

Branch	#1	#2
PL_2	10 ¾" CS	10 ¾" CS
PL_1	10 ¾" CS	8 5/8" CS
FL_01	6" GRE, 6 5/8" CS, 5 9/16" CS, 4 1/2" CS	6" GRE, 6 5/8" CS
FL_02	6" GRE, 6 5/8" CS, 5 9/16" CS	6" GRE, 6 5/8" CS
FL_03	6" GRE, 6 5/8" CS	6" GRE
FL_04	6" GRE, 6 5/8" CS, 5 9/16" CS	6" GRE, 6 5/8" CS
FL_05	6" GRE, 6 5/8" CS, 5 9/16" CS	6" GRE, 6 5/8" CS

### 5.1.4 Discussion: Erosional Velocity Ratio (EVR)

The erosional velocity ratio (EVR) is defined in OLGA as [6]:

$$EVR = U_{ACTUAL}/U_{EROSIONAL} \dots\dots\dots (8)$$

$$U_{ACTUAL} = |USG| + |USL| + |USD| \dots\dots\dots (9)$$

$$U_{EROSIONAL} = c/\sqrt{\rho_{MIX}} \dots\dots\dots (10)$$

$$\rho_{MIX} = [\rho_G|USG| + \rho_L(|USL| + |USD|)]/(|USG| + |USL| + |USD|) \dots\dots\dots (11)$$

Where EVR is the erosional velocity ratio [-],  $U_{ACTUAL}$  is the actual mixture velocity [ft/s],  $U_{EROSIONAL}$  is the erosional velocity [ft/s],  $USG$  is the superficial velocity for gas [ft/s],  $USL$  is the superficial velocity for liquid film [ft/s],  $USD$  is the superficial velocity for liquid droplets [ft/s],  $\rho_{MIX}$  is the mixture density at flowing pressure and temperature [lb/ft<sup>3</sup>],  $\rho_G$  is the gas density [lb/ft<sup>3</sup>],  $\rho_L$  is the liquid density [lb/ft<sup>3</sup>], and  $c$  is an empirical constant that is equal to 100 lb<sup>1/2</sup>/s·ft<sup>1/2</sup> for velocities in ft/s and densities in lb/ft<sup>3</sup>, or 122 kg<sup>1/2</sup>/s·m<sup>1/2</sup> for velocities in m/s and densities in kg/m<sup>3</sup>.

This definition is based on the API RP-14E; the Recommended Practice for Design and Installation of Offshore Production Platform Sizing Systems and has been widely used in the oil and gas industry in the last 40 years. Under its section that describes the sizing criteria for gas/liquid two-phase lines, the API RP-14E recommends that the velocity of a fluid mixture flowing in a pipe should be maintained below the erosional velocity, as defined in Eq. 10, when there is no specific information available about the erosive or corrosive properties of the fluid [34].

API RP-14E states that for solid-free fluids, using a value of 100 for the empirical constant  $c$  during continuous service is considered conservative, and that values of 150 to 200 could be used for such fluids when corrosion is either unanticipated, or mitigated by corrosion inhibitors or by using corrosion resistant alloys (CRAs). Higher values of  $c$  could be used for intermittent service. On the other hand, if solid production is expected, then fluid velocities should be significantly reduced.

The erosional velocity equation is easy to apply and requires only little input, which explains how popular it is, but for the same reason it becomes an oversimplification that does not explain how it could take into account scenarios that cover multi-phase flow with and without solid production, corrosion inhibition, and the application of CRAs. The origin of the equation itself is subject of controversy and many have questioned the validity of its use [12].

The API RP-14E equation was assessed in the literature and was found to have underpredicted the erosional velocity in some cases and overpredicted it in other cases. Some producers had to adopt modified versions of the equation with values of  $c$  factors other than those in the RP, and other producers quit using the equation and switched to other models for predicting the erosional velocity [12].

Because of that, in this task 5.1, while the EVR was calculated by OLGA using the default value of  $c = 100$  and was reported in the results as required by the operator, it was not considered as a basis of design for the line sizes. For example, the 5 9/16" CS pipe was considered a valid choice for FL\_04 because the inlet pressure was well below the design pressure at the maximum flowrate while the EVR was 1.7, meaning that the actual fluid velocity in the pipe is 1.7 times the calculated erosional velocity using the API RP-14E equation.

## 5.2 Pipeline Parameters Based on Production Profiles

### 5.2.1 Objective

The objective of this task is to determine the pressure, temperature, velocity, liquid hold-up, and flow regimes in the pipeline based on the production profiles.

### 5.2.2 Setup

As discussed in 4.1.3, six different points in the lifetime of the field were chosen to perform this task. Since the task intends to check the pipeline performance at these different dates and not to come up with any design parameters for the pipeline network, the task will be simulated using the summer and winter average ambient conditions (SA and WA) as defined in Table 17; not the design ambient conditions. Table 21 lists the different well gas flowrates at these points. This results in a total of 6 points x 2 ambient conditions = 12 simulation cases.

Table 21 – Well gas flowrate over time [yy/mm]

	Gas flowrate [MMscfd]					
	01/01	02/01	09/04	13/10	14/09	21/01
<b>Well_01</b>	9.2	8.1	6.5	4.9	-	-
<b>Well_02</b>	9.5	8.2	6.5	4.5	4.3	-
<b>Well_03</b>	13.7	12.1	12.1	9.2	8.9	7.0
<b>Well_04</b>	20.6	18.7	21.5	17.9	17.3	14.5
<b>Well_05</b>	-	5.9	6.5	5.4	5.2	4.5
<b>Total</b>	<b>53.0</b>	<b>53.0</b>	<b>53.0</b>	<b>41.9</b>	<b>35.7</b>	<b>25.9</b>

The decline in reservoir pressure with time as in Table 8 will be accounted for in setting up the cases along with using different C values for the IPRs of Well\_05 as listed in Table 14. Different PVT tables will be used to account for the change in the gas condensate composition starting from the point 09/04 as discussed in 4.1.3. The hydrate curves at 0 wt% methanol for both pure and saline water content as in Appendix C will be used to calculate the hydrate subcooling, and the  $C_v$  tables discussed in 4.2.3 will be used for the choke valves and the SDV.

Cases will be run using the hydrate table with the pure water only and will not be repeated using the table with saline water. Then, after extracting the results from OLGA into Excel, the difference between the hydrate formation temperature and the fluid temperature (DTHYD) at the outlet of each branch will be calculated for the cases of pure and saline water content using a lookup function.

The lookup function will search the hydrate tables in Excel for the hydrate formation temperature at the outlet pressure of a branch, then the fluid temperature at the same point will be subtracted from this value. DTHYD is positive when the fluid temperature is below the hydrate formation temperature, indicating that a hydrate phase exists, and negative when the

fluid temperature is above the hydrate formation temperature. DTHYD, as calculated by OLGA (pure water) and by Excel (pure and saline water), will be presented in the results.

Going back to Table 21, to get the target flowrate from a well, the right backpressure needs to be exerted on the well by adjusting the opening of the choke valve. Therefore, the relative openings of the different choke valves need to be determined in order to achieve the required flowrates in the table.

To do so, a transmitter is inserted upstream each of the choke valves that measures the gas flowrate, and a proportional–integral–derivative (PID) controller is set up to receive the reading from the transmitter and automatically manipulate the opening of the choke valve in order to achieve the target flowrate. Fig. 34 shows how this pipeline network in OLGA looks like.

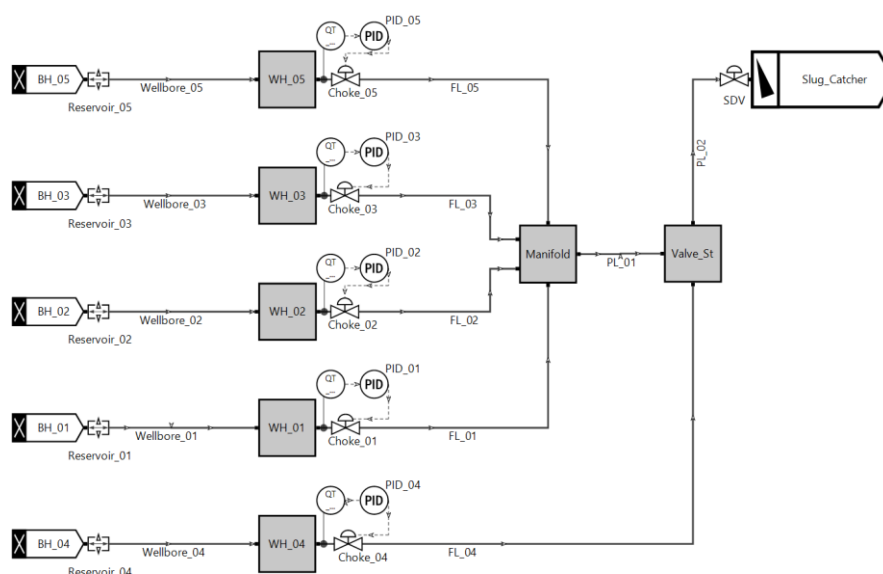


Fig. 34 – Network schematic in OLGA with well models

The PID is set up so that the time it takes to change the choke opening from completely open to completely closed or vice versa- known as the STROKETIME- is one minute. By default, the initial relative valve opening in OLGA at the beginning of a simulation run- known as the BIAS- is given a value of 0.2. That is the valve is only 20% open. The steady state pre-processor would then initialize the case by solving for the flowrates using this bias, then the PID starts to manipulate the choke openings until a steady target flowrate- the SETPOINT- is achieved. Typically, the choke opening at this point might still oscillate slightly around the setpoint depending on how the PID is set-up.

However, reaching a thermal steady-state in the system after the flowrates have been manipulated can take a very long time. To overcome this, instead of simulating a case in one run, another approach was adopted. First, cases will be run for one hour only, allowing enough time for the wells to reach their target flowrates. The choke openings at the end of the run will be recorded. Then, these choke openings will be used to initialize another six-

hour run by adjusting the bias values accordingly. Now, the pre-processor is going to solve the system for the target flowrates directly and thermal equilibrium can be achieved in a very short time.

In summary, each case will be run in transient mode for one hour using automatic PIDs to arrive to target flowrates and their related choke openings. The case will then be run again for six hours using PIDs with initial biases that are equal to the recorded choke openings from the previous run.

### 5.2.3 Results

Table 22 shows the different choke openings at the end of the first run after allowing the target flowrates to be achieved.

Table 22 – Choke openings over time (after a one-hour run)

	Relative choke opening [-]					
	01/01	02/01	09/04	13/10	14/09	21/01
Well_01	0.262	0.254	0.301	0.276	-	-
Well_02	0.268	0.261	0.332	0.279	0.277	-
Well_03	0.289	0.283	0.419	0.350	0.346	0.320
Well_04	0.325	0.333	0.450	0.406	0.394	0.374
Well_05	-	0.232	0.344	0.309	0.309	0.305

Table 23 shows the results of the runs at the point 02/01 in both winter average (WA) and summer average (SA) ambient conditions. The results of all the different points are provided in Table H.1 of Appendix H.

Temperature values that fall below WAT are marked with a **(W)** for “Wax” and formatted in **bold**. Positive DTHYD values indicating hydrate formation are formatted similarly and marked with an **(H)** for “Hydrate.” The same is done with QLT values that show fluctuations with time as a result of slugging behavior. In this case, the reported value is an average of the lowest and the highest encountered values, and it is marked with an **(S)** for “Slugging.”

The reported flow regimes (ID) are those observed in a branch regardless of how prevailing they are, and the liquid holdup (HOL) is reported as an average value for each ID in the branch. A short description of the reported variables can be found in Appendix G.

Table 23 – Pipeline parameters at 02/01

02/01_WA							
Branch	QGST [MMscfd]	PT <sub>in</sub> [barg]	PT <sub>out</sub> [barg]	DP [barg]	TM <sub>in</sub> [°C]	TM <sub>out</sub> [°C]	DTHYD <sub>out</sub> OP [°C]
PL_2	52.9	56.8	45.0	11.8	25.2	20.2	-4.1
PL_1	34.2	59.1	56.8	2.3	17.8	<b>(W) 16.2</b>	<b>(H) 1.4</b>
FL_01	8.0	59.8	59.1	0.6	33.5	22.0	-4.2
FL_02	8.2	61.3	59.1	2.1	34.5	<b>(W) 4.8</b>	<b>(H) 13.0</b>

FL_03	12.1	61.4	59.1	2.2	40.1	23.3	-5.5
FL_04	18.7	58.5	56.9	1.7	45.5	41.5	-24.0
FL_05	5.8	59.5	59.1	0.4	27.9	19.1	-1.3
Branch	ID [-]	HOL <sub>avg</sub> [-]	LIQC [bbl]	QLT <sub>out</sub> [bbl/day]	EVR <sub>max</sub> [-]	UG <sub>max</sub> [m/s]	UL <sub>max</sub> [m/s]
PL_2	1, 3	0.168, 0.106	449	12,968	0.55	7.6	5.0
PL_1	1	0.210	360	8,837	0.31	4.1	2.6
FL_01	1, 3	0.229, 0.282	54	2,057	0.20	2.7	2.0
FL_02	1, 3	0.236, 0.311	235	2,224	0.20	2.6	2.0
FL_03	1, 3	0.191, 0.225	86	3,086	0.29	3.7	2.3
FL_04	1	0.170	19	4,480	0.48	6.1	3.3
FL_05	1, 3	0.274, 0.346	42	1,495	0.14	2.4	1.8

## 02/01\_SA

Branch	QGST [MMscfd]	PT <sub>in</sub> [barg]	PT <sub>out</sub> [barg]	DP [barg]	TM <sub>in</sub> [°C]	TM <sub>out</sub> [°C]	DTHYD <sub>out</sub> OP [°C]
PL_2	52.9	57.3	45.0	12.3	31.0	26.6	-10.5
PL_1	34.2	59.7	57.3	2.4	25.6	24.4	-6.8
FL_01	8.0	60.4	59.7	0.6	33.9	27.5	-9.7
FL_02	8.2	61.9	59.7	2.2	34.9	18.2	-0.3
FL_03	12.1	62.0	59.7	2.3	40.4	30.0	-12.1
FL_04	18.7	59.0	57.4	1.7	45.7	43.0	-25.4
FL_05	5.8	60.1	59.7	0.4	28.3	24.2	-6.3
Branch	ID [-]	HOL <sub>avg</sub> [-]	LIQC [bbl]	QLT <sub>out</sub> [bbl/day]	EVR <sub>max</sub> [-]	UG <sub>max</sub> [m/s]	UL <sub>max</sub> [m/s]
PL_2	1, 3	0.162, 0.101	432	12,712	0.56	7.9	5.2
PL_1	1	0.201	340	8,647	0.31	4.2	2.6
FL_01	1, 3	0.225, 0.275	53	2,026	0.19	2.7	2.0
FL_02	1, 3	0.223, 0.288	222	2,129	0.19	2.7	2.0
FL_03	1, 3	0.187, 0.217	84	3,029	0.29	3.7	2.3
FL_04	1	0.170	19	4,469	0.48	6.1	3.3
FL_05	1, 3	0.271, 0.338	41	1,460	0.14	2.4	1.8

## 5.2.4 Discussion

### 5.2.4.1 Considering Water Salinity

The DTHYD values reported in Table H.1 were calculated in OLGA assuming pure water content. Table 24 compares these values to the ones calculated in Excel using the lookup functions, assuming pure and saline water content. Calculations for saline water content are only performed for those points in time where liquid condensation in the reservoir is expected after the reservoir pressure drops below the dewpoint.

The table shows good consistency between the interpolation in OLGA and the interpolation in Excel with the lookup functions. Naturally, when the salt content in the produced water is accounted for, hydrate requires more subcooling in order to form compared to assuming a pure water content.

Table 24 – DTHYD calculations for pure and saline water content for different points in time

Branch	01/01_WA			01/01_SA		
	DTHYD <sub>out</sub> OP [°C]	DTHYD <sub>out</sub> EP [°C]	DTHYD <sub>out</sub> ES [°C]	DTHYD <sub>out</sub> OP [°C]	DTHYD <sub>out</sub> EP [°C]	DTHYD <sub>out</sub> ES [°C]
PL_2	-6.7	-6.8	-	-12.8	-13.0	-
PL_1	-0.7	-0.9	-	-8.9	-9.1	-
FL_01	-6.8	-7.2	-	-11.7	-12.2	-
FL_02	<b>(H) 10.9</b>	<b>(H) 10.5</b>	-	-1.7	-2.2	-
FL_03	-8.3	-8.7	-	-14.3	-14.8	-
FL_04	-25.3	-25.5	-	-26.6	-26.8	-
Branch	02/01_WA			02/01_SA		
	DTHYD <sub>out</sub> OP [°C]	DTHYD <sub>out</sub> EP [°C]	DTHYD <sub>out</sub> ES [°C]	DTHYD <sub>out</sub> OP [°C]	DTHYD <sub>out</sub> EP [°C]	DTHYD <sub>out</sub> ES [°C]
PL_2	-4.1	-4.3	-	-10.5	-10.7	-
PL_1	<b>(H) 1.4</b>	<b>(H) 1.2</b>	-	-6.8	-7.0	-
FL_01	-4.2	-4.6	-	-9.7	-10.1	-
FL_02	<b>(H) 13.0</b>	<b>(H) 12.6</b>	-	-0.3	-0.8	-
FL_03	-5.5	-5.9	-	-12.1	-12.6	-
FL_04	-24.0	-24.1	-	-25.4	-25.6	-
FL_05	-1.3	-1.7	-	-6.3	-6.8	-
Branch	09/04_WA			09/04_SA		
	DTHYD <sub>out</sub> OP [°C]	DTHYD <sub>out</sub> EP [°C]	DTHYD <sub>out</sub> ES [°C]	DTHYD <sub>out</sub> OP [°C]	DTHYD <sub>out</sub> EP [°C]	DTHYD <sub>out</sub> ES [°C]
PL_2	-1.7	-2.0	-14.9	-8.5	-8.7	-21.6
PL_1	<b>(H) 3.0</b>	<b>(H) 2.2</b>	-10.1	-6.3	-7.0	-19.4
FL_01	<b>(H) 1.1</b>	<b>(H) 0.8</b>	-12.2	-6.3	-6.6	-19.6
FL_02	<b>(H) 17.2</b>	<b>(H) 17.0</b>	<b>(H) 4.0</b>	<b>(H) 1.9</b>	<b>(H) 1.6</b>	-11.4
FL_03	-3.3	-3.5	-16.5	-10.7	-11.0	-24.0
FL_04	-17.8	-18.6	-30.9	-19.3	-20.1	-32.4
FL_05	-5.5	-5.7	-18.7	-10.7	-11.0	-24.0
Branch	13/10_WA			13/10_SA		
	DTHYD <sub>out</sub> OP [°C]	DTHYD <sub>out</sub> EP [°C]	DTHYD <sub>out</sub> ES [°C]	DTHYD <sub>out</sub> OP [°C]	DTHYD <sub>out</sub> EP [°C]	DTHYD <sub>out</sub> ES [°C]
PL_2	<b>(H) 1.8</b>	<b>(H) 1.5</b>	-11.4	-6.1	-6.4	-19.3
PL_1	<b>(H) 8.2</b>	<b>(H) 7.9</b>	-5.0	-2.7	-3.0	-15.9
FL_01	<b>(H) 7.7</b>	<b>(H) 7.3</b>	-5.6	-1.7	-2.1	-15.1
FL_02	<b>(H) 19.5</b>	<b>(H) 19.1</b>	<b>(H) 6.2</b>	<b>(H) 3.0</b>	<b>(H) 2.6</b>	-10.4
FL_03	<b>(H) 3.7</b>	<b>(H) 3.3</b>	-9.7	-5.7	-6.2	-19.1
FL_04	-14.4	-14.7	-27.6	-16.2	-16.5	-29.5
FL_05	<b>(H) 0.2</b>	-0.2	-13.2	-6.2	-6.7	-19.6
Branch	14/09_WA			14/09_SA		
	DTHYD <sub>out</sub> OP [°C]	DTHYD <sub>out</sub> EP [°C]	DTHYD <sub>out</sub> ES [°C]	DTHYD <sub>out</sub> OP [°C]	DTHYD <sub>out</sub> EP [°C]	DTHYD <sub>out</sub> ES [°C]
PL_2	<b>(H) 1.1</b>	<b>(H) 0.8</b>	-12.1	-6.7	-7.1	-20.0
PL_1	<b>(H) 8.6</b>	<b>(H) 7.7</b>	-4.5	-2.7	-3.6	-15.8



<b>FL_02</b>	<b>(H) 19.5</b>	<b>(H) 19.3</b>	<b>(H) 6.3</b>	<b>(H) 2.9</b>	<b>(H) 2.6</b>	-10.3
<b>FL_03</b>	<b>(H) 4.6</b>	<b>(H) 4.4</b>	-8.6	-5.1	-5.4	-18.3
<b>FL_04</b>	-13.7	-14.6	-26.7	-15.6	-16.5	-28.7
<b>FL_05</b>	<b>(H) 0.8</b>	<b>(H) 0.5</b>	-12.4	-5.9	-6.1	-19.1
	<b>21/01_WA</b>			<b>21/01_SA</b>		
<b>Branch</b>	<b>DTHYD<sub>out</sub> OP [°C]</b>	<b>DTHYD<sub>out</sub> EP [°C]</b>	<b>DTHYD<sub>out</sub> ES [°C]</b>	<b>DTHYD<sub>out</sub> OP [°C]</b>	<b>DTHYD<sub>out</sub> EP [°C]</b>	<b>DTHYD<sub>out</sub> ES [°C]</b>
<b>PL_2</b>	<b>(H) 1.6</b>	<b>(H) 1.2</b>	-11.7	-6.4	-6.8	-19.7
<b>PL_1</b>	<b>(H) 9.6</b>	<b>(H) 8.9</b>	-4.0	-1.8	-2.5	-15.4
<b>FL_03</b>	<b>(H) 9.2</b>	<b>(H) 8.4</b>	-3.8	-2.2	-3.0	-15.2
<b>FL_04</b>	-11.5	-12.2	-25.1	-13.8	-14.5	-27.4
<b>FL_05</b>	<b>(H) 3.9</b>	<b>(H) 3.0</b>	-9.1	-3.7	-4.5	-16.7

#### 5.2.4.2 Well Models vs Mass Sources

A few FA studies were reviewed at the preparation phase for this study; all of which used mass nodes or mass sources to simulate the feed of the produced fluids to the pipeline(s). The use of mass nodes/sources was not explicitly reported in the FA studies, but they all assumed some values for temperatures at the inlet of the pipeline branch(es), which implies the use of mass nodes/sources.

The way the inlet temperatures were assumed was mostly inaccurate; as in assuming a constant inlet temperature for all values of flowrate or assuming the inlet temperature at flowing conditions to be the same as the ambient temperature. While this might be sufficient to calculate the pipeline inlet pressures, for example, it cannot be relied on in the prediction of hydrate and wax formation that is highly sensitive to temperature. It was only in a few cases that more work was done in attempt to arrive at values that are more accurate.

In this FA study, it was initially intended to use the typical mass sources to simulate the feed of the gas condensate to the system at wellheads during steady-state production instead of using the well models as part of the FA cases. The motive behind that was to reduce the runtime of the cases compared to integrating the well models that continuously need to solve for the IPRs and the fluid flow in wellbores, but only if accurate pipeline inlet conditions could be used to define the mass sources.

The way this was expected to work is as follows: the well model is used in a separate case to come up with the wellhead pressures (WHP) and temperatures (WHT) that correspond to the target steady-state flowrates that need to be simulated, the WHTs are used in the simulation model of the pipeline network along with the values of the flowrates to define the mass sources at the wellheads, chokes are inserted downstream the mass sources to calculate the pressure drops across the choke and achieve realistic temperatures downstream the chokes, while the choke openings are manipulated by PIDs that aim to maintain the pressures upstream the chokes at the WHP values from the well models. Fig. 35 shows how this pipeline network looks like in OLGA.

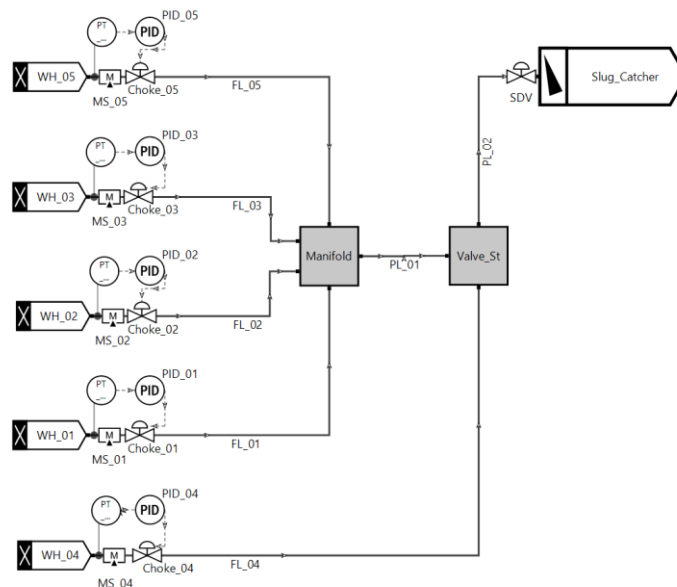


Fig. 35 – Network schematic in OLGA with mass sources (MS)

The well model was used to determine the wellhead conditions at the flowrates in Table 21 and the results are listed in Table 25. These conditions were then used to set up the cases in this task.

Table 25 – Wellhead conditions over time

Date	Well_01		Well_02		Well_03		Well_04		Well_05	
	WHP [barg]	WHT [°C]	WHP [barg]	WHT [°C]	WHP [barg]	WHT [°C]	WHP [barg]	WHT [°C]	WHP [barg]	WHT [°C]
01/01	187.2	54.3	175.2	54.1	205.0	61.4	207.9	66.5	-	-
02/01	175.4	51.6	166.0	51.4	190.8	58.6	191.5	64.3	162.7	45.4
09/04	85.1	39.8	74.1	39.2	84.2	46.6	92.5	50.6	69.1	39.0
13/10	77.9	33.9	74.1	32.6	80.8	43.0	87.2	47.8	69.1	35.3
14/09	-	-	73.6	31.5	79.8	42.3	86.5	47.8	67.5	34.7
21/01	-	-	-	-	75.9	38.6	82.7	46.3	65.0	31.5

However, upon initializing the cases, the simulation stopped because pressure values were encountered upstream the chokes that are higher than the upper limit in the PVT table, which means that OLGA cannot solve for the fluid properties at such pressures. This happened because, at the default BIAS of the choke valves of 0.2 and the given flowrates, OLGA calculated very high pressures upstream the choke valves. The solution to this is to use a higher BIAS and see when the case will successfully initialize. Note that mass sources are not pressure-driven, as in the case of well IPRs, and they will always give the flowrate assigned to them. That is why a lot of attention needs to be paid to them if they are expected to be exposed to back-pressure.

A user might be initially tempted to re-create the PVT table so that it covers fluid properties at higher pressures, but it does not guarantee that even higher pressures would not be

encountered during initialization. A good understanding of why a certain error occurs and stops the simulation is key to efficient troubleshooting.

Taking only one point in time as an example here, Table 26 lists the pressures and temperatures across the choke valves at the given flowrates of the point 02/01 at the winter average (WA) ambient conditions. The results are consistent with the wellhead conditions in Table 25 and the flowline inlet conditions in Table 23 for this point.

Table 26 – Pressures and temperatures across the choke valves at 02/01\_WA

Well	QGST [MMscfd]	WHP [barg]	PT <sub>DSC</sub> [barg]	WHT [°C]	TM <sub>DSC</sub> [°C]
Well_01	8.1	175.4	59.8	51.5	33.9
Well_02	8.2	166.0	61.3	51.2	34.9
Well_03	12.1	190.8	61.5	58.5	40.5
Well_04	18.7	191.6	58.6	64.2	45.6
Well_05	5.8	162.7	59.6	45.2	28.3

In comparison to the case run with well the models, the case with the mass sources initialized faster and the simulation time was around 80% of that of with the well models. Nevertheless, the cases with the mass sources required some prep work to come up with the wellhead conditions at the desired flowrates.

Mass sources were found to be able to simulate steady-state production to a good level of accuracy, but with prep work that requires using well models anyway. To use mass sources to simulate cases like ramp-ups and pipeline packing, for example, will require the sources to be manipulated manually, which is counter-intuitive because it is required to find out how the sources will react to backpressure in such cases; not to assume how they will do that. They will not be able to capture such events as accurately as pressure-driven sources, and therefore only well models will be used for such cases.

### 5.2.4.3 Black-oil Model vs Compositional Model

Although it was already established that the black-oil model for fluid properties is not suitable for modelling gas condensate or volatile oils, as was mentioned in 4.1.1, it was still of interest to briefly look into how the solution of the pipeline network would differ from that with the compositional model. The case at 02/01 and winter average conditions (WA) was run using black-oil model, and the results were compared to those in Table 22.

A black-oil feed was created in OLGA that consists of an oil component and a gas component. No water production takes place at this point, and the volume of condensed water along the flow paths is insignificant compared to the whole produced stream, so no water component was created. The properties of the oil and the gas at standard conditions from Table B.7 in Appendix B were used to define the oil and gas components, and the default black-oil correlation in OLGA (Lasater) was used to calculate the fluid properties during the run.

Table 27 shows the pipeline parameters at 02/01 with the black-oil model. A few variables were picked to compare the results of the run to those with the compositional model. The values of the variables from the compositional model simulation are subtracted from those of the black-oil and the differences are included in parentheses in the table.

Table 27 – Pipeline parameters at 02/01 (black-oil), and the differences between black-oil and compositional model solutions

02/01_WA							
Branch	QGST [MMscfd]	PT <sub>in</sub> [barg]	DP [barg]	TM <sub>in</sub> [°C]	TM <sub>out</sub> [°C]	LIQC [bbl]	QLT <sub>out</sub> [bbl/day]
PL_2	53.1 (0.1)	57.9 (1.1)	12.9 (1.1)	18.0 (-7.1)	<b>(W) 11.0</b> (-9.2)	351 (-99)	9,831 (-3,137)
PL_1	34.4 (0.1)	60.6 (1.5)	2.7 (0.4)	<b>(W) 12.1</b> (-5.8)	<b>(W) 10.6</b> (-5.6)	288 (-71)	6,596 (-2,241)
FL_01	8.1 (0.0)	61.3 (1.5)	0.7 (0.1)	29.1 (-4.5)	<b>(W) 15.6</b> (-6.4)	45 (-9)	1,566 (-491)
FL_02	8.2 (0.0)	63.0 (1.7)	2.4 (0.3)	31.3 (-3.3)	<b>(W) 4.2</b> (-0.6)	192 (-43)	1,585 (-639)
FL_03	12.2 (0.0)	63.2 (1.8)	2.6 (0.3)	36.7 (-3.4)	<b>(W) 16.5</b> (-6.8)	71 (-15)	2,356 (-730)
FL_04	18.8 (0.0)	59.7 (1.2)	1.8 (0.1)	39.2 (-6.2)	36.4 (-5.2)	15 (-3)	3,642 (-838)
FL_05	5.9 (0.0)	61.0 (1.5)	0.4 (0.0)	22.0 (-5.9)	<b>(W) 13.0</b> (-6.1)	35 (-7)	1,136 (-359)

The first difference that can be observed immediately is that in the liquid flowrates between the two models, and hence in the related liquid contents of the branches. The black-oil model calculated liquid flowrates that are 25% lower on average than those in the compositional model under the in-situ conditions in the pipeline. Note that the total gas flowrate running in the network in both cases is ~53 MMscfd at the same GOR, which means the oil flowrates at the standard conditions are still the same in both cases.

Since more gas is running in the network with the black-oil model under in-situ conditions, the temperature profile in the network is lower than that in the compositional model due to the low specific heat capacity of the gas.

Using the black-oil model in this FA study, for which it is not intended, would result in separator sizes and/or drain rates that are insufficient to handle the actual liquid flowrates in the network, and in hydrate inhibition requirements that are higher than necessary.

## 5.3 Turndown Rates

### 5.3.1 Objective

The objective of this task is to define the predominant flow regimes and the liquid hold-ups in the flowlines and the trunk-line at different turndown rates, and to determine the minimum stable flowrate (MSFR) into the slug catcher.

### 5.3.2 Setup

As mentioned in 4.1.3, the point 02/01 will be chosen as the base case where the FA simulations will be done. In this task, the pipeline parameters will be checked at flowrates that are equal to 20%, 40%, 60%, 80% and 100% of the values at the production plateau. Cases will be run considering two scenarios: 0% WC, and 26% WC. At 26% WC, the GCR will be producing 500 Sm<sup>3</sup>/day of water at the production plateau, which is the maximum water handling capacity of the facilities. The cases will be run at the winter design ambient conditions (WD), which is the most critical condition for hydrate and wax formation, as well as liquid condensation that can promote slugging.

Table 28 lists the different gas turndown flowrates including the values at 100% of the production plateau flowrate. This results in a total of 5 turndown flowrates x 2 WCs = 10 simulation cases.

Table 28 – Gas turndown flowrates

	Gas flowrate [MMscfd]				
	100%	80%	60%	40%	20%
<b>Well_01</b>	8.1	6.4	4.8	3.2	1.6
<b>Well_02</b>	8.2	6.6	4.9	3.3	1.6
<b>Well_03</b>	12.1	9.7	7.3	4.9	2.4
<b>Well_04</b>	18.7	15.0	11.2	7.5	3.7
<b>Well_05</b>	5.9	4.7	3.5	2.3	1.2
<b>Total</b>	<b>53.0</b>	<b>42.4</b>	<b>31.8</b>	<b>21.2</b>	<b>10.6</b>

Note that the flowrate at the production plateau in this FA study will also be referred to as the “design flowrate”, or the “100% turndown flowrate” as in Table 28, even though it does not represent a decline from another reference flowrate. The turndown percentage here, as in 60% for example, does not mean the flowrate has been reduced by 60%; it means the flowrate is 60% of the design flowrate.

As in the previous task 5.2, each case will be run first in transient mode for one hour using automatic PIDs to arrive to target flowrates and their related choke openings. The PID can still be allowed to run automatically in the second run to make sure the target rate is continuously achieved with great accuracy, or it can be frozen in the second run at the opening that was recorded at the end of the previous run. This recorded opening might not achieve the target flowrates in Table 28 to the same exact decimal digit because it is just a snapshot of the choke opening as it oscillates slightly around the setpoint.

However, since achieving the flowrates in Table 28 to a great accuracy is not critical, and what actually matters is to describe the pipeline performance at a number of varying flowrates, it was decided to keep the PID frozen in the second run. This is expected to save the time required for the PID calculations, and to avoid any small fluctuations in the flowrate and the rest of the pipeline parameters that might be caused by the slightly oscillating choke opening, allowing to focus only on those changes that are related to the flow regimes.

The fact that the PID was decided to be frozen and the choke opening to be fixed during the second simulation run, which means there is no transient event to be simulated that we know of yet, makes the run a candidate for steady-state simulation as well and might eliminate the need to execute it in transient mode. An ideal approach here would be to perform the second run in steady-state, and only repeat a case in transient mode if the steady-state pre-processor fails to converge or if an event best captured by transient simulation, like slug flow for example, is observed in the results and motivates the user to get a closer look into it. This is highly expected in this task, where the flowrate will be turned down and the probability of slug flow to take place will increase.

However, since this thesis does not only aim to perform the FA study, but also to assess the different methods of running a certain a case and to compare the results of these methods, the second run was decided to be performed in transient mode for 12 hours in all the cases. This is to check if the conditions in the pipeline network during this period will have changed compared to the beginning of the run. Note that the results of the transient run at 0 seconds represent the solution of the steady-state pre-processor, which is equivalent to running the case in steady-state by setting the ENDTIME key in OLGA to 0 seconds.

In summary, each case will be run in transient mode for one hour using automatic PIDs to arrive to target flowrates and their related choke openings. The case will then be run in transient mode for 12 hours using frozen PIDs at initial biases that are equal to the recorded choke openings from the previous run. The results of the second run at the end of the 12 hours will be compared to their initial values at 0 seconds to see if the longer runtime has added any value to the simulation.

### 5.3.3 Results

Table 29 shows the different choke openings at the end of the first run after allowing the target flowrates to be achieved.

Table 29 – Choke opening for different turndown rates

	Relative choke opening [-]									
	0% WC					26% WC				
	100%	80%	60%	40%	20%	100%	80%	60%	40%	20%
<b>Well_01</b>	0.254	0.227	0.203	0.179	0.154	0.274	0.241	0.216	0.186	0.160
<b>Well_02</b>	0.261	0.231	0.206	0.180	0.154	0.280	0.249	0.218	0.188	0.161
<b>Well_03</b>	0.285	0.254	0.227	0.197	0.168	0.310	0.274	0.239	0.210	0.171
<b>Well_04</b>	0.334	0.293	0.259	0.224	0.184	0.381	0.321	0.278	0.237	0.189

	Relative choke opening [-]									
	0% WC					26% WC				
	100%	80%	60%	40%	20%	100%	80%	60%	40%	20%
<b>Well_05</b>	0.233	0.208	0.187	0.168	0.144	0.249	0.222	0.198	0.174	0.155

Table 30 shows the results of the runs at the design flowrate (100%). The full list of the results at the different turndown percentages (100, 80, 60, 40, 20), both for 0% WC and 26% WC, are provided in Table H.2 of Appendix H. Temperature values below WAT are marked with a **(W)** and formatted in **bold**, and positive DTHYD values indicating hydrate formation are formatted similarly and marked with an **(H)**. The same is done with QGST and QLT values that show fluctuations with time as a result of slugging behavior, and they are marked with an **(S)**.

The reported flow regimes (ID) are those observed in a branch regardless of how prevailing they are, but the percentage of the branch length that shows a certain ID is reported under ID<sub>pct</sub> to indicate which flow regime is predominant. The liquid holdup (HOL) is reported as an average value for each ID. A short description of the reported variables can be found in Appendix G.

Table 30 – Pipeline parameters at the design flowrates (transient)

WC0_100							
Branch	QGST [MMscfd]	PT <sub>in</sub> [barg]	PT <sub>out</sub> [barg]	DP [barg]	TM <sub>in</sub> [°C]	TM <sub>out</sub> [°C]	DTHYD <sub>in</sub> OP [°C]
PL_2	52.1	56.2	45.0	11.2	22.4	<b>(W) 17.4</b>	-4.9
PL_1	33.9	58.5	56.3	2.2	<b>(W) 14.5</b>	<b>(W) 12.6</b>	<b>(H) 3.2</b>
FL_01	8.0	59.1	58.5	0.6	33.2	19.6	-15.4
FL_02	8.2	60.6	58.5	2.1	34.2	<b>(W) -0.8</b>	-16.3
FL_03	11.9	60.7	58.5	2.2	39.8	20.4	-21.8
FL_04	18.2	57.9	56.3	1.6	45.0	40.5	-27.4
FL_05	5.8	58.9	58.5	0.4	27.6	<b>(W) 17.1</b>	-9.8
Branch	DTHYD <sub>out</sub> OP [°C]	ID [-]	HOL <sub>avg</sub> [-]	ID <sub>pct</sub> [%]	LIQC [bbl]	QLT <sub>out</sub> [bbl/day]	
PL_2	-1.3	1, 3	0.171, 0.109	~100.0, ~0.0	457	12,891	
PL_1	<b>(H) 4.9</b>	1	0.216	100.0	367	8,855	
FL_01	-1.9	1, 3	0.225, 0.285	99.7, 0.3	54	2,051	
FL_02	<b>(H) 18.5</b>	1, 3	0.240, 0.320	99.9, 0.1	240	2,252	
FL_03	-2.7	1, 3	0.189, 0.228	99.8, 0.2	87	3,063	
FL_04	-23.0	1	0.150	100.0	19	4,375	
FL_05	<b>(H) 0.7</b>	1, 3	0.270, 0.348	97.2, 2.8	42	1,497	
WC26_100							
Branch	QGST [MMscfd]	PT <sub>in</sub> [barg]	PT <sub>out</sub> [barg]	DP [barg]	TM <sub>in</sub> [°C]	TM <sub>out</sub> [°C]	DTHYD <sub>in</sub> OP [°C]
PL_2	51.9	59.6	45.0	14.6	33.0	28.1	-15.2
PL_1	33.5	62.3	59.7	2.6	24.7	22.8	-6.6
FL_01	7.9	63.1	62.3	0.7	44.5	30.7	-26.4

FL_02	8.0	64.7	62.3	2.3	45.2	<b>(W) 6.3</b>	-26.9
FL_03	11.9	64.9	62.3	2.5	50.7	31.6	-32.3
FL_04	18.4	61.7	59.7	2.0	55.6	51.4	-37.5
FL_05	5.7	62.8	62.3	0.5	39.3	28.2	-21.1
Branch	DTHYD <sub>out</sub> OP [°C]	ID [-]	HOL <sub>avg</sub> [-]	ID <sub>pct</sub> [%]	LIQC [bbf]	QLT <sub>out</sub> [bbf/day]	
PL_2	-12.0	1, 3	0.195, 0.113	~100.0, ~0.0	522	15,511	
PL_1	-4.9	1, 3	0.251, 0.323	96.6, 3.4	431	10,539	
FL_01	-12.6	1, 3	0.266, 0.312	99.8, 0.2	64	2,449	
FL_02	<b>(H) 11.9</b>	1, 3	0.281, 0.352	98.8, 1.2	282	2,648	
FL_03	-13.5	1, 3	0.223, 0.253	99.9, 0.1	102	3,678	
FL_04	-33.6	1	0.177	100.0	22	5,427	
FL_05	-10.1	1, 3	0.290, 0.403	87.1, 12.9	48	1,794	

Fig. 36 shows the total liquid content in each of the branches (LIQC) at the different turndown flowrates, at 0% WC (left) and 26% WC (right). The order of the branches in the legend of the figure reflects the order of LIQC in the branches from higher to lower.

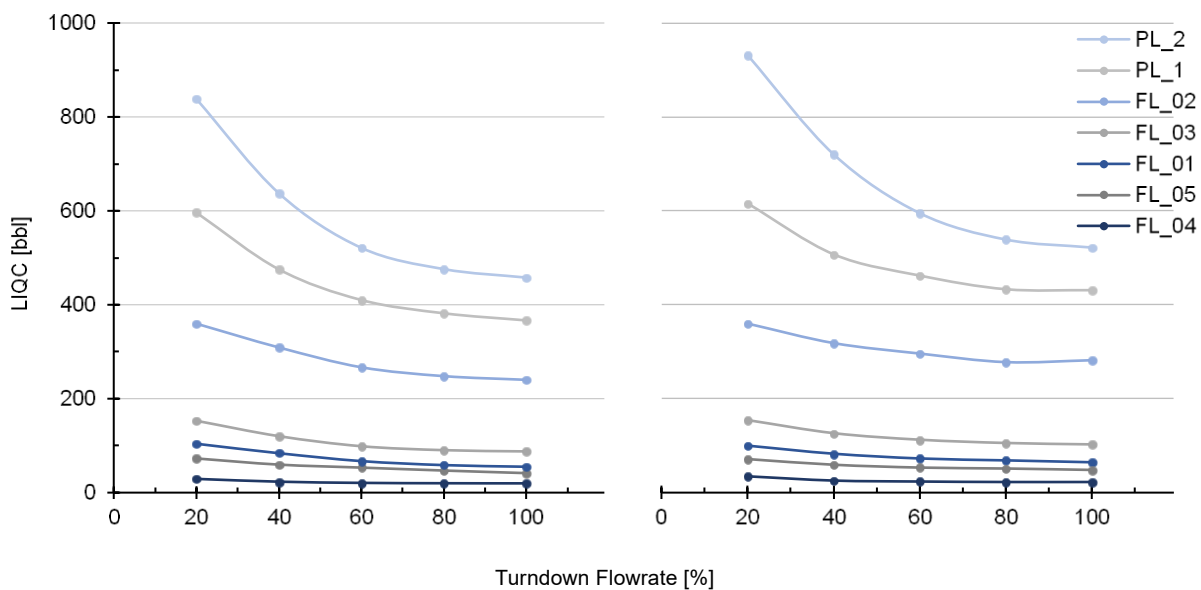


Fig. 36 – Total liquid content in each of the branches at the different turndown flowrates, at 0% WC (left) and 26% WC (right).

## 5.3.4 Discussion

### 5.3.4.1 Minimum Stable Flowrate (MSFR)

In the cases at 0% WC, where the liquid in the system comes from condensation that takes place as the pressure of the produced fluid drops along the pipeline network, the effect of the slug flow starts to appear at 80% turndown flowrate as the liquid flowrate observed at the end of the branches (QLT<sub>out</sub>) starts to fluctuate.

This fluctuation is mild at the beginning and it does not occur in all the branches, but it increases as the flowrate is turned down further. At 20% turndown, all the branches in the



network are showing the same behavior. At 26% WC,  $QLT_{out}$  is observed to be more stable, and it is only at 20% turndown flowrate that the network branches start to exhibit fluctuations in  $QLT_{out}$ .

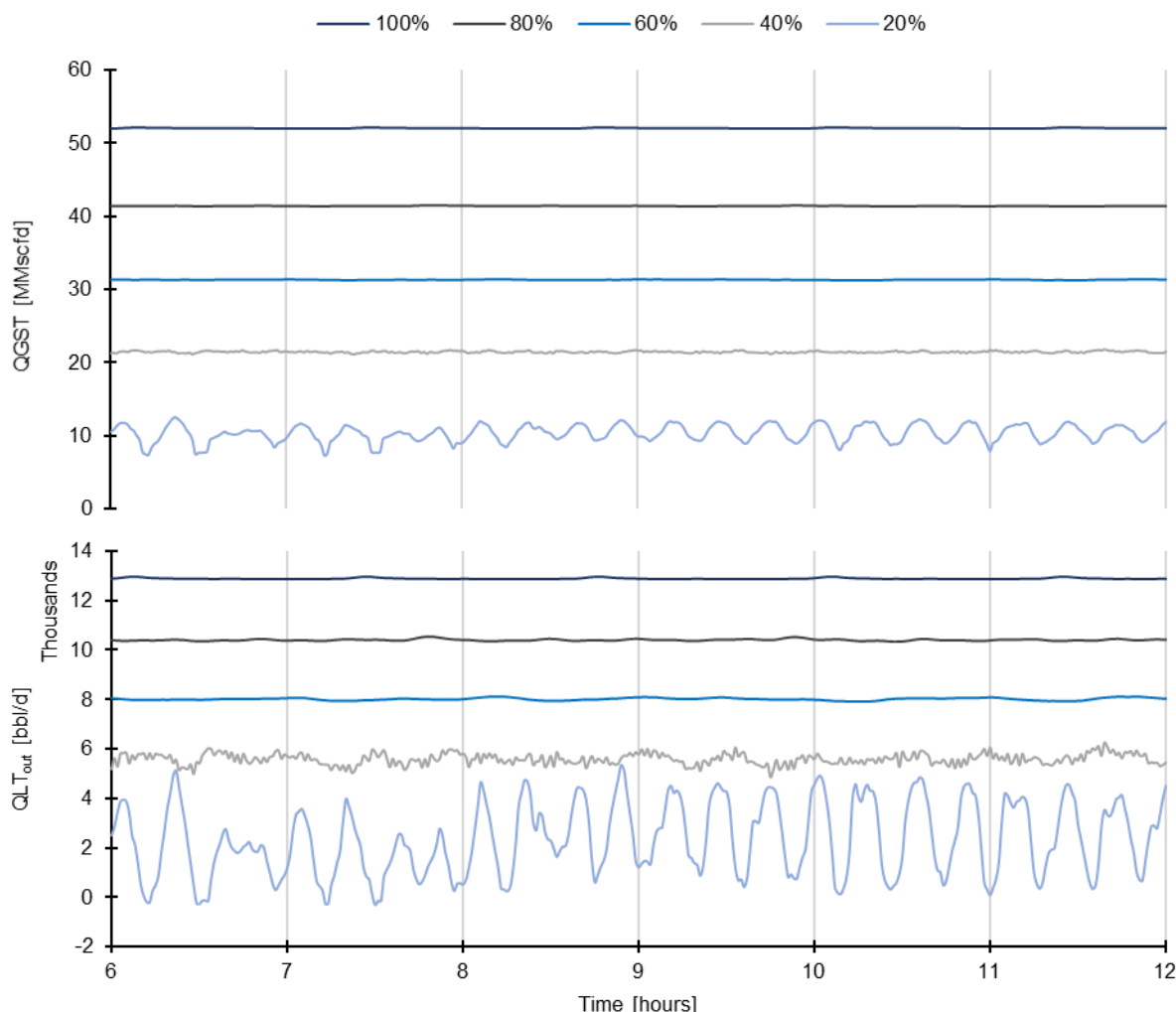


Fig. 37 – QLT and QGST into the slug catcher at different turndown flowrates

Fig. 37 shows  $QLT_{out}$  and QGST at the end of the pipeline network into the slug catcher at 0% WC in the last six hours of the runs. It can be observed that to ensure a stable flow into the process, the flowrate needs to stay above 20% turndown. The trend of  $QLT_{out}$  shows negative values sometimes at 20% turndown, indicating reverse liquid flow into the trunk-line at the section boundary where  $QLT_{out}$  is calculated.

### 5.3.4.2 Considering Water Salinity

The DTHYD values reported in Table H.2 were calculated in OLGA assuming pure water content. Table 31 compares these values at the outlet of the branches to the ones calculated in Excel using the lookup functions, assuming pure and saline water content. Calculations for saline water content are only performed for those points where formation water production is assumed.

Table 31 – DTHYD calculations for pure and saline water content at different turndown flowrates

Branch	WC0_100			WC26_100		
	DTHYD <sub>out</sub> OP [°C]	DTHYD <sub>out</sub> EP [°C]	DTHYD <sub>out</sub> ES [°C]	DTHYD <sub>out</sub> OP [°C]	DTHYD <sub>out</sub> EP [°C]	DTHYD <sub>out</sub> ES [°C]
PL_2	-1.3	-1.4	-	-12.0	-12.2	-24.2
PL_1	(H) 4.9	(H) 4.8	-	-4.9	-5.4	-17.6
FL_01	-1.9	-2.2	-	-12.6	-12.7	-25.0
FL_02	(H) 18.5	(H) 18.2	-	(H) 11.9	(H) 11.7	-0.6
FL_03	-2.7	-3.0	-	-13.5	-13.6	-25.9
FL_04	-23.0	-23.1	-	-33.6	-34.0	-46.3
FL_05	(H) 0.7	(H) 0.3	-	-10.1	-10.2	-22.5
Branch	WC0_80			WC26_80		
	DTHYD <sub>out</sub> OP [°C]	DTHYD <sub>out</sub> EP [°C]	DTHYD <sub>out</sub> ES [°C]	DTHYD <sub>out</sub> OP [°C]	DTHYD <sub>out</sub> EP [°C]	DTHYD <sub>out</sub> ES [°C]
PL_2	(H) 3.0	(H) 2.9	-	-8.4	-8.6	-20.6
PL_1	(H) 10.1	(H) 9.8	-	-1.5	-2.1	-14.2
FL_01	(H) 4.1	(H) 3.6	-	-7.0	-7.1	-19.3
FL_02	(H) 22.0	(H) 21.6	-	(H) 11.8	(H) 11.7	-0.5
FL_03	(H) 3.2	(H) 2.7	-	-9.1	-9.2	-21.5
FL_04	-18.9	-19.2	-	-28.0	-28.5	-40.7
FL_05	(H) 7.0	(H) 6.5	-	-3.6	-3.7	-15.9
Branch	WC0_60			WC26_60		
	DTHYD <sub>out</sub> OP [°C]	DTHYD <sub>out</sub> EP [°C]	DTHYD <sub>out</sub> ES [°C]	DTHYD <sub>out</sub> OP [°C]	DTHYD <sub>out</sub> EP [°C]	DTHYD <sub>out</sub> ES [°C]
PL_2	(H) 8.0	(H) 7.8	-	-1.3	-1.5	-13.5
PL_1	(H) 15.5	(H) 14.8	-	(H) 7.3	(H) 7.3	-5.6
FL_01	(H) 10.8	(H) 10.7	-	(H) 0.8	(H) 0.6	-11.6
FL_02	(H) 24.7	(H) 24.6	-	(H) 21.2	(H) 21.0	(H) 8.9
FL_03	(H) 9.7	(H) 9.6	-	-0.1	-0.3	-12.4
FL_04	-13.7	-14.4	-	-25.0	-25.0	-37.8
FL_05	(H) 13.7	(H) 13.6	-	(H) 2.8	(H) 2.6	-9.5
Branch	WC0_40			WC26_40		
	DTHYD <sub>out</sub> OP [°C]	DTHYD <sub>out</sub> EP [°C]	DTHYD <sub>out</sub> ES [°C]	DTHYD <sub>out</sub> OP [°C]	DTHYD <sub>out</sub> EP [°C]	DTHYD <sub>out</sub> ES [°C]
PL_2	(H) 14.6	(H) 14.4	-	(H) 6.7	(H) 6.5	-5.6
PL_1	(H) 21.2	(H) 20.8	-	(H) 15.2	(H) 14.6	(H) 2.6
FL_01	(H) 17.9	(H) 17.3	-	(H) 10.2	(H) 9.5	-2.6
FL_02	(H) 26.3	(H) 25.6	-	(H) 24.9	(H) 24.1	(H) 12.1
FL_03	(H) 17.6	(H) 17.0	-	(H) 9.5	(H) 8.8	-3.3
FL_04	-4.9	-5.4	-	-17.0	-17.6	-29.6
FL_05	(H) 20.3	(H) 19.7	-	(H) 11.6	(H) 10.9	-1.2
Branch	WC0_20			WC26_20		
	DTHYD <sub>out</sub> OP [°C]	DTHYD <sub>out</sub> EP [°C]	DTHYD <sub>out</sub> ES [°C]	DTHYD <sub>out</sub> OP [°C]	DTHYD <sub>out</sub> EP [°C]	DTHYD <sub>out</sub> ES [°C]
PL_2	(H) 21.1	(H) 20.9	-	(H) 18.3	(H) 18.2	(H) 6.1

PL_1	(H) 24.9	(H) 24.5	-	(H) 22.7	(H) 22.2	(H) 10.2
FL_01	(H) 23.4	(H) 22.8	-	(H) 21.4	(H) 20.7	(H) 8.6
FL_02	(H) 26.7	(H) 26.1	-	(H) 26.2	(H) 25.5	(H) 13.5
FL_03	(H) 24.7	(H) 24.1	-	(H) 22.0	(H) 21.3	(H) 9.2
FL_04	(H) 2.4	(H) 2.0	-	-0.5	-0.9	-13.0
FL_05	(H) 24.4	(H) 23.8	-	(H) 17.9	(H) 17.3	(H) 5.2

The produced water is keeping the fluid temperature at higher values compared to the cases with 0% WC due to the high specific heat capacity of the water and the increased thermal mass of the fluid due to the increased mass flowrate in the pipeline network.

When the salt content in the produced water is accounted for, hydrate is found to require more subcooling to form compared to assuming a pure water content. In fact, at the operating pressure range in the network and 0 wt% methanol in the gas condensate, hydrate is found to form at temperatures that are 12-13 °C below those where pure water content is assumed. This also means that ignoring the salinity of the produced water will result in more conservative- and more expensive- measures to avoid hydrate formation in the network, like higher-than-necessary methanol injection flowrates and/or flowline insulation thicknesses.

### 5.3.4.3 Steady-state vs Transient Simulation

Table H.3 of Appendix H shows the pipeline parameters at 0 seconds for the different turndown flowrates, which is the solution of the steady-state pre-processor. Table 32 shows the parameters at the design flowrate only. A few variables were picked to compare the transient solution at the end of the 12-hour runs to the steady-state solution. The values of the variables from the transient runs are subtracted from those of the steady-state solution and the differences are given in parentheses. The pre-processor did not converge at initializing the cases of 20% turndown, and the solution at 0 seconds was checked and found to be invalid. That is why Table H.3 does not include cases for 20% turndown.

Table 32 – Pipeline parameters at the design flowrate (steady-state), and the differences between steady-state and transient solutions

WC0_100							
Branch	QGST [MMscfd]	PT <sub>in</sub> [barg]	DP [barg]	TM <sub>out</sub> [°C]	DTHYD <sub>out</sub> OP [°C]	LIQC [bbl]	QLT <sub>out</sub> [bbl/day]
PL_2	52.2 (0.1)	56.3 (0.0)	11.3 (0.0)	(W) 17.4 (0.0)	-1.3 (0.0)	457 (0)	12,915 (25)
PL_1	33.9 (0.0)	58.5 (0.0)	2.2 (0.0)	(W) 12.7 (0.0)	(H) 4.8 (0.0)	367 (0)	8,861 (6)
FL_01	8.0 (0.0)	59.2 (0.1)	0.6 (0.0)	19.6 (0.0)	-1.9 (0.0)	54 (0)	2,058 (7)
FL_02	8.2 (0.0)	60.7 (0.1)	2.1 (0.0)	(W) -0.8 (0.0)	(H) 18.5 (0.0)	240 (0)	2,253 (1)
FL_03	11.9 (0.0)	60.7 (0.0)	2.2 (0.0)	20.4 (0.0)	-2.7 (0.0)	87 (0)	3,063 (0)

<b>FL_04</b>	18.3 (0.0)	57.9 (0.0)	1.6 (0.0)	40.6 (0.0)	-23.1 (0.0)	19 (0)	4,385 (10)
<b>FL_05</b>	5.8 (0.0)	59.0 (0.0)	0.4 (0.0)	<b>(W) 17.1</b> (0.0)	<b>(H) 0.7</b> (0.0)	41 (-1)	1,506 (9)

**WC26\_100**

<b>Branch</b>	<b>QGST</b> <b>[MMscfd]</b>	<b>PT<sub>in</sub></b> <b>[barg]</b>	<b>DP</b> <b>[barg]</b>	<b>TM<sub>out</sub> [°C]</b>	<b>DTHYD<sub>out</sub></b> <b>OP [°C]</b>	<b>LIQC</b> <b>[bbf]</b>	<b>QLT<sub>out</sub></b> <b>[bbf/day]</b>
<b>PL_2</b>	52.0 (0.1)	59.7 (0.1)	14.7 (0.1)	28.1 (0.0)	-12.0 (0.0)	522 (0)	15,545 (34)
<b>PL_1</b>	33.6 (0.1)	62.4 (0.1)	2.6 (0.0)	22.8 (0.0)	-5.0 (0.0)	431 (0)	10,566 (27)
<b>FL_01</b>	7.9 (0.0)	63.1 (0.1)	0.7 (0.0)	30.7 (0.0)	-12.6 (0.0)	64 (0)	2,455 (6)
<b>FL_02</b>	8.0 (0.0)	64.8 (0.1)	2.4 (0.0)	<b>(W) 6.3</b> (0.0)	<b>(H) 11.8</b> (0.0)	283 (1)	2,655 (7)
<b>FL_03</b>	11.9 (0.0)	65.0 (0.1)	2.6 (0.0)	31.6 (0.0)	-13.5 (0.0)	102 (0)	3,687 (9)
<b>FL_04</b>	18.4 (0.0)	61.8 (0.1)	2.0 (0.0)	51.4 (0.0)	-33.6 (0.0)	22 (0)	5,437 (10)
<b>FL_05</b>	5.8 (0.0)	62.9 (0.1)	0.5 (0.0)	28.2 (0.0)	-10.1 (0.0)	48 (0)	1,799 (5)

Since the steady-state pre-processor gives a snapshot of the simulation model at the beginning of the run, it cannot capture the fluctuation in the flowrate that was exhibited earlier by the transient solution. However, the comparison shows that depending on the objective of running the model, the steady-state simulation can be used when there is confidence in the stability of the variables, and its results can be trusted as long as the solution converges.

## 5.4 Methanol Injection under Flowing Conditions

### 5.4.1 Objective

The objective of this task is to determine the methanol injection rates required to avoid hydrate formation during production (active inhibition).

### 5.4.2 Setup

In OLGA, the inhibitor tracking module is used to track a hydrate inhibitor as it flows in the pipeline. With specifying hydrate curves at different inhibitor concentrations, the inhibitor tracking module interpolates between the curves to find the hydrate formation temperature at the in-situ inhibitor concentration in a pipe section [19]. The amount of inhibitor can then be modified to make sure it is sufficient to prevent hydrate formation. The hydrate inhibitors that can be tracked in OLGA are methanol (MeOH), ethanol (EtOH), and mono-ethylene glycol (MEG).

In this task, the point 02/01 is chosen to run the cases at the different turndown flowrates, considering 0% WC (pure water content) and 26% WC (pure and saline water content), and using the related hydrate curves that were discussed in 4.1.4.

Ideally, cases would be run in steady-state using the inhibitor tracking module, and a sensitivity analysis- known in OLGA as a parametric study- would be performed at different methanol injection flowrates to find the ones at which no hydrate is being formed in the network. It is already known from the results of the previous task 5.3 that the solution of the cases at 20% turndown flowrates did not converge at initialization and could only be run in transient mode to provide valid results. Therefore, these cases would also need to be run in transient mode for this task.

However, after setting up the inhibitor tracking for methanol and running a few cases, the steady-state pre-processor did not converge, and the solution of the network was too far from correct compared to the results from the turndown cases. This meant that all the cases needed to be run in transient. A different approach was adopted, though. Instead of running all the cases in transient mode using inhibitor tracking and trying to find the methanol injection rate required to avoid hydrate formation, which is a very time-consuming task, this rate was calculated in Excel instead using the results of the turndown cases, then one case was run afterwards in transient mode with inhibitor tracking to validate the calculated results.

DTHYD at the outlet of each branch is calculated for all the hydrate curves (different methanol wt%) using a lookup function. As described in 5.2.2, the lookup function will search the hydrate tables in Excel for the hydrate formation temperature at the outlet pressure of a branch. Then, the fluid temperature at the same point will be subtracted from this value. This gives the difference between the hydrate formation temperature at each methanol wt% and the in-situ fluid temperature, which, by definition, is DTHYD.

Now, it is required to find the methanol wt% that will keep the fluid above the hydrate formation temperature by a margin of, say, 5 °C. This is done in Excel by linear interpolation

between the two hydrate curves that confine the value of DTHYD = -5 °C. The methanol injection rate can then be determined using Eq. 5 using mass flowrates instead of mass and given the interpolated wt% and the total mass flow rate of water- including vapor- that is flowing in each branch (GLWVT).

Fig. 38 shows an example that graphically illustrates the interpolation between the hydrate curves to find the methanol wt% that will provide a hydrate subcooling of 5 °C. The cross represents the conditions at the outlet of FL\_02 at the design flowrate and 0% WC, the values next to the arrows represent DTHYD for the different hydrate curves, and the triangle represents the interpolated methanol wt% between the two curves confining DTHYD = -5 °C. The required wt% in this case is 52%.

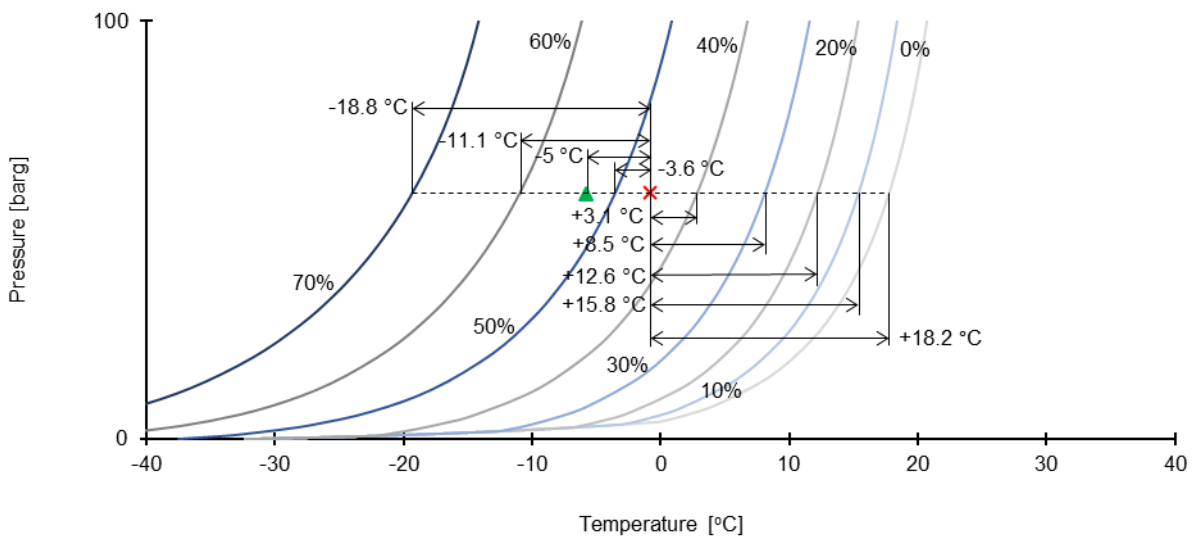


Fig. 38 – Interpolating between hydrate curves (methanol wt%)

The calculations are done for the in-situ conditions at the outlet of each branch because this is where the lowest temperature is expected to exist under steady-state production.

### 5.4.3 Results

Table 33 shows the results of the runs at the design flowrate. The full list of the results at the different turndown percentages (100, 80, 60, 40, 20), both for 0% WC and 26% WC, are given in Table H.4 of Appendix H. Positive DTHYD values indicating hydrate formation are formatted in **bold** and marked with an **(H)**. Required methanol wt% (MeOH wt%) and injection rate (QMeOH) are calculated for all the branches in the network. A short description of the reported variables can be found in Appendix G.

However, it might be the case that the required methanol injection rate to prevent hydrate formation in the trunk-line is higher than the sum of the rates sufficient to prevent hydrate formation in each of the flowlines. In this case, since methanol injection takes place upstream the choke valves only, the injection rates at the wells are increased to account for hydrate suppression in the trunk-line as well, resulting in even higher hydrate suppression in the flowlines.

Table 33 – Methanol injection rates at the design flowrate

WC0_100							
Branch	Pure				Saline		
	GLWVT [kg/h]	DTHYD <sub>out</sub> EP [°C]	MeOH wt% [%]	QMeOH [kg/h]	DTHYD <sub>out</sub> ES [°C]	MeOH wt% [%]	QMeOH [kg/h]
PL_2	247.9	-1.4	13.7	-	-	-	-
PL_1	157.6	(H) 4.8	30.2	-	-	-	-
FL_01	36.7	-2.2	11.3	7.7	-	-	-
FL_02	37.1	(H) 18.2	51.8	42.9	-	-	-
FL_03	57.7	-3.0	8.1	8.2	-	-	-
FL_04	90.3	-23.1	0.0	0.0	-	-	-
FL_05	26.2	(H) 0.3	19.4	9.3	-	-	-

WC26_100							
Branch	Pure				Saline		
	GLWVT [kg/h]	DTHYD <sub>out</sub> EP [°C]	MeOH wt% [%]	QMeOH [kg/h]	DTHYD <sub>out</sub> ES [°C]	MeOH wt% [%]	QMeOH [kg/h]
PL_2	20,613.1	-12.2	0.0	-	-24.2	0.0	-
PL_1	13,297.0	-5.4	0.0	-	-17.6	0.0	-
FL_01	3,130.0	-12.7	0.0	0.0	-25.0	0.0	0.0
FL_02	3,174.8	(H) 11.7	31.1	1,433.1	-0.6	7.6	261.1
FL_03	4,713.5	-13.6	0.0	0.0	-25.9	0.0	0.0
FL_04	7,316.0	-34.0	0.0	0.0	-46.3	0.0	0.0
FL_05	2,278.8	-10.2	0.0	0.0	-22.5	0.0	0.0

Fig. 39 shows the required methanol flowrates for the whole network at 0% WC (left) and 26% WC (right), for both pure and saline produced water contents. It shows that assuming a pure water content for the produced water has led to methanol requirements that are three to six times higher than those when the produced water salinity is accounted for.

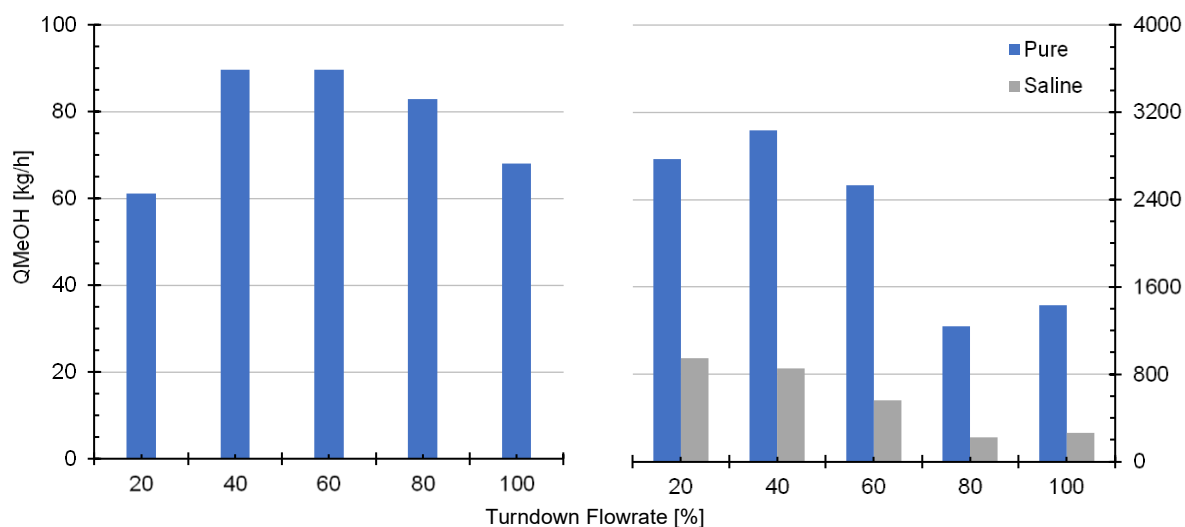


Fig. 39 – Required methanol flowrates for the whole network at 0% WC (left) and 26% WC (right), for both pure and saline produced water contents, at different turndown flowrates

### 5.4.4 Discussion: Validating the Results

To validate the Excel calculations performed to come up with the required methanol injection flowrates to avoid hydrate formation, the case at the design flowrate and 0% WC (WC0\_100) is considered to be run in transient mode using the injection rates calculated in Excel. This is to check if hydrate formation was avoided as expected or not, and how far the temperatures at the outlets of the branches are from the hydrate formation temperatures.

In Excel, the methanol wt% required to avoid hydrate formation in each branch by a margin of 5 °C was determined by interpolation as described in 5.4.2 and the results are given in column (3) of Table 34. The corresponding methanol flowrates were then calculated, and the results are given in column (4). However, the sum of methanol injection rates in the wellheads resulted in a methanol flowrate in PL\_1 of the trunk-line that is lower than required to avoid hydrate formation at the outlet of the branch. That is  $4.7 + 39.9 + 5.1 + 6.3 = 56.0$  kg/hr < 68.1 kg/hr. Therefore, the injection rates in the wells were increased by a total amount of  $68.1 - 56.0 = 12.1$  kg/hr that was divided equally on the wells where injection took place, and the corrected flowrates are given in column (5).

Columns (3) and (5) are those reported earlier in the results in Table 33. Here, only the flowrates at the wells are given because, in practice, no methanol injection will take place directly into the trunk-line. Note that if the methanol injection flowrates in the wellheads are already sufficient to prevent hydrate formation in the trunk-line, then the corrected values in column (5) will be the same as those in column (4).

Columns (6) and (7) give the actual methanol flowrates in all the branches and the resulting methanol wt%. It can be seen that the values in column (7) are eventually higher than those in column (3) except for PL\_1, which was the reason for such increase in the other branches, and FL\_04, where no methanol injection was required in the first place. This means that it is expected to see a DTHYD value of -5 °C at the outlet of PL\_1 and even lower values at the outlets of the other branches.

Table 34 – Methanol injection calculations in Excel for the case at design flowrate and 0% WC

WC0_100							
Branch	(1) GLWVT [kg/h]	(2) DTHYD <sub>out</sub> EP [°C]	(3) Required MeOH wt% [%]	(4) Required QMeOH [kg/h]	(5) Corrected QMeOH [kg/h]	(6) Actual QMeOH [kg/h]	(7) Actual MeOH wt% [%]
PL_2	247.9	-1.4	13.7	39.4	-	68.1	21.6
PL_1	157.6	<b>(H) 4.8</b>	30.2	68.1	-	68.1	30.2
FL_01	36.7	-2.2	11.3	4.7	7.7	7.7	17.4
FL_02	37.1	<b>(H) 18.2</b>	51.8	39.9	42.9	42.9	53.7
FL_03	57.7	-3.0	8.1	5.1	8.2	8.2	12.4
FL_04	90.3	-23.1	0.0	0.0	0.0	0.0	0.0
FL_05	26.2	<b>(H) 0.3</b>	19.4	6.3	9.3	9.3	26.3



The case WC0\_100 was run in transient mode for six hours using inhibitor tracking for methanol by adjusting the keyword COMPOSITIONAL = MEOH under the case options, and the results at the end of the run are shown in Table 35.

Table 35 – Results of running the case WC0\_100 in OLGA using inhibitor tracking

WC0_100							
Branch	QGST [MMscfd]	PT <sub>in</sub> [barg]	PT <sub>out</sub> [barg]	DP [barg]	TM <sub>in</sub> [°C]	TM <sub>out</sub> [°C]	DTHYD <sub>out</sub> OP [°C]
PL_2	52.8	56.6	45.0	11.6	21.1	<b>(W) 17.5</b>	-4.3
PL_1	34.3	58.9	56.6	2.2	<b>(W) 13.4</b>	<b>(W) 11.9</b>	-0.2
FL_01	8.1	59.5	58.9	0.6	25.8	<b>(W) 17.2</b>	-2.1
FL_02	8.2	60.9	58.9	2.1	27.0	<b>(W) 0.6</b>	-1.0
FL_03	12.1	61.0	58.9	2.1	33.5	19.3	-3.3
FL_04	18.7	58.2	56.6	1.6	42.1	38.3	-20.7
FL_05	5.8	59.3	58.9	0.4	19.3	<b>(W) 14.2</b>	-0.7

DTHYD values at the outlets of the branches show that no hydrate was formed, and that hydrate suppression was higher in all the branches compared to PL\_1, which supports the validity of the calculations that were done in Excel. However, although a DTHYD value of -5 °C was anticipated at the outlet of PL\_1, the result was found to be only -0.2 °C.

Another observation is that the values of the fluid temperatures here are different than those that were reported in Table 33, and on which the Excel calculations were based. In general, the temperatures in this case are 1-8 °C lower than in the original case, and only in two branch outlets that they are slightly higher. DTHYD values would have been lower if the fluid temperature at the outlets of the branches were higher.

The temperature profiles in the wellbores were also checked and found to be 3-8 °C lower than in the original turndown case, which means that this difference is not related to the methanol injection on the surface, but might be due to how calculations are done in OLGA when inhibitor tracking is activated.

Another run was carried out using inhibitor tracking but without injecting any methanol into the network, and the temperature profiles were still found to be lower than in the original turndown case without inhibitor tracking. This agrees to the assumption that this discrepancy is related to the inhibitor tracking module. However, no more investigation was performed to find out where this discrepancy originates from.

The Excel calculation method was proven to give valid results, and the 5 °C margin used was found to be a good choice to account for the uncertainty in the calculations. This method is going to be used to calculate the methanol injection rates in the rest of the FA study.

## 5.5 Methanol Injection under Shut-in Conditions

### 5.5.1 Objective

The objective of this task is to determine the methanol injection rates that allow for the required no-touch time of 6 hours that is set by the operator (shut-in scenario).

### 5.5.2 Setup

In this task, the point 02/01 is chosen to run shutdown cases starting from the different turndown flowrates, considering 0% WC (pure water content) and 26% WC (pure and saline water content), and using the related hydrate curves that were discussed in 4.1.4.

In OLGA, a case can be set up to continue from a previous run, which is known as a RESTART case. In this task, the shutdown cases will be set up to restart from the end of the turndown cases. The choke valves of the wells and the SDV at the inlet of the slug catcher will close at the beginning of the restart run and will be kept this way for six hours until the end of the run. Since the calculation method described in the previous task 5.4 for the methanol injection flowrate in Excel was proved reliable, it is going to be used here as well based on the results of the shutdown cases.

The difference is that in this task, each branch will be checked at the end of the six hours for the point where the hydrate formation is most critical (highest positive DTHYD), and the calculations will be performed for the in-situ conditions at this point. Here, it is not necessarily going to be the outlet of the branch. This is because unlike the steady-state production, where the temperature profile along a branch is uniform and decreasing with distance, the shutdown will result in a temperature profile that is highly dependent on the geometry of the branch and the variations in the liquid hold up of its sections.

### 5.5.3 Results

First, Table 36 lists the parameters of the branches at the end of the six-hour shutdown period for the design flowrate. The full list of the results for the different turndown percentages (100, 80, 60, 40, 20), both for 0% WC and 26% WC, are given in Table H.5 of Appendix H. The maximum DTHYD value in each branch is reported, in addition to the pressure and temperature at this point. The average pressure and temperature of each branch are also reported. Temperature values below WAT are marked with a **(W)** and formatted in **bold**, and positive DTHYD values indicating hydrate formation are formatted similarly and marked with an **(H)**. A short description of the reported variables can be found in Appendix G.

Table 36 – Pipeline parameters after a six-hour shutdown for the design flowrate

WC0_100							
Branch	DTHYD <sub>max</sub> OP [°C]	DTHYD <sub>max</sub> EP [°C]	DTHYD <sub>max</sub> ES [°C]	PT <sub>DTHYD</sub> [barg]	TM <sub>DTHYD</sub> [°C]	PT <sub>avg</sub> [barg]	TM <sub>avg</sub> [°C]
PL_2	<b>(H) 5.8</b>	<b>(H) 5.4</b>	-	53.1	<b>(W) 11.3</b>	53.2	<b>(W) 16.1</b>

PL_1	(H) 13.0	(H) 12.6	-	52.9	(W) 4.1	53.1	(W) 9.9
FL_01	(H) 13.5	(H) 13.2	-	52.9	(W) 3.6	52.9	(W) 9.5
FL_02	(H) 22.1	(H) 21.7	-	52.9	(W) -5.0	52.6	(W) 2.3
FL_03	(H) 13.5	(H) 13.1	-	52.9	(W) 3.6	52.8	(W) 11.5
FL_04	(H) 1.0	(H) 0.6	-	53.1	(W) 16.1	53.1	(W) 19.2
FL_05	(H) 13.8	(H) 13.4	-	52.9	(W) 3.3	52.9	(W) 7.2

## WC26\_100

Branch	DTHYD <sub>max</sub> OP [°C]	DTHYD <sub>max</sub> EP [°C]	DTHYD <sub>max</sub> ES [°C]	PT <sub>DTHYD</sub> [barg]	TM <sub>DTHYD</sub> [°C]	PT <sub>avg</sub> [barg]	TM <sub>avg</sub> [°C]
PL_2	-1.7	-1.7	-14.6	55.4	19.1	55.4	25.5
PL_1	(H) 7.2	(H) 6.5	-5.6	55.0	(W) 10.2	55.2	18.8
FL_01	(H) 8.6	(H) 8.0	-4.2	55.0	(W) 8.8	54.9	(W) 16.3
FL_02	(H) 18.5	(H) 17.9	(H) 5.7	55.0	(W) -1.1	54.6	(W) 8.0
FL_03	(H) 9.2	(H) 8.5	-3.6	55.0	(W) 8.2	54.9	18.1
FL_04	-4.7	-4.7	-17.6	55.4	22.1	55.3	25.6
FL_05	(H) 8.8	(H) 8.1	-4.0	55.0	(W) 8.6	55.0	(W) 14.0

Table 37 shows the methanol injection rates required for a no-touch time of six hours based on the values of the maximum DTHYD in each branch at the end of the runs of the design flowrate. Table H.6 of Appendix H gives the full list of the results for the different turndown flowrates. The values of the total water mass flowrates (GLWVT) in the tables are those that took place during the flowing period before the shutdown, and on which the required methanol wt% (MeOH wt%) and injection rate (QMeOH) calculations are based.

Table 37 – Methanol injection rates required for a no-touch time of six hours for the design flowrate

## WC0\_100

Branch	GLWVT [kg/h]	Pure			Saline		
		DTHYD <sub>max</sub> EP [°C]	MeOH wt% [%]	QMeOH [kg/h]	DTHYD <sub>max</sub> ES [°C]	MeOH wt% [%]	QMeOH [kg/h]
PL_2	247.9	(H) 5.4	31.2	-	-	-	-
PL_1	157.6	(H) 12.6	43.4	-	-	-	-
FL_01	36.7	(H) 13.2	44.2	29.0	-	-	-
FL_02	37.1	(H) 21.7	56.1	47.3	-	-	-
FL_03	57.7	(H) 13.1	44.1	45.6	-	-	-
FL_04	90.3	(H) 0.6	20.1	22.7	-	-	-
FL_05	26.2	(H) 13.4	44.6	21.0	-	-	-

## WC26\_100

Branch	GLWVT [kg/h]	Pure			Saline		
		DTHYD <sub>max</sub> EP [°C]	MeOH wt% [%]	QMeOH [kg/h]	DTHYD <sub>max</sub> ES [°C]	MeOH wt% [%]	QMeOH [kg/h]
PL_2	20,613.1	-1.7	7.0	-	-14.6	0.0	-
PL_1	13,297.0	(H) 6.5	23.8	-	-5.6	0.0	-
FL_01	3,130.0	(H) 8.0	26.1	1,107.7	-4.2	1.5	48.5
FL_02	3,174.8	(H) 17.9	40.5	2,159.8	(H) 5.7	18.7	730.0

<b>FL_03</b>	4,713.5	<b>(H) 8.5</b>	27.1	1,750.7	-3.6	2.6	127.3
<b>FL_04</b>	7,316.0	-4.7	0.6	41.9	-17.6	0.0	0.0
<b>FL_05</b>	2,278.8	<b>(H) 8.1</b>	26.4	818.9	-4.0	1.9	43.5

Fig. 40 shows the required methanol flowrates for the whole network at 0% WC (left) and 26% WC (right), for both pure and saline produced water contents. It shows that assuming a pure water content in the cases where formation water production takes place has led to methanol requirements that are three to seven times higher than those when the produced water salinity is accounted for.

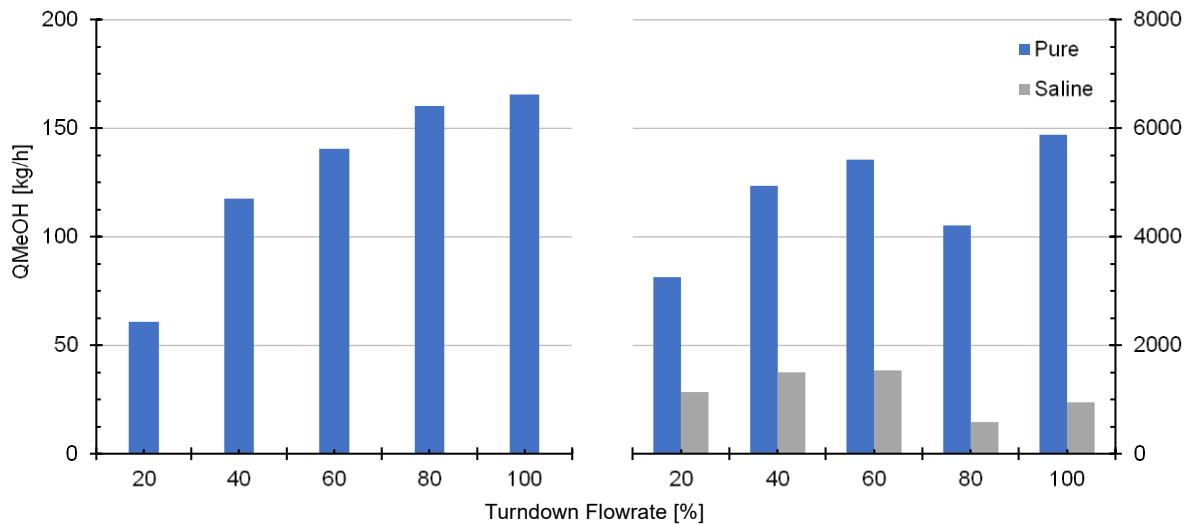


Fig. 40 – Required methanol flowrates for the whole network for a no-touch time of six hours, at 0% WC (left) and 26% WC (right), and both pure and saline produced water contents

## 5.6 Insulation Thickness under Flowing Conditions

### 5.6.1 Objective

The objective of this task is to determine the required flowline insulation thickness to prevent hydrate and/or wax formation during production (passive inhibition).

### 5.6.2 Setup

In this task, the point 02/01 is chosen to run the cases at the different turndown flowrates, considering 0% WC (pure water content) and 26% WC (pure and saline water content), and using the related hydrate curves that were discussed in 4.1.4. For each turndown case, four different flowline insulation thicknesses, as listed in Table 12, will be tested by selecting the related pipe wall in the simulation model.

Another additional case will be considered where the thermal conductivity of the insulation material ( $\lambda$ ) is set to an extremely small value of  $10^{-12}$  W/m·K (perfect insulation). This is to examine the effect of the inevitable heat loss in the branches due to expansion cooling only (Joule-Thomson effect) by eliminating the heat loss to the surroundings and ignoring the potential energy losses due to the small elevation change in the network.

A maximum of 5 turndown flowrates x 5 insulation cases x 2 WC = 50 cases could be run in this task. However, if a certain insulation thickness is sufficient to avoid hydrate and wax formation at some turndown flowrate, no higher thicknesses will need to be tested, and the next case to run will be that of the perfect insulation. Cases will be run in steady-state mode as long as the pre-processor can converge.

### 5.6.3 Results

Table H.7 of Appendix H shows the results of the runs at the different turndown percentages (100, 80, 60, 40), both for 0% WC and 26% WC, and under different flowline insulations (0", 1.17", 1.75", 2.43", 3.19",  $\lambda \sim 0$  W/m·K). The steady-state solution of the turndown cases from the task 5.3 were included in the table for comparison purposes, as they represent the base-case of the pipeline network without flowline insulation (0"). The solution of the cases at 20% turndown rate did not converge in steady-state mode, but they eventually were not run in transient mode instead because the status of the pipeline could mostly be deduced from other cases. Table 38 shows an example of the results at the design flowrate, 0% WC, and 1.17" flowline insulation thickness.

Temperature values below WAT are marked with a **(W)** and formatted in **bold**, positive DTHYD values indicating hydrate formation are formatted similarly and marked with an **(H)**. Required methanol wt% (MeOH wt%) and injection rate (QMeOH) to avoid hydrate formation by a margin of 5 °C are calculated for all the branches in the network. The overall heat transfer coefficient (Q2) for each branch is also reported. A short description of the reported variables can be found in Appendix G.

Table 38 – Pipeline parameters and methanol injection rates at the design flowrate, 0% WC, and 1.17" flowline insulation thickness

WC0_100_1.17"							
Branch	QGST [MMscfd]	PT <sub>in</sub> [barg]	PT <sub>out</sub> [barg]	DP [barg]	TM <sub>in</sub> [°C]	TM <sub>out</sub> [°C]	Q2 [W/m <sup>2</sup> ·K]
PL_2	52.2	57.0	45.0	12.0	32.7	27.0	0.65
PL_1	33.9	59.5	57.1	2.4	29.0	26.4	0.65
FL_01	8.0	60.1	59.5	0.6	33.8	30.3	1.14
FL_02	8.2	61.7	59.5	2.2	34.9	21.7	1.14
FL_03	11.9	61.8	59.5	2.3	40.3	34.9	1.14
FL_04	18.3	58.7	57.1	1.6	45.4	44.1	1.14
FL_05	5.8	59.9	59.5	0.4	28.3	25.6	1.14
Branch	DTHYD <sub>out</sub> OP [°C]	DTHYD <sub>out</sub> EP [°C]	DTHYD <sub>out</sub> ES [°C]	QMeOH EP [kg/h]	QMeOH ES [kg/h]	LIQC [bbl]	QLT <sub>out</sub> [bbl/day]
PL_2	-10.9	-11.1	-	-	-	429	12,539
PL_1	-8.9	-9.0	-	-	-	333	8,495
FL_01	-12.4	-12.9	-	0.0	-	53	1,995
FL_02	-3.8	-4.3	-	1.2	-	216	2,092
FL_03	-17.1	-17.5	-	0.0	-	83	2,937
FL_04	-26.6	-26.7	-	0.0	-	19	4,350
FL_05	-7.8	-8.2	-	0.0	-	40	1,469

Table 39 shows whether hydrate and/or wax will be formed in any of the network branches for the different turndown flowrates under the examined insulations and assuming no methanol injection. The total methanol injection flowrate required to avoid hydrate formation in the whole network by a margin of 5 °C is reported in kg/h in parentheses assuming both pure/saline, when applicable. When a case shows no hydrate formation yet methanol injection flowrate is still reported, it means that the hydrate subcooling in one or more of the branches is less than 5 °C.

Note that in this table, whether hydrate is said to have formed or not, this comes from the more conservative cases, where pure water content is assumed.

Table 39 – Hydrate and/or wax formation for different turndown flowrates under different insulations, and required methanol injection flowrates in kg/h for pure/saline water content

Case	Flowline insulation					
	0"	1.17"	1.75"	2.43"	3.19"	λ ~ 0
WC0_100	H, W (68/-)	-	*-	*-	*-	-
WC0_80	H, W (83/-)	H, W (12/-)	W (0/-)	- (0/-)	*-	-
WC0_60	H, W (90/-)	*H, W	H, W (29/-)	H, W (25/-)	H, W (22/-)	H, W (7/-)
WC0_40	H, W (90/-)	*H, W	*H, W	*H, W	*H, W	H, W (23/-)

Case	Flowline insulation					
	0"	1.17"	1.75"	2.43"	3.19"	$\lambda \sim 0$
WC0_20	*H, W (54/-)	*H, W	*H, W	*H, W	*H, W	*H, W
WC26_100	H, W (1433/260)	*_	*_	*_	*_	-
WC26_80	H, W (1577/451)	-	*_	*_	*_	-
WC26_60	H, W (2387/535)	-	*_	*_	*_	-
WC26_40	H, W (3038/852)	H, W (773/12)	H, W (551/0)	H, W (397/0)	H, W (324/0)	-
WC26_20	*H, W (2773/945)	*H, W	*H, W	*H, W	*H, W	N/A

\*Cases are not reported in Table H.7 but the results can be deduced from other cases

Not all the results mentioned here were reported in Table H.7; some could be deduced from the results of the cases that were run in this task or in task 5.3. For example, the fact that hydrate and wax are found to form for the 60% turndown flowrate with 0% WC under all insulations means that the same will happen for the 40% and 20% turndown flowrates as well because lower temperatures are expected to take place in the network. The status of the pipeline under the 20% turndown rate with perfect insulation could not be deduced from the other results, but it was not critical to run it in transient mode, and therefore it was ignored.

### 5.6.4 Discussion: 1D vs 2D Heat Transfer

The difference between the one-dimensional and the two-dimensional heat transfer in OLGA was described in 4.3.1. The two-dimensional heat transfer using FEMTherm was chosen to perform all the runs in the FA study. Here, a comparison between the two methods will be carried out to see how the method of heat transfer calculations could affect the choice of insulation thickness and the determination of the methanol injection requirements.

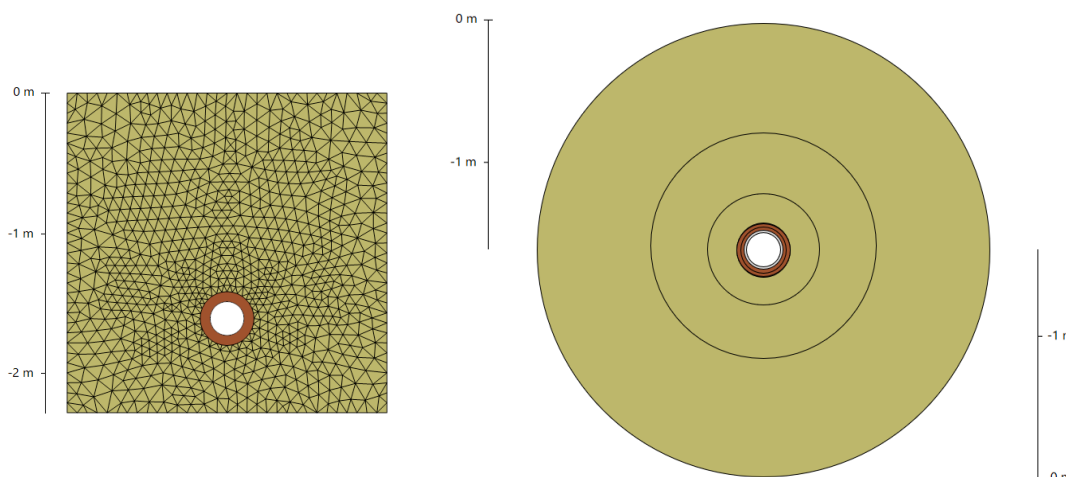


Fig. 41 – Trunk-line surroundings in 2D heat transfer (left) vs 1D heat transfer (right)

The cases at the design flowrate and both 0% and 26% WC will be run using one-dimensional heat transfer, and their results will be compared to the cases run earlier in this task and reported in Table H.7. If a certain insulation thickness is sufficient to avoid hydrate and wax formation, no higher thicknesses will be examined.

Fig. 41 shows the difference between the solid bundle around the trunk-line in FEMTherm (left) and the pipe wall “10 3/4 CS + 2.00 PUR + Soil” that is used for the trunk-line in the cases where one-dimensional heat transfer is set up. A list of all the walls including the materials of the layers and the discretization of the thicknesses is attached in Appendix E.

In FEMTherm’s solid bundle, the ambient temperature above the top side of the square is -43 °C in the winter design (WD) conditions, and the temperature at the bottom side is 0.8 °C. The heat transfer in the solid bundle is complex and asymmetrical around the pipe. On the other hand, in the one-dimensional heat transfer, the ambient conditions surround the outer boundary of the pipe wall from all directions, and heat transfer takes place symmetrically in the radial direction through the wall layers, which include the soil layers. The same applies to all the flowlines as well. Table H.8 of Appendix H lists the results of the runs at the design flowrate. An example of these results at 0% WC and 1.17” flowline insulation thickness is shown in Table 40.

Table 40 – Pipeline parameters and methanol injection rates at the design flowrate, 0% WC, and 1.17” flowline insulation thickness, using 1D heat transfer

WC0_100_1.17”							
Branch	QGST [MMscfd]	PT <sub>in</sub> [barg]	PT <sub>out</sub> [barg]	DP [barg]	TM <sub>in</sub> [°C]	TM <sub>out</sub> [°C]	Q2 [W/m <sup>2</sup> ·K]
PL_2	52.2	56.7	45.0	11.7	28.8	21.9	0.56
PL_1	33.9	59.1	56.7	2.4	24.7	20.9	0.56
FL_01	8.0	59.7	59.1	0.6	33.7	27.7	0.93
FL_02	8.2	61.3	59.1	2.2	34.7	<b>(W) 12.6</b>	0.93
FL_03	11.9	61.3	59.1	2.3	40.2	31.7	0.93
FL_04	18.3	58.3	56.7	1.6	45.3	43.5	0.93
FL_05	5.8	59.5	59.1	0.4	28.1	23.3	0.93
Branch	DTHYD <sub>out</sub> OP [°C]	DTHYD <sub>out</sub> EP [°C]	DTHYD <sub>out</sub> ES [°C]	QMeOH EP [kg/h]	QMeOH ES [kg/h]	LIQC [bbl]	QLT <sub>out</sub> [bbl/day]
PL_2	-5.8	-5.9	-	-	-	441	12,734
PL_1	-3.3	-3.5	-	-	-	344	8,635
FL_01	-9.9	-10.3	-	0.0	-	53	2,009
FL_02	<b>(H) 5.1</b>	<b>(H) 4.8</b>	-	16.0	-	223	2,152
FL_03	-13.9	-14.3	-	0.0	-	83	2,961
FL_04	-26.0	-26.1	-	0.0	-	19	4,353
FL_05	-5.5	-5.9	-	0.0	-	41	1,478

Lower fluid temperature profiles along the branches are observed compared to 2D heat transfer, especially in the cases where no flowline insulation is applied. Lower temperatures result in more condensation, and consequently in a higher liquid content in the branches and



a higher liquid flowrate at the outlet of the pipeline. Hydrate and wax were found to have formed under flowline insulation thicknesses that could actually manage to prevent their formation. This effect is clearly observed in FL\_02 because it is the longest flowline and Well\_02 is producing only 8.2 MMscfd of gas, so a longer time is allowed for heat transfer between the gas condensate in the flowline and its surroundings compared to the rest of the flowlines.

Table 41 summarizes the comparison between the results of the two heat transfer calculations in terms of whether hydrate and/or wax will be formed in any of the network branches assuming no methanol injection, and the total methanol injection flowrate required to avoid hydrate formation in the whole network considering a margin of 5 °C.

Table 41 – Hydrate and/or wax formation and required methanol injection flowrates in kg/h for pure/saline water content at design flowrate for 1D and 2D heat transfer

Case	Flowline insulation				
	0"	1.17"	1.75"	2.43"	3.19"
WC0_100 (2D)	H, W (68/-)	-	*-	*-	*-
WC0_100 (1D)	H, W (216/-)	H, W (16/-)	H, W (9/-)	- (4/-)	*-
WC26_100 (2D)	H, W (1433/260)	*-	*-	*-	*-
WC26_100 (1D)	H, W (3943/1698)	- (0/0)	*-	*-	*-

\*Cases were not run, but results can be deduced from other cases

The table shows that using one-dimensional heat transfer for this FA study under such extreme ambient conditions would have resulted in much higher methanol injection requirements, especially considering water production; and in a choice of a thicker insulation, based on the operator's criteria; leading the operator to go for more conservative- and more expensive- options than what the operator might actually require.

## 5.7 Insulation Thickness under Shut-in Conditions

### 5.7.1 Objective

The objective of this task is to determine the flowline insulation thickness that allows for the required no-touch time of 6 hours that is set by the operator (shut-in scenario).

### 5.7.2 Setup

In this task, the point 02/01 is chosen to run the shutdown cases starting from the different turndown flowrates, considering 0% WC (pure water content) and 26% WC (pure and saline water content), and using the related hydrate curves that were discussed in 4.1.4.

The shutdown cases here cannot be run as restart cases from the turndown ones in 5.3 because a pipe wall cannot be changed in a restart case. Recall that the turndown cases were run without flowline insulation, while here it is required to test different pipe walls. For each shutdown case, only those flowline insulation thicknesses that could prevent hydrate and/or wax formation under flowing conditions will be tested, and no cases with perfect insulation will be considered. As in the previous task 5.6, if a certain insulation thickness is sufficient to avoid hydrate and wax formation at some turndown flowrate, no higher thicknesses will be tested. This makes a total of 19 cases that could be run in this task as can be seen in Table 39.

One minute will be allowed at the beginning of each run for steady production before shutdown is commenced. The choke valves of the wells and the SDV at the inlet of the slug catcher will then close and will be kept this way for six hours until the end of the run.

It was found already from the results of the task 5.3 that the steady-state solution (at 0 seconds) of the turndown flowrates above 20% gave consistent results with reference to the transient solution of the same cases after 12 hours of runtime. So, there is no gain from allowing for a long period of steady production before the shutdown.

### 5.7.3 Results

Table H.9 of Appendix H lists the parameters of the branches at the end of the six-hour shutdown period that started at the different turndown percentages examined (100, 80, 60), both for 0% WC and 26% WC, and under different flowline insulations (1.17", 1.75", 2.43", 3.19"). The maximum DTHYD value in each branch is reported, in addition to the pressure and temperature at this point. The average pressure and temperature of each branch are also reported. Table 42 shows an example of the results at the design flowrate, 0% WC, and 1.17" flowline insulation thickness.

Temperature values below WAT are marked with a **(W)** and formatted in **bold**, and positive DTHYD values indicating hydrate formation are formatted similarly and marked with an **(H)**. Required methanol wt% (MeOH wt%) and injection rate (QMeOH) to avoid hydrate formation with a margin of 5 °C are calculated for all the branches in the network. The overall heat

transfer coefficient (Q2) for each branch is also reported. A short description of the reported variables can be found in Appendix G.

Table 42 – Pipeline parameters and methanol injection rates after a six-hour shutdown for the design flowrate, 0% WC, and 1.17” flowline insulation thickness

WC0_100_1.17”					
Branch	PT <sub>DTHYD</sub> [barg]	TM <sub>DTHYD</sub> [°C]	PT <sub>avg</sub> [barg]	TM <sub>avg</sub> [°C]	Q2 [W/m <sup>2</sup> ·K]
PL_2	53.4	22.0	53.6	24.8	0.64
PL_1	53.3	19.8	53.4	22.2	0.64
FL_01	53.3	<b>(W) 13.9</b>	53.3	<b>(W) 17.0</b>	1.11
FL_02	53.3	<b>(W) 9.2</b>	53.0	<b>(W) 14.6</b>	1.11
FL_03	53.3	<b>(W) 16.0</b>	53.2	20.3	1.11
FL_04	53.5	19.3	53.5	24.8	1.11
FL_05	53.3	<b>(W) 11.3</b>	53.3	<b>(W) 13.9</b>	1.11
Branch	DTHYD <sub>max</sub> OP [°C]	DTHYD <sub>max</sub> EP [°C]	DTHYD <sub>max</sub> ES [°C]	QMeOH EP [kg/h]	QMeOH ES [kg/h]
PL_2	-4.8	-5.2	-	-	-
PL_1	-2.6	-3.0	-	-	-
FL_01	<b>(H) 3.2</b>	<b>(H) 2.8</b>	-	12.5	-
FL_02	<b>(H) 8.0</b>	<b>(H) 7.6</b>	-	20.1	-
FL_03	<b>(H) 1.2</b>	<b>(H) 0.7</b>	-	14.8	-
FL_04	-2.1	-2.6	-	10.0	-
FL_05	<b>(H) 5.9</b>	<b>(H) 5.5</b>	-	12.0	-

Table 43 shows whether hydrate and/or wax will be formed in any of the branches at the end of the shutdown under the examined insulations and assuming no methanol injection. The total methanol injection flowrate required to avoid hydrate formation in the whole network by a margin of 5 °C is reported in kg/h in parentheses assuming both pure/saline water content, when applicable. When a case shows no hydrate formation yet methanol injection flowrate is still reported, it means that the hydrate subcooling in one or more of the branches is less than 5 °C. Note that in this table, whether hydrate is said to have formed or not, this comes from the more conservative cases, where pure water content is assumed.

Table 43 – Hydrate and/or wax formation after a six-hour shutdown under different insulation thicknesses, and required methanol injection flowrates in kg/h for pure/saline water content

Case	Flowline insulation				
	0”	1.17”	1.75”	2.43”	3.19”
WC0_100	*H, W (166/-)	H, W (69/-)	H, W (36/-)	H, W (18/-)	- (9/-)
WC0_80	*H, W (160/-)	*H, W	*H, W	*H, W	H, W (33/-)
WC0_60	*H, W (141/-)	*H, W	*H, W	*H, W	*H, W

Case	Flowline insulation				
	0"	1.17"	1.75"	2.43"	3.19"
<b>WC0_40</b>	*H, W (118/-)	*H, W	*H, W	*H, W	*H, W
<b>WC0_20</b>	*H, W (61/-)	*H, W	*H, W	*H, W	*H, W
<b>WC26_100</b>	*H, W (5879/949)	H, W (875/0)	- (110/0)	*- (0/0)	*- (371/0)
<b>WC26_80</b>	*H, W (4208/584)	*H, W	H, W (514/0)	- (0/0)	*- (371/0)
<b>WC26_60</b>	*H, W (5420/1542)	*H, W	*H, W	H, W (731/0)	W (371/0)
<b>WC26_40</b>	*H, W (4943/1507)	*H, W	*H, W	*H, W	*H, W
<b>WC26_20</b>	*H, W (3263/1134)	*H, W	*H, W	*H, W	*H, W

\*Cases are not reported in Table H.9 but the results can be deduced from other cases

As in the results of the previous task 5.6.3, not all the results mentioned here were detailed in Table H.9; some could be deduced from the results of other cases. For example, the fact that hydrate and wax were found to form for the 60% turndown flowrate with 0% WC under all insulations during flowing conditions means that the same will happen for this turndown flowrate and the smaller ones during shutdown conditions, where lower temperatures are expected to take place in the network.

## 5.8 Ramp-up Rates

### 5.8.1 Objective

The objective of this task is to determine the proper flowrate ramp-ups and to examine the related slugging characteristics and liquid handling capabilities.

### 5.8.2 Setup

In this task, the point 02/01 is chosen to run flowrate ramp-up cases starting from the different turndown flowrates, considering 0% WC and 26% WC. The ramp-up cases will be set up to restart from the end of the turndown cases and run for 12 hours. The opening of the choke valves will increase at the beginning of the restart run from their initial values that correspond to the specific turndown flowrates to the values at the design flowrate.

First, choke openings will be allowed to increase immediately and simultaneously at the beginning of each run, and the liquid handling capabilities of the slug catcher will be examined at different drain rates. The liquid surge volume (SURGELIQ) into the slug catcher is calculated in OLGA based on the drain rate, and its maximum value is compared to the design surge capacity of 50 m<sup>3</sup> as mentioned in 3.2.4. If the maximum SURGELIQ exceeds 50 m<sup>3</sup>, it means that the drain rate is not sufficient to avoid surging the slug catcher.

To assume some realistic drain rates, a number of commercially available control valves were considered. Table 44 lists different valve designs from Kimray Inc. up to 4" that could be installed downstream the slug catcher [35], in addition to the maximum liquid drain rates at different pressure values downstream the valves, as calculated using Kimray's online valve sizing tool [36]. The pressure upstream the valves is the pressure in the slug catcher, which is 45 barg. However, there is no available information about the operating pressures of the separator downstream the slug catcher, and therefore different pressure values were considered.

Table 44 – Slug catcher drain rates for different control valve designs

#	Flange size [in]	Trim size [in]	Max C <sub>v</sub> [gpm/psi <sup>1/2</sup> ]	Slug catcher maximum drain rate [bbl/d] at downstream pressure of:			
				1 barg	20 barg	30 barg	40 barg
1	2, 3	1.5	28.6	17,754	17,262	13,371	7,720
2	2, 3	2.0	57.0	35,384	34,404	26,649	15,386
3	3	3.0	107.0	66,423	64,582	50,025	28,882
4	4	3.0	115.0	71,389	69,411	53,766	31,042
5	4	4.0	222.0	137,812	133,993	103,791	59,924

If the drain rates required to avoid surging the slug catcher exceed those that could be achieved with the valves in Table 44, a slower ramp-up rate will need to be determined to avoid surging the slug catcher. This makes a minimum of 8 cases to be run in the task. Eventually, it is up to the operator to decide whether to use a larger drain valve or to adopt a slower ramp-up rate.

### 5.8.3 Results

Instead of calculating SURGELIQ at all the drain rates listed in Table 44, only a few representative values are considered. In addition, OLGA calculates the average liquid flowrate exiting the pipeline ( $QLT_{out}$ ) over the whole period of the run and SURGELIQ is initially calculated by default using this average value as the drain rate. Table 45 lists the maximum SURGELIQ at different slug catcher drain rates for all the cases. Maximum SURGELIQ values that exceed the slug catcher design capacity of  $50 \text{ m}^3$  (314.5 bbl) are formatted in **bold**.

Table 45 – Maximum SURGELIQ during ramp-up at different slug catcher drain rates

Case	Average $QLT_{out}$ [bbl/d]	Maximum SURGELIQ [bbl] ( $\text{m}^3$ ) at slug catcher drain rate of:				
		Average $QLT_{out}$	15,000 bbl/d	20,000 bbl/d	30,000 bbl/d	50,000 bbl/d
WC0_80	13,255	51 (8.1)	0 (0.0)	0 (0.0)	0 (0.0)	0 (0.0)
WC0_60	13,574	117 (18.6)	25 (4.0)	13 (2.1)	6 (1.0)	0 (0.0)
WC0_40	14,228	251 (39.9)	153 (24.3)	11 (1.8)	2 (0.4)	0 (0.0)
WC0_20	15,238	<b>524 (83.3)</b>	<b>555 (88.3)</b>	174 (27.6)	6 (0.9)	0 (0.0)
WC26_80	15,941	53 (8.4)	<b>&gt;487 (77.4)*</b>	14 (2.2)	7 (1.1)	0 (0.0)
WC26_60	16,224	141 (22.5)	<b>&gt;639 (101.6)*</b>	17 (2.7)	9 (1.4)	0 (0.0)
WC26_40	16,784	258 (41.0)	<b>&gt;918 (145.9)*</b>	22 (3.5)	9 (1.4)	0 (0.0)
WC26_20	17,814	<b>491 (78.1)</b>	<b>&gt;1421 (226.0)*</b>	275 (43.7)	23 (3.7)	10 (1.5)

\*SURGELIQ was still increasing with time at the end of the 12-hour runtime

The table shows that a drain rate of 20,000 bbl/d is sufficient to handle the liquid volumes entering the slug catcher for all the cases. Such rate could be achieved using a valve with a trim size of 2" or 3", depending on the pressure downstream the valve.

### 5.8.4 Discussion: Slugging Characteristics

To take a look at the slugging behavior in this task, ramping up from 20% turndown flowrate at 0% WC (WC0\_20) is considered. In the discussion of task 5.3, it was recommended not to go down to such low flowrate to ensure a stable flow of gas and liquids into the slug catcher. This case is considered here because at this low flowrate the liquid holdup in the branches is relatively high, and the slugging behavior during ramp-up will be easy to capture and describe.

Fig. 42 shows the liquid holdup in the trunk-line in the OlgaViewer tool during ramp-up at 20-minute intervals until the gas and liquid flow into the slug catcher became stable. The time starts from 720 minutes (12 hours) because it continues from the end of the turndown case that was run for 12 hours.

The clear variation in the liquid holdup between the different sections of the trunk-line at the beginning of the run is due to the geometry of the line, which is not captured in the figure, where the trunk-line has been flattened horizontally. The arrows in the figure indicate a clear movement of slug fronts during ramp-up as observed in the OlgaViewer animation.

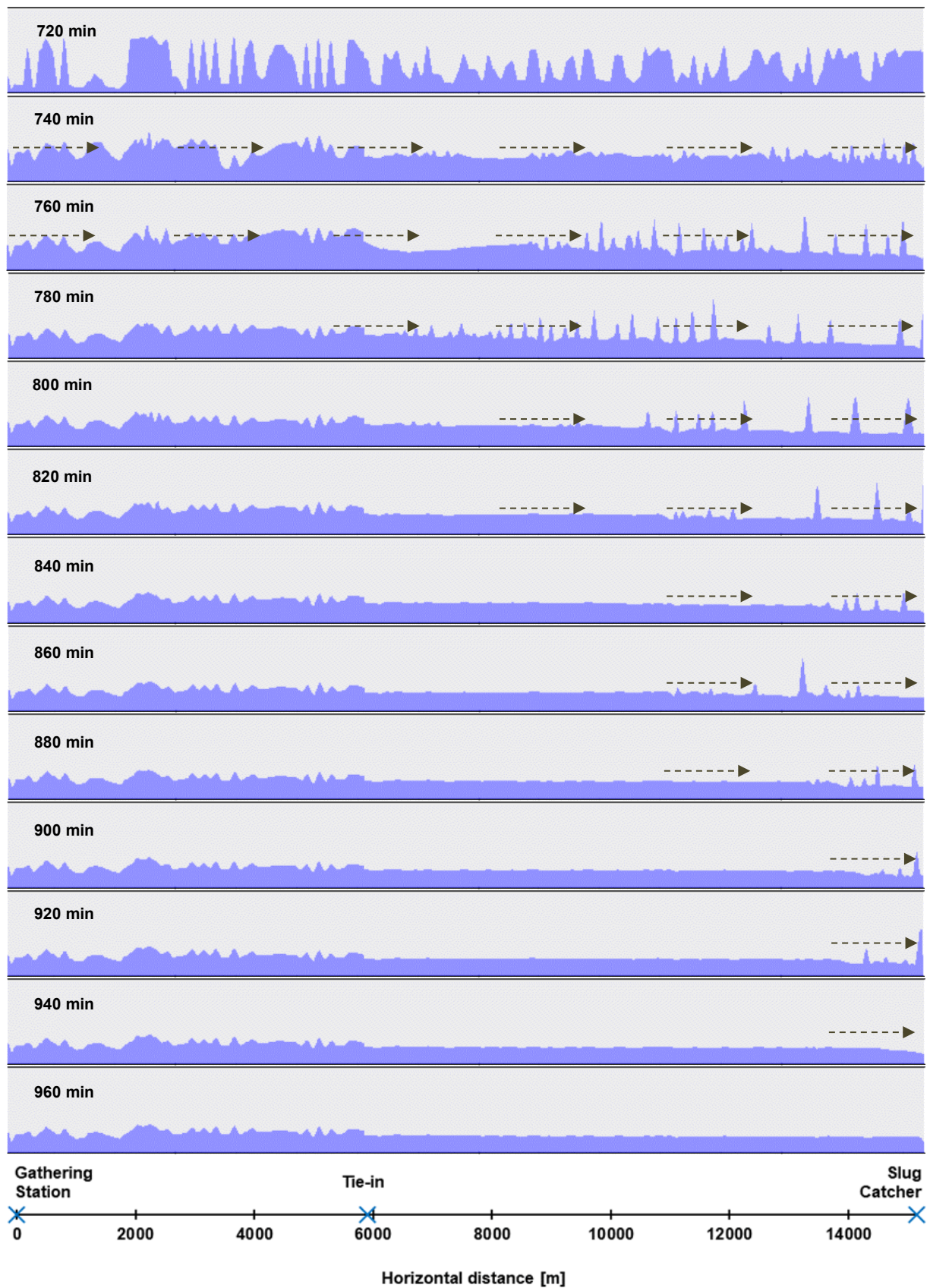


Fig. 42 – Liquid holdup in the trunk-line during ramp-up from 20% turndown at 0% WC

At the beginning of ramp-up, slugs are created and transferred along the whole trunk-line. The slugs are fast, and frequently created; especially in the second half of the line. As ramp-up continues, the slug flow becomes observed only closer and closer to the trunk-line outlet

while the rest of the line stabilizes at a stratified flow regime. The length of the slugs passing a control point located in a relatively flat part of the trunk-line that is located 250 m upstream the slug catcher ranges from 35-120 m. The snapshot at 960 min shows the liquid holdup in the trunk-line at the design flowrate.

Note that the choke valves were ramped up in around one minute only, and the flowrates of the wells at the wellheads reached their design rate in the simulation model in about the same time, but it eventually took around four hours for the gas condensate arriving at the slug catcher to stabilize at the design flowrate.

Fig. 43 shows the surge volume into the slug catcher at drain rates of 15,000 bbl/d, 15,238 bbl/d; which is the average liquid flowrate into the slug catcher during the run, and 20,000 bbl/d. As reported in Table 45, the maximum surge volume is below the design surge capacity of the slug catcher at the drain rate of 20,000 bbl/d, but not at the other two. The liquid flowrate at the outlet of the trunk-line shows some spikes that go up to 80,000-100,000 bbl/d.

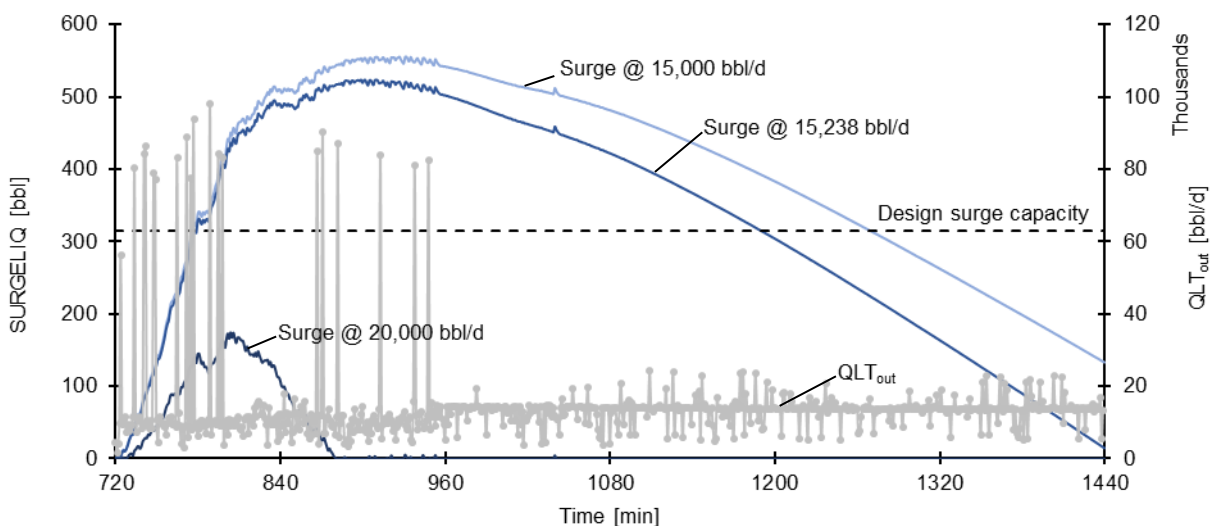


Fig. 43 – SURGELIQ during ramp-up from 20% turndown at different drain rates

Appendix I shows the surge volume at different slug catcher drain rates for all the cases that were run in this task, and the liquid flowrate at the outlet of the trunk-line.



## 5.9 Pigging

### 5.9.1 Objective

The objective of this task is to determine a proper pigging speed that avoids surging the slug catcher, and to examine the related slugging characteristics and liquid handling capabilities.

### 5.9.2 Setup

In this task, the point 02/01 is chosen to run the pigging cases for all the network branches at different well turndown flowrates, considering 0% WC and 26% WC, except for FL\_04 that is planned to be flushed instead.

Typical velocities for utility pigs are in the range of 2-7 m/s in the case of on-stream gas, and 1-5 m/s in the case of on-stream liquids [8]. In this task, pigging velocities will be examined in order to maintain them below 7 m/s to avoid frictional heating that might result in the damage of pig components or aquaplaning that can decrease the pigging performance. All cases will be run first at the design flowrate. If at a given flowrate, the pig velocity is not below 7 m/s, a lower turndown flowrate will need to be examined.

Cases will be run for seven hours. All the cases will start while the wells are producing at their design rate. The well whose flowline is going to be pigged at a lower flowrate will be choked down after 30 minutes to this rate, and pigging will be commenced 30 minutes later.

In the case of pigging the trunk-line at a turndown flowrate, all the wells will be choked down simultaneously after 30 minutes from the beginning of the run, and the pig will be launched one hour later to allow for enough time to reduce the flowrate in the trunk-line for pig velocity control. While choking all the wells might not be a practical procedure for pigging the trunk-line, it intends to simulate the pigging at different velocities; not to find exactly which wells shall best be choked down to perform the pigging.

The liquid handling capabilities of the slug catcher will be examined at different drain rates that are representative of the values in Table 44, as explained in the previous task 5.8. The liquid surge volume (SURGELIQ) into the slug catcher is calculated in OLGA based on the drain rate, and its maximum value is compared to the design surge capacity of 50 m<sup>3</sup>. If the maximum SURGELIQ exceeds 50 m<sup>3</sup>, it means that the drain rate is not sufficient to avoid surging the slug catcher.

If the drain rates required to avoid surging the slug catcher exceed those that could be achieved with the valves in Table 44, a different pigging procedure will need to be determined.

### 5.9.3 Results

Table 46 lists the average pig velocity ( $UPIG_{avg}$ ) as it travels along a branch and the maximum pig velocity encountered during its travel ( $UPIG_{max}$ ). Velocity values equal to or exceeding 7 m/s are formatted in **bold**.

Table 46 – Average and maximum pig velocities

Case	PL_1		PL_2		FL_01	
	UPIG <sub>avg</sub>	UPIG <sub>max</sub>	UPIG <sub>avg</sub>	UPIG <sub>max</sub>	UPIG <sub>avg</sub>	UPIG <sub>max</sub>
	[m/s]	[m/s]	[m/s]	[m/s]	[m/s]	[m/s]
WC0_100	3.1	3.3	5.3	<b>10.2</b>	2.1	2.2
WC0_80	2.7	2.9	4.4	<b>7.0</b>	-	-
WC0_60	2.2	2.4	3.5	6.4	-	-
WC26_100	3.2	3.3	5.4	<b>10.0</b>	2.1	2.2
WC26_80	2.8	3.1	4.6	<b>8.0</b>	-	-
WC26_60	2.3	2.6	3.6	6.3	-	-

Case	FL_02		FL_03		FL_05	
	UPIG <sub>avg</sub>	UPIG <sub>max</sub>	UPIG <sub>avg</sub>	UPIG <sub>max</sub>	UPIG <sub>avg</sub>	UPIG <sub>max</sub>
	[m/s]	[m/s]	[m/s]	[m/s]	[m/s]	[m/s]
WC0_100	1.9	2.2	3.0	3.6	1.5	1.6
WC26_100	1.9	2.3	3.1	3.8	1.5	1.6

For pigging the trunk-line, the flowrate had to be turned down to 60% of the design rate to achieve pigging velocities below 7 m/s. The flowlines, though, could be pigged at the design flowrate without concerns about the pigging velocity.

As in the previous case 5.8, four different slug catcher drain rates, based on Table 44, are considered to calculate the surge volume into the slug catcher (SURGELIQ), in addition to OLGA's default calculations at the average liquid flowrate exiting the pipeline (QLT<sub>out</sub>) over the whole period of the run. Table 47 lists the maximum SURGELIQ at different slug catcher drain rates for all the cases. Maximum SURGELIQ values that exceed the slug catcher design capacity of 50 m<sup>3</sup> (314.5 bbl) are formatted in **bold**.

Table 47 – Maximum SURGELIQ during pigging at different slug catcher drain rates

PL						
Case	Average QLT <sub>out</sub> [bbl/d]	Maximum SURGELIQ [bbl] (m <sup>3</sup> ) at slug catcher drain rate of:				
		Average	15,000	20,000	30,000	50,000
		QLT <sub>out</sub> [bbl/d]	bbl/d	bbl/d	bbl/d	bbl/d
WC0_100	12,897	<b>394 (62.7)</b>	<b>384 (61.1)</b>	<b>360 (57.2)</b>	311 (49.5)	214 (34.0)
WC0_80	10,589	<b>419 (66.6)</b>	<b>397 (63.2)</b>	<b>373 (59.3)</b>	<b>325 (51.8)</b>	242 (38.5)
WC0_60	7,938	<b>481 (76.5)</b>	<b>411 (65.3)</b>	<b>383 (60.9)</b>	<b>327 (52.1)</b>	228 (36.3)
WC26_100	15,529	<b>452 (71.9)</b>	<b>456 (72.5)</b>	<b>425 (67.5)</b>	<b>362 (57.6)</b>	250 (39.8)
WC26_80	12,863	<b>482 (76.6)</b>	<b>469 (74.5)</b>	<b>437 (69.5)</b>	<b>375 (59.6)</b>	260 (41.3)
WC26_60	9,779	<b>558 (88.7)</b>	<b>494 (78.6)</b>	<b>463 (73.6)</b>	<b>400 (63.7)</b>	283 (45.0)

FL_01						
Case	Average QLT <sub>out</sub> [bbl/d]	Maximum SURGELIQ [bbl] (m <sup>3</sup> ) at slug catcher drain rate of:				
		Average	15,000	20,000	30,000	50,000
		QLT <sub>out</sub> [bbl/d]	bbl/d	bbl/d	bbl/d	bbl/d
WC0_100	12,888	27 (4.3)	15 (2.3)	9 (1.4)	2 (0.3)	0 (0.0)
WC26_100	15,510	52 (8.3)	149 (23.6)	35 (5.5)	21 (3.4)	8 (1.2)

FL_02						
Case	Average QLT <sub>out</sub> [bbl/d]	Maximum SURGELIQ [bbl] (m <sup>3</sup> ) at slug catcher drain rate of:				
		Average QLT <sub>out</sub>	15,000 bbl/d	20,000 bbl/d	30,000 bbl/d	50,000 bbl/d
WC0_100	12,893	113 (18.0)	79 (12.6)	22 (3.5)	1 (0.2)	0 (0.0)
WC26_100	15,543	138 (22.0)	190 (30.3)	79 (12.6)	6 (0.9)	0 (0.0)

FL_03						
Case	Average QLT <sub>out</sub> [bbl/d]	Maximum SURGELIQ [bbl] (m <sup>3</sup> ) at slug catcher drain rate of:				
		Average QLT <sub>out</sub>	15,000 bbl/d	20,000 bbl/d	30,000 bbl/d	50,000 bbl/d
WC0_100	12,888	39 (6.2)	21 (3.3)	8 (1.3)	0 (0.0)	0 (0.0)
WC26_100	15,511	65 (10.4)	149 (23.7)	39 (6.2)	9 (1.5)	0 (0.0)

FL_05						
Case	Average QLT <sub>out</sub> [bbl/d]	Maximum SURGELIQ [bbl] (m <sup>3</sup> ) at slug catcher drain rate of:				
		Average QLT <sub>out</sub>	15,000 bbl/d	20,000 bbl/d	30,000 bbl/d	50,000 bbl/d
WC0_100	12,889	22 (3.6)	16 (2.5)	10 (1.5)	3 (0.4)	0 (0.0)
WC26_100	15,510	47 (7.6)	149 (23.7)	31 (4.9)	19 (3.0)	5 (0.8)

The table shows that pigging the flowlines does not represent any challenge to the liquid handling capability of the slug catcher at relatively low drain rates. However, for pigging the trunk-line, drain rates between 30,000 bbl/d and 50,000 bbl/d were required to avoid surging the slug catcher.

#### 5.9.4 Discussion: Slugging Characteristics

To take a look at the slugging behavior in this task, the case where the trunk-line was pigged after going down to 60% turndown flowrate at 0% WC (WC0\_60) is considered. Fig. 44 shows the liquid holdup in the trunk-line in the OlgaViewer tool during pigging at 10-minute intervals, starting from pig launch until the pig is trapped in the pig receiver, then at 30-minute intervals until the flow into the slug catcher has stabilized. Note that in practice, flowrate would have been ramped up again right after the pig has been trapped.

After the pig is launched, it continues to build a large slug in front of it as it travels down the trunk-line until it is trapped. A control point located in a relatively flat part of the trunk-line 250 m upstream the slug catcher witnesses one slug during the pigging that is around 1730 meters long. Compare this to the ramp-up task 5.8, where a lot of slugs were created and the longest one was 120 meters long.

Fig. 45 shows the surge volume into the slug catcher for this case at drain rates of 15,000 bbl/d, 30,000 bbl/d, and 50,000 bbl/d. As reported in Table 47, the 30,000 bbl/d drain rate resulted in a maximum surge volume that is only 1.8 m<sup>3</sup> above the design surge capacity of the slug catcher, and the 50,000 bbl/d drain rate was more than enough to avoid surging the slug catcher. In fact, a slug catcher drain rate of 32,500 bbl/d was found to be sufficient to avoid surging the vessel in this case. The liquid flowrate at the outlet of the trunk-line shows

a rapid surge that goes from 4000 bbl/d to 145,000 bbl/d in seven minutes before it drops again in one minute.

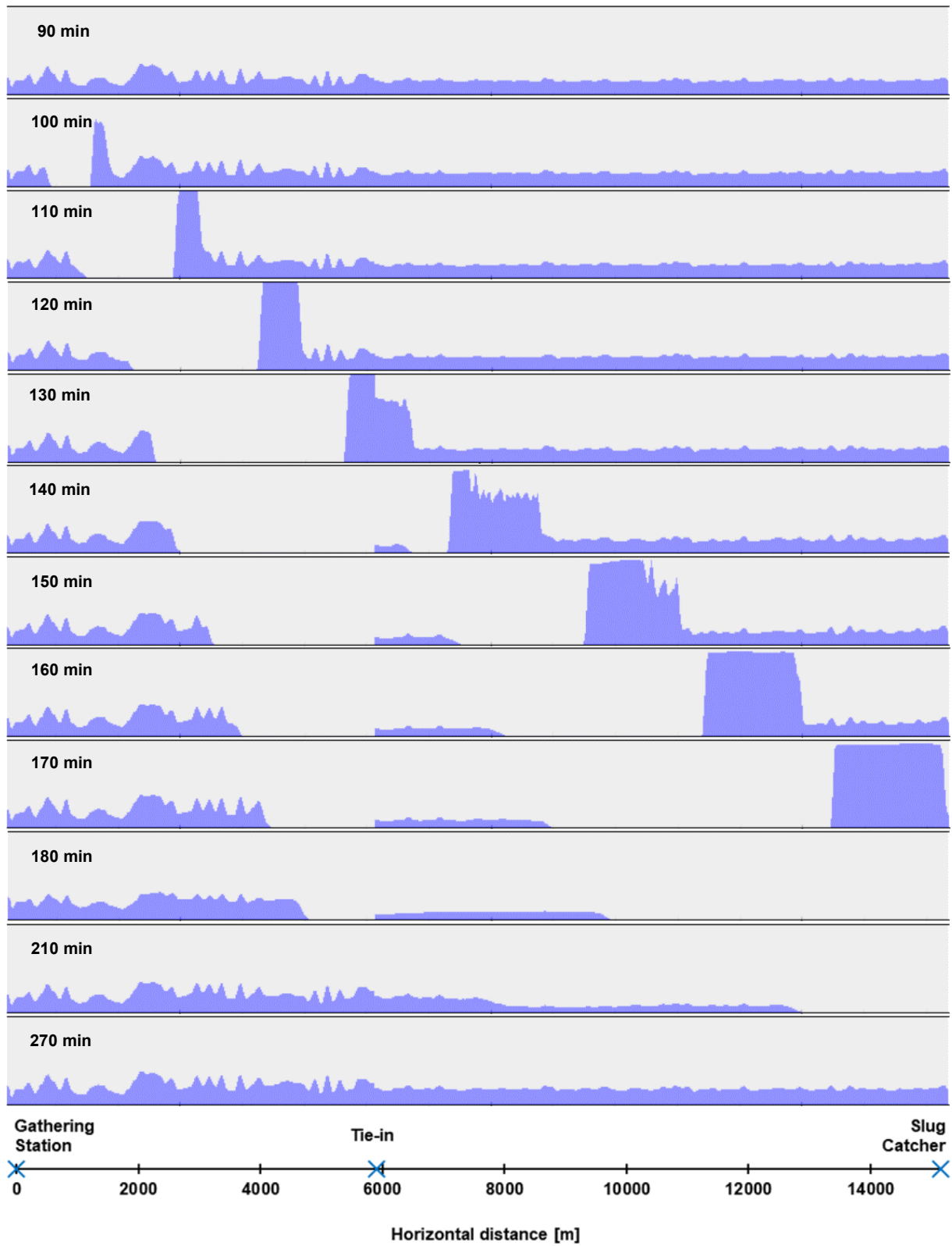


Fig. 44 – Liquid holdup in the trunk-line during pigging at 60% turndown flowrate

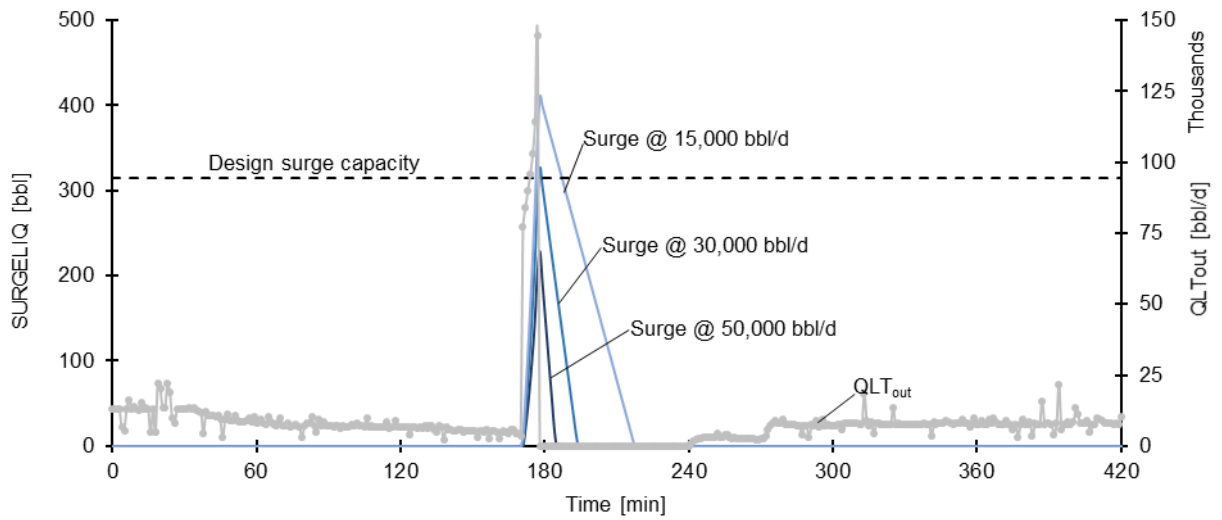


Fig. 45 – SURGELIQ during pigging the trunk-line at 60% turndown and different drain rates

Appendix J shows the surge volume at different slug catcher drain rates for all the cases that were run in this task, and the liquid flowrate at the outlet of the trunk-line.

## 5.10 Pipeline Packing

### 5.10.1 Objective

The objective of this task is to perform a pipeline packing analysis and determine the time required to reach pipeline and equipment design pressure of 100 barg.

### 5.10.2 Setup

In this task, the point 02/01 is chosen to run pipeline packing cases starting from the different turndown flowrates and considering 0% WC and 26% WC. The cases will be set up to restart from the end of the turndown cases and run for 12 hours. The SDV upstream the slug catcher will be closed at the beginning of the runs, and the opening of the choke valves will remain fixed at their initial values allowing the produced fluids to continue to flow into the pipeline network, resulting in a continuous increase in the network pressure.

On each flowline, a valve is installed at the wellhead to resemble the wing valve (WV) of the X-mas tree, a transmitter is installed downstream the choke valve to measure the pressure at this point, and an emergency shutdown (ESD) controller is set up to shut down the WV as soon as the pressure measured by the transmitter reaches the design pressure of the pipeline at 100 barg. Fig. 46 shows how the pipeline network in OLGA looks like in this task. This task consists of a total of 5 turndown cases x 2 WCs = 10 cases.

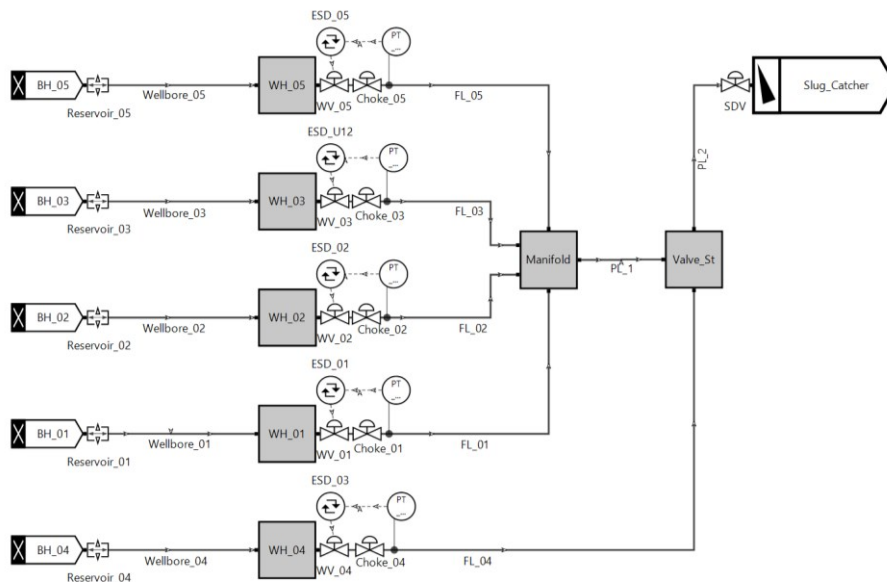


Fig. 46 – Network schematic in OLGA with WVs and ESD

### 5.10.3 Results

Table 48 lists the results of the runs showing the time it takes each flowline to reach the pipeline design pressure downstream the chokes during a process shutdown.

Table 48 – Time until pipeline design pressure is reached during a process shutdown

Case	Time to reach design pressure downstream the choke [min]				
	Well_01	Well_02	Well_03	Well_04	Well_05
WC0_100	770	770	769	771	771
WC0_80	791	790	790	793	791
WC0_60	822	821	821	826	822
WC0_40	875	873	875	884	876
WC0_20	1021	1022	1020	1040	1021
WC26_100	761	760	760	762	761
WC26_80	778	777	778	781	779
WC26_60	806	805	806	811	807
WC26_40	855	853	854	863	855
WC26_20	991	988	989	1013	992





## 6 Conclusion

### 6.1 Summary

The thesis provided a flow assurance (FA) study of a gas condensate pipeline network that is planned to be constructed onshore in a continental climate with extreme ambient conditions. The design basis of the gas condensate field (GCF) was summarized and served as the input to the FA study. Building a preliminary simulation model in OLGA was discussed that was used to set up and run the different simulation cases of the FA study. The simulation cases were then covered: the objective of each case, the model set-up, and the simulation results were presented, and different approaches for simulating the cases were examined.

### 6.2 Building the Model

Multiflash was used to create the PVT tables for OLGA. The effect of condensate drop-out in the reservoir on the composition of the gas condensate flowing into the network was approximated to enable the simulation of the pipeline network in different points over the life of the field. Different hydrate tables were created for the gas condensate at varying concentrations of methanol and taking into account the effects of formation water production, the salinity of produced water, and the different gas condensate compositions on the hydrate formation conditions.

In addition to the pipeline sizes in the basis of design, more sizes were selected according to API Spec 5L to check their applicability, and different flowline insulation thicknesses were chosen to study their effect on hydrate and wax formation. Well IPRs were generated that could match the given production profiles, and well models were built to simulate the inflow to the simulation model. A choke model was defined with the help of the MFSizing tool for the prediction of pressure drop across the valves and, very importantly for the FA study, the flowlines inlet temperatures. 2D heat transfer was set up in OLGA for the pipelines using the FEMTherm module with optimized spatial and temporal discretization, and 1D heat transfer was set up for the well models. The effect of well path discretization on the geothermal gradient near the surface was examined, where the temperature at the surface was found to have very little effect on the top section of the geothermal gradient after discretization.

### 6.3 Results

- The pipeline sizes in the basis of design were confirmed, based on the pipeline pressure rating of 100 barg, and more sizes were proposed. If consistency in size within the trunk-line parts and the flowlines is required, 10 3/4" CS would be chosen for the trunk-line, and either 6" GRE or 6 5/8" CS would be chosen for the flowlines. If consistency is not required, Table 20 provides other possible combinations of line sizes.
- The pressures, temperatures, velocities, liquid hold-up, and flow regimes in the pipeline branches were determined based on the production profiles at different points in the lifetime of the field, and the results are listed in Table H.1.

- The predominant flow regimes and the liquid hold-ups in the flowlines and the trunk-line at different turndown rates were determined, as can be seen in Table H.2. It was found that to ensure a stable flow into the process, the flowrate needs to stay above 20% of its value at the design flowrate.
- At the operating pressure range in the network and 0 wt% methanol in the gas condensate, taking the produced water salinity into account has resulted in hydrate formation temperatures that are 12-13 °C below those where pure water content is assumed. This difference goes up to 16 °C at higher methanol wt%. This means that ignoring the salinity of the produced water would result in more conservative- and more expensive- measures to avoid hydrate formation in the network, like higher-than-necessary methanol injection flowrates and/or flowline insulation thicknesses.
- The methanol injection rates required to avoid hydrate formation in the pipeline network during production were estimated for the different turndown flowrates and the result are listed in Table H.4. Assuming a pure water content in the cases where formation water production takes place would lead to methanol requirements that are three to six times higher than those when the produced water salinity is accounted for.
- The methanol injection rates that would allow for the required no-touch time of 6 hours that is set by the operator were estimated and the results are given in Table H.6. Assuming a pure water content in the cases where formation water production takes place would lead to methanol requirements that are three to seven times higher than those when the produced water salinity is accounted for.
- The required flowline insulation thicknesses that could prevent hydrate and/or wax formation during production were checked under the different turndown flowrates and the results are summarized in Table 39. No insulation could totally prevent hydrate or wax formation in the network at flowrates that are 60% of the design flowrate or lower when no water production takes place. At 26% WC, none of the proposed flowline insulation thicknesses could prevent hydrate or wax formation at 40% turndown flowrates or lower. In these cases, active hydrate inhibition by methanol injection is also required.
- The flowline insulation thicknesses that would allow for the required no-touch time of 6 hours that is set by the operator were checked and the results are summarized in Table 43. The results show that hydrate and wax formation cannot be avoided exclusively by passive inhibition when shutdown commences at flowrates that are below the design flowrate when no water production takes place. A combination of passive and active hydrate inhibition is required.
- Flowrate ramp-ups were simulated from the different turndown rates to the design rate, the slug catcher's liquid handling capabilities were examined, and the results are summarized in Table 45. A slug catcher drain rate of 20,000 bbl/d was found sufficient to handle the liquid volumes entering the slug catcher when ramp-up is carried out immediately and simultaneously in all the wells. Such rate could be achieved using a drain valve from the ones proposed in Table 44 with a trim size of 2" or 3", depending on the pressure downstream the valve. The slugging behavior during ramp-up from 20% turndown flowrate was examined. Slugs were frequently

created in the second half of the trunk-line particularly, and their lengths, as observed from a point upstream the slug catcher, were 35-120 m.

- Pipeline pigging was simulated for the different network branches to determine proper pigging velocities that would avoid surging the slug catcher, the liquid handling capabilities of the slug catcher were examined, and the results are listed in Table 46 and Table 47. Pigging velocities were meant to be maintained below 7 m/s to avoid frictional heating or aquaplaning. All the flowlines could be pigged at the design flowrates at proper velocities and without any challenge to the liquid handling capability of the slug catcher at relatively low drain rates. However, for pigging the trunk-line, the flowrate needed to be turned down to below 80% of the design rate to keep the pig velocity below 7 m/s, and drain rates between 30,000 bbl/d and 50,000 bbl/d were required to avoid surging the slug catcher. The slugging behavior during pigging the trunk-line at 60% turndown flowrate was examined. The pig continued to build a large slug in front of it as it travelled down the trunk-line that grew to a length of 1730 m, as observed from a point upstream the slug catcher.
- Packing analysis was performed during a process shutdown at the slug catcher for the different turndown flowrates, and the times it took to reach the pipeline and equipment design pressure of 100 barg in all the flowlines were observed. This ranged from 760-1040 minutes, as reported in Table 48.

## 6.4 Remarks

- The API RP-14E erosional velocity equation was found to have underpredicted the erosional velocity in some cases in the literature and overpredicted it in other cases. The origin of the equation is subject of controversy and many have questioned the validity of its use. Therefore, the equation was not chosen as a criterion for pipeline size selection in this FA study.
- Mass sources were found to be able to simulate steady-state production to a good level of accuracy and resulted in a faster runtime compared to the cases with integrated well models. However, well models were still needed to run separately to predict the wellhead conditions that were used to define the mass sources, which reduced the value of the mentioned faster runtime. Special care should be paid to setting up the cases with mass sources if their flow is intended to be choked.
- Using the black-oil model to simulate the gas condensate, for which it is not intended, resulted in liquid flowrates that are 25% lower on average than those in the compositional model under the in-situ conditions in the pipeline at the design flowrate, and temperatures profiles that are 1-9 °C lower. This would result in separator sizes and/or drain rates that are insufficient to handle the actual liquid flowrates in the network, and in hydrate inhibition requirements that are higher than necessary.
- In the turndown cases where no transient phenomenon was initially intended to be simulated, the solution of the steady-state pre-processor down to 40% turndown flowrate matched that of the transient simulation at the end of the runs. The added value of the time-consuming transient simulation was to demonstrate the slight fluctuations in the liquid and gas flowrates that the pre-processor naturally cannot

capture. When the flowrate became significantly unstable at lower flowrates, the solution of the pre-processor was invalid, and the transient simulation was indispensable. In general, the steady-state simulation can be used when there is confidence in the stability of the variables, and its results can be trusted as long as the solution converges.

- Methanol injection calculations were performed in Excel to come up with the required methanol injection flowrates to avoid hydrate formation by a margin of 5 °C, and the results were validated against a simulation case in OLGA at the design flowrate. The Excel calculation method was proven to give valid results, and the 5 °C margin used was found to be a good choice to account for the uncertainty in the calculations.
- The temperature profiles in the pipeline network while activating the inhibitor tracking module (COMPOSITIONAL = MEOH) were found to be lower than OLGA's default calculations without any component tracking (COMPOSITIONAL = OFF).
- Using 1D heat transfer calculations for the pipeline network resulted in lower temperature profiles, higher liquid flowrates, and higher liquid contents in the branches compared to 2D heat transfer with the FEMTherm module, and hydrate and wax were found to have formed under flowline insulation thicknesses that could actually manage to prevent their formation. This would lead to methanol injection requirements, especially under water production, and flowline insulation thicknesses that are higher than necessary.
- The runtime of the different cases that were performed for this FA study is provided in Appendix K.

---

## References

- [1] T. Y. Makogon, *Handbook of Multiphase Flow Assurance*, Cambridge, MA: Gulf Professional Publishing, 2019.
- [2] J. P. Brill and E. M. Al-Safran, *Applied Multiphase Flow in Pipes and Flow Assurance*, Richardson, TX: Society of Petroleum Engineers, 2017.
- [3] T. Bikmukhametov and J. Jäschke, "First Principles and Machine Learning Virtual Flow Metering: A Literature Review," *Journal of Petroleum Science and Engineering*, vol. 184, January 2020.
- [4] M. Shippen and W. Bailey, "Steady-State Multiphase Flow—Past, Present, and Future, with a Perspective on Flow Assurance," *Energy & Fuels*, vol. 26, no. 07, pp. 4145-4157, 08 June 2012.
- [5] J. P. Brill and S. J. Arirachakaran, "State of the Art in Multiphase Flow," *Journal of Petroleum Technology*, vol. 44, no. 05, pp. 538 - 541, May 1992.
- [6] OLGA 2018 [Version 2018.1] User Manual, Schlumberger, 2018.
- [7] C. A. Koh, E. D. Sloan, A. K. Sum and D. T. Wu, "Fundamentals and Applications of Gas Hydrates," *Annual Review of Chemical and Biomolecular Engineering*, vol. 2, pp. 237-257, 08 March 2011.
- [8] J. Cordell and H. Vanzant, *The Pipeline Pigging Handbook*, Houston, TX: Clarion Technical Publishers and Scientific Surveys Ltd, 2003.
- [9] "OptionAll™ Pigs," January 2007. [Online]. Available: <http://www.tdwilliamson.com/content/Bulletins/OptionAll%20Cleaning%20Pigs.pdf>.
- [10] I. N. Forsdyke, "Flow Assurance in Multiphase Environments," in *International Symposium on Oilfield Chemistry*, Houston, TX, 18-21 February 1997.
- [11] K. G. Jordan, "Erosion in Multiphase Production of Oil & Gas," in *CORROSION 98*, San Diego, CA, 22-27 March 1998.
- [12] F. M. Sani, S. Nesic, K. Esaklul and S. Huizinga, "Review of the API RP 14E Erosional Velocity Equation: Origin, Applications, Misuses and limitations," in *CORROSION 2019*, Nashville, Tennessee, 24-28 March 2019.
- [13] M. Dular, T. Požar, J. Zevnik and R. Petkovšek, "High speed observation of damage created by a collapse of a single cavitation bubble," *Wear*, Vols. 418-419, pp. 13-23, 08

November 2018.

- [14] Recommended Practice RP O501: Erosive Wear in Piping Systems, Det Norske Veritas (DNV), 2011.
- [15] "GAP," Petroleum Experts Ltd., 2015. [Online]. Available: <https://www.petex.com/media/2274/gap-brochure.pdf>.
- [16] "Raw natural gas," Schlumberger, 26 May 2017. [Online]. Available: [https://www.glossary.oilfield.slb.com/en/Terms/r/raw\\_natural\\_gas.aspx](https://www.glossary.oilfield.slb.com/en/Terms/r/raw_natural_gas.aspx).
- [17] D. Thompson, "Characteristics of Sandy Loam Soil," 09 December 2018. [Online]. Available: <https://homeguides.sfgate.com/characteristics-sandy-loam-soil-50765.html>.
- [18] "Choke Valve Sizing Software & App," 2018. [Online]. Available: <https://www.masterflo.com/en/resources/choke-valve-sizing-software-app/>.
- [19] OLGA Flow Assurance Workflow/Solutions Training, Schlumberger Software Integrated Solutions (SIS), 2018.
- [20] R. J. Wheaton and H. R. Zhang, "Condensate Banking Dynamics in Gas Condensate Fields: Compositional Changes and Condensate Accumulation Around Production Wells," in *SPE Annual Technical Conference and Exhibition*, Dallas, TX, 1-4 October, 2000.
- [21] Multiflash User Guide for Models and Physical Properties [Version 7.0], Walton on Thames, Surrey, UK: KBC Advanced Technologies Ltd, 2017.
- [22] M. Moshfeghian, "Quick Determination of the Methanol Injection Rate for Natural-Gas Hydrate Inhibition," PetroSkills, 01 April 2009. [Online]. Available: <http://www.jmcampbell.com/tip-of-the-month/2009/04/quick-determination-of-the-methanol-injection-rate-for-natural-gas-hydrate-inhibition/>.
- [23] E. D. Solan and C. A. Koh, *Clathrate Hydrates of Natural Gases*, Boca Raton, FL: CRC Press, Taylor & Francis Group, LLC, 2008.
- [24] B. Edmonds, R. A. S. Moorwood and R. Szczepanski, "A Practical Model for the Effect of Salinity on Gas Hydrate Formation," in *European Production Operations Conference and Exhibition*, Stavanger, Norway, 16-17 April, 1996.
- [25] API SPECIFICATION 5L: Specification for Line Pipe, Washington, DC: American Petroleum Institute (API), 2004.
- [26] "STAR Fiberglass Pipe," July 2016. [Online]. Available: <https://www.nov.com/-/media/nov/files/products/caps/fiber-glass-systems/star-fiberglass-pipe/star-super-seal->

---

api-15hr-design-data-sheet.pdf.

- [27] EN 253:2009 (E): District heating pipes - Preinsulated bonded pipe systems for directly buried hot water networks - Pipe assembly of steel service pipe, polyurethane thermal insulation and outer casing of polyethylene, Brussels: European Committee for Standardization (CEN), 2009.
- [28] H. Deng, J. Ramos and P. Yang, "Thermal Properties of a Glass Fiber Filled Epoxy (Sumitomo E264H)," in *The Rio Grande Symposium on Advanced Materials*, Albuquerque, NM, 2 October 2015.
- [29] Thermal insulation materials made of rigid polyurethane foam (PUR/PIR), Brussels: Federation of European Rigid Polyurethane Foam Associations (PU Europe), 2006.
- [30] K. A. Thakare, H. G. Vishwakarma and A. G. Bhave, "Experimental Investigation of Possible Use of HDPE as Thermal Storage Material in Thermal Storage Type Solar Cookers," *International Journal of Research in Engineering and Technology*, vol. 4, no. 12, pp. 92-99, December 2015.
- [31] Y. Dong, J. S. McCartney and N. Lu, "Critical Review of Thermal Conductivity Models for Unsaturated Soils," *Geotechnical and Geological Engineering*, vol. 33, no. 2, pp. 207-221, 13 January 2015.
- [32] "P3E Choke Valve," 2018. [Online]. Available: <https://www.masterflo.com/en/products/choke-valves/p3e-choke-valve/>.
- [33] "KLINGER Ballostar® KHI ball valves," 2017. [Online]. Available: [https://www.klinger.kfc.at/en/ballostar-khi?file=files/KLINGER\\_Fluid\\_Control/downloads/kugelhahn/Produktkatalog-KHI-EN.pdf](https://www.klinger.kfc.at/en/ballostar-khi?file=files/KLINGER_Fluid_Control/downloads/kugelhahn/Produktkatalog-KHI-EN.pdf).
- [34] API RP 14E: Recommended Practice for Design and Installation of Offshore Production Platform Piping Systems, Washington, DC: American Petroleum Institute (API), 1991.
- [35] "High Pressure Cage Guided Balanced," Kimray Inc., 2020. [Online]. Available: <https://kimray.com/Products/SubItems/4>.
- [36] "Liquid Sizing (Simplified) and Product Selection," Kimray Inc., 2020. [Online]. Available: <https://kimray.com/Sizing/LiquidSimplified>.

## List of Tables

Table 1 – Expected range of gas flowrate for each well .....	19
Table 2 – Reservoir fluid composition .....	20
Table 3 – Parameters of pseudo-components.....	21
Table 4 – Chemical analysis of formation water .....	22
Table 5 – Design ambient parameters .....	25
Table 6 – Compatibility between fluid/solid models and PVT methods [6, p. 58] .....	29
Table 7 – Important dates in the GCF life.....	30
Table 8 – Reservoir pressure and GOR over time.....	31
Table 9 – wt% of methanol in different phases.....	37
Table 10 – Water mass fraction at different water production rates.....	37
Table 11 – Trunk-line and flowline dimensions for 100 barg rating pressure .....	42
Table 12 – Line dimensions including PUR-foam insulation and PE outer casing .....	43
Table 13 – Thermal properties of wall layers.....	44
Table 14 – Constants of backpressure inflow equation .....	48
Table 15 – Temperature calculation settings in OLGA [6, p. 91].....	48
Table 16 – FEMTherm time constant of different layers .....	51
Table 17 – FEMTherm ambient conditions.....	52
Table 18 – Input to ambient conditions in the well editor .....	52
Table 19 – Pressure and EVR of different branch sizes at maximum gas flowrate .....	58
Table 20 – Possible combinations of network line sizes .....	59
Table 21 – Well gas flowrate over time [yy/mm].....	62
Table 22 – Choke openings over time (after a one-hour run) .....	64
Table 23 – Pipeline parameters at 02/01.....	64
Table 24 – DTHYD calculations for pure and saline water content for different points in time .....	66
Table 25 – Wellhead conditions over time.....	68
Table 26 – Pressures and temperatures across the choke valves at 02/01_WA .....	69
Table 27 – Pipeline parameters at 02/01 (black-oil), and the differences between black-oil and compositional model solutions .....	70
Table 28 – Gas turndown flowrates.....	71



Table 29 – Choke opening for different turndown rates .....	72
Table 30 – Pipeline parameters at the design flowrates (transient) .....	73
Table 31 – DTHYD calculations for pure and saline water content at different turndown flowrates .....	76
Table 32 – Pipeline parameters at the design flowrate (steady-state), and the differences between steady-state and transient solutions .....	77
Table 33 – Methanol injection rates at the design flowrate .....	81
Table 34 – Methanol injection calculations in Excel for the case at design flowrate and 0% WC .....	82
Table 35 – Results of running the case WC0_100 in OLGA using inhibitor tracking .....	83
Table 36 – Pipeline parameters after a six-hour shutdown for the design flowrate .....	84
Table 37 – Methanol injection rates required for a no-touch time of six hours for the design flowrate .....	85
Table 38 – Pipeline parameters and methanol injection rates at the design flowrate, 0% WC, and 1.17" flowline insulation thickness .....	88
Table 39 – Hydrate and/or wax formation for different turndown flowrates under different insulations, and required methanol injection flowrates in kg/h for pure/saline water content.....	88
Table 40 – Pipeline parameters and methanol injection rates at the design flowrate, 0% WC, and 1.17" flowline insulation thickness, using 1D heat transfer .....	90
Table 41 – Hydrate and/or wax formation and required methanol injection flowrates in kg/h for pure/saline water content at design flowrate for 1D and 2D heat transfer .....	91
Table 42 – Pipeline parameters and methanol injection rates after a six-hour shutdown for the design flowrate, 0% WC, and 1.17" flowline insulation thickness.....	93
Table 43 – Hydrate and/or wax formation after a six-hour shutdown under different insulation thicknesses, and required methanol injection flowrates in kg/h for pure/saline water content.....	93
Table 44 – Slug catcher drain rates for different control valve designs.....	95
Table 45 – Maximum SURGELIQ during ramp-up at different slug catcher drain rates .....	96
Table 46 – Average and maximum pig velocities .....	100
Table 47 – Maximum SURGELIQ during pigging at different slug catcher drain rates.....	100
Table 48 – Time until pipeline design pressure is reached during a process shutdown .....	105

## List of Figures

Fig. 1 – Calculation process of pressure gradient. A modification of the figure in [2, p. 47] ....	4
Fig. 2 – Flow patterns in horizontal and slightly-inclined pipes [2, p. 48].....	5
Fig. 3 – Inertia vs Gravity matrix of flow patterns [2, p. 50] .....	6
Fig. 4 – Black-oil model. A modification of the figure in [2, p. 282].....	8
Fig. 5 – Compositional model [2, p. 314] .....	9
Fig. 6 – Evolution of Multiphase flow modelling [4, p. 4147] .....	9
Fig. 7 – Gas Hydrate Structures, from [7, p. 242] .....	12
Fig. 8 – Methane hydrate curves for a multiphase flow in a subsea pipeline [7, p. 244].....	12
Fig. 9 – Cleaning pigs [9] .....	13
Fig. 10 – Severe and terrain slugging [2, p. 194].....	15
Fig. 11 – Cavitation erosion [13, p. 14].....	16
Fig. 12 – Flow assurance (FA) workflow [2, p. 210].....	16
Fig. 13 – Production profile of the GCF's initial development plan.....	20
Fig. 14 – Hydrate formation curve and possible flowing operating conditions .....	22
Fig. 15 – Simplified layout of the GCF's pipeline network.....	23
Fig. 16 – Flowlines and trunk-line lengths in kilometers.....	24
Fig. 17 – Air and soil temperatures around the year .....	25
Fig. 18 – Procedure of calculating new fluid compositions .....	33
Fig. 19 – Composition of produced fluid over time.....	34
Fig. 20 – Hydrate curves (Multiflash vs Third-party) .....	34
Fig. 21 – Hydrate curves at different methanol wt% .....	35
Fig. 22 – Hydrate curves at different methanol wt% during formation water production.....	36
Fig. 23 – Hydrates curves at different water mass fractions .....	37
Fig. 24 – Hydrate curves at different methanol wt% during formation water production and considering water salinity.....	38
Fig. 25 – Hydrate curves at different compositions considering pure and saline water content .....	39
Fig. 26 – Hydrate curves at different compositions and 50 wt% methanol in pure water.....	40
Fig. 27 – Simulation network sketch.....	41
Fig. 28 – Cv curve for choke valve model P3 .....	45

---

Fig. 29 – Completion schematic of the well model.....	46
Fig. 30 – Procedure of matching the IPR models .....	47
Fig. 31 – Solid bundles around the trunk-line (left) and a flowline (right) .....	50
Fig. 32 – Geothermal gradients: before discretization (left), after discretization (middle), and after manual editing (right) .....	53
Fig. 33 – Network schematic in OLGA (base case).....	56
Fig. 34 – Network schematic in OLGA with well models.....	63
Fig. 35 – Network schematic in OLGA with mass sources (MS).....	68
Fig. 36 – Total liquid content in each of the branches at the different turndown flowrates, at 0% WC (left) and 26% WC (right). .....	74
Fig. 37 – QLT and QGST into the slug catcher at different turndown flowrates .....	75
Fig. 38 – Interpolating between hydrate curves (methanol wt%) .....	80
Fig. 39 – Required methanol flowrates for the whole network at 0% WC (left) and 26% WC (right), for both pure and saline produced water contents, at different turndown flowrates .....	81
Fig. 40 – Required methanol flowrates for the whole network for a no-touch time of six hours, at 0% WC (left) and 26% WC (right), and both pure and saline produced water contents .....	86
Fig. 41 – Trunk-line surroundings in 2D heat transfer (left) vs 1D heat transfer (right).....	89
Fig. 42 – Liquid holdup in the trunk-line during ramp-up from 20% turndown at 0% WC .....	97
Fig. 43 – SURGELIQ during ramp-up from 20% turndown at different drain rates.....	98
Fig. 44 – Liquid holdup in the trunk-line during pigging at 60% turndown flowrate.....	102
Fig. 45 – SURGELIQ during pigging the trunk-line at 60% turndown and different drain rates .....	103
Fig. 46 – Network schematic in OLGA with WVs and ESD.....	104

---

## Abbreviations

API	American Petroleum Institute
ASME	American Society of Mechanical Engineers
BHP	Bottom-hole Pressure
BHT	Bottom-hole Temperature
CGR	Condensate Gas Ratio
CPU	Central Processing Unit
CRA	Corrosion Resistant Alloy
CS	Carbon Steel
DST	Drill-Stem Test
EN	European Standard (Norm)
EoS	Equation of State
FA	Flow Assurance
FEED	Front-End Engineering Design
FEM	Finite Element Method
FL	Flowline
FLP	Flowline Pressure
FLT	Flowline Temperature
GCF	Gas Condensate Field
GCR	Gas Condensate Reservoir
GOR	Gas Oil Ratio
GRE	Glass Reinforced Epoxy
HDPE	High-density Polyethylene
HIPPS	High-Integrity Pressure Protection System
ID	Inner Diameter
IFE	Institute for Energy Technology
IPR	Inflow Performance Relationship
LGTM	Linear Gradient Theory Model
MS	Mass Source
MSFR	Minimum Stable Flow Rate
N/A	Not Applicable
OD	Outer Diameter
PC	Personal Computer
PE	Polyethylene
PL	Pipeline
PR78A	Peng-Robinson 1978 Advanced
PUR	Polyurethane
SA	Summer Average
SD	Summer Design
SDV	Shutdown Valve
SG	Specific Gravity

---

SPT	Scandpower Petroleum Technology
SR	Split Ratio
THI	Thermodynamic Hydrate Inhibitor
WA	Winter Average
WAT	Wax Appearance Temperature
WC	Water Cut
WD	Winter Design
WHP	Wellhead Pressure
WHT	Wellhead Temperature
WV	Wing Valve

## Nomenclature

$C$	Flow coefficient in IPR equation
$c$	Empirical constant in erosional velocity equation
$C_{avg}$	Mean of calculated flow coefficient vector
$C_{calc}$	Calculated flow coefficient vector
$C_D$	Discharge coefficient
$C_g$	Gas flow coefficient
$Cond_{drop}$	Condensate drop-out in miles
$Cond_{prod}$	Condensate produced in moles
$Cond_{res}$	Condensate remaining in reservoir in moles
$C_p$	Specific heat capacity
$C_v$	Liquid flow coefficient
$Gas_{prod}$	Gas produced in moles
$GC_{prod}$	Gas condensate produced in moles
$K_v$	Flow factor
$L$	Layer thickness
$L/F$	Liquid mole fraction (moles of liquid/total number of moles)
$\dot{m}_T$	Total mass flowrate
$n$	Deliverability constant
$p$	Pressure
$P_d$	Dewpoint pressure
$P_{res}$	Reservoir pressure
$P_{wf}$	Bottom-hole flowing pressure
$Q_{calc}$	Calculated flowrate vector
$q_g$	Gas flowrate
$q_L$	Liquid flowrate
$q_v$	Vapor flowrate
$R_s$	Gas solubility in oil
$R_{sw}$	Gas solubility in water
$T$	Temperature
$TC$	Time constant
$U_{ACTUAL}$	Actual fluid velocity
$U_{EROSIONAL}$	Erosional velocity
$V/F$	Vapor mole fraction (moles of vapor/total number of moles)
$wt\%$	Weight percent
$X_i$	Component $i$ liquid amount in moles
$x_i$	Component $i$ liquid mole fraction
$Y_i$	Component $i$ vapor amount in moles
$y_i$	Component $i$ vapor mole fraction
$Z_i$	Component $i$ overall amount in moles
$z_i$	Component $i$ overall mole fraction

---

$\beta_G$	Gas formation volume factor
$\beta_O$	Oil formation volume factor
$\beta_W$	Water formation volume factor
$\gamma_{API}$	API gravity
$\gamma_G$	Gas specific gravity
$\gamma_W$	Water specific gravity
$\lambda$	Thermal conductivity
$\mu_G$	Gas viscosity
$\mu_L$	Liquid viscosity
$\mu_O$	Oil viscosity
$\mu_v$	Vapor viscosity
$\mu_W$	Water viscosity
$\rho$	Density
$\rho_G$	Gas density
$\rho_L$	Liquid density
$\rho_O$	Oil density
$\rho_v$	Vapor density
$\rho_W$	Water density
$\rho_{MIX}$	Fluid mixture density
$\sigma_L$	Liquid surface tension
$\sigma_O$	Oil surface tension
$\sigma_W$	Water surface tension

## Appendices

### A. Keyword-based PVT Table

Keyword: PVTTABLE

Key	Parameter set	Unit	Description
LABEL		[-]	Name of the table.
PHASE	TWO, THREE	[-]	Two or three phase table.
EOS		[-]	Equation of state used in generating the PVT table. Optional.
MESHTYPE	STANDARD, FREEPRES, FREETEMP	[-]	STANDARD: Both temperature and pressure points are fixed independently. FREEPRES: Temperature points are fixed first and the pressure points are specified for each of the individual temperature points. FREETEMP: Pressure points are fixed first and the temperature points are specified for each of the individual pressure points.
COMPONENTS		[-]	List of names of the components in the composition. Optional.
MOLES		[-]	Mole fraction for each of the components in the composition. Optional.
DENSITY		[kg/m <sup>3</sup> ]	Density for each of the components in the composition. Optional. Set to -999 if not available.
MOLWEIGHT		[g/mol]	Molecular weight for each of the components in the composition. Optional.
STDPRESSURE	1 ATM	[Pa]	Pressure at standard conditions (1 atm). Optional.
STDTEMPERATURE	15.5 °C	[°C]	Temperature at standard conditions (15.5 °C). Optional.
GOR		[Sm <sup>3</sup> /Sm <sup>3</sup> ]	Gas/oil ratio at standard conditions. For two-phase flow, GOR is interpreted as gas/liquid ratio, that is, it is ratio of gas volume fraction to the liquid volume fraction at standard conditions. For cases where there is no oil/liquid, set GOR = -999.
GLR		[Sm <sup>3</sup> /Sm <sup>3</sup> ]	Gas/liquid ratio at standard conditions. For cases where there is no liquid, set GLR = -999.
WC		[-]	Water cut at standard conditions, for three-phase table only.
STDGASDENSITY		[kg/m <sup>3</sup> ]	Gas density at standard conditions.
STDOILDENSITY		[kg/m <sup>3</sup> ]	Oil density at standard conditions.
STDLIQDENSITY		[kg/m <sup>3</sup> ]	Liquid density at standard conditions. This key is only used in two-phase fluid tables



		generated from a composition with water, in which case it replaces STDOILDENSITY.
STDWATDENSITY	[kg/m <sup>3</sup> ]	Water density at standard conditions.
TOTWATERFRACTION	[-]	Mass fraction of water component in the composition.
DEWPRESSURES	[Pa]	Dewpoint pressures. The subkeys DEWPRESSURES and DEWTEMPERATURES are optional. Leave out these two subkeys if no dew point curve is found.
DEWTEMPERATURES	[°C]	Dewpoint temperatures corresponding to the dewpoint pressure given in keyword DEWPRESSURES.
BUBBLEPRESSURES	[Pa]	Bubble point pressures.
BUBBLETEMPERATURES	[°C]	Bubble point temperatures corresponding to the bubble point pressures given in keyword BUBBLEPRESSURES. The subkeys BUBBLEPRESSURE and BUBBLETEMPERATURE are optional. Leave out these two subkeys if no bubble point curve is found.
CRITICALPRESSURE	[Pa]	Pressure at the critical point.
CRITICALTEMPERATURE	[°C]	Temperature at the critical point. The subkeys CRITICALPRESSURE and CRITICALTEMPERATURE are optional. If the critical point is not found, either set the values of critical pressure and temperature to -999 or leave out these two subkeys.
NOPRES	[-]	Number of pressure points for each of temperature points given in subkey TEMPERATURE. Only if MESHTYPE = FREEPRES.
TEMPERATURE	[°C]	Temperature points if MESHTYPE = FREEPRES or STANDARD.
NOTEMP	[-]	Number of temperature points for each of pressure points given in subkey PRESSURE. Only if MESHTYPE = FREETEMP.
PRESSURE	[Pa]	Pressure points if MESHTYPE = FREETEMP or STANDARD.
COLUMNS	[-]	Specify orders and units of parameters for a table point.
	TM	[°C] Temperature.
	PT	[Pa] Pressure.
	RS	[-] Gas mass fraction in gas/oil mixture.
	RSW	[-] Water vapor mass fraction in gas phase.
	ROG	[kg/m <sup>3</sup> ] Gas density.
	DROGDP	[s <sup>2</sup> /m <sup>2</sup> ] Derivative of gas density with respect to

		pressure.
DROGDT	[kg/m <sup>3</sup> ·°C]	Derivative of gas density with respect to temperature.
ROHL	[kg/m <sup>3</sup> ]	Oil density.
DROHLDP	[s <sup>2</sup> /m <sup>2</sup> ]	Derivative of oil density with respect to pressure.
DROHLDT	[kg/m <sup>3</sup> ·°C]	Derivative of oil density with respect to temperature.
ROWT	[kg/m <sup>3</sup> ]	Water density.
DROWTDP	[s <sup>2</sup> /m <sup>2</sup> ]	Derivative of water density with respect to pressure.
DROWTDT	[kg/m <sup>3</sup> ·°C]	Derivative of water density with respect to temperature.
TCG	[W/m·°C]	Gas thermal conductivity.
TCHL	[W/m·°C]	Oil thermal conductivity.
TCWT	[W/m·°C]	Water thermal conductivity.
CPG	[J/kg·°C]	Gas thermal capacity.
CPHL	[J/kg·°C]	Oil thermal capacity.
CPWT	[J/kg·°C]	Water thermal capacity.
HG	[J/kg]	Gas enthalpy.
HHL	[J/kg]	Oil enthalpy.
HWT	[J/kg]	Water enthalpy.
VISG	[N·s/m <sup>2</sup> ]	Gas viscosity.
VISHL	[N·s/m <sup>2</sup> ]	Oil viscosity.
VISWT	[N·s/m <sup>2</sup> ]	Water viscosity.
SEG	[J/kg·°C]	Gas entropy.
SEHL	[J/kg·°C]	Oil entropy.
SEWT	[J/kg·°C]	Water entropy.
SIGGHL	[N/m]	Surface tension between gas and oil.
SIGGWT	[N/m]	Surface tension between gas and water.
SIGHLWT	[N/m]	Surface tension between oil and water.
POINT		Values of parameters.

## B. Composition of Produced Fluid over Time

Table B.1 – Reservoir Pressures, GOR, and SR over time

Date	P <sub>res</sub> [barg]	Target GOR [scf/STB]	SR [-]	Achieved GOR [scf/STB]
01/01	494.5	5,119	N/A	6,027
02/01	464.3	5,119	N/A	6,027
09/04	324.3	11,296	0.1850	11,298
13/10	277.2	16,101	0.1335	16,096
14/09	270.5	17,031	0.1270	17,017
21/01	237.8	22,680	0.1000	22,679

Table B.2 – Composition of gas condensate in 01/01 and 02/01

Component	Z <sub>i</sub>	[Y <sub>i</sub> ] <sub>prod</sub>	[X <sub>i</sub> ] <sub>drop</sub>	[X <sub>i</sub> ] <sub>prod</sub>	[Z <sub>i</sub> ] <sub>prod</sub>	[z <sub>i</sub> ] <sub>prod</sub>
Nitrogen	2.87	2.8700	0.0000	0.0000	2.8700	0.0287
CO <sub>2</sub>	1.35	1.3500	0.0000	0.0000	1.3500	0.0135
H <sub>2</sub> S	0.90	0.9000	0.0000	0.0000	0.9000	0.0090
H <sub>2</sub> O	0.50	0.5000	0.0000	0.0000	0.5000	0.0050
Methane	66.59	66.5900	0.0000	0.0000	66.5900	0.6659
Ethane	8.10	8.1000	0.0000	0.0000	8.1000	0.0810
Propane	4.63	4.6300	0.0000	0.0000	4.6300	0.0463
i-Butane	1.07	1.0700	0.0000	0.0000	1.0700	0.0107
n-Butane	2.07	2.0700	0.0000	0.0000	2.0700	0.0207
i-Pentane	0.75	0.7500	0.0000	0.0000	0.7500	0.0075
n-Pentane	0.80	0.8000	0.0000	0.0000	0.8000	0.0080
n-Hexane	1.15	1.1500	0.0000	0.0000	1.1500	0.0115
n-Heptane	1.32	1.3200	0.0000	0.0000	1.3200	0.0132
C <sub>8</sub> -C <sub>9</sub>	2.65	2.6500	0.0000	0.0000	2.6500	0.0265
C <sub>10</sub> -C <sub>12</sub>	2.03	2.0300	0.0000	0.0000	2.0300	0.0203
C <sub>13</sub> -C <sub>15</sub>	1.19	1.1900	0.0000	0.0000	1.1900	0.0119
C <sub>16</sub> -C <sub>19</sub>	0.87	0.8700	0.0000	0.0000	0.8700	0.0087
C <sub>20</sub> -C <sub>25</sub>	0.66	0.6600	0.0000	0.0000	0.6600	0.0066
C <sub>26</sub> -C <sub>31</sub>	0.31	0.3100	0.0000	0.0000	0.3100	0.0031
C <sub>32+</sub>	0.19	0.1900	0.0000	0.0000	0.1900	0.0019
<b>Total</b>	<b>100.00</b>	<b>100.0000</b>	<b>0.0000</b>	<b>0.0000</b>	<b>100.0000</b>	<b>1.0000</b>

Table B.3 – Composition of gas condensate in 09/04

Component	Z <sub>i</sub>	[Y <sub>i</sub> ] <sub>prod</sub>	[X <sub>i</sub> ] <sub>drop</sub>	[X <sub>i</sub> ] <sub>prod</sub>	[Z <sub>i</sub> ] <sub>prod</sub>	[z <sub>i</sub> ] <sub>prod</sub>
Nitrogen	2.87	2.2571	0.6129	0.1134	2.3705	0.0317
CO <sub>2</sub>	1.35	0.9497	0.4003	0.0740	1.0238	0.0137
H <sub>2</sub> S	0.90	0.5793	0.3207	0.0593	0.6386	0.0085
H <sub>2</sub> O	0.50	0.3558	0.1442	0.0267	0.3825	0.0051
Methane	66.59	49.5022	17.0878	3.1613	52.6634	0.7033
Ethane	8.10	5.6589	2.4411	0.4516	6.1105	0.0816

Component	Z <sub>i</sub>	[Y <sub>i</sub> ] <sub>prod</sub>	[X <sub>i</sub> ] <sub>drop</sub>	[X <sub>i</sub> ] <sub>prod</sub>	[Z <sub>i</sub> ] <sub>prod</sub>	[z <sub>i</sub> ] <sub>prod</sub>
Propane	4.63	3.0933	1.5367	0.2843	3.3776	0.0451
i-Butane	1.07	0.6924	0.3776	0.0698	0.7623	0.0102
n-Butane	2.07	1.3127	0.7573	0.1401	1.4528	0.0194
i-Pentane	0.75	0.4501	0.2999	0.0555	0.5055	0.0068
n-Pentane	0.80	0.4732	0.3268	0.0605	0.5337	0.0071
n-Hexane	1.15	0.6085	0.5415	0.1002	0.7086	0.0095
n-Heptane	1.32	0.6528	0.6672	0.1234	0.7762	0.0104
C <sub>8</sub> -C <sub>9</sub>	2.65	1.1860	1.4640	0.2708	1.4568	0.0195
C <sub>10</sub> -C <sub>12</sub>	2.03	0.7514	1.2786	0.2365	0.9879	0.0132
C <sub>13</sub> -C <sub>15</sub>	1.19	0.3409	0.8491	0.1571	0.4980	0.0067
C <sub>16</sub> -C <sub>19</sub>	0.87	0.1766	0.6934	0.1283	0.3049	0.0041
C <sub>20</sub> -C <sub>25</sub>	0.66	0.1048	0.5552	0.1027	0.2075	0.0028
C <sub>26</sub> -C <sub>31</sub>	0.31	0.0239	0.2861	0.0529	0.0768	0.0010
C <sub>32+</sub>	0.19	0.0079	0.1821	0.0337	0.0416	0.0006
<b>Total</b>	<b>100.00</b>	<b>69.1773</b>	<b>30.8227</b>	<b>5.7022</b>	<b>74.8795</b>	<b>1.0000</b>

Table B.4 – Composition of gas condensate in 13/10

Component	Z <sub>i</sub>	[Y <sub>i</sub> ] <sub>prod</sub>	[X <sub>i</sub> ] <sub>drop</sub>	[X <sub>i</sub> ] <sub>prod</sub>	[Z <sub>i</sub> ] <sub>prod</sub>	[z <sub>i</sub> ] <sub>prod</sub>
Nitrogen	2.87	2.3900	0.4800	0.0641	2.4541	0.0326
CO <sub>2</sub>	1.35	0.9897	0.3603	0.0481	1.0378	0.0138
H <sub>2</sub> S	0.90	0.5908	0.3092	0.0413	0.6320	0.0084
H <sub>2</sub> O	0.50	0.3710	0.1290	0.0172	0.3882	0.0052
Methane	66.59	52.0802	14.5098	1.9371	54.0173	0.7185
Ethane	8.10	5.8557	2.2443	0.2996	6.1553	0.0819
Propane	4.63	3.1466	1.4834	0.1980	3.3447	0.0445
i-Butane	1.07	0.6942	0.3758	0.0502	0.7444	0.0099
n-Butane	2.07	1.3057	0.7643	0.1020	1.4077	0.0187
i-Pentane	0.75	0.4369	0.3131	0.0418	0.4787	0.0064
n-Pentane	0.80	0.4562	0.3438	0.0459	0.5021	0.0067
n-Hexane	1.15	0.5589	0.5911	0.0789	0.6379	0.0085
n-Heptane	1.32	0.5768	0.7432	0.0992	0.6760	0.0090
C <sub>8</sub> -C <sub>9</sub>	2.65	0.9913	1.6587	0.2214	1.2127	0.0161
C <sub>10</sub> -C <sub>12</sub>	2.03	0.5574	1.4726	0.1966	0.7540	0.0100
C <sub>13</sub> -C <sub>15</sub>	1.19	0.2143	0.9757	0.1303	0.3446	0.0046
C <sub>16</sub> -C <sub>19</sub>	0.87	0.0893	0.7807	0.1042	0.1936	0.0026
C <sub>20</sub> -C <sub>25</sub>	0.66	0.0457	0.6143	0.0820	0.1277	0.0017
C <sub>26</sub> -C <sub>31</sub>	0.31	0.0069	0.3031	0.0405	0.0474	0.0006
C <sub>32+</sub>	0.19	0.0017	0.1883	0.0251	0.0268	0.0004
<b>Total</b>	<b>100.00</b>	<b>71.3596</b>	<b>28.6404</b>	<b>3.8235</b>	<b>75.1831</b>	<b>1.0000</b>

Table B.5 – Composition of gas condensate in 14/09

Component	Z <sub>i</sub>	[Y <sub>i</sub> ] <sub>prod</sub>	[X <sub>i</sub> ] <sub>drop</sub>	[X <sub>i</sub> ] <sub>prod</sub>	[Z <sub>i</sub> ] <sub>prod</sub>	[z <sub>i</sub> ] <sub>prod</sub>
Nitrogen	2.87	2.4083	0.4617	0.0586	2.4669	0.0328

Component	Z <sub>i</sub>	[Y <sub>i</sub> ] <sub>prod</sub>	[X <sub>i</sub> ] <sub>drop</sub>	[X <sub>i</sub> ] <sub>prod</sub>	[Z <sub>i</sub> ] <sub>prod</sub>	[z <sub>i</sub> ] <sub>prod</sub>
CO <sub>2</sub>	1.35	0.9961	0.3539	0.0449	1.0410	0.0138
H <sub>2</sub> S	0.90	0.5931	0.3069	0.0390	0.6321	0.0084
H <sub>2</sub> O	0.50	0.3734	0.1266	0.0161	0.3895	0.0052
Methane	66.59	52.4618	14.1282	1.7943	54.2561	0.7205
Ethane	8.10	5.8871	2.2129	0.2810	6.1681	0.0819
Propane	4.63	3.1559	1.4741	0.1872	3.3431	0.0444
i-Butane	1.07	0.6948	0.3752	0.0477	0.7424	0.0099
n-Butane	2.07	1.3052	0.7648	0.0971	1.4023	0.0186
i-Pentane	0.75	0.4352	0.3148	0.0400	0.4751	0.0063
n-Pentane	0.80	0.4538	0.3462	0.0440	0.4978	0.0066
n-Hexane	1.15	0.5520	0.5980	0.0759	0.6279	0.0083
n-Heptane	1.32	0.5660	0.7540	0.0958	0.6617	0.0088
C <sub>8</sub> -C <sub>9</sub>	2.65	0.9641	1.6859	0.2141	1.1783	0.0156
C <sub>10</sub> -C <sub>12</sub>	2.03	0.5316	1.4984	0.1903	0.7219	0.0096
C <sub>13</sub> -C <sub>15</sub>	1.19	0.1990	0.9910	0.1259	0.3249	0.0043
C <sub>16</sub> -C <sub>19</sub>	0.87	0.0802	0.7898	0.1003	0.1805	0.0024
C <sub>20</sub> -C <sub>25</sub>	0.66	0.0401	0.6199	0.0787	0.1188	0.0016
C <sub>26</sub> -C <sub>31</sub>	0.31	0.0057	0.3043	0.0386	0.0444	0.0006
C <sub>32+</sub>	0.19	0.0013	0.1887	0.0240	0.0253	0.0003
<b>Total</b>	<b>100.00</b>	<b>71.7048</b>	<b>28.2952</b>	<b>3.5935</b>	<b>75.2983</b>	<b>1.0000</b>

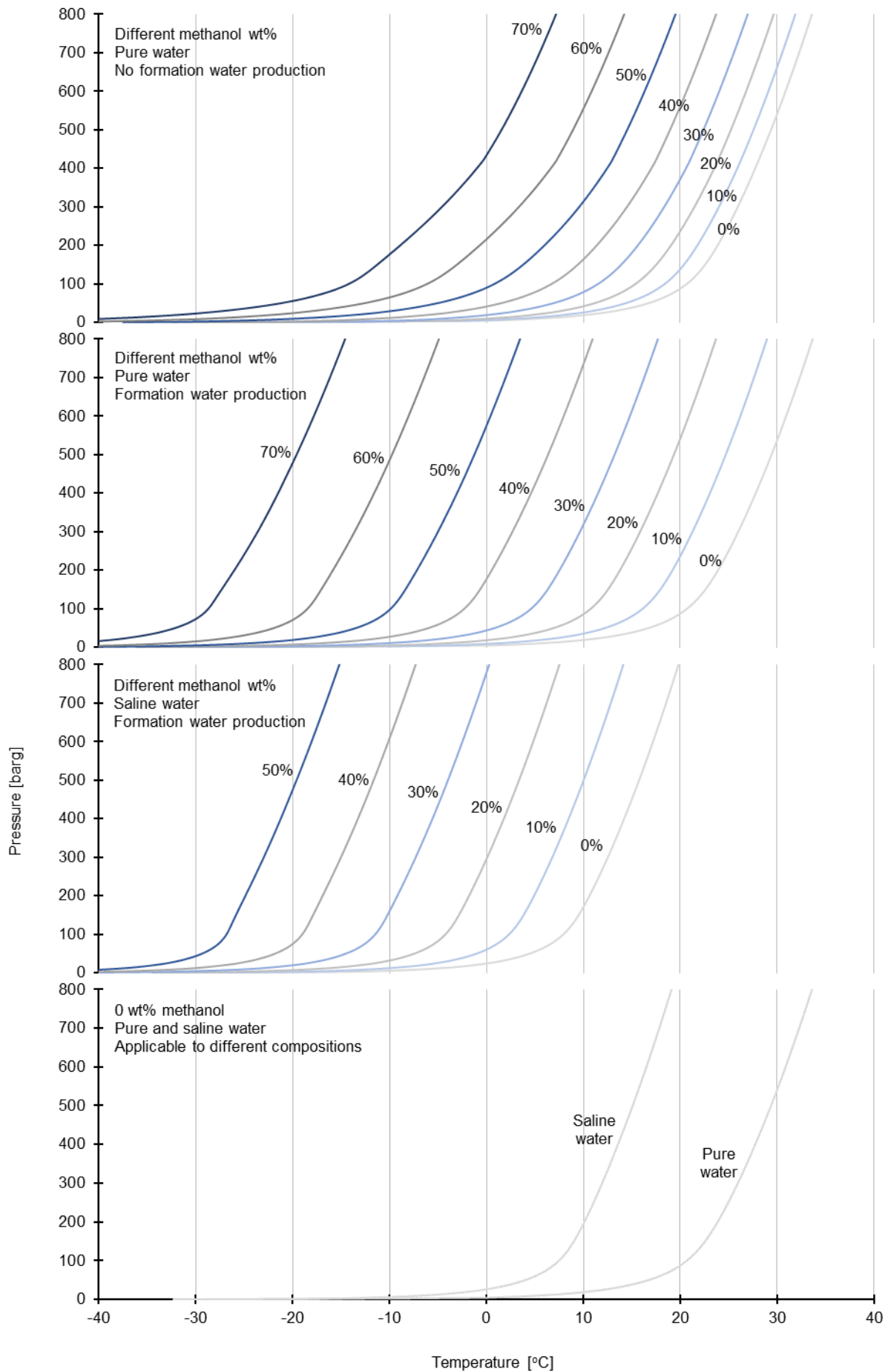
Table B.6 – Composition of gas condensate in 21/01

Component	Z <sub>i</sub>	[Y <sub>i</sub> ] <sub>prod</sub>	[X <sub>i</sub> ] <sub>drop</sub>	[X <sub>i</sub> ] <sub>prod</sub>	[Z <sub>i</sub> ] <sub>prod</sub>	[z <sub>i</sub> ] <sub>prod</sub>
Nitrogen	2.87	2.4943	0.3757	0.0376	2.5318	0.0333
CO <sub>2</sub>	1.35	1.0291	0.3209	0.0321	1.0612	0.0139
H <sub>2</sub> S	0.90	0.6070	0.2930	0.0293	0.6363	0.0084
H <sub>2</sub> O	0.50	0.3857	0.1143	0.0114	0.3971	0.0052
Methane	66.59	54.3458	12.2442	1.2244	55.5703	0.7301
Ethane	8.10	6.0498	2.0502	0.2050	6.2548	0.0822
Propane	4.63	3.2061	1.4239	0.1424	3.3485	0.0440
i-Butane	1.07	0.6979	0.3721	0.0372	0.7351	0.0097
n-Butane	2.07	1.3037	0.7663	0.0766	1.3803	0.0181
i-Pentane	0.75	0.4264	0.3236	0.0324	0.4587	0.0060
n-Pentane	0.80	0.4421	0.3579	0.0358	0.4779	0.0063
n-Hexane	1.15	0.5174	0.6326	0.0633	0.5807	0.0076
n-Heptane	1.32	0.5123	0.8077	0.0808	0.5931	0.0078
C <sub>8</sub> -C <sub>9</sub>	2.65	0.8324	1.8176	0.1818	1.0141	0.0133
C <sub>10</sub> -C <sub>12</sub>	2.03	0.4126	1.6174	0.1617	0.5743	0.0075
C <sub>13</sub> -C <sub>15</sub>	1.19	0.1338	1.0562	0.1056	0.2394	0.0031
C <sub>16</sub> -C <sub>19</sub>	0.87	0.0451	0.8249	0.0825	0.1276	0.0017
C <sub>20</sub> -C <sub>25</sub>	0.66	0.0201	0.6399	0.0640	0.0840	0.0011
C <sub>26</sub> -C <sub>31</sub>	0.31	0.0021	0.3079	0.0308	0.0329	0.0004
C <sub>32+</sub>	0.19	0.0004	0.1896	0.0190	0.0193	0.0003
<b>Total</b>	<b>100.00</b>	<b>73.4639</b>	<b>26.5361</b>	<b>2.6536</b>	<b>76.1175</b>	<b>1.0000</b>

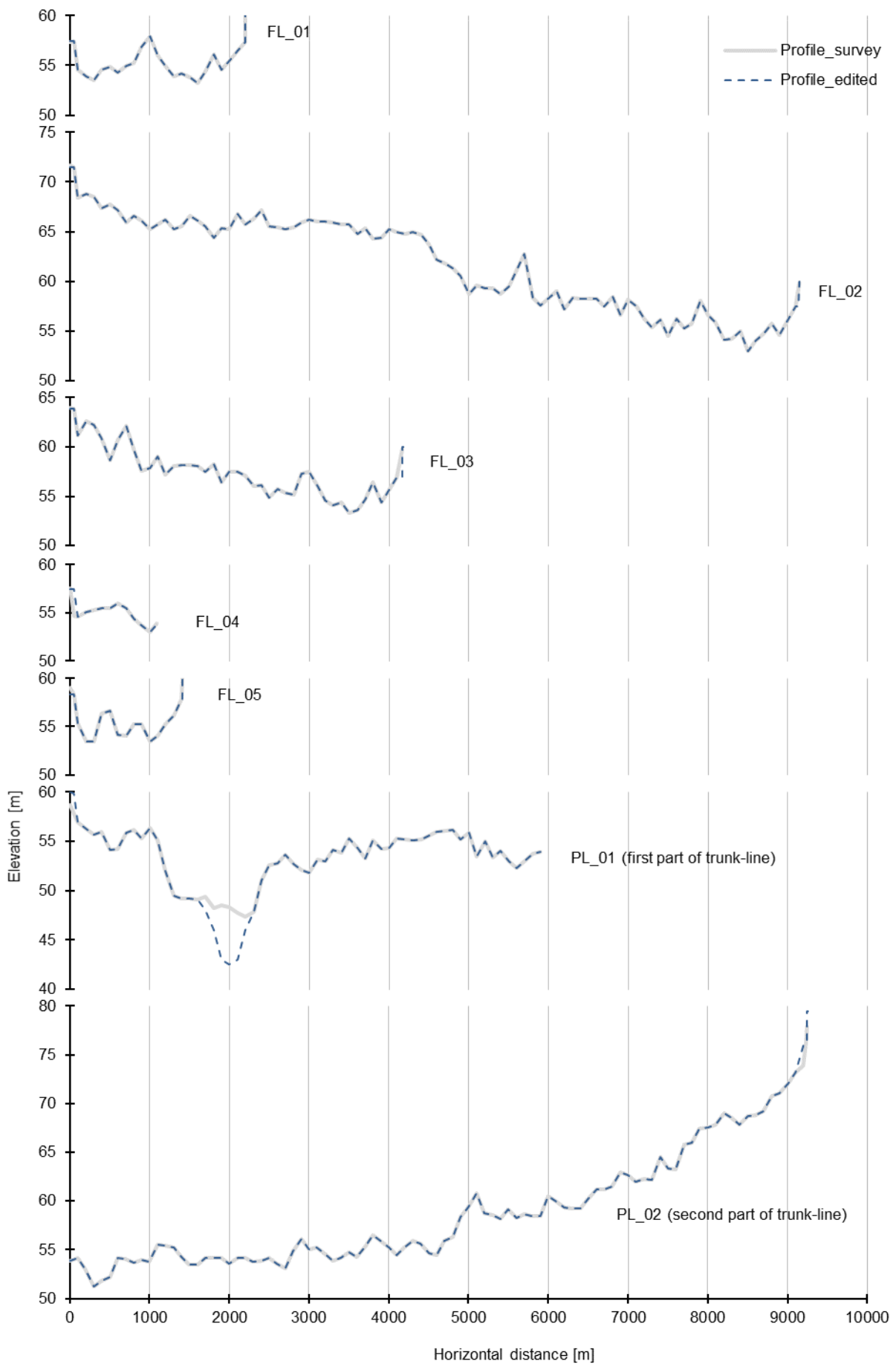
Table B.7 – Properties of produced fluid over time at standard conditions (for definition of black-oil components)

<b>Date</b>	<b>GOR</b> <b>[scf/STB]</b>	<b>Oil SG</b> <b>[-]</b>	<b>Gas SG</b> <b>[-]</b>	<b>[y<sub>H2S</sub>]<sub>prod</sub></b> <b>[-]</b>	<b>[y<sub>CO2</sub>]<sub>prod</sub></b> <b>[-]</b>	<b>[y<sub>N2</sub>]<sub>prod</sub></b> <b>[-]</b>
01/01, 02/01	6,027	0.7856	0.7996	0.0099	0.0149	0.0317
09/04	11,497	0.7747	0.7904	0.0090	0.0145	0.0335
13/10	16,384	0.7714	0.7857	0.0087	0.0144	0.0340
14/09	17,322	0.7710	0.7850	0.0087	0.0144	0.0341
21/01	23,090	0.7697	0.7814	0.0086	0.0144	0.0343

### C. Hydrate Formation Curves



## D. Pipeline Profiles





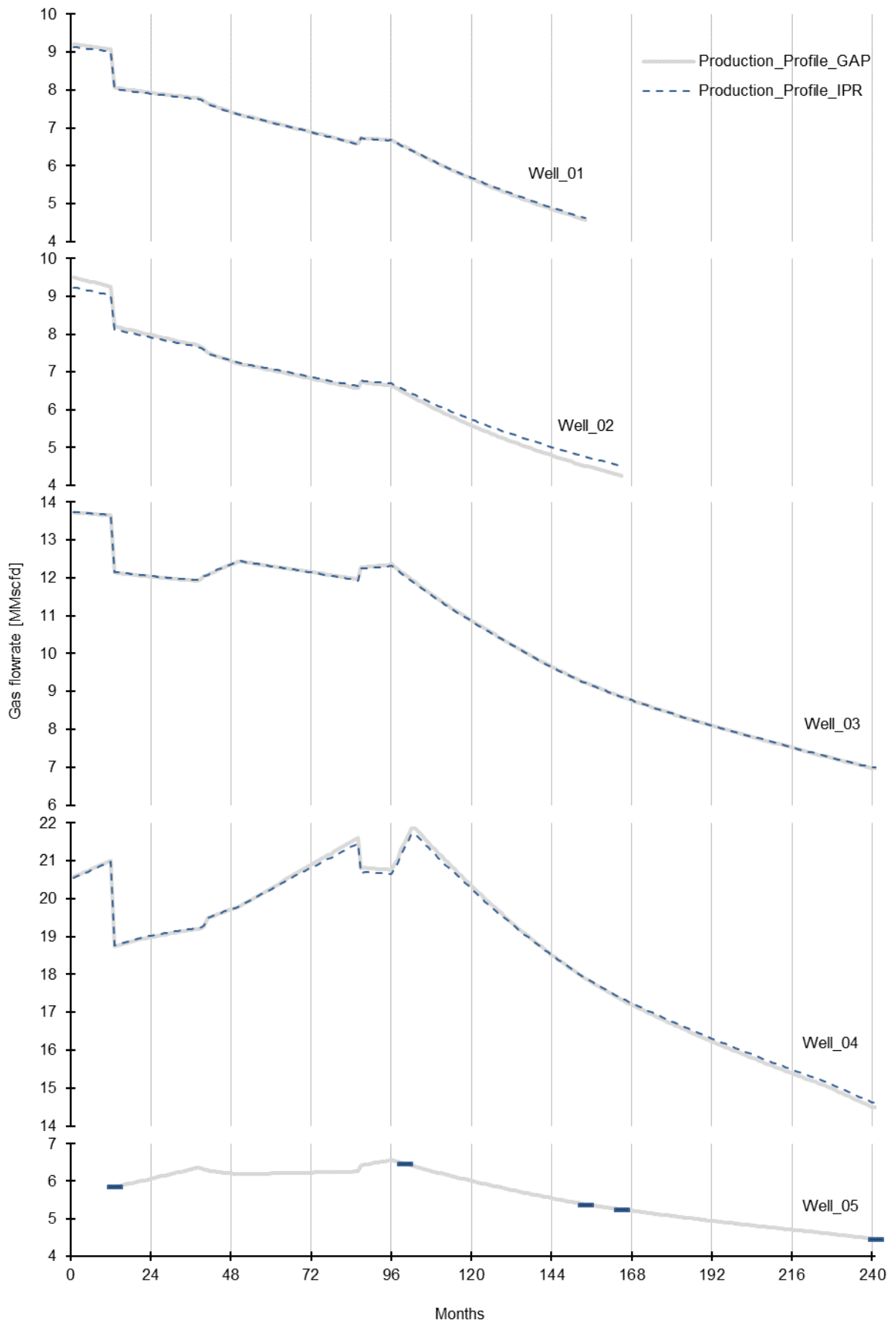
## E. Pipeline Walls

**Note:** The walls without the soil layers are defined to be applied in one-dimensional heat transfer calculations, while the ones with the soil layers are defined to be applied with FEMTherm, where the soil is modelled separately using a solid bundle.

Wall label	Material	Thickness [in]
10 3/4 CS + 2.00 PUR	CS	0.625
	PUR	1.000
	PUR	1.000
	HDPE	0.190
6 GRE	GRE	0.690
6 GRE + 1.17 PUR	GRE	0.690
	PUR	0.585
	PUR	0.585
	HDPE	0.140
6 GRE + 1.75 PUR	GRE	0.690
	PUR	0.875
	PUR	0.875
	HDPE	0.150
6 GRE + 2.43 PUR	GRE	0.690
	PUR	1.215
	PUR	1.215
	HDPE	0.160
6 GRE + 3.19 PUR	GRE	0.690
	PUR	1.063
	PUR	1.063
	PUR	1.063
HDPE	0.180	
8 5/8 CS + 2.0 PUR	CS	0.562
	PUR	1.000
	PUR	1.000
	HDPE	0.180
6 5/8 CS + 2.05 PUR	CS	0.500
	PUR	1.025
	PUR	1.025
	HDPE	0.150
5 9/16 CS + 2.0 PUR	CS	0.500
	PUR	1.000
	PUR	1.000
	HDPE	0.140
4 1/2 CS + 2.05 PUR	CS	0.438
	PUR	0.683
	PUR	0.683
	PUR	0.683
HDPE	0.130	
10 3/4 CS + 2.00 PUR + Soil	CS	0.625
	PUR	1.000

Wall label	Material	Thickness [in]
	PUR	1.000
	HDPE	0.190
	Soil	7.962
	Soil	15.925
	Soil	31.849
6 GRE + Soil	GRE	0.690
	Soil	9.091
	Soil	18.182
	Soil	36.364
6 GRE + 1.17 PUR + Soil	GRE	0.690
	PUR	0.585
	PUR	0.585
	HDPE	0.140
	Soil	8.717
	Soil	17.433
	Soil	34.866
6 GRE + 1.75 PUR + Soil	GRE	0.690
	PUR	0.875
	PUR	0.875
	HDPE	0.150
	Soil	8.545
	Soil	17.090
	Soil	34.181
6 GRE + 2.43 PUR + Soil	GRE	0.690
	PUR	1.215
	PUR	1.215
	HDPE	0.160
	Soil	8.351
	Soil	16.702
	Soil	33.404
6 GRE + 3.19 PUR + Soil	GRE	0.690
	PUR	1.063
	PUR	1.063
	PUR	1.063
	HDPE	0.180
	Soil	8.128
	Soil	16.256
	Soil	32.512

## F. Production Profiles



## G. Variables

Name	Unit	Description
ACCLIQ	[bb]	Accumulated liquid volume flow (usually located at the pipe outlet)
ACCLIQBR	[bb]	Accumulated liquid volume along branch
DP	[bar]	Pressure difference along a branch
DPPIG	[bar]	Pressure difference across pig
DTHYD	[°C]	Difference between hydrate formation and section temperature
DTHYD <sub>max</sub>	[°C]	Maximum DTHYD in a branch
DTHYD <sub>max</sub> EP	[°C]	DTHYD <sub>max</sub> calculated in "Excel" considering "Pure" water
DTHYD <sub>max</sub> ES	[°C]	DTHYD <sub>max</sub> calculated in "Excel" considering "Pure" water
DTHYD <sub>max</sub> OP	[°C]	DTHYD <sub>max</sub> calculated in "Excel" considering "Pure" water
DTHYD <sub>out</sub>	[°C]	DTHYD at the outlet of a branch
DTHYD <sub>out</sub> EP	[°C]	DTHYD <sub>out</sub> calculated in "Excel" considering "Pure" water
DTHYD <sub>out</sub> ES	[°C]	DTHYD <sub>out</sub> calculated in "Excel" considering "Saline" water
DTHYD <sub>out</sub> OP	[°C]	DTHYD <sub>out</sub> calculated in "OLGA" considering "Pure" water
EVR	[-]	Erosional velocity ratio
EVR <sub>max</sub>	[-]	Maximum EVR in a branch
GG	[kg/h]	Gas mass flow
GL	[kg/h]	Liquid bulk mass flow
GLT	[kg/h]	Liquid total mass flow rate
GLTHL	[kg/h]	Mass flow rate of oil
GLTWT	[kg/h]	Mass flow rate of water excluding vapor
GLWVT	[kg/h]	Total mass flow rate of water including vapor
GT	[kg/h]	Total mass flow
HOL	[-]	Holdup (liquid volume fraction including solids)
HOL <sub>avg</sub>	[-]	Average HOL in a branch (optional: for each ID)
HOLHL	[-]	Oil volume fraction
HOLWT	[-]	Water volume fraction
ID	[-]	Flow regime: 1=stratified, 2=annular, 3=slug, 4=bubble
ID <sub>pct</sub>	[%]	Percentage of branch length with a certain ID
INHIBMASS	[kg]	Total mass of inhibitor in branch
INHIBMFR	[%]	Inhibitor mass fraction in water
LIQC	[bb]	Total liquid content in branch
LSLEXP	[m]	Slug length (0 = no slug)
MeOH wt%	[%]	Total methanol mass fraction in water + vapor
NSLUG	[-]	Total number of slugs in the pipeline
PT	[barg]	Pressure
PT <sub>avg</sub>	[barg]	Average PT in a branch
PT <sub>DTHYD</sub>	[barg]	PT at the section where DTHYD is reported
PT <sub>DSC</sub>	[barg]	PT downstream the choke
PT <sub>in</sub>	[barg]	PT at the inlet of a branch
PT <sub>out</sub>	[barg]	PT at the outlet of a branch
Q2	[W/m <sup>2</sup> ·K]	Overall heat transfer coefficient
QGST	[MMscfd]	Gas volume flow at standard conditions
QGST <sub>tot</sub>	[MMscfd]	Total QGST (flowing out of the pipeline network)
QLT	[bb/d]	Total liquid volume flow

QLT <sub>out</sub>	[bbl/d]	Total liquid volume flow at the outlet of a branch
QMeOH	[kg/h]	Mass flowrate of methanol
QMeOH EP	[kg/h]	QMeOH calculated in "Excel" considering "Pure" water
QMeOH ES	[kg/h]	QMeOH calculated in "Excel" considering "Saline" water
RWINHIBTOT	[%]	Total mass fraction of inhibitor in water phase in branch
SURGELIQ	[bbl]	Surge volume (post-processed variable based on ACCLIQ)
TINHIBMFR	[%]	Total inhibitor mass fraction in water + vapor
TM	[°C]	Fluid temperature
TM <sub>avg</sub>	[°C]	Average TM in a branch
TM <sub>DTHYD</sub>	[°C]	TM at the section where DTHYD is reported
TM <sub>DSC</sub>	[°C]	TM downstream the choke
TM <sub>in</sub>	[°C]	TM at the inlet of a branch
TM <sub>out</sub>	[°C]	TM at the outlet of a branch
UG	[m/s]	Gas velocity
UG <sub>max</sub>	[m/s]	Maximum UG in a branch
UL	[m/s]	Liquid velocity
UL <sub>max</sub>	[m/s]	Maximum UL in a branch
UPIG	[m/s]	Pig velocity
UPIG <sub>avg</sub>	[m/s]	Average pig velocity
UPIG <sub>max</sub>	[m/s]	Maximum pig velocity
USD	[m/s]	Superficial liquid droplet velocity
USG	[m/s]	Superficial gas velocity
USL	[m/s]	Superficial liquid film velocity
VALVOP	[-]	Relative valve opening
VOLGBL	[-]	Global max volume error since last write
ZPIG	[m]	Pig position in branch
ZZPIG	[m]	Pig total distance traveled

## H. Simulation Results

Table H.1 – Pipeline parameters over time

01/01_WA							
Branch	QGST [MMscfd]	PT <sub>in</sub> [barg]	PT <sub>out</sub> [barg]	DP [barg]	TM <sub>in</sub> [°C]	TM <sub>out</sub> [°C]	DTHYD <sub>out</sub> OP [°C]
PL_2	52.9	57.0	45.0	12.0	27.9	22.8	-6.7
PL_1	32.4	59.1	57.0	2.1	20.1	18.3	-0.7
FL_01	9.2	59.9	59.1	0.8	35.5	24.6	-6.8
FL_02	9.5	61.9	59.1	2.7	36.7	<b>(W) 6.9</b>	<b>(H) 10.9</b>
FL_03	13.7	62.1	59.1	2.9	42.3	26.1	-8.3
FL_04	20.5	59.2	57.1	2.1	46.8	42.9	-25.3
Branch	ID [-]	HOL <sub>avg</sub> [-]	LIQC [bbl]	QLT <sub>out</sub> [bbl/day]	EVR <sub>max</sub> [-]	UG <sub>max</sub> [m/s]	UL <sub>max</sub> [m/s]
PL_2	1, 3	0.165, 0.104	442	12,874	0.55	7.7	5.1
PL_1	1	0.210	359	8,319	0.29	3.9	2.6
FL_01	1, 3	0.213, 0.259	51	2,329	0.22	3.0	2.0
FL_02	1, 3	0.223, 0.285	222	2,549	0.23	2.9	2.1
FL_03	1, 3	0.184, 0.207	83	3,456	0.33	4.2	2.5
FL_04	1	0.160	18	4,903	0.53	6.7	3.6
01/01_SA							
Branch	QGST [MMscfd]	PT <sub>in</sub> [barg]	PT <sub>out</sub> [barg]	DP [barg]	TM <sub>in</sub> [°C]	TM <sub>out</sub> [°C]	DTHYD <sub>out</sub> OP [°C]
PL_2	52.9	57.5	45.0	12.5	33.4	28.9	-12.8
PL_1	32.4	59.7	57.5	2.2	27.7	26.5	-8.9
FL_01	9.2	60.5	59.7	0.8	35.8	29.6	-11.7
FL_02	9.5	62.5	59.7	2.8	37.0	19.6	-1.7
FL_03	13.7	62.7	59.7	3.0	42.5	32.2	-14.3
FL_04	20.5	59.6	57.5	2.1	47.0	44.2	-26.6
Branch	ID [-]	HOL <sub>avg</sub> [-]	LIQC [bbl]	QLT <sub>out</sub> [bbl/day]	EVR <sub>max</sub> [-]	UG <sub>max</sub> [m/s]	UL <sub>max</sub> [m/s]
PL_2	1, 3	0.159, 0.010	426	12,644	0.56	8.0	5.2
PL_1	1	0.200	341	8,120	0.30	4.1	2.6
FL_01	1, 3	0.210, 0.253	50	2,298	0.22	3.0	2.0
FL_02	1, 3	0.211, 0.264	210	2,448	0.23	3.0	2.1
FL_03	1, 3	0.181, 0.202	82	3,400	0.33	4.2	2.4
FL_04	1	0.160	18	4,892	0.53	6.7	3.6
02/01_WA							
Branch	QGST [MMscfd]	PT <sub>in</sub> [barg]	PT <sub>out</sub> [barg]	DP [barg]	TM <sub>in</sub> [°C]	TM <sub>out</sub> [°C]	DTHYD <sub>out</sub> OP [°C]
PL_2	52.9	56.8	45.0	11.8	25.2	20.2	-4.1
PL_1	34.2	59.1	56.8	2.3	17.8	<b>(W) 16.2</b>	<b>(H) 1.4</b>
FL_01	8.0	59.8	59.1	0.6	33.5	22.0	-4.2
FL_02	8.2	61.3	59.1	2.1	34.5	<b>(W) 4.8</b>	<b>(H) 13.0</b>
FL_03	12.1	61.4	59.1	2.2	40.1	23.3	-5.5
FL_04	18.7	58.5	56.9	1.7	45.5	41.5	-24.0

Branch	ID [-]	HOL <sub>avg</sub> [-]	LIQC [bbl]	QLT <sub>out</sub> [bbl/day]	EVR <sub>max</sub> [-]	UG <sub>max</sub> [m/s]	UL <sub>max</sub> [m/s]
FL_05	5.8	59.5	59.1	0.4	27.9	19.1	-1.3
PL_2	1, 3	0.168, 0.106	449	12,968	0.55	7.6	5.0
PL_1	1	0.210	360	8,837	0.31	4.1	2.6
FL_01	1, 3	0.229, 0.282	54	2,057	0.20	2.7	2.0
FL_02	1, 3	0.236, 0.311	235	2,224	0.20	2.6	2.0
FL_03	1, 3	0.191, 0.225	86	3,086	0.29	3.7	2.3
FL_04	1	0.170	19	4,480	0.48	6.1	3.3
FL_05	1, 3	0.274, 0.346	42	1,495	0.14	2.4	1.8

## 02/01\_SA

Branch	QGST [MMscfd]	PT <sub>in</sub> [barg]	PT <sub>out</sub> [barg]	DP [barg]	TM <sub>in</sub> [°C]	TM <sub>out</sub> [°C]	DTHYD <sub>out</sub> OP [°C]
PL_2	52.9	57.3	45.0	12.3	31.0	26.6	-10.5
PL_1	34.2	59.7	57.3	2.4	25.6	24.4	-6.8
FL_01	8.0	60.4	59.7	0.6	33.9	27.5	-9.7
FL_02	8.2	61.9	59.7	2.2	34.9	18.2	-0.3
FL_03	12.1	62.0	59.7	2.3	40.4	30.0	-12.1
FL_04	18.7	59.0	57.4	1.7	45.7	43.0	-25.4
FL_05	5.8	60.1	59.7	0.4	28.3	24.2	-6.3

Branch	ID [-]	HOL <sub>avg</sub> [-]	LIQC [bbl]	QLT <sub>out</sub> [bbl/day]	EVR <sub>max</sub> [-]	UG <sub>max</sub> [m/s]	UL <sub>max</sub> [m/s]
PL_2	1, 3	0.162, 0.101	432	12,712	0.56	7.9	5.2
PL_1	1	0.201	340	8,647	0.31	4.2	2.6
FL_01	1, 3	0.225, 0.275	53	2,026	0.19	2.7	2.0
FL_02	1, 3	0.223, 0.288	222	2,129	0.19	2.7	2.0
FL_03	1, 3	0.187, 0.217	84	3,029	0.29	3.7	2.3
FL_04	1	0.170	19	4,469	0.48	6.1	3.3
FL_05	1, 3	0.271, 0.338	41	1,460	0.14	2.4	1.8

## 09/04\_WA

Branch	QGST [MMscfd]	PT <sub>in</sub> [barg]	PT <sub>out</sub> [barg]	DP [barg]	TM <sub>in</sub> [°C]	TM <sub>out</sub> [°C]	DTHYD <sub>out</sub> OP [°C]
PL_2	53.0	54.8	45.0	9.8	22.9	17.9	-1.7
PL_1	31.5	56.4	54.8	1.6	<b>(W) 16.2</b>	<b>(W) 14.5</b>	<b>(H) 3.0</b>
FL_01	6.5	56.9	56.5	0.5	31.2	<b>(W) 16.6</b>	<b>(H) 1.1</b>
FL_02	6.4	57.8	56.5	1.4	33.6	<b>(W) 0.4</b>	<b>(H) 17.2</b>
FL_03	12.1	58.4	56.5	1.9	39.0	20.9	-3.3
FL_04	21.5	56.7	54.8	1.9	39.0	35.3	-17.8
FL_05	6.4	56.8	56.5	0.4	34.4	23.1	-5.5

Branch	ID [-]	HOL <sub>avg</sub> [-]	LIQC [bbl]	QLT <sub>out</sub> [bbl/day]	EVR <sub>max</sub> [-]	UG <sub>max</sub> [m/s]	UL <sub>max</sub> [m/s]
PL_2	1, 3	0.113, 0.083	302	8,015	0.48	7.3	4.0
PL_1	1	0.150	250	5,080	0.25	3.8	2.3
FL_01	1, 3	0.184, 0.275	44	1,043	0.14	2.5	1.6
FL_02	1, 3	0.189, 0.303	188	1,113	0.14	2.4	1.7
FL_03	1, 3	0.123, 0.184	56	1,905	0.27	3.8	2.1
FL_04	1	0.100	12	3,125	0.49	6.8	3.4

FL_05	1, 3	0.187, 0.265	28	989	0.14	2.7	1.6
-------	------	--------------	----	-----	------	-----	-----

## 09/04\_SA

Branch	QGST [MMscfd]	PT <sub>in</sub> [barg]	PT <sub>out</sub> [barg]	DP [barg]	TM <sub>in</sub> [°C]	TM <sub>out</sub> [°C]	DTHYD <sub>out</sub> OP [°C]
PL_2	53.0	55.2	45.0	10.2	29.1	24.7	-8.5
PL_1	31.5	57.0	55.2	1.7	24.9	23.8	-6.3
FL_01	6.5	57.4	57.0	0.5	31.6	24.0	-6.3
FL_02	6.4	58.4	57.0	1.4	34.1	<b>(W) 15.8</b>	<b>(H) 1.9</b>
FL_03	12.1	58.9	57.0	1.9	39.3	28.4	-10.7
FL_04	21.5	57.1	55.3	1.9	39.2	36.9	-19.3
FL_05	6.4	57.3	57.0	0.3	34.8	28.4	-10.7

Branch	ID [-]	HOL <sub>avg</sub> [-]	LIQC [bbl]	QLT <sub>out</sub> [bbl/day]	EVR <sub>max</sub> [-]	UG <sub>max</sub> [m/s]	UL <sub>max</sub> [m/s]
PL_2	1, 3	0.107, 0.079	302	8,015	0.48	7.3	4.0
PL_1	1	0.140	250	5,080	0.25	3.8	2.3
FL_01	1, 3	0.178, 0.265	44	1,043	0.14	2.5	1.6
FL_02	1, 3	0.171, 0.308	188	1,113	0.14	2.4	1.7
FL_03	1, 3	0.119, 0.176	56	1,905	0.27	3.8	2.1
FL_04	1	0.100	12	3,125	0.49	6.8	3.4
FL_05	1, 3	0.176, 0.292	28	989	0.14	2.7	1.6

## 13/10\_WA

Branch	QGST [MMscfd]	PT <sub>in</sub> [barg]	PT <sub>out</sub> [barg]	DP [barg]	TM <sub>in</sub> [°C]	TM <sub>out</sub> [°C]	DTHYD <sub>out</sub> OP [°C]
PL_2	41.9	50.5	45.0	5.5	18.3	<b>(W) 14.4</b>	<b>(H) 1.8</b>
PL_1	24.0	51.6	50.5	1.1	<b>(W) 10.4</b>	<b>(W) 8.8</b>	<b>(H) 8.2</b>
FL_01	4.8	52.2	51.7	0.5	24.6	<b>(W) 9.4</b>	<b>(H) 7.7</b>
FL_02	4.6	53.1	51.7	1.4	24.7	<b>(W) -2.4</b>	<b>(H) 19.5</b>
FL_03	9.2	52.7	51.7	1.1	33.7	<b>(W) 13.4</b>	<b>(H) 3.7</b>
FL_04	17.9	51.8	50.6	1.2	35.6	31.4	-14.4
FL_05	5.4	52.0	51.7	0.4	28.6	<b>(W) 16.9</b>	<b>(H) 0.2</b>

Branch	ID [-]	HOL <sub>avg</sub> [-]	LIQC [bbl]	QLT <sub>out</sub> [bbl/day]	EVR <sub>max</sub> [-]	UG <sub>max</sub> [m/s]	UL <sub>max</sub> [m/s]
PL_2	1, 3	0.096, 0.080	257	5,075	0.36	5.7	2.6
PL_1	1, 3	0.135, 0.291	237	3,131	0.19	3.5	2.0
FL_01	1, 3	0.221, 0.357	54	<b>(S) 653</b>	0.10	2.3	1.4
FL_02	1, 3	0.192, 0.421	218	<b>(S) 553</b>	0.10	2.2	1.4
FL_03	1, 3	0.106, 0.199	48	1,166	0.20	3.2	1.7
FL_04	1	0.080	9	2,005	0.40	6.1	2.8
FL_05	1, 3	0.182, 0.325	32	<b>(S) 663</b>	0.12	2.6	1.5

## 13/10\_SA

Branch	QGST [MMscfd]	PT <sub>in</sub> [barg]	PT <sub>out</sub> [barg]	DP [barg]	TM <sub>in</sub> [°C]	TM <sub>out</sub> [°C]	DTHYD <sub>out</sub> OP [°C]
PL_2	41.8	50.8	45.0	5.8	25.5	22.3	-6.1
PL_1	24.0	51.9	50.8	1.1	20.7	19.7	-2.7
FL_01	4.8	52.4	51.9	0.5	25.1	18.9	-1.7
FL_02	4.4	53.3	51.9	1.4	25.1	<b>(W) 14.2</b>	<b>(H) 3.0</b>



FL_03	9.2	53.0	51.9	1.1	34.0	22.9	-5.7
FL_04	17.9	52.1	50.8	1.2	35.8	33.3	-16.2
FL_05	5.4	52.3	51.9	0.4	29.1	23.4	-6.2
Branch	ID [-]	HOL <sub>avg</sub> [-]	LIQC [bbl]	QLT <sub>out</sub> [bbl/day]	EVR <sub>max</sub> [-]	UG <sub>max</sub> [m/s]	UL <sub>max</sub> [m/s]
PL_2	1, 3	0.089, 0.074	237	4,730	0.37	6.0	2.6
PL_1	1, 3	0.122, 0.277	210	2,902	0.20	3.6	1.9
FL_01	1, 3	0.206, 0.358	51	<b>(S) 592</b>	0.10	2.4	1.4
FL_02	1, 3	0.183, 0.404	202	<b>(S) 499</b>	0.10	2.3	1.4
FL_03	1, 3	0.100, 0.188	45	1,100	0.20	3.3	1.7
FL_04	1	0.080	9	1,984	0.40	6.1	2.8
FL_05	1, 3	0.200, 0.288	31	<b>(S) 639</b>	0.12	2.6	1.5
14/09_WA							
Branch	QGST [MMscfd]	PT <sub>in</sub> [barg]	PT <sub>out</sub> [barg]	DP [barg]	TM <sub>in</sub> [°C]	TM <sub>out</sub> [°C]	DTHYD <sub>out</sub> OP [°C]
PL_2	35.7	49.0	45.0	4.0	18.9	<b>(W) 15.2</b>	<b>(H) 1.1</b>
PL_1	18.4	50.1	49.1	1.0	<b>(W) 9.6</b>	<b>(W) 8.3</b>	<b>(H) 8.6</b>
FL_02	4.4	51.5	50.1	1.4	23.4	<b>(W) -2.5</b>	<b>(H) 19.5</b>
FL_03	8.8	51.1	50.1	1.0	32.7	<b>(W) 12.4</b>	<b>(H) 4.6</b>
FL_04	17.3	50.3	49.1	1.2	34.9	30.5	-13.7
FL_05	5.2	50.5	50.1	0.4	27.9	<b>(W) 16.2</b>	<b>(H) 0.8</b>
Branch	ID [-]	HOL <sub>avg</sub> [-]	LIQC [bbl]	QLT <sub>out</sub> [bbl/day]	EVR <sub>max</sub> [-]	UG <sub>max</sub> [m/s]	UL <sub>max</sub> [m/s]
PL_2	1, 3	0.097, 0.084	256	<b>(S) 4,118</b>	0.31	6.8	2.0
PL_1	1, 3	0.151, 0.358	280	<b>(S) 2,314</b>	0.15	3.2	1.9
FL_02	1, 3	0.202, 0.413	220	<b>(S) 549</b>	0.09	2.2	1.4
FL_03	1, 3	0.103, 0.199	46	1,078	0.20	3.1	1.7
FL_04	1	0.080	9	1,863	0.39	6.0	2.7
FL_05	1, 3	0.200, 0.318	31	<b>(S) 529</b>	0.12	2.7	1.4
14/09_SA							
Branch	QGST [MMscfd]	PT <sub>in</sub> [barg]	PT <sub>out</sub> [barg]	DP [barg]	TM <sub>in</sub> [°C]	TM <sub>out</sub> [°C]	DTHYD <sub>out</sub> OP [°C]
PL_2	35.7	49.2	45.0	4.2	25.7	23.0	-6.7
PL_1	18.4	50.2	49.2	1.0	20.3	19.5	-2.7
FL_02	4.3	51.6	50.3	1.4	23.8	<b>(W) 14.1</b>	<b>(H) 2.9</b>
FL_03	8.9	51.3	50.3	1.0	32.9	22.1	-5.1
FL_04	17.3	50.4	49.3	1.2	35.0	32.5	-15.6
FL_05	5.2	50.6	50.3	0.4	28.3	22.9	-5.9
Branch	ID [-]	HOL <sub>avg</sub> [-]	LIQC [bbl]	QLT <sub>out</sub> [bbl/day]	EVR <sub>max</sub> [-]	UG <sub>max</sub> [m/s]	UL <sub>max</sub> [m/s]
PL_2	1, 3	0.089, 0.078	233	<b>(S) 3,903</b>	0.31	7.0	2.0
PL_1	1, 3	0.143, 0.372	256	<b>(S) 2,081</b>	0.15	3.3	1.8
FL_02	1, 3	0.173, 0.383	201	<b>(S) 453</b>	0.09	2.3	1.4
FL_03	1, 3	0.096, 0.187	43	1,013	0.20	3.3	1.7
FL_04	1	0.080	9	1,841	0.39	6.1	2.7
FL_05	1, 3	0.182, 0.337	30	<b>(S) 505</b>	0.12	2.6	1.4

## 21/01\_WA

Branch	QGST [MMscfd]	PT <sub>in</sub> [barg]	PT <sub>out</sub> [barg]	DP [barg]	TM <sub>in</sub> [°C]	TM <sub>out</sub> [°C]	DTHYD <sub>out</sub> OP [°C]
PL_2	26.0	47.2	45.0	2.2	18.4	(W) 14.7	(H) 1.6
PL_1	11.5	48.3	47.2	1.1	(W) 9.8	(W) 7.0	(H) 9.6
FL_03	7.0	49.1	48.3	0.7	28.8	(W) 7.6	(H) 9.2
FL_04	14.5	48.0	47.2	0.8	33.1	28.1	-11.5
FL_05	4.5	48.7	48.3	0.4	24.9	(W) 12.9	(H) 3.9
Branch	ID [-]	HOL <sub>avg</sub> [-]	LIQC [bbl]	QLT <sub>out</sub> [bbl/day]	EVR <sub>max</sub> [-]	UG <sub>max</sub> [m/s]	UL <sub>max</sub> [m/s]
PL_2	1, 3	0.095, 0.090	246	(S) 2,530	0.22	6.2	1.5
PL_1	1, 3	0.195, 0.423	381	(S) 1,244	0.09	2.8	1.6
FL_03	1, 3	0.108, 0.220	49	732	0.16	2.9	1.5
FL_04	1	0.070	8	1,286	0.33	5.3	2.3
FL_05	1, 3	0.192, 0.384	33	(S) 377	0.10	2.4	1.3

## 21/01\_SA

Branch	QGST [MMscfd]	PT <sub>in</sub> [barg]	PT <sub>out</sub> [barg]	DP [barg]	TM <sub>in</sub> [°C]	TM <sub>out</sub> [°C]	DTHYD <sub>out</sub> OP [°C]
PL_2	25.9	47.2	45.0	2.2	25.1	22.7	-6.4
PL_1	11.4	48.4	47.2	1.1	19.5	18.4	-1.8
FL_03	7.0	49.1	48.4	0.7	29.1	19.0	-2.2
FL_04	14.5	48.0	47.3	0.8	33.2	30.5	-13.8
FL_05	4.3	48.8	48.4	0.4	25.3	20.5	-3.7
Branch	ID [-]	HOL <sub>avg</sub> [-]	LIQC [bbl]	QLT <sub>out</sub> [bbl/day]	EVR <sub>max</sub> [-]	UG <sub>max</sub> [m/s]	UL <sub>max</sub> [m/s]
PL_2	1, 3	0.087, 0.085	225	(S) 2,300	0.22	6.3	1.5
PL_1	1, 3	0.159, 0.457	352	(S) 1,131	0.09	2.8	1.5
FL_03	1, 3	0.098, 0.203	45	662	0.15	2.9	1.5
FL_04	1	0.060	8	1,262	0.33	5.3	2.3
FL_05	1, 3	0.196, 0.304	33	(S) 364	0.10	2.5	1.3

Table H.2 – Pipeline parameters for different turndown flowrates (transient)

## WC0\_100

Branch	QGST [MMscfd]	PT <sub>in</sub> [barg]	PT <sub>out</sub> [barg]	DP [barg]	TM <sub>in</sub> [°C]	TM <sub>out</sub> [°C]	DTHYD <sub>in</sub> OP [°C]
PL_2	52.1	56.2	45.0	11.2	22.4	(W) 17.4	-4.9
PL_1	33.9	58.5	56.3	2.2	(W) 14.5	(W) 12.6	(H) 3.2
FL_01	8.0	59.1	58.5	0.6	33.2	19.6	-15.4
FL_02	8.2	60.6	58.5	2.1	34.2	(W) -0.8	-16.3
FL_03	11.9	60.7	58.5	2.2	39.8	20.4	-21.8
FL_04	18.2	57.9	56.3	1.6	45.0	40.5	-27.4
FL_05	5.8	58.9	58.5	0.4	27.6	(W) 17.1	-9.8
Branch	DTHYD <sub>out</sub> OP [°C]	ID [-]	HOL <sub>avg</sub> [-]	ID <sub>pct</sub> [%]	LIQC [bbl]	QLT <sub>out</sub> [bbl/day]	

PL_2	-1.3	1, 3	0.171, 0.109	~100.0, ~0.0	457	12,891
PL_1	<b>(H) 4.9</b>	1	0.216	100.0	367	8,855
FL_01	-1.9	1, 3	0.225, 0.285	99.7, 0.3	54	2,051
FL_02	<b>(H) 18.5</b>	1, 3	0.240, 0.320	99.9, 0.1	240	2,252
FL_03	-2.7	1, 3	0.189, 0.228	99.8, 0.2	87	3,063
FL_04	-23.0	1	0.150	100.0	19	4,375
FL_05	<b>(H) 0.7</b>	1, 3	0.270, 0.348	97.2, 2.8	42	1,497

**WC0\_80**

Branch	QGST [MMscfd]	PT <sub>in</sub> [barg]	PT <sub>out</sub> [barg]	DP [barg]	TM <sub>in</sub> [°C]	TM <sub>out</sub> [°C]	DTHYD <sub>in</sub> OP [°C]
PL_2	41.4	51.9	45.0	6.9	<b>(W) 17.1</b>	<b>(W) 13.1</b>	-0.1
PL_1	26.9	53.6	52.0	1.6	<b>(W) 8.6</b>	<b>(W) 6.9</b>	<b>(H) 8.6</b>
FL_01	6.4	54.1	53.6	0.5	27.1	<b>(W) 13.1</b>	-9.8
FL_02	6.4	55.2	53.6	1.6	27.8	<b>(W) -4.8</b>	-10.4
FL_03	9.4	55.0	53.6	1.5	34.7	<b>(W) 14.0</b>	-17.3
FL_04	14.5	53.0	52.0	1.0	41.0	35.9	-23.8
FL_05	4.6	54.0	53.6	0.4	20.6	<b>(W) 10.2</b>	-3.4

Branch	DTHYD <sub>out</sub> OP [°C]	ID [-]	HOL <sub>avg</sub> [-]	ID <sub>pct</sub> [%]	LIQC [bbl]	QLT <sub>out</sub> [bbl/day]
PL_2	<b>(H) 3.0</b>	1, 3	0.178, 0.122	~100.0, ~0.0	475	<b>(S) 10,405</b>
PL_1	<b>(H) 10.1</b>	1, 3	0.221, 0.322	97.2, 2.8	382	<b>(S) 7,065</b>
FL_01	<b>(H) 4.1</b>	1, 3	0.239, 0.308	99.7, 0.3	58	1,649
FL_02	<b>(H) 22.0</b>	1, 3	0.248, 0.299	99.6, 0.4	248	<b>(S) 1,820</b>
FL_03	<b>(H) 3.2</b>	1, 3	0.195, 0.250	99.8, 0.2	89	2,432
FL_04	-18.9	1	0.150	100.0	19	3,489
FL_05	<b>(H) 7.0</b>	1, 3	0.294, 0.355	93.8, 6.2	47	<b>(S) 1,175</b>

**WC0\_60**

Branch	QGST [MMscfd]	PT <sub>in</sub> [barg]	PT <sub>out</sub> [barg]	DP [barg]	TM <sub>in</sub> [°C]	TM <sub>out</sub> [°C]	DTHYD <sub>in</sub> OP [°C]
PL_2	31.5	49.0	45.0	4.0	<b>(W) 11.3</b>	<b>(W) 8.1</b>	<b>(H) 5.3</b>
PL_1	20.5	50.2	49.0	1.2	<b>(W) 2.3</b>	<b>(W) 1.2</b>	<b>(H) 14.5</b>
FL_01	4.8	50.7	50.2	0.5	20.0	<b>(W) 6.0</b>	-3.2
FL_02	<b>(S) 5.0</b>	51.6	50.2	1.4	20.7	<b>(W) -7.9</b>	-3.7
FL_03	7.2	51.2	50.2	1.0	28.5	<b>(W) 7.1</b>	-11.6
FL_04	11.0	49.6	49.0	0.6	36.2	30.3	-19.5
FL_05	<b>(S) 3.5</b>	50.7	50.2	0.5	<b>(W) 13.7</b>	<b>(W) 3.1</b>	<b>(H) 3.2</b>

Branch	DTHYD <sub>out</sub> OP [°C]	ID [-]	HOL <sub>avg</sub> [-]	ID <sub>pct</sub> [%]	LIQC [bbl]	QLT <sub>out</sub> [bbl/day]
PL_2	<b>(H) 8.0</b>	1, 3	0.197, 0.143	~100.0, ~0.0	522	<b>(S) 8,030</b>
PL_1	<b>(H) 15.5</b>	1, 3	0.236, 0.394	96.6, 3.4	410	<b>(S) 5,410</b>
FL_01	<b>(H) 10.8</b>	1, 3	0.269, 0.391	96.6, 3.4	66	<b>(S) 1,270</b>
FL_02	<b>(H) 24.7</b>	1, 3	0.265, 0.430	98.4, 1.6	267	<b>(S) 1,310</b>
FL_03	<b>(H) 9.7</b>	1, 3	0.213, 0.285	99.8, 0.2	98	1,865
FL_04	-13.7	1	0.157	100.0	20	2,648
FL_05	<b>(H) 13.7</b>	1, 3	0.307, 0.495	81.6, 18.4	54	<b>(S) 600</b>

**WC0\_40**

Branch	QGST [MMscfd]	PT <sub>in</sub> [barg]	PT <sub>out</sub> [barg]	DP [barg]	TM <sub>in</sub> [°C]	TM <sub>out</sub> [°C]	DTHYD <sub>in</sub> OP [°C]
PL_2	(S) 21.4	47.3	45.0	2.3	(W) 3.7	(W) 1.5	(H) 12.7
PL_1	(S) 14.1	48.5	47.3	1.1	(W) -4.0	(W) -4.8	(H) 20.5
FL_01	(S) 3.3	49.1	48.5	0.6	(W) 11.3	(W) -1.4	(H) 5.3
FL_02	(S) 3.5	50.0	48.5	1.6	(W) 12.0	(W) -9.7	(H) 4.7
FL_03	(S) 4.9	49.3	48.5	0.8	19.7	(W) -1.0	-3.0
FL_04	7.4	47.6	47.3	0.2	28.2	21.3	-11.7
FL_05	(S) 2.4	49.0	48.5	0.5	(W) 5.2	(W) -3.7	(H) 11.4
Branch	DTHYD <sub>out</sub> OP [°C]	ID [-]	HOL <sub>avg</sub> [-]	ID <sub>pct</sub> [%]	LIQC [bbl]	QLT <sub>out</sub> [bbl/day]	
PL_2	(H) 14.6	1, 3	0.240, 0.260	96.9, 3.1	638	(S) 5,385	
PL_1	(H) 21.2	1, 3	0.251, 0.439	85.3, 14.7	475	(S) 3,915	
FL_01	(H) 17.9	1, 3	0.295, 0.523	82.9, 17.1	84	(S) 785	
FL_02	(H) 26.3	1, 3	0.285, 0.531	90.4, 9.6	309	(S) 1,175	
FL_03	(H) 17.6	1, 3	0.252, 0.401	95.9, 4.1	120	(S) 1,415	
FL_04	-4.9	1	0.176	100.0	23	1,820	
FL_05	(H) 20.3	1, 3	0.344, 0.565	76.9, 23.1	59	(S) 765	

## WC0\_20

Branch	QGST [MMscfd]	PT <sub>in</sub> [barg]	PT <sub>out</sub> [barg]	DP [barg]	TM <sub>in</sub> [°C]	TM <sub>out</sub> [°C]	DTHYD <sub>in</sub> OP [°C]
PL_2	(S) 10.5	46.9	45.0	1.9	(W) -1.1	(W) -5.0	(H) 17.5
PL_1	(S) 6.8	48.2	46.9	1.3	(W) -8.2	(W) -8.5	(H) 24.7
FL_01	(S) 1.4	48.9	48.2	0.7	(W) 8.3	(W) -6.8	(H) 8.4
FL_02	(S) 1.4	50.0	48.2	1.7	(W) 8.9	(W) -10.2	(H) 7.9
FL_03	(S) 2.8	49.2	48.2	1.0	(W) 7.0	(W) -8.1	(H) 9.7
FL_04	3.9	47.0	46.9	0.1	21.2	(W) 13.9	-4.8
FL_05	(S) 1.2	48.8	48.2	0.6	(W) 4.2	(W) -7.9	(H) 12.5
Branch	DTHYD <sub>out</sub> OP [°C]	ID [-]	HOL <sub>avg</sub> [-]	ID <sub>pct</sub> [%]	LIQC [bbl]	QLT <sub>out</sub> [bbl/day]	
PL_2	(H) 21.1	1, 3	0.308, 0.432	83.3, 16.7	837	(S) 2,585	
PL_1	(H) 24.9	1, 3	0.300, 0.517	81.9, 18.1	594	(S) 1,725	
FL_01	(H) 23.4	1, 3	0.251, 0.708	58.8, 41.2	101	(S) 383	
FL_02	(H) 26.7	1, 3	0.308, 0.587	78.8, 21.2	360	(S) 405	
FL_03	(H) 24.7	1, 3	0.282, 0.466	79.9, 20.1	154	(S) 875	
FL_04	(H) 2.4	1, 3	0.224, 0.467	94.1, 5.9	29	(S) 985	
FL_05	(H) 24.4	1, 3	0.345, 0.733	57.7, 42.3	74	(S) 335	

## WC26\_100

Branch	QGST [MMscfd]	PT <sub>in</sub> [barg]	PT <sub>out</sub> [barg]	DP [barg]	TM <sub>in</sub> [°C]	TM <sub>out</sub> [°C]	DTHYD <sub>in</sub> OP [°C]
PL_2	51.9	59.6	45.0	14.6	33.0	28.1	-15.2
PL_1	33.5	62.3	59.7	2.6	24.7	22.8	-6.6
FL_01	7.9	63.1	62.3	0.7	44.5	30.7	-26.4
FL_02	8.0	64.7	62.3	2.3	45.2	(W) 6.3	-26.9
FL_03	11.9	64.9	62.3	2.5	50.7	31.6	-32.3
FL_04	18.4	61.7	59.7	2.0	55.6	51.4	-37.5
FL_05	5.7	62.8	62.3	0.5	39.3	28.2	-21.1

Branch	DTHYD <sub>out</sub> OP [°C]	ID [-]	HOL <sub>avg</sub> [-]	ID <sub>pct</sub> [%]	LIQC [bbbl]	QLT <sub>out</sub> [bbbl/day]
PL_2	-12.0	1, 3	0.195, 0.113	~100.0, ~0.0	522	15,511
PL_1	-4.9	1, 3	0.251, 0.323	96.6, 3.4	431	10,539
FL_01	-12.6	1, 3	0.266, 0.312	99.8, 0.2	64	2,449
FL_02	<b>(H) 11.9</b>	1, 3	0.281, 0.352	98.8, 1.2	282	2,648
FL_03	-13.5	1, 3	0.223, 0.253	99.9, 0.1	102	3,678
FL_04	-33.6	1	0.177	100.0	22	5,427
FL_05	-10.1	1, 3	0.290, 0.403	87.1, 12.9	48	1,794

## WC26\_80

Branch	QGST [MMscfd]	PT <sub>in</sub> [barg]	PT <sub>out</sub> [barg]	DP [barg]	TM <sub>in</sub> [°C]	TM <sub>out</sub> [°C]	DTHYD <sub>in</sub> OP [°C]
PL_2	41.9	54.3	45.0	9.3	28.0	24.5	-10.8
PL_1	27.3	56.3	54.4	2.0	20.0	18.8	-2.5
FL_01	6.4	57.0	56.3	0.6	31.1	24.5	-13.5
FL_02	6.6	58.3	56.3	2.0	32.8	<b>(W) 5.7</b>	-15.1
FL_03	9.6	58.1	56.3	1.8	40.5	26.6	-22.8
FL_04	14.6	55.7	54.4	1.3	48.8	45.2	-31.4
FL_05	4.7	56.8	56.3	0.5	23.7	21.1	-6.1

Branch	DTHYD <sub>out</sub> OP [°C]	ID [-]	HOL <sub>avg</sub> [-]	ID <sub>pct</sub> [%]	LIQC [bbbl]	QLT <sub>out</sub> [bbbl/day]
PL_2	-8.4	1, 3	0.203, 0.126	~100.0, ~0.0	539	12,615
PL_1	-1.5	1, 3	0.254, 0.351	96.6, 3.4	433	8,555
FL_01	-7.0	1, 3	0.276, 0.331	99.8, 0.2	68	1,999
FL_02	<b>(H) 11.8</b>	1, 3	0.274, 0.377	92.4, 7.6	278	2,163
FL_03	-9.1	1, 3	0.226, 0.269	99.9, 0.1	105	2,959
FL_04	-28.0	1	0.176	100.0	22	4,315
FL_05	-3.6	1, 3	0.259, 0.433	65.2, 34.8	51	1,471

## WC26\_60

Branch	QGST [MMscfd]	PT <sub>in</sub> [barg]	PT <sub>out</sub> [barg]	DP [barg]	TM <sub>in</sub> [°C]	TM <sub>out</sub> [°C]	DTHYD <sub>in</sub> OP [°C]
PL_2	31.1	49.9	45.0	4.9	20.7	<b>(W) 17.4</b>	-4.0
PL_1	20.2	51.4	49.9	1.4	<b>(W) 11.1</b>	<b>(W) 9.4</b>	<b>(H) 5.8</b>
FL_01	4.7	52.0	51.4	0.6	32.7	<b>(W) 16.2</b>	-15.7
FL_02	4.8	53.1	51.4	1.7	33.2	<b>(W) -4.3</b>	-16.1
FL_03	7.1	52.6	51.4	1.2	40.7	<b>(W) 17.0</b>	-23.6
FL_04	10.9	50.6	49.9	0.7	47.4	41.7	-30.5
FL_05	3.5	51.9	51.4	0.5	26.5	<b>(W) 14.1</b>	-9.5

Branch	DTHYD <sub>out</sub> OP [°C]	ID [-]	HOL <sub>avg</sub> [-]	ID <sub>pct</sub> [%]	LIQC [bbbl]	QLT <sub>out</sub> [bbbl/day]
PL_2	-1.3	1, 3	0.223, 0.224	98.0, 2.0	595	9,536
PL_1	<b>(H) 7.3</b>	1, 3	0.256, 0.368	86.4, 13.6	462	6,412
FL_01	<b>(H) 0.8</b>	1, 3	0.251, 0.394	69.0, 31.0	72	1,492
FL_02	<b>(H) 21.2</b>	1, 3	0.268, 0.397	78.1, 21.9	296	1,594
FL_03	-0.1	1, 3	0.239, 0.318	95.0, 5.0	112	2,216
FL_04	-25.0	1	0.179	100.0	23	3,207
FL_05	<b>(H) 2.8</b>	1, 3	0.245, 0.474	57.9, 42.1	53	1,116

## WC26\_40

Branch	QGST [MMscfd]	PT <sub>in</sub> [barg]	PT <sub>out</sub> [barg]	DP [barg]	TM <sub>in</sub> [°C]	TM <sub>out</sub> [°C]	DTHYD <sub>in</sub> OP [°C]
PL_2	21.2	47.8	45.0	2.8	(W) 12.4	(W) 9.4	(H) 4.1
PL_1	13.8	49.1	47.8	1.3	(W) 2.9	(W) 1.3	(H) 13.8
FL_01	3.2	49.7	49.1	0.7	23.8	(W) 6.5	-7.0
FL_02	3.3	50.8	49.1	1.7	24.7	(W) -8.2	-7.8
FL_03	4.9	50.1	49.1	1.0	32.9	(W) 7.1	-16.1
FL_04	7.4	48.1	47.8	0.3	40.7	33.5	-24.2
FL_05	2.4	49.6	49.1	0.5	(W) 17.5	(W) 5.0	-0.8
Branch	DTHYD <sub>out</sub> OP [°C]	ID [-]	HOL <sub>avg</sub> [-]	ID <sub>pct</sub> [%]	LIQC [bbl]	QLT <sub>out</sub> [bbl/day]	
PL_2	(H) 6.7	1, 3	0.266, 0.318	92.6, 7.4	720	6,631	
PL_1	(H) 15.2	1, 3	0.254, 0.410	72.3, 27.7	507	4,446	
FL_01	(H) 10.2	1, 3	0.239, 0.476	59.7, 40.3	82	1,025	
FL_02	(H) 24.9	1, 3	0.255, 0.447	67.1, 32.9	318	1,101	
FL_03	(H) 9.5	1, 3	0.245, 0.371	75.6, 24.4	126	1,546	
FL_04	-17.0	1	0.199	100.0	25	2,196	
FL_05	(H) 11.6	1, 3	0.253, 0.530	50.6, 49.4	59	773	

## WC26\_20

Branch	QGST [MMscfd]	PT <sub>in</sub> [barg]	PT <sub>out</sub> [barg]	DP [barg]	TM <sub>in</sub> [°C]	TM <sub>out</sub> [°C]	DTHYD <sub>in</sub> OP [°C]
PL_2	(S) 10.3	47.4	45.0	2.4	(W) 0.3	(W) -2.2	(H) 16.1
PL_1	(S) 6.9	48.8	47.4	1.4	(W) -5.6	(W) -6.3	(H) 22.2
FL_01	1.7	49.6	48.8	0.7	(W) 10.1	(W) -4.8	(H) 6.6
FL_02	(S) 1.5	50.7	48.8	1.9	26.1	(W) -9.6	-9.3
FL_03	2.3	49.9	48.8	1.0	17.7	(W) -5.3	-1.0
FL_04	3.7	47.5	47.4	0.1	26.4	(W) 16.9	-10.0
FL_05	1.2	49.5	48.8	0.6	18.2	(W) -1.3	-1.5
Branch	DTHYD <sub>out</sub> OP [°C]	ID [-]	HOL <sub>avg</sub> [-]	ID <sub>pct</sub> [%]	LIQC [bbl]	QLT <sub>out</sub> [bbl/day]	
PL_2	(H) 18.3	1, 3	0.297, 0.457	67.0, 33.0	931	(S) 3,270	
PL_1	(H) 22.7	1, 3	0.266, 0.518	65.0, 35.0	615	(S) 1,959	
FL_01	(H) 21.4	1, 3	0.222, 0.604	47.5, 52.5	99	(S) 509	
FL_02	(H) 26.2	1, 3	0.244, 0.543	60.5, 39.5	359	(S) 642	
FL_03	(H) 22.0	1, 3	0.247, 0.495	61.2, 38.8	154	884	
FL_04	-0.5	1, 3	0.258, 0.474	94.1, 5.9	34	1,146	
FL_05	(H) 17.9	1, 3	0.313, 0.650	50.9, 49.1	71	(S) 428	

Table H.3 – Pipeline parameters for different turndown flowrates (steady-state), and the differences between steady-state and transient solutions

## WC0\_100

Branch	QGST [MMscfd]	PT <sub>in</sub> [barg]	DP [barg]	TM <sub>out</sub> [°C]	DTHYD <sub>out</sub> OP [°C]	LIQC [bbl]	QLT <sub>out</sub> [bbl/day]
--------	------------------	----------------------------	--------------	------------------------	---------------------------------	---------------	---------------------------------

<b>PL_2</b>	52.2 (0.1)	56.3 (0.0)	11.3 (0.0)	<b>(W) 17.4</b> (0.0)	-1.3 (0.0)	457 (0)	12,915 (25)
<b>PL_1</b>	33.9 (0.0)	58.5 (0.0)	2.2 (0.0)	<b>(W) 12.7</b> (0.0)	<b>(H) 4.8</b> (0.0)	367 (0)	8,861 (6)
<b>FL_01</b>	8.0 (0.0)	59.2 (0.1)	0.6 (0.0)	19.6 (0.0)	-1.9 (0.0)	54 (0)	2,058 (7)
<b>FL_02</b>	8.2 (0.0)	60.7 (0.1)	2.1 (0.0)	<b>(W) -0.8</b> (0.0)	<b>(H) 18.5</b> (0.0)	240 (0)	2,253 (1)
<b>FL_03</b>	11.9 (0.0)	60.7 (0.0)	2.2 (0.0)	20.4 (0.0)	-2.7 (0.0)	87 (0)	3,063 (0)
<b>FL_04</b>	18.3 (0.0)	57.9 (0.0)	1.6 (0.0)	40.6 (0.0)	-23.1 (0.0)	19 (0)	4,385 (10)
<b>FL_05</b>	5.8 (0.0)	59.0 (0.0)	0.4 (0.0)	<b>(W) 17.1</b> (0.0)	<b>(H) 0.7</b> (0.0)	41 (-1)	1,506 (9)

**WC0\_80**

<b>Branch</b>	<b>QGST</b> [MMscfd]	<b>PT<sub>in</sub></b> [barg]	<b>DP</b> [barg]	<b>TM<sub>out</sub> [°C]</b>	<b>DTHYD<sub>out</sub></b> <b>OP [°C]</b>	<b>LIQC</b> [bbl]	<b>QLT<sub>out</sub></b> [bbl/day]
<b>PL_2</b>	41.5 (0.0)	52.0 (0.0)	7.0 (0.0)	<b>(W) 13.1</b> (0.0)	<b>(H) 3.0</b> (0.0)	475 (0)	10,400 (-5)
<b>PL_1</b>	26.9 (0.0)	53.6 (0.0)	1.6 (0.0)	<b>(W) 6.9</b> (0.0)	<b>(H) 10.1</b> (0.0)	382 (0)	7,058 (-7)
<b>FL_01</b>	6.4 (0.0)	54.1 (0.0)	0.5 (0.0)	<b>(W) 13.1</b> (0.0)	<b>(H) 4.1</b> (0.0)	58 (0)	1,650 (1)
<b>FL_02</b>	6.5 (0.0)	55.2 (0.1)	1.6 (0.0)	<b>(W) -4.8</b> (0.0)	<b>(H) 22.0</b> (0.0)	248 (0)	1,779 (-41)
<b>FL_03</b>	9.4 (0.0)	55.1 (0.0)	1.5 (0.0)	<b>(W) 14.0</b> (0.0)	<b>(H) 3.2</b> (0.0)	89 (0)	2,431 (0)
<b>FL_04</b>	14.6 (0.0)	53.0 (0.0)	1.0 (0.0)	36.0 (0.0)	-18.9 (0.0)	19 (0)	3,497 (8)
<b>FL_05</b>	4.6 (0.0)	54.0 (0.0)	0.4 (0.0)	<b>(W) 10.2</b> (0.0)	<b>(H) 7.0</b> (0.0)	45 (-2)	1,204 (29)

**WC0\_60**

<b>Branch</b>	<b>QGST</b> [MMscfd]	<b>PT<sub>in</sub></b> [barg]	<b>DP</b> [barg]	<b>TM<sub>out</sub> [°C]</b>	<b>DTHYD<sub>out</sub></b> <b>OP [°C]</b>	<b>LIQC</b> [bbl]	<b>QLT<sub>out</sub></b> [bbl/day]
<b>PL_2</b>	31.4 (0.0)	49.0 (0.0)	4.0 (0.0)	<b>(W) 8.0</b> (-0.1)	<b>(H) 8.1</b> (0.1)	522 (1)	8,014 (-16)
<b>PL_1</b>	20.5 (0.0)	50.2 (0.0)	1.2 (0.0)	<b>(W) 1.2</b> (0.0)	<b>(H) 15.5</b> (0.0)	409 (-1)	5,419 (9)
<b>FL_01</b>	4.8 (0.0)	50.7 (0.0)	0.5 (0.0)	<b>(W) 6.0</b> (0.0)	<b>(H) 10.8</b> (0.0)	65 (-2)	1,261 (-9)
<b>FL_02</b>	4.9 (-0.1)	51.7 (0.0)	1.4 (0.0)	<b>(W) -7.9</b> (0.0)	<b>(H) 24.7</b> (0.0)	263 (-4)	1,344 (34)
<b>FL_03</b>	7.2 (0.0)	51.2 (0.0)	1.0 (0.0)	<b>(W) 7.1</b> (0.0)	<b>(H) 9.7</b> (0.0)	98 (0)	1,871 (7)
<b>FL_04</b>	11.0 (0.0)	49.6 (0.0)	0.6 (0.0)	30.0 (-0.3)	-13.4 (0.3)	20 (0)	2,653 (5)

<b>FL_05</b>	3.6	50.7	0.4	<b>(W) 3.8</b>	<b>(H) 13.0</b>	49	941
	(0.1)	(0.0)	(0.0)	(0.7)	(-0.7)	(-5)	(341)

**WC0\_40**

<b>Branch</b>	<b>QGST [MMscfd]</b>	<b>PT<sub>in</sub> [barg]</b>	<b>DP [barg]</b>	<b>TM<sub>out</sub> [°C]</b>	<b>DTHYD<sub>out</sub> OP [°C]</b>	<b>LIQC [bbl]</b>	<b>QLT<sub>out</sub> [bbl/day]</b>
<b>PL_2</b>	21.4	47.3	2.3	<b>(W) 1.5</b>	<b>(H) 14.6</b>	636	5,586
	(0.1)	(0.0)	(0.0)	(0.0)	(0.0)	(-2)	(201)
<b>PL_1</b>	14.0	48.5	1.1	<b>(W) -4.8</b>	<b>(H) 21.2</b>	461	3,772
	(0.0)	(0.0)	(0.0)	(0.0)	(0.0)	(-15)	(-143)
<b>FL_01</b>	3.3	49.0	0.6	<b>(W) -1.4</b>	<b>(H) 18.0</b>	76	886
	(0.1)	(0.0)	(-0.1)	(-0.1)	(0.1)	(-9)	(101)
<b>FL_02</b>	3.4	50.0	1.5	<b>(W) -9.7</b>	<b>(H) 26.3</b>	293	930
	(-0.1)	(-0.1)	(-0.1)	(0.0)	(0.0)	(-17)	(-245)
<b>FL_03</b>	4.9	49.3	0.9	<b>(W) -1.0</b>	<b>(H) 17.6</b>	115	1,294
	(0.0)	(0.0)	(0.0)	(0.0)	(0.0)	(-5)	(-121)
<b>FL_04</b>	7.4	47.6	0.2	21.3	-4.9	23	1,827
	(0.0)	(0.0)	(0.0)	(0.0)	(0.0)	(0)	(7)
<b>FL_05</b>	2.5	48.9	0.5	<b>(W) -3.0</b>	<b>(H) 19.6</b>	56	662
	(0.1)	(0.0)	(0.0)	(0.7)	(-0.7)	(-3)	(-103)

**WC26\_100**

<b>Branch</b>	<b>QGST [MMscfd]</b>	<b>PT<sub>in</sub> [barg]</b>	<b>DP [barg]</b>	<b>TM<sub>out</sub> [°C]</b>	<b>DTHYD<sub>out</sub> OP [°C]</b>	<b>LIQC [bbl]</b>	<b>QLT<sub>out</sub> [bbl/day]</b>
<b>PL_2</b>	52.0	59.7	14.7	28.1	-12.0	522	15,545
	(0.1)	(0.1)	(0.1)	(0.0)	(0.0)	(0)	(34)
<b>PL_1</b>	33.6	62.4	2.6	22.8	-5.0	431	10,566
	(0.1)	(0.1)	(0.0)	(0.0)	(0.0)	(0)	(27)
<b>FL_01</b>	7.9	63.1	0.7	30.7	-12.6	64	2,455
	(0.0)	(0.1)	(0.0)	(0.0)	(0.0)	(0)	(6)
<b>FL_02</b>	8.0	64.8	2.4	<b>(W) 6.3</b>	<b>(H) 11.8</b>	283	2,655
	(0.0)	(0.1)	(0.0)	(0.0)	(0.0)	(1)	(7)
<b>FL_03</b>	11.9	65.0	2.6	31.6	-13.5	102	3,687
	(0.0)	(0.1)	(0.0)	(0.0)	(0.0)	(0)	(9)
<b>FL_04</b>	18.4	61.8	2.0	51.4	-33.6	22	5,437
	(0.0)	(0.1)	(0.0)	(0.0)	(0.0)	(0)	(10)
<b>FL_05</b>	5.8	62.9	0.5	28.2	-10.1	48	1,799
	(0.0)	(0.1)	(0.0)	(0.0)	(0.0)	(0)	(5)

**WC26\_80**

<b>Branch</b>	<b>QGST [MMscfd]</b>	<b>PT<sub>in</sub> [barg]</b>	<b>DP [barg]</b>	<b>TM<sub>out</sub> [°C]</b>	<b>DTHYD<sub>out</sub> OP [°C]</b>	<b>LIQC [bbl]</b>	<b>QLT<sub>out</sub> [bbl/day]</b>
<b>PL_2</b>	41.5	54.1	9.1	23.4	-7.3	542	12,556
	(-0.4)	(-0.2)	(-0.2)	(-1.1)	(1.1)	(3)	(-59)
<b>PL_1</b>	27.0	56.1	1.9	<b>(W) 16.6</b>	<b>(H) 0.6</b>	439	8,510
	(-0.3)	(-0.2)	(0.0)	(-2.2)	(2.1)	(6)	(-46)
<b>FL_01</b>	6.3	56.7	0.6	24.2	-6.7	67	1,974
	(-0.1)	(-0.2)	(0.0)	(-0.3)	(0.2)	(-1)	(-25)
<b>FL_02</b>	6.6	58.1	2.0	<b>(W) 1.3</b>	<b>(H) 16.1</b>	284	2,171



	(-0.1)	(-0.2)	(0.0)	(-4.3)	(4.3)	(5)	(7)
<b>FL_03</b>	9.5	57.9	1.8	25.2	-7.7	104	2,940
	(-0.1)	(-0.2)	(0.0)	(-1.4)	(1.4)	(-1)	(-19)
<b>FL_04</b>	14.5	55.5	1.3	47.2	-29.9	22	4,273
	(-0.1)	(-0.2)	(0.0)	(1.9)	(-1.9)	(0)	(-42)
<b>FL_05</b>	4.6	56.6	0.5	21.3	-3.9	50	1,440
	(-0.1)	(-0.2)	(0.0)	(0.3)	(-0.3)	(-1)	(-32)

**WC26\_60**

<b>Branch</b>	<b>QGST</b> [MMscfd]	<b>PT<sub>in</sub></b> [barg]	<b>DP</b> [barg]	<b>TM<sub>out</sub> [°C]</b>	<b>DTHYD<sub>out</sub></b> <b>OP [°C]</b>	<b>LIQC</b> [bbl]	<b>QLT<sub>out</sub></b> [bbl/day]
<b>PL_2</b>	31.2	49.9	4.9	17.9	-1.8	593	9,552
	(0.1)	(0.0)	(0.0)	(0.4)	(-0.4)	(-3)	(16)
<b>PL_1</b>	20.2	51.4	1.5	<b>(W) 10.1</b>	<b>(H) 6.7</b>	461	6,416
	(0.0)	(0.1)	(0.0)	(0.7)	(-0.7)	(-1)	(4)
<b>FL_01</b>	4.8	52.0	0.6	<b>(W) 17.4</b>	-0.5	72	1,487
	(0.0)	(0.1)	(0.0)	(1.3)	(-1.3)	(0)	(-5)
<b>FL_02</b>	4.8	53.2	1.8	<b>(W) -3.8</b>	<b>(H) 20.8</b>	296	1,596
	(0.0)	(0.1)	(0.1)	(0.4)	(-0.4)	(0)	(2)
<b>FL_03</b>	7.1	52.6	1.2	<b>(W) 17.0</b>	-0.1	112	2,220
	(0.0)	(0.1)	(0.0)	(0.0)	(0.0)	(0)	(3)
<b>FL_04</b>	10.9	50.7	0.7	41.7	-25.0	23	3,219
	(0.0)	(0.0)	(0.0)	(0.0)	(0.0)	(0)	(12)
<b>FL_05</b>	3.6	51.9	0.5	<b>(W) 15.9</b>	<b>(H) 1.1</b>	52	1,115
	(0.0)	(0.1)	(0.0)	(1.8)	(-1.8)	(-1)	(-1)

**WC26\_40**

<b>Branch</b>	<b>QGST</b> [MMscfd]	<b>PT<sub>in</sub></b> [barg]	<b>DP</b> [barg]	<b>TM<sub>out</sub> [°C]</b>	<b>DTHYD<sub>out</sub></b> <b>OP [°C]</b>	<b>LIQC</b> [bbl]	<b>QLT<sub>out</sub></b> [bbl/day]
<b>PL_2</b>	21.2	47.8	2.8	<b>(W) 9.5</b>	<b>(H) 6.6</b>	718	6,643
	(0.1)	(0.0)	(0.0)	(0.0)	(0.0)	(-2)	(12)
<b>PL_1</b>	13.8	49.1	1.3	<b>(W) 1.3</b>	<b>(H) 15.1</b>	510	4,466
	(0.1)	(0.0)	(0.0)	(0.1)	(-0.1)	(3)	(20)
<b>FL_01</b>	3.2	49.8	0.6	<b>(W) 6.5</b>	<b>(H) 10.1</b>	81	1,030
	(0.0)	(0.0)	(0.0)	(0.1)	(-0.1)	(0)	(5)
<b>FL_02</b>	3.3	50.9	1.8	<b>(W) -8.2</b>	<b>(H) 24.9</b>	321	1,107
	(0.0)	(0.1)	(0.0)	(0.0)	(0.0)	(3)	(6)
<b>FL_03</b>	4.9	50.1	1.0	<b>(W) 7.2</b>	<b>(H) 9.5</b>	126	1,551
	(0.0)	(0.1)	(0.0)	(0.0)	(0.0)	(0)	(5)
<b>FL_04</b>	7.4	48.1	0.3	33.5	-17.0	25	2,200
	(0.0)	(0.0)	(0.0)	(0.0)	(0.0)	(0)	(4)
<b>FL_05</b>	2.4	49.6	0.5	<b>(W) 5.1</b>	<b>(H) 11.5</b>	60	778
	(0.0)	(0.0)	(0.0)	(0.1)	(-0.1)	(0)	(5)

Table H.4 – Methanol injection rates for different turndown flowrates

**WC0\_100**

Branch	Pure				Saline		
	GLWVT	DTHYD <sub>out</sub>	MeOH	QMeOH	DTHYD <sub>out</sub>	MeOH	QMeOH
	[kg/h]	EP [°C]	wt% [%]	[kg/h]	ES [°C]	wt% [%]	[kg/h]
PL_2	247.9	-1.4	13.7	-	-	-	-
PL_1	157.6	<b>(H) 4.8</b>	30.2	-	-	-	-
FL_01	36.7	-2.2	11.3	7.7	-	-	-
FL_02	37.1	<b>(H) 18.2</b>	51.8	42.9	-	-	-
FL_03	57.7	-3.0	8.1	8.2	-	-	-
FL_04	90.3	-23.1	0.0	0.0	-	-	-
FL_05	26.2	<b>(H) 0.3</b>	19.4	9.3	-	-	-

## WC0\_80

Branch	Pure				Saline		
	GLWVT	DTHYD <sub>out</sub>	MeOH	QMeOH	DTHYD <sub>out</sub>	MeOH	QMeOH
	[kg/h]	EP [°C]	wt% [%]	[kg/h]	ES [°C]	wt% [%]	[kg/h]
PL_2	200.8	<b>(H) 2.9</b>	25.4	-	-	-	-
PL_1	128.7	<b>(H) 9.8</b>	39.2	-	-	-	-
FL_01	30.3	<b>(H) 3.6</b>	27.4	13.0	-	-	-
FL_02	30.3	<b>(H) 21.6</b>	56.3	40.5	-	-	-
FL_03	46.8	<b>(H) 2.7</b>	25.1	17.3	-	-	-
FL_04	72.0	-19.2	0.0	0.0	-	-	-
FL_05	21.4	<b>(H) 6.5</b>	33.2	12.2	-	-	-

## WC0\_60

Branch	Pure				Saline		
	GLWVT	DTHYD <sub>out</sub>	MeOH	QMeOH	DTHYD <sub>out</sub>	MeOH	QMeOH
	[kg/h]	EP [°C]	wt% [%]	[kg/h]	ES [°C]	wt% [%]	[kg/h]
PL_2	154.3	<b>(H) 7.8</b>	35.3	-	-	-	-
PL_1	100.1	<b>(H) 14.8</b>	47.3	-	-	-	-
FL_01	23.7	<b>(H) 10.7</b>	40.6	16.7	-	-	-
FL_02	23.7	<b>(H) 24.6</b>	59.8	35.7	-	-	-
FL_03	35.6	<b>(H) 9.6</b>	38.6	22.9	-	-	-
FL_04	54.3	-14.4	0.0	0.0	-	-	-
FL_05	17.1	<b>(H) 13.6</b>	44.8	14.4	-	-	-

## WC0\_40

Branch	Pure				Saline		
	GLWVT	DTHYD <sub>out</sub>	MeOH	QMeOH	DTHYD <sub>out</sub>	MeOH	QMeOH
	[kg/h]	EP [°C]	wt% [%]	[kg/h]	ES [°C]	wt% [%]	[kg/h]
PL_2	106.5	<b>(H) 14.4</b>	45.6	-	-	-	-
PL_1	69.7	<b>(H) 20.8</b>	54.2	-	-	-	-
FL_01	16.5	<b>(H) 17.3</b>	51.3	18.8	-	-	-
FL_02	16.8	<b>(H) 25.6</b>	61.9	28.7	-	-	-
FL_03	24.1	<b>(H) 17.0</b>	50.8	26.3	-	-	-
FL_04	36.8	-5.4	0.0	0.0	-	-	-
FL_05	12.3	<b>(H) 19.7</b>	54.4	16.0	-	-	-

## WC0\_20

Branch	Pure				Saline		
	GLWVT [kg/h]	DTHYD <sub>out</sub> EP [°C]	MeOH wt% [%]	QMeOH [kg/h]	DTHYD <sub>out</sub> ES [°C]	MeOH wt% [%]	QMeOH [kg/h]
PL_2	51.2	(H) 20.9	54.4	-	-	-	-
PL_1	31.8	(H) 24.5	59.0	-	-	-	-
FL_01	4.6	(H) 22.8	58.5	7.9	-	-	-
FL_02	4.9	(H) 26.1	62.4	9.6	-	-	-
FL_03	13.5	(H) 24.1	60.1	21.8	-	-	-
FL_04	19.4	(H) 2.0	23.4	7.4	-	-	-
FL_05	8.8	(H) 23.8	59.8	14.5	-	-	-

## WC26\_100

Branch	Pure				Saline		
	GLWVT [kg/h]	DTHYD <sub>out</sub> EP [°C]	MeOH wt% [%]	QMeOH [kg/h]	DTHYD <sub>out</sub> ES [°C]	MeOH wt% [%]	QMeOH [kg/h]
PL_2	20,613.1	-12.2	0.0	-	-24.2	0.0	-
PL_1	13,297.0	-5.4	0.0	-	-17.6	0.0	-
FL_01	3,130.0	-12.7	0.0	0.0	-25.0	0.0	0.0
FL_02	3,174.8	(H) 11.7	31.1	1,433.1	-0.6	7.6	261.1
FL_03	4,713.5	-13.6	0.0	0.0	-25.9	0.0	0.0
FL_04	7,316.0	-34.0	0.0	0.0	-46.3	0.0	0.0
FL_05	2,278.8	-10.2	0.0	0.0	-22.5	0.0	0.0

## WC26\_80

Branch	Pure				Saline		
	GLWVT [kg/h]	DTHYD <sub>out</sub> EP [°C]	MeOH wt% [%]	QMeOH [kg/h]	DTHYD <sub>out</sub> ES [°C]	MeOH wt% [%]	QMeOH [kg/h]
PL_2	16,678.1	-8.6	0.0	-	-20.6	0.0	-
PL_1	10,864.9	-2.1	7.4	-	-14.2	0.0	-
FL_01	2,556.0	-7.1	0.0	0.0	-19.3	0.0	0.0
FL_02	2,639.3	(H) 11.7	31.0	1,186.4	-0.5	7.7	219.7
FL_03	3,803.8	-9.2	0.0	0.0	-21.5	0.0	0.0
FL_04	5,813.2	-28.5	0.0	0.0	-40.7	0.0	0.0
FL_05	1,865.8	-3.7	2.8	53.8	-15.9	0.0	0.0

## WC26\_60

Branch	Pure				Saline		
	GLWVT [kg/h]	DTHYD <sub>out</sub> EP [°C]	MeOH wt% [%]	QMeOH [kg/h]	DTHYD <sub>out</sub> ES [°C]	MeOH wt% [%]	QMeOH [kg/h]
PL_2	12,362.4	-1.5	7.5	-	-13.5	0.0	-
PL_1	8,026.6	(H) 7.3	24.0	-	-5.6	0.0	-
FL_01	1,887.1	(H) 0.6	11.7	290.3	-11.6	0.0	0.0
FL_02	1,911.8	(H) 21.0	44.6	1,581.3	(H) 8.9	22.8	563.7
FL_03	2,818.3	-0.3	10.1	357.5	-12.4	0.0	0.0
FL_04	4,335.7	-25.0	0.0	0.0	-37.8	0.0	0.0
FL_05	1,409.4	(H) 2.6	15.7	301.0	-9.5	0.0	0.0

## WC26\_40

Branch	Pure				Saline		
	GLWVT [kg/h]	DTHYD <sub>out</sub> EP [°C]	MeOH wt% [%]	QMeOH [kg/h]	DTHYD <sub>out</sub> ES [°C]	MeOH wt% [%]	QMeOH [kg/h]
PL_2	8,409.4	(H) 6.5	22.7	-	-5.6	0.0	-
PL_1	5,476.3	(H) 14.6	35.7	-	(H) 2.6	13.5	-
FL_01	1,279.9	(H) 9.5	28.8	542.0	-2.6	4.7	97.0
FL_02	1,312.7	(H) 24.1	48.9	1,279.1	(H) 12.1	28.0	545.0
FL_03	1,928.3	(H) 8.8	27.7	762.8	-3.3	3.4	101.2
FL_04	2,933.0	-17.6	0.0	0.0	-29.6	0.0	0.0
FL_05	955.5	(H) 10.9	31.0	452.2	-1.2	7.4	110.8

## WC26\_20

Branch	Pure				Saline		
	GLWVT [kg/h]	DTHYD <sub>out</sub> EP [°C]	MeOH wt% [%]	QMeOH [kg/h]	DTHYD <sub>out</sub> ES [°C]	MeOH wt% [%]	QMeOH [kg/h]
PL_2	4,204.5	(H) 18.2	39.7	-	(H) 6.1	18.4	-
PL_1	2,747.8	(H) 22.2	46.4	-	(H) 10.2	24.4	-
FL_01	663.7	(H) 20.7	44.3	597.3	(H) 8.6	23.1	215.7
FL_02	632.2	(H) 25.5	50.6	717.4	(H) 13.5	30.0	286.2
FL_03	967.4	(H) 21.3	45.1	863.1	(H) 9.2	24.0	320.6
FL_04	1,456.7	-0.9	8.6	206.9	-13.0	0.0	0.0
FL_05	484.5	(H) 17.3	39.7	388.6	(H) 5.2	18.1	122.6

Table H.5 – Pipeline parameters after a six-hour shutdown

## WC0\_100

Branch	DTHYD <sub>max</sub> OP [°C]	DTHYD <sub>max</sub> EP [°C]	DTHYD <sub>max</sub> ES [°C]	PT <sub>DTHYD</sub> [barg]	TM <sub>DTHYD</sub> [°C]	PT <sub>avg</sub> [barg]	TM <sub>avg</sub> [°C]
PL_2	(H) 5.8	(H) 5.4	-	53.1	(W) 11.3	53.2	(W) 16.1
PL_1	(H) 13.0	(H) 12.6	-	52.9	(W) 4.1	53.1	(W) 9.9
FL_01	(H) 13.5	(H) 13.2	-	52.9	(W) 3.6	52.9	(W) 9.5
FL_02	(H) 22.1	(H) 21.7	-	52.9	(W) -5.0	52.6	(W) 2.3
FL_03	(H) 13.5	(H) 13.1	-	52.9	(W) 3.6	52.8	(W) 11.5
FL_04	(H) 1.0	(H) 0.6	-	53.1	(W) 16.1	53.1	(W) 19.2
FL_05	(H) 13.8	(H) 13.4	-	52.9	(W) 3.3	52.9	(W) 7.2

## WC0\_80

Branch	DTHYD <sub>max</sub> OP [°C]	DTHYD <sub>max</sub> EP [°C]	DTHYD <sub>max</sub> ES [°C]	PT <sub>DTHYD</sub> [barg]	TM <sub>DTHYD</sub> [°C]	PT <sub>avg</sub> [barg]	TM <sub>avg</sub> [°C]
PL_2	(H) 9.0	(H) 9.0	-	49.7	(W) 7.7	49.7	(W) 11.8
PL_1	(H) 15.8	(H) 15.0	-	49.6	(W) 0.9	49.7	(W) 4.9
FL_01	(H) 16.4	(H) 15.6	-	49.6	(W) 0.3	49.6	(W) 6.0
FL_02	(H) 24.0	(H) 23.2	-	49.6	(W) -7.2	49.5	(W) -0.9
FL_03	(H) 16.1	(H) 15.3	-	49.6	(W) 0.6	49.5	(W) 8.1
FL_04	(H) 3.1	(H) 3.1	-	49.8	(W) 13.7	49.7	(W) 16.8
FL_05	(H) 16.8	(H) 16.0	-	49.6	(W) 0.0	49.6	(W) 3.5

## WC0\_60

Branch	DTHYD <sub>max</sub> OP [°C]	DTHYD <sub>max</sub> EP [°C]	DTHYD <sub>max</sub> ES [°C]	PT <sub>DTHYD</sub> [barg]	TM <sub>DTHYD</sub> [°C]	PT <sub>avg</sub> [barg]	TM <sub>avg</sub> [°C]
PL_2	(H) 12.2	(H) 11.7	-	47.6	(W) 4.3	47.5	(W) 7.0
PL_1	(H) 18.9	(H) 18.4	-	47.6	(W) -2.5	47.6	(W) 0.0
FL_01	(H) 19.2	(H) 18.7	-	47.6	(W) -2.7	47.6	(W) 2.1
FL_02	(H) 25.4	(H) 24.8	-	47.7	(W) -8.9	47.6	(W) -4.0
FL_03	(H) 19.4	(H) 18.9	-	47.6	(W) -2.9	47.5	(W) 4.3
FL_04	(H) 5.7	(H) 5.2	-	47.6	(W) 10.8	47.5	(W) 13.9
FL_05	(H) 19.7	(H) 19.2	-	47.6	(W) -3.2	47.7	(W) -0.1

## WC0\_40

Branch	DTHYD <sub>max</sub> OP [°C]	DTHYD <sub>max</sub> EP [°C]	DTHYD <sub>max</sub> ES [°C]	PT <sub>DTHYD</sub> [barg]	TM <sub>DTHYD</sub> [°C]	PT <sub>avg</sub> [barg]	TM <sub>avg</sub> [°C]
PL_2	(H) 16.6	(H) 16.4	-	45.9	(W) -0.4	46.3	(W) 1.0
PL_1	(H) 22.6	(H) 22.2	-	46.8	(W) -6.3	46.6	(W) -5.2
FL_01	(H) 22.7	(H) 22.3	-	46.8	(W) -6.4	46.9	(W) -2.3
FL_02	(H) 26.2	(H) 25.8	-	46.8	(W) -9.9	47.1	(W) -6.8
FL_03	(H) 22.7	(H) 22.3	-	46.8	(W) -6.4	46.7	(W) -0.5
FL_04	(H) 10.3	(H) 10.0	-	46.5	(W) 6.0	46.4	(W) 9.2
FL_05	(H) 23.0	(H) 22.6	-	46.8	(W) -6.7	46.9	(W) -4.4

## WC0\_20

Branch	DTHYD <sub>max</sub> OP [°C]	DTHYD <sub>max</sub> EP [°C]	DTHYD <sub>max</sub> ES [°C]	PT <sub>DTHYD</sub> [barg]	TM <sub>DTHYD</sub> [°C]	PT <sub>avg</sub> [barg]	TM <sub>avg</sub> [°C]
PL_2	(H) 19.8	(H) 19.5	-	46.1	(W) -3.6	46.2	(W) -1.8
PL_1	(H) 25.6	(H) 25.1	-	47.4	(W) -9.1	47.0	(W) -8.8
FL_01	(H) 24.9	(H) 24.4	-	47.4	(W) -8.5	47.5	(W) -6.0
FL_02	(H) 26.5	(H) 26.1	-	47.4	(W) -10.1	47.7	(W) -8.6
FL_03	(H) 25.6	(H) 25.1	-	47.4	(W) -9.1	47.3	(W) -6.1
FL_04	(H) 11.7	(H) 11.3	-	46.6	(W) 4.6	46.5	(W) 7.8
FL_05	(H) 25.1	(H) 24.6	-	47.4	(W) -8.7	47.5	(W) -7.1

## WC26\_100

Branch	DTHYD <sub>max</sub> OP [°C]	DTHYD <sub>max</sub> EP [°C]	DTHYD <sub>max</sub> ES [°C]	PT <sub>DTHYD</sub> [barg]	TM <sub>DTHYD</sub> [°C]	PT <sub>avg</sub> [barg]	TM <sub>avg</sub> [°C]
PL_2	-1.7	-1.7	-14.6	55.4	19.1	55.4	25.5
PL_1	(H) 7.2	(H) 6.5	-5.6	55.0	(W) 10.2	55.2	18.8
FL_01	(H) 8.6	(H) 8.0	-4.2	55.0	(W) 8.8	54.9	(W) 16.3
FL_02	(H) 18.5	(H) 17.9	(H) 5.7	55.0	(W) -1.1	54.6	(W) 8.0
FL_03	(H) 9.2	(H) 8.5	-3.6	55.0	(W) 8.2	54.9	18.1
FL_04	-4.7	-4.7	-17.6	55.4	22.1	55.3	25.6
FL_05	(H) 8.8	(H) 8.1	-4.0	55.0	(W) 8.6	55.0	(W) 14.0

## WC26\_80

Branch	DTHYD <sub>max</sub> OP [°C]	DTHYD <sub>max</sub> EP [°C]	DTHYD <sub>max</sub> ES [°C]	PT <sub>DTHYD</sub> [barg]	TM <sub>DTHYD</sub> [°C]	PT <sub>avg</sub> [barg]	TM <sub>avg</sub> [°C]
PL_2	(H) 0.4	(H) 0.1	-12.0	51.6	(W) 16.6	51.5	21.9
PL_1	(H) 7.8	(H) 7.6	-4.6	51.7	(W) 9.2	51.7	(W) 15.4

FL_01	(H) 6.1	(H) 5.8	-6.3	51.7	(W) 10.9	51.7	18.0
FL_02	(H) 18.1	(H) 17.9	(H) 5.7	51.7	(W) -1.2	51.5	(W) 9.3
FL_03	(H) 7.6	(H) 7.4	-4.8	51.7	(W) 9.4	51.6	19.0
FL_04	-6.5	-6.8	-18.9	51.6	23.5	51.6	26.7
FL_05	(H) 5.9	(H) 5.6	-6.5	51.7	(W) 11.1	51.8	(W) 16.4
<b>WC26_60</b>							
Branch	DTHYD <sub>max</sub> OP [°C]	DTHYD <sub>max</sub> EP [°C]	DTHYD <sub>max</sub> ES [°C]	PT <sub>DTHYD</sub> [barg]	TM <sub>DTHYD</sub> [°C]	PT <sub>avg</sub> [barg]	TM <sub>avg</sub> [°C]
PL_2	(H) 5.3	(H) 4.7	-7.3	48.0	(W) 11.2	47.9	(W) 15.3
PL_1	(H) 13.6	(H) 13.0	(H) 0.9	47.9	(W) 2.9	48.0	(W) 7.5
FL_01	(H) 14.4	(H) 13.9	(H) 1.8	47.9	(W) 2.1	47.9	(W) 8.8
FL_02	(H) 23.4	(H) 22.9	(H) 10.8	48.0	(W) -6.9	47.9	(W) 0.5
FL_03	(H) 14.9	(H) 14.3	(H) 2.3	47.9	(W) 1.6	47.8	(W) 10.9
FL_04	-0.2	-0.8	-12.8	48.0	(W) 16.7	48.0	20.5
FL_05	(H) 14.7	(H) 14.2	(H) 2.1	47.9	(W) 1.7	48.0	(W) 6.4
<b>WC26_40</b>							
Branch	DTHYD <sub>max</sub> OP [°C]	DTHYD <sub>max</sub> EP [°C]	DTHYD <sub>max</sub> ES [°C]	PT <sub>DTHYD</sub> [barg]	TM <sub>DTHYD</sub> [°C]	PT <sub>avg</sub> [barg]	TM <sub>avg</sub> [°C]
PL_2	(H) 10.1	(H) 9.7	-2.4	46.7	(W) 6.3	46.5	(W) 8.3
PL_1	(H) 18.4	(H) 18.0	(H) 5.9	47.0	(W) -2.0	46.9	(W) 0.4
FL_01	(H) 19.0	(H) 18.6	(H) 6.5	47.0	(W) -2.7	47.0	(W) 3.5
FL_02	(H) 25.4	(H) 25.0	(H) 12.9	47.0	(W) -9.1	47.2	(W) -3.6
FL_03	(H) 19.2	(H) 18.7	(H) 6.7	47.0	(W) -2.8	46.8	(W) 5.7
FL_04	(H) 4.4	(H) 4.0	-8.1	46.7	(W) 11.9	46.6	(W) 16.4
FL_05	(H) 19.1	(H) 18.7	(H) 6.6	47.0	(W) -2.8	47.0	(W) 1.3
<b>WC26_20</b>							
Branch	DTHYD <sub>max</sub> OP [°C]	DTHYD <sub>max</sub> EP [°C]	DTHYD <sub>max</sub> ES [°C]	PT <sub>DTHYD</sub> [barg]	TM <sub>DTHYD</sub> [°C]	PT <sub>avg</sub> [barg]	TM <sub>avg</sub> [°C]
PL_2	(H) 19.6	(H) 19.3	(H) 7.3	45.8	(W) -3.4	46.5	(W) -1.0
PL_1	(H) 23.5	(H) 23.1	(H) 11.0	47.0	(W) -7.1	47.3	(W) -6.5
FL_01	(H) 23.9	(H) 23.4	(H) 11.3	47.8	(W) -7.5	48.0	(W) -3.8
FL_02	(H) 26.2	(H) 25.7	(H) 13.6	47.8	(W) -9.7	48.2	(W) -5.5
FL_03	(H) 24.1	(H) 23.5	(H) 11.5	47.8	(W) -7.6	47.7	(W) -2.7
FL_04	(H) 12.8	(H) 12.4	(H) 0.4	46.9	(W) 3.5	46.9	(W) 8.0
FL_05	(H) 22.5	(H) 22.0	(H) 9.9	47.8	(W) -6.1	47.9	(W) -1.6

Table H.6 - Methanol injection rates required for a no-touch time of six hours

<b>WC0_100</b>							
Branch	Pure				Saline		
	GLWVT [kg/h]	DTHYD <sub>max</sub> EP [°C]	MeOH wt% [%]	QMeOH [kg/h]	DTHYD <sub>max</sub> ES [°C]	MeOH wt% [%]	QMeOH [kg/h]
PL_2	247.9	(H) 5.4	31.2	-	-	-	-
PL_1	157.6	(H) 12.6	43.4	-	-	-	-
FL_01	36.7	(H) 13.2	44.2	29.0	-	-	-

FL_02	37.1	(H) 21.7	56.1	47.3	-	-	-
FL_03	57.7	(H) 13.1	44.1	45.6	-	-	-
FL_04	90.3	(H) 0.6	20.1	22.7	-	-	-
FL_05	26.2	(H) 13.4	44.6	21.0	-	-	-

---

**WC0\_80**


---

Branch	Pure				Saline		
	GLWVT [kg/h]	DTHYD <sub>max</sub> EP [°C]	MeOH wt% [%]	QMeOH [kg/h]	DTHYD <sub>max</sub> ES [°C]	MeOH wt% [%]	QMeOH [kg/h]
PL_2	200.8	(H) 9.0	37.2	-	-	-	-
PL_1	128.7	(H) 15.0	48.1	-	-	-	-
FL_01	30.3	(H) 15.6	48.9	29.0	-	-	-
FL_02	30.3	(H) 23.2	59.0	43.6	-	-	-
FL_03	46.8	(H) 15.3	48.5	44.1	-	-	-
FL_04	72.0	(H) 3.1	24.0	22.8	-	-	-
FL_05	21.4	(H) 16.0	49.4	20.9	-	-	-

---

**WC0\_60**


---

Branch	Pure				Saline		
	GLWVT [kg/h]	DTHYD <sub>max</sub> EP [°C]	MeOH wt% [%]	QMeOH [kg/h]	DTHYD <sub>max</sub> ES [°C]	MeOH wt% [%]	QMeOH [kg/h]
PL_2	154.3	(H) 11.7	41.7	-	-	-	-
PL_1	100.1	(H) 18.4	51.1	-	-	-	-
FL_01	23.7	(H) 18.7	51.5	25.1	-	-	-
FL_02	23.7	(H) 24.8	59.5	34.7	-	-	-
FL_03	35.6	(H) 18.9	51.7	38.1	-	-	-
FL_04	54.3	(H) 5.2	30.7	24.0	-	-	-
FL_05	17.1	(H) 19.2	52.1	18.6	-	-	-

---

**WC0\_40**


---

Branch	Pure				Saline		
	GLWVT [kg/h]	DTHYD <sub>max</sub> EP [°C]	MeOH wt% [%]	QMeOH [kg/h]	DTHYD <sub>max</sub> ES [°C]	MeOH wt% [%]	QMeOH [kg/h]
PL_2	106.5	(H) 16.4	48.3	-	-	-	-
PL_1	69.7	(H) 22.2	56.1	-	-	-	-
FL_01	16.5	(H) 22.3	56.2	21.2	-	-	-
FL_02	16.8	(H) 25.8	60.7	26.0	-	-	-
FL_03	24.1	(H) 22.3	56.2	30.9	-	-	-
FL_04	36.8	(H) 10.0	39.1	23.6	-	-	-
FL_05	12.3	(H) 22.6	56.6	16.0	-	-	-

---

**WC0\_20**


---

Branch	Pure				Saline		
	GLWVT [kg/h]	DTHYD <sub>max</sub> EP [°C]	MeOH wt% [%]	QMeOH [kg/h]	DTHYD <sub>max</sub> ES [°C]	MeOH wt% [%]	QMeOH [kg/h]
PL_2	51.2	(H) 19.5	52.6	-	-	-	-
PL_1	31.8	(H) 25.1	59.8	-	-	-	-
FL_01	4.6	(H) 24.4	59.0	6.7	-	-	-
FL_02	4.9	(H) 26.1	61.1	7.7	-	-	-

FL_03	13.5	(H) 25.1	59.8	20.1	-	-	-
FL_04	19.4	(H) 11.3	41.1	13.6	-	-	-
FL_05	8.8	(H) 24.6	59.2	12.8	-	-	-

## WC26\_100

Branch	Pure				Saline		
	GLWVT [kg/h]	DTHYD <sub>max</sub> EP [°C]	MeOH wt% [%]	QMeOH [kg/h]	DTHYD <sub>max</sub> ES [°C]	MeOH wt% [%]	QMeOH [kg/h]
PL_2	20,613.1	-1.7	7.0	-	-14.6	0.0	-
PL_1	13,297.0	(H) 6.5	23.8	-	-5.6	0.0	-
FL_01	3,130.0	(H) 8.0	26.1	1,107.7	-4.2	1.5	48.5
FL_02	3,174.8	(H) 17.9	40.5	2,159.8	(H) 5.7	18.7	730.0
FL_03	4,713.5	(H) 8.5	27.1	1,750.7	-3.6	2.6	127.3
FL_04	7,316.0	-4.7	0.6	41.9	-17.6	0.0	0.0
FL_05	2,278.8	(H) 8.1	26.4	818.9	-4.0	1.9	43.5

## WC26\_80

Branch	Pure				Saline		
	GLWVT [kg/h]	DTHYD <sub>max</sub> EP [°C]	MeOH wt% [%]	QMeOH [kg/h]	DTHYD <sub>max</sub> ES [°C]	MeOH wt% [%]	QMeOH [kg/h]
PL_2	16,678.1	(H) 0.1	10.9	-	-12.0	0.0	-
PL_1	10,864.9	(H) 7.6	24.4	-	-4.6	0.7	-
FL_01	2,556.0	(H) 5.8	21.6	702.2	-6.3	0.0	0.0
FL_02	2,639.3	(H) 17.9	40.5	1,796.0	(H) 5.7	17.8	570.3
FL_03	3,803.8	(H) 7.4	24.1	1,206.5	-4.8	0.4	13.7
FL_04	5,813.2	-6.8	0.0	0.0	-18.9	0.0	0.0
FL_05	1,865.8	(H) 5.6	21.2	503.2	-6.5	0.0	0.0

## WC26\_60

Branch	Pure				Saline		
	GLWVT [kg/h]	DTHYD <sub>max</sub> EP [°C]	MeOH wt% [%]	QMeOH [kg/h]	DTHYD <sub>max</sub> ES [°C]	MeOH wt% [%]	QMeOH [kg/h]
PL_2	12,362.4	(H) 4.7	19.7	-	-7.3	0.0	-
PL_1	8,026.6	(H) 13.0	33.1	-	(H) 0.9	11.1	-
FL_01	1,887.1	(H) 13.9	34.5	992.2	(H) 1.8	12.4	266.4
FL_02	1,911.8	(H) 22.9	47.2	1,708.8	(H) 10.8	25.2	645.4
FL_03	2,818.3	(H) 14.3	35.2	1,531.2	(H) 2.3	13.1	423.4
FL_04	4,335.7	-0.8	9.0	430.7	-12.8	0.0	0.0
FL_05	1,409.4	(H) 14.2	34.9	757.0	(H) 2.1	12.8	207.2

## WC26\_40

Branch	Pure				Saline		
	GLWVT [kg/h]	DTHYD <sub>max</sub> EP [°C]	MeOH wt% [%]	QMeOH [kg/h]	DTHYD <sub>max</sub> ES [°C]	MeOH wt% [%]	QMeOH [kg/h]
PL_2	8,409.4	(H) 9.7	27.9	-	-2.4	4.4	-
PL_1	5,476.3	(H) 18.0	40.7	-	(H) 5.9	18.1	-
FL_01	1,279.9	(H) 18.6	41.5	908.7	(H) 6.5	19.1	301.3
FL_02	1,312.7	(H) 25.0	50.0	1,313.0	(H) 12.9	28.2	516.7
FL_03	1,928.3	(H) 18.7	41.7	1,380.8	(H) 6.7	19.3	461.4



WC26_20							
Branch	Pure				Saline		
	GLWVT [kg/h]	DTHYD <sub>max</sub> EP [°C]	MeOH wt% [%]	QMeOH [kg/h]	DTHYD <sub>max</sub> ES [°C]	MeOH wt% [%]	QMeOH [kg/h]
FL_04	2,933.0	(H) 4.0	18.3	657.7	-8.1	0.0	0.0
FL_05	955.5	(H) 18.7	41.7	682.6	(H) 6.6	19.2	227.6
PL_2	4,204.5	(H) 19.3	42.5	-	(H) 7.3	20.2	-
PL_1	2,747.8	(H) 23.1	47.5	-	(H) 11.0	25.5	-
FL_01	663.7	(H) 23.4	47.9	609.9	(H) 11.3	26.0	232.9
FL_02	632.2	(H) 25.7	50.8	652.9	(H) 13.6	29.2	260.6
FL_03	967.4	(H) 23.5	48.0	894.8	(H) 11.5	26.1	342.5
FL_04	1,456.7	(H) 12.4	32.2	692.2	(H) 0.4	9.1	145.2
FL_05	484.5	(H) 22.0	46.0	413.2	(H) 9.9	24.0	152.9

Table H.7 – Pipeline parameters and methanol injection rates under different flowline insulation thicknesses

WC0_100_0"							
Branch	QGST [MMscfd]	PT <sub>in</sub> [barg]	PT <sub>out</sub> [barg]	DP [barg]	TM <sub>in</sub> [°C]	TM <sub>out</sub> [°C]	Q2 [W/m <sup>2</sup> ·K]
PL_2	52.2	56.3	45.0	11.3	22.4	(W) 17.4	0.65
PL_1	33.9	58.5	56.3	2.2	(W) 14.5	(W) 12.7	0.65
FL_01	8.0	59.2	58.6	0.6	33.2	19.6	24.49
FL_02	8.2	60.7	58.6	2.1	34.2	(W) -0.8	24.49
FL_03	11.9	60.7	58.6	2.2	39.8	20.4	24.68
FL_04	18.3	57.9	56.3	1.6	45.0	40.6	24.85
FL_05	5.8	59.0	58.6	0.4	27.6	(W) 17.1	24.31
Branch	DTHYD <sub>out</sub> OP [°C]	DTHYD <sub>out</sub> EP [°C]	DTHYD <sub>out</sub> ES [°C]	QMeOH EP [kg/h]	QMeOH ES [kg/h]	LIQC [bbl]	QLT <sub>out</sub> [bbl/day]
PL_2	-1.3	-1.4	-	-	-	457	12,915
PL_1	(H) 4.8	(H) 4.7	-	-	-	367	8,861
FL_01	-1.9	-2.2	-	7.7	-	54	2,058
FL_02	(H) 18.5	(H) 18.2	-	43.0	-	240	2,253
FL_03	-2.7	-3.0	-	8.1	-	87	3,063
FL_04	-23.1	-23.2	-	0.0	-	19	4,385
FL_05	(H) 0.7	(H) 0.3	-	9.3	-	41	1,506
WC0_100_1.17"							
Branch	QGST [MMscfd]	PT <sub>in</sub> [barg]	PT <sub>out</sub> [barg]	DP [barg]	TM <sub>in</sub> [°C]	TM <sub>out</sub> [°C]	Q2 [W/m <sup>2</sup> ·K]
PL_2	52.2	57.0	45.0	12.0	32.7	27.0	0.65
PL_1	33.9	59.5	57.1	2.4	29.0	26.4	0.65
FL_01	8.0	60.1	59.5	0.6	33.8	30.3	1.14
FL_02	8.2	61.7	59.5	2.2	34.9	21.7	1.14
FL_03	11.9	61.8	59.5	2.3	40.3	34.9	1.14
FL_04	18.3	58.7	57.1	1.6	45.4	44.1	1.14

FL_05	5.8	59.9	59.5	0.4	28.3	25.6	1.14
Branch	DTHYD <sub>out</sub> OP [°C]	DTHYD <sub>out</sub> EP [°C]	DTHYD <sub>out</sub> ES [°C]	QMeOH EP [kg/h]	QMeOH ES [kg/h]	LIQC [bbl]	QLT <sub>out</sub> [bbl/day]
PL_2	-10.9	-11.1	-	-	-	429	12,539
PL_1	-8.9	-9.0	-	-	-	333	8,495
FL_01	-12.4	-12.9	-	0.0	-	53	1,995
FL_02	-3.8	-4.3	-	1.2	-	216	2,092
FL_03	-17.1	-17.5	-	0.0	-	83	2,937
FL_04	-26.6	-26.7	-	0.0	-	19	4,350
FL_05	-7.8	-8.2	-	0.0	-	40	1,469

## WC0\_100\_λ0

Branch	QGST [MMscfd]	PT <sub>in</sub> [barg]	PT <sub>out</sub> [barg]	DP [barg]	TM <sub>in</sub> [°C]	TM <sub>out</sub> [°C]	Q2 [W/m <sup>2</sup> ·K]
PL_2	52.2	57.5	45.0	12.5	38.4	34.8	0.00
PL_1	33.9	60.1	57.6	2.5	35.3	34.7	0.00
FL_01	8.0	60.8	60.1	0.6	34.1	33.9	0.00
FL_02	8.2	62.4	60.1	2.3	35.1	34.6	0.00
FL_03	11.9	62.4	60.1	2.3	40.5	40.0	0.00
FL_04	18.3	59.2	57.6	1.6	45.6	45.2	0.00
FL_05	5.8	60.5	60.1	0.4	28.6	28.5	0.00

Branch	DTHYD <sub>out</sub> OP [°C]	DTHYD <sub>out</sub> EP [°C]	DTHYD <sub>out</sub> ES [°C]	QMeOH EP [kg/h]	QMeOH ES [kg/h]	LIQC [bbl]	QLT <sub>out</sub> [bbl/day]
PL_2	-18.7	-18.9	-	-	-	411	12,257
PL_1	-17.0	-17.3	-	-	-	319	8,299
FL_01	-16.0	-16.5	-	0.0	-	52	1,977
FL_02	-16.7	-17.2	-	0.0	-	207	2,014
FL_03	-22.1	-22.6	-	0.0	-	82	2,899
FL_04	-27.6	-27.8	-	0.0	-	19	4,343
FL_05	-10.6	-11.1	-	0.0	-	40	1,458

## WC0\_80\_0"

Branch	QGST [MMscfd]	PT <sub>in</sub> [barg]	PT <sub>out</sub> [barg]	DP [barg]	TM <sub>in</sub> [°C]	TM <sub>out</sub> [°C]	Q2 [W/m <sup>2</sup> ·K]
PL_2	41.5	52.0	45.0	7.0	(W) 17.1	(W) 13.1	0.65
PL_1	26.9	53.6	52.0	1.6	(W) 8.6	(W) 6.9	0.65
FL_01	6.4	54.1	53.6	0.5	27.1	(W) 13.1	24.34
FL_02	6.5	55.2	53.6	1.6	27.8	(W) -4.8	24.32
FL_03	9.4	55.1	53.6	1.5	34.7	(W) 14.0	24.54
FL_04	14.6	53.0	52.0	1.0	41.0	36.0	24.74
FL_05	4.6	54.0	53.6	0.4	20.6	(W) 10.2	24.25

Branch	DTHYD <sub>out</sub> OP [°C]	DTHYD <sub>out</sub> EP [°C]	DTHYD <sub>out</sub> ES [°C]	QMeOH EP [kg/h]	QMeOH ES [kg/h]	LIQC [bbl]	QLT <sub>out</sub> [bbl/day]
PL_2	(H) 3.0	(H) 2.8	-	-	-	475	10,400
PL_1	(H) 10.1	(H) 9.8	-	-	-	382	7,058
FL_01	(H) 4.1	(H) 3.6	-	13.0	-	58	1,650
FL_02	(H) 22.0	(H) 21.5	-	40.5	-	248	1,779
FL_03	(H) 3.2	(H) 2.7	-	17.3	-	89	2,431
FL_04	-18.9	-19.2	-	0.0	-	19	3,497

FL_05	(H) 7.0	(H) 6.5	-	12.2	-	45	1,204
<b>WC0_80_1.17"</b>							
Branch	QGST [MMscfd]	PT <sub>in</sub> [barg]	PT <sub>out</sub> [barg]	DP [barg]	TM <sub>in</sub> [°C]	TM <sub>out</sub> [°C]	Q2 [W/m <sup>2</sup> ·K]
PL_2	41.5	52.4	45.0	7.4	27.1	22.4	0.65
PL_1	26.9	54.1	52.4	1.7	22.7	20.1	0.65
FL_01	6.4	54.6	54.1	0.5	27.7	23.9	1.14
FL_02	6.5	55.8	54.1	1.7	28.4	<b>(W) 14.8</b>	1.14
FL_03	9.4	55.7	54.1	1.5	35.2	29.3	1.14
FL_04	14.6	53.5	52.4	1.0	41.3	40.0	1.14
FL_05	4.6	54.5	54.1	0.4	21.3	18.5	1.14
Branch	DTHYD <sub>out</sub> OP [°C]	DTHYD <sub>out</sub> EP [°C]	DTHYD <sub>out</sub> ES [°C]	QMeOH EP [kg/h]	QMeOH ES [kg/h]	LIQC [bbl]	QLT <sub>out</sub> [bbl/day]
PL_2	-6.4	-6.5	-	-	-	444	10,097
PL_1	-3.0	-3.4	-	-	-	347	6,767
FL_01	-6.6	-7.2	-	0.0	-	56	1,597
FL_02	<b>(H) 2.5</b>	<b>(H) 2.0</b>	-	9.2	-	225	1,664
FL_03	-12.0	-12.5	-	0.0	-	84	2,321
FL_04	-22.9	-23.3	-	0.0	-	19	3,460
FL_05	-1.3	-1.8	-	3.1	-	44	1,172
<b>WC0_80_1.75"</b>							
Branch	QGST [MMscfd]	PT <sub>in</sub> [barg]	PT <sub>out</sub> [barg]	DP [barg]	TM <sub>in</sub> [°C]	TM <sub>out</sub> [°C]	Q2 [W/m <sup>2</sup> ·K]
PL_2	41.4	52.4	45.0	7.4	28.1	23.4	0.65
PL_1	26.9	54.2	52.5	1.7	24.1	21.5	0.65
FL_01	6.4	54.7	54.2	0.5	27.7	24.8	0.82
FL_02	6.5	55.8	54.2	1.7	28.5	<b>(W) 17.5</b>	0.82
FL_03	9.4	55.7	54.2	1.5	35.2	30.6	0.82
FL_04	14.6	53.5	52.5	1.0	41.4	40.3	0.82
FL_05	4.6	54.6	54.2	0.4	21.4	19.2	0.82
Branch	DTHYD <sub>out</sub> OP [°C]	DTHYD <sub>out</sub> EP [°C]	DTHYD <sub>out</sub> ES [°C]	QMeOH EP [kg/h]	QMeOH ES [kg/h]	LIQC [bbl]	QLT <sub>out</sub> [bbl/day]
PL_2	-7.3	-7.4	-	-	-	441	10,069
PL_1	-4.4	-4.7	-	-	-	344	6,739
FL_01	-7.5	-8.1	-	0.0	-	56	1,592
FL_02	-0.2	-0.8	-	5.7	-	223	1,650
FL_03	-13.3	-13.8	-	0.0	-	84	2,312
FL_04	-23.2	-23.6	-	0.0	-	19	3,457
FL_05	-1.9	-2.5	-	2.5	-	44	1,170
<b>WC0_80_2.43"</b>							
Branch	QGST [MMscfd]	PT <sub>in</sub> [barg]	PT <sub>out</sub> [barg]	DP [barg]	TM <sub>in</sub> [°C]	TM <sub>out</sub> [°C]	Q2 [W/m <sup>2</sup> ·K]
PL_2	41.4	52.5	45.0	7.5	28.8	24.0	0.65
PL_1	26.9	54.2	52.5	1.7	25.1	22.4	0.65
FL_01	6.4	54.7	54.2	0.5	27.8	25.4	0.64
FL_02	6.5	55.9	54.2	1.7	28.5	19.4	0.64

FL_03	9.4	55.8	54.2	1.5	35.3	31.4	0.64
FL_04	14.6	53.5	52.5	1.0	41.4	40.5	0.64
FL_05	4.6	54.6	54.2	0.4	21.4	19.6	0.64

Branch	DTHYD <sub>out</sub> OP [°C]	DTHYD <sub>out</sub> EP [°C]	DTHYD <sub>out</sub> ES [°C]	QMeOH EP [kg/h]	QMeOH ES [kg/h]	LIQC [bbl]	QLT <sub>out</sub> [bbl/day]
PL_2	-7.9	-8.0	-	-	-	439	10,050
PL_1	-5.3	-5.6	-	-	-	342	6,720
FL_01	-8.1	-8.6	-	0.0	-	56	1,590
FL_02	-2.1	-2.7	-	3.2	-	221	1,640
FL_03	-14.2	-14.7	-	0.0	-	84	2,306
FL_04	-23.4	-23.7	-	0.0	-	19	3,456
FL_05	-2.4	-2.9	-	2.0	-	44	1,168

## WC0\_80\_λ0

Branch	QGST [MMscfd]	PT <sub>in</sub> [barg]	PT <sub>out</sub> [barg]	DP [barg]	TM <sub>in</sub> [°C]	TM <sub>out</sub> [°C]	Q2 [W/m <sup>2</sup> ·K]
PL_2	41.4	52.7	45.0	7.7	33.2	30.9	0.00
PL_1	26.9	54.5	52.8	1.7	29.3	28.9	0.00
FL_01	6.4	55.0	54.5	0.5	27.9	27.8	0.00
FL_02	6.5	56.2	54.5	1.7	28.6	28.2	0.00
FL_03	9.4	56.1	54.5	1.6	35.4	35.0	0.00
FL_04	14.6	53.8	52.8	1.0	41.5	41.2	0.00
FL_05	4.6	54.9	54.5	0.4	21.6	21.4	0.00

Branch	DTHYD <sub>out</sub> OP [°C]	DTHYD <sub>out</sub> EP [°C]	DTHYD <sub>out</sub> ES [°C]	QMeOH EP [kg/h]	QMeOH ES [kg/h]	LIQC [bbl]	QLT <sub>out</sub> [bbl/day]
PL_2	-14.8	-15.0	-	-	-	423	9,846
PL_1	-11.8	-12.1	-	-	-	330	6,593
FL_01	-10.5	-11.0	-	0.0	-	55	1,579
FL_02	-10.9	-11.5	-	0.0	-	215	1,597
FL_03	-17.7	-18.3	-	0.0	-	83	2,284
FL_04	-24.1	-24.5	-	0.0	-	19	3,450
FL_05	-4.1	-4.7	-	0.3	-	44	1,162

## WC0\_60\_0''

Branch	QGST [MMscfd]	PT <sub>in</sub> [barg]	PT <sub>out</sub> [barg]	DP [barg]	TM <sub>in</sub> [°C]	TM <sub>out</sub> [°C]	Q2 [W/m <sup>2</sup> ·K]
PL_2	31.4	49.0	45.0	4.0	(W) 11.2	(W) 8.0	0.65
PL_1	20.5	50.2	49.0	1.2	(W) 2.7	(W) 1.2	0.65
FL_01	4.8	50.7	50.2	0.5	20.1	(W) 6.0	24.16
FL_02	4.9	51.7	50.2	1.4	20.7	(W) -7.9	24.09
FL_03	7.2	51.2	50.2	1.0	28.5	(W) 7.1	24.38
FL_04	11.0	49.6	49.0	0.6	35.8	30.0	24.59
FL_05	3.6	50.7	50.2	0.4	(W) 13.7	(W) 3.8	24.07

Branch	DTHYD <sub>out</sub> OP [°C]	DTHYD <sub>out</sub> EP [°C]	DTHYD <sub>out</sub> ES [°C]	QMeOH EP [kg/h]	QMeOH ES [kg/h]	LIQC [bbl]	QLT <sub>out</sub> [bbl/day]
PL_2	(H) 8.1	(H) 7.9	-	-	-	522	8,014
PL_1	(H) 15.5	(H) 14.8	-	-	-	409	5,419
FL_01	(H) 10.8	(H) 10.7	-	16.8	-	65	1,261
FL_02	(H) 24.7	(H) 24.6	-	35.9	-	263	1,344

FL_03	(H) 9.7	(H) 9.6	-	23.0	-	98	1,871
FL_04	-13.4	-14.1	-	0.0	-	20	2,653
FL_05	(H) 13.0	(H) 12.9	-	14.0	-	49	941

## WC0\_60\_1.75"

Branch	QGST [MMscfd]	PT <sub>in</sub> [barg]	PT <sub>out</sub> [barg]	DP [barg]	TM <sub>in</sub> [°C]	TM <sub>out</sub> [°C]	Q2 [W/m <sup>2</sup> ·K]
PL_2	31.4	49.2	45.0	4.2	21.7	17.6	0.65
PL_1	20.4	50.5	49.3	1.2	(W) 17.1	(W) 14.4	0.65
FL_01	4.8	51.0	50.5	0.5	20.7	(W) 17.5	0.82
FL_02	4.9	51.9	50.5	1.4	21.3	(W) 10.1	0.82
FL_03	7.2	51.5	50.5	1.0	29.1	24.0	0.82
FL_04	11.0	49.8	49.3	0.6	36.2	35.1	0.82
FL_05	3.6	50.9	50.5	0.4	(W) 14.4	(W) 12.2	0.82

Branch	DTHYD <sub>out</sub> OP [°C]	DTHYD <sub>out</sub> EP [°C]	DTHYD <sub>out</sub> ES [°C]	QMeOH EP [kg/h]	QMeOH ES [kg/h]	LIQC [bbl]	QLT <sub>out</sub> [bbl/day]
PL_2	-1.5	-1.6	-	-	-	482	7,765
PL_1	(H) 2.2	(H) 1.5	-	-	-	374	5,182
FL_01	-0.7	-0.8	-	6.1	-	62	1,214
FL_02	(H) 6.7	(H) 6.6	-	13.6	-	241	1,261
FL_03	-7.1	-7.2	-	0.0	-	91	1,773
FL_04	-18.4	-19.2	-	0.0	-	19	2,615
FL_05	(H) 4.6	(H) 4.5	-	8.9	-	48	915

## WC0\_60\_2.43"

Branch	QGST [MMscfd]	PT <sub>in</sub> [barg]	PT <sub>out</sub> [barg]	DP [barg]	TM <sub>in</sub> [°C]	TM <sub>out</sub> [°C]	Q2 [W/m <sup>2</sup> ·K]
PL_2	31.4	49.3	45.0	4.3	22.3	18.2	0.65
PL_1	20.4	50.5	49.3	1.2	18.1	(W) 15.3	0.65
FL_01	4.8	51.0	50.5	0.5	20.7	18.2	0.64
FL_02	4.9	51.9	50.5	1.4	21.3	(W) 12.0	0.64
FL_03	7.2	51.5	50.5	1.0	29.1	24.9	0.64
FL_04	11.0	49.9	49.3	0.6	36.3	35.3	0.64
FL_05	3.6	50.9	50.5	0.4	(W) 14.4	(W) 12.6	0.64

Branch	DTHYD <sub>out</sub> OP [°C]	DTHYD <sub>out</sub> EP [°C]	DTHYD <sub>out</sub> ES [°C]	QMeOH EP [kg/h]	QMeOH ES [kg/h]	LIQC [bbl]	QLT <sub>out</sub> [bbl/day]
PL_2	-2.1	-2.2	-	-	-	480	7,750
PL_1	(H) 1.3	(H) 0.6	-	-	-	371	5,167
FL_01	-1.3	-1.4	-	5.2	-	62	1,212
FL_02	(H) 4.9	(H) 4.8	-	11.6	-	240	1,253
FL_03	-8.1	-8.2	-	0.0	-	91	1,768
FL_04	-18.6	-19.4	-	0.0	-	19	2,613
FL_05	(H) 4.2	(H) 4.1	-	8.3	-	48	913

## WC0\_60\_3.19"

Branch	QGST [MMscfd]	PT <sub>in</sub> [barg]	PT <sub>out</sub> [barg]	DP [barg]	TM <sub>in</sub> [°C]	TM <sub>out</sub> [°C]	Q2 [W/m <sup>2</sup> ·K]
PL_2	31.4	49.3	45.0	4.3	22.8	18.6	0.65
PL_1	20.4	50.5	49.3	1.2	18.8	(W) 16.0	0.65

FL_01	4.8	51.0	50.5	0.5	20.7	18.6	0.52
FL_02	4.9	51.9	50.5	1.4	21.3	<b>(W) 13.3</b>	0.52
FL_03	7.2	51.6	50.5	1.0	29.1	25.5	0.52
FL_04	11.0	49.9	49.3	0.6	36.3	35.5	0.52
FL_05	3.6	51.0	50.5	0.4	<b>(W) 14.4</b>	<b>(W) 12.9</b>	0.52
Branch	DTHYD <sub>out</sub> OP [°C]	DTHYD <sub>out</sub> EP [°C]	DTHYD <sub>out</sub> ES [°C]	QMeOH EP [kg/h]	QMeOH ES [kg/h]	LIQC [bbl]	QLT <sub>out</sub> [bbl/day]
PL_2	-2.5	-2.7	-	-	-	478	7,740
PL_1	<b>(H) 0.7</b>	<b>(H) 0.0</b>	-	-	-	370	5,156
FL_01	-1.7	-1.8	-	4.5	-	62	1,210
FL_02	<b>(H) 3.6</b>	<b>(H) 3.5</b>	-	9.9	-	238	1,248
FL_03	-8.7	-8.8	-	0.0	-	91	1,764
FL_04	-18.8	-19.5	-	0.0	-	19	2,612
FL_05	<b>(H) 3.9</b>	<b>(H) 3.8</b>	-	7.7	-	48	912

## WC0\_60\_λ0

Branch	QGST [MMscfd]	PT <sub>in</sub> [barg]	PT <sub>out</sub> [barg]	DP [barg]	TM <sub>in</sub> [°C]	TM <sub>out</sub> [°C]	Q2 [W/m <sup>2</sup> ·K]
PL_2	31.4	49.3	45.0	4.3	22.8	18.6	0.65
PL_1	20.4	50.5	49.3	1.2	18.8	<b>(W) 16.0</b>	0.65
FL_01	4.8	51.0	50.5	0.5	20.7	18.6	0.52
FL_02	4.9	51.9	50.5	1.4	21.3	<b>(W) 13.3</b>	0.52
FL_03	7.2	51.6	50.5	1.0	29.1	25.5	0.52
FL_04	11.0	49.9	49.3	0.6	36.3	35.5	0.52
FL_05	3.6	51.0	50.5	0.4	<b>(W) 14.4</b>	<b>(W) 12.9</b>	0.52
Branch	DTHYD <sub>out</sub> OP [°C]	DTHYD <sub>out</sub> EP [°C]	DTHYD <sub>out</sub> ES [°C]	QMeOH EP [kg/h]	QMeOH ES [kg/h]	LIQC [bbl]	QLT <sub>out</sub> [bbl/day]
PL_2	-2.5	-2.7	-	-	-	478	7,740
PL_1	<b>(H) 0.7</b>	<b>(H) 0.0</b>	-	-	-	370	5,156
FL_01	-1.7	-1.8	-	4.5	-	62	1,210
FL_02	<b>(H) 3.6</b>	<b>(H) 3.5</b>	-	9.9	-	238	1,248
FL_03	-8.7	-8.8	-	0.0	-	91	1,764
FL_04	-18.8	-19.5	-	0.0	-	19	2,612
FL_05	<b>(H) 3.9</b>	<b>(H) 3.8</b>	-	7.7	-	48	912

## WC0\_40\_0"

Branch	QGST [MMscfd]	PT <sub>in</sub> [barg]	PT <sub>out</sub> [barg]	DP [barg]	TM <sub>in</sub> [°C]	TM <sub>out</sub> [°C]	Q2 [W/m <sup>2</sup> ·K]
PL_2	21.4	47.3	45.0	2.3	<b>(W) 4.1</b>	<b>(W) 1.5</b>	0.65
PL_1	14.0	48.5	47.3	1.1	<b>(W) -3.6</b>	<b>(W) -4.8</b>	0.65
FL_01	3.3	49.0	48.5	0.6	<b>(W) 11.3</b>	<b>(W) -1.4</b>	23.96
FL_02	3.4	50.0	48.5	1.5	<b>(W) 12.0</b>	<b>(W) -9.7</b>	23.78
FL_03	4.9	49.3	48.5	0.9	19.7	<b>(W) -1.0</b>	24.12
FL_04	7.4	47.6	47.3	0.2	28.2	21.3	24.34
FL_05	2.5	48.9	48.5	0.5	<b>(W) 5.2</b>	<b>(W) -3.0</b>	23.73
Branch	DTHYD <sub>out</sub> OP [°C]	DTHYD <sub>out</sub> EP [°C]	DTHYD <sub>out</sub> ES [°C]	QMeOH EP [kg/h]	QMeOH ES [kg/h]	LIQC [bbl]	QLT <sub>out</sub> [bbl/day]
PL_2	<b>(H) 14.6</b>	<b>(H) 14.5</b>	-	-	-	636	5,586
PL_1	<b>(H) 21.2</b>	<b>(H) 20.8</b>	-	-	-	461	3,772

FL_01	(H) 18.0	(H) 17.4	-	18.9	-	76	886
FL_02	(H) 26.3	(H) 25.6	-	28.7	-	293	930
FL_03	(H) 17.6	(H) 17.0	-	26.4	-	115	1,294
FL_04	-4.9	-5.4	-	0.0	-	23	1,827
FL_05	(H) 19.6	(H) 19.0	-	15.5	-	56	662

## WC0\_40\_λ0

Branch	QGST [MMscfd]	PT <sub>in</sub> [barg]	PT <sub>out</sub> [barg]	DP [barg]	TM <sub>in</sub> [°C]	TM <sub>out</sub> [°C]	Q2 [W/m <sup>2</sup> ·K]
PL_2	21.4	47.4	45.0	2.4	18.7	17.9	0.00
PL_1	14.0	48.5	47.4	1.1	(W) 13.8	(W) 13.5	0.00
FL_01	3.3	49.1	48.5	0.6	(W) 12.1	(W) 11.9	0.00
FL_02	3.4	50.0	48.5	1.4	(W) 12.8	(W) 12.4	0.00
FL_03	4.9	49.3	48.5	0.8	20.4	20.2	0.00
FL_04	7.4	47.6	47.4	0.2	28.7	28.7	0.00
FL_05	2.5	49.0	48.5	0.5	(W) 6.1	(W) 5.9	0.00

Branch	DTHYD <sub>out</sub> OP [°C]	DTHYD <sub>out</sub> EP [°C]	DTHYD <sub>out</sub> ES [°C]	QMeOH EP [kg/h]	QMeOH ES [kg/h]	LIQC [bbl]	QLT <sub>out</sub> [bbl/day]
PL_2	-1.8	-1.9	-	-	-	566	5,286
PL_1	(H) 2.9	(H) 2.4	-	-	-	415	3,538
FL_01	(H) 4.7	(H) 4.0	-	6.8	-	73	845
FL_02	(H) 4.2	(H) 3.6	-	6.5	-	268	859
FL_03	-3.6	-4.2	-	1.1	-	106	1,205
FL_04	-12.2	-12.7	-	0.0	-	22	1,786
FL_05	(H) 10.7	(H) 10.0	-	8.2	-	55	640

## WC26\_100\_0"

Branch	QGST [MMscfd]	PT <sub>in</sub> [barg]	PT <sub>out</sub> [barg]	DP [barg]	TM <sub>in</sub> [°C]	TM <sub>out</sub> [°C]	Q2 [W/m <sup>2</sup> ·K]
PL_2	52.0	59.7	45.0	14.7	33.0	28.1	0.65
PL_1	33.6	62.4	59.8	2.6	24.7	22.8	0.65
FL_01	7.9	63.1	62.4	0.7	44.6	30.7	24.75
FL_02	8.0	64.8	62.4	2.4	45.2	(W) 6.3	24.75
FL_03	11.9	65.0	62.4	2.6	50.7	31.6	24.86
FL_04	18.4	61.8	59.8	2.0	55.6	51.4	24.95
FL_05	5.8	62.9	62.4	0.5	39.3	28.2	24.63

Branch	DTHYD <sub>out</sub> OP [°C]	DTHYD <sub>out</sub> EP [°C]	DTHYD <sub>out</sub> ES [°C]	QMeOH EP [kg/h]	QMeOH ES [kg/h]	LIQC [bbl]	QLT <sub>out</sub> [bbl/day]
PL_2	-12.0	-12.2	-24.2	-	-	522	15,545
PL_1	-5.0	-5.4	-17.7	-	-	431	10,566
FL_01	-12.6	-12.7	-25.0	0.0	0.0	64	2,455
FL_02	(H) 11.8	(H) 11.7	-0.6	1,433.2	259.6	283	2,655
FL_03	-13.5	-13.6	-26.0	0.0	0.0	102	3,687
FL_04	-33.6	-34.1	-46.3	0.0	0.0	22	5,437
FL_05	-10.1	-10.2	-22.5	0.0	0.0	48	1,799

## WC26\_100\_λ0

Branch	QGST [MMscfd]	PT <sub>in</sub> [barg]	PT <sub>out</sub> [barg]	DP [barg]	TM <sub>in</sub> [°C]	TM <sub>out</sub> [°C]	Q2 [W/m <sup>2</sup> ·K]
--------	------------------	----------------------------	-----------------------------	-----------	-----------------------	------------------------	-----------------------------

PL_2	52.0	61.1	45.0	16.1	49.4	46.1	0.00
PL_1	33.5	64.1	61.1	2.9	46.4	45.9	0.00
FL_01	7.9	64.8	64.1	0.7	45.3	45.1	0.00
FL_02	8.0	66.6	64.1	2.5	45.9	45.5	0.00
FL_03	11.9	66.7	64.1	2.6	51.3	50.9	0.00
FL_04	18.4	63.1	61.2	2.0	56.0	55.7	0.00
FL_05	5.7	64.6	64.1	0.5	40.1	40.1	0.00

Branch	DTHYD <sub>out</sub> OP [°C]	DTHYD <sub>out</sub> EP [°C]	DTHYD <sub>out</sub> ES [°C]	QMeOH EP [kg/h]	QMeOH ES [kg/h]	LIQC [bbl]	QLT <sub>out</sub> [bbl/day]
PL_2	-30.0	-30.1	-42.2	-	-	473	14,942
PL_1	-27.9	-27.9	-40.7	-	-	380	10,038
FL_01	-26.9	-27.2	-39.5	0.0	0.0	63	2,383
FL_02	-27.3	-27.6	-39.9	0.0	0.0	248	2,414
FL_03	-32.6	-32.9	-45.2	0.0	0.0	98	3,541
FL_04	-37.7	-37.7	-50.6	0.0	0.0	22	5,404
FL_05	-21.8	-22.1	-34.4	0.0	0.0	47	1,755

## WC26\_80\_0"

Branch	QGST [MMscfd]	PT <sub>in</sub> [barg]	PT <sub>out</sub> [barg]	DP [barg]	TM <sub>in</sub> [°C]	TM <sub>out</sub> [°C]	Q2 [W/m <sup>2</sup> ·K]
PL_2	41.5	54.1	45.0	9.1	27.3	23.4	0.65
PL_1	27.0	56.1	54.2	1.9	18.4	<b>(W) 16.6</b>	0.65
FL_01	6.3	56.7	56.1	0.6	39.4	24.2	24.65
FL_02	6.6	58.1	56.1	2.0	40.3	<b>(W) 1.3</b>	24.65
FL_03	9.5	57.9	56.1	1.8	46.5	25.2	24.77
FL_04	14.5	55.5	54.2	1.3	51.9	47.2	24.87
FL_05	4.6	56.6	56.1	0.5	33.2	21.3	24.49

Branch	DTHYD <sub>out</sub> OP [°C]	DTHYD <sub>out</sub> EP [°C]	DTHYD <sub>out</sub> ES [°C]	QMeOH EP [kg/h]	QMeOH ES [kg/h]	LIQC [bbl]	QLT <sub>out</sub> [bbl/day]
PL_2	-7.3	-7.4	-19.5	-	-	542	12,556
PL_1	<b>(H) 0.6</b>	<b>(H) 0.1</b>	-12.1	-	-	439	8,510
FL_01	-6.7	-6.8	-19.6	0.0	0.0	67	1,974
FL_02	<b>(H) 16.1</b>	<b>(H) 16.0</b>	<b>(H) 3.2</b>	1,535.3	451.2	284	2,171
FL_03	-7.7	-7.8	-20.6	0.0	0.0	104	2,940
FL_04	-29.9	-30.4	-42.6	0.0	0.0	22	4,273
FL_05	-3.9	-4.0	-16.8	42.0	0.0	50	1,440

## WC26\_80\_1.17"

Branch	QGST [MMscfd]	PT <sub>in</sub> [barg]	PT <sub>out</sub> [barg]	DP [barg]	TM <sub>in</sub> [°C]	TM <sub>out</sub> [°C]	Q2 [W/m <sup>2</sup> ·K]
PL_2	41.5	54.7	45.0	9.7	38.7	34.2	0.65
PL_1	27.0	56.8	54.8	2.0	34.6	32.1	0.65
FL_01	6.3	57.5	56.8	0.6	39.9	36.0	1.14
FL_02	6.6	58.8	56.8	2.0	40.9	26.6	1.14
FL_03	9.5	58.6	56.8	1.8	46.9	41.2	1.14
FL_04	14.5	56.1	54.8	1.3	52.3	51.0	1.14
FL_05	4.6	57.3	56.8	0.5	33.9	30.8	1.14

Branch	DTHYD <sub>out</sub> OP [°C]	DTHYD <sub>out</sub> EP [°C]	DTHYD <sub>out</sub> ES [°C]	QMeOH EP [kg/h]	QMeOH ES [kg/h]	LIQC [bbl]	QLT <sub>out</sub> [bbl/day]
--------	---------------------------------	---------------------------------	---------------------------------	--------------------	--------------------	---------------	---------------------------------



PL_2	-18.1	-18.2	-30.3	-	-	508	12,244
PL_1	-14.7	-15.4	-27.5	-	-	401	8,204
FL_01	-18.5	-18.6	-30.9	0.0	0.0	65	1,921
FL_02	-9.0	-9.2	-21.4	0.0	0.0	258	2,033
FL_03	-23.6	-23.8	-36.0	0.0	0.0	99	2,836
FL_04	-33.7	-34.3	-46.4	0.0	0.0	22	4,244
FL_05	-13.3	-13.4	-25.7	0.0	0.0	49	1,409

## WC26\_80\_λ0

Branch	QGST [MMscfd]	PT <sub>in</sub> [barg]	PT <sub>out</sub> [barg]	DP [barg]	TM <sub>in</sub> [°C]	TM <sub>out</sub> [°C]	Q2 [W/m <sup>2</sup> ·K]
PL_2	41.5	55.2	45.0	10.2	45.0	42.8	0.00
PL_1	27.0	57.3	55.2	2.1	41.5	41.1	0.00
FL_01	6.3	57.9	57.3	0.6	40.1	40.0	0.00
FL_02	6.6	59.3	57.3	2.0	41.1	40.7	0.00
FL_03	9.5	59.1	57.3	1.8	47.1	46.8	0.00
FL_04	14.5	56.5	55.2	1.3	52.4	52.2	0.00
FL_05	4.6	57.8	57.3	0.5	34.1	34.0	0.00

Branch	DTHYD <sub>out</sub> OP [°C]	DTHYD <sub>out</sub> EP [°C]	DTHYD <sub>out</sub> ES [°C]	QMeOH EP [kg/h]	QMeOH ES [kg/h]	LIQC [bbl]	QLT <sub>out</sub> [bbl/day]
PL_2	-26.7	-26.9	-38.9	-	-	487	12,017
PL_1	-23.8	-24.4	-36.6	-	-	384	8,045
FL_01	-22.4	-22.6	-34.8	0.0	0.0	65	1,906
FL_02	-23.1	-23.3	-35.6	0.0	0.0	249	1,969
FL_03	-29.2	-29.4	-41.6	0.0	0.0	97	2,805
FL_04	-34.8	-35.4	-47.6	0.0	0.0	22	4,238
FL_05	-16.4	-16.6	-28.8	0.0	0.0	49	1,400

## WC26\_60\_0''

Branch	QGST [MMscfd]	PT <sub>in</sub> [barg]	PT <sub>out</sub> [barg]	DP [barg]	TM <sub>in</sub> [°C]	TM <sub>out</sub> [°C]	Q2 [W/m <sup>2</sup> ·K]
PL_2	31.2	49.9	45.0	4.9	21.2	17.9	0.65
PL_1	20.2	51.4	50.0	1.5	<b>(W) 11.9</b>	<b>(W) 10.1</b>	0.65
FL_01	4.8	52.0	51.4	0.6	34.7	<b>(W) 17.4</b>	24.50
FL_02	4.8	53.2	51.4	1.8	36.7	<b>(W) -3.8</b>	24.45
FL_03	7.1	52.6	51.4	1.2	40.7	<b>(W) 17.0</b>	24.66
FL_04	10.9	50.7	50.0	0.7	47.4	41.7	24.76
FL_05	3.6	51.9	51.4	0.5	29.2	<b>(W) 15.9</b>	24.31

Branch	DTHYD <sub>out</sub> OP [°C]	DTHYD <sub>out</sub> EP [°C]	DTHYD <sub>out</sub> ES [°C]	QMeOH EP [kg/h]	QMeOH ES [kg/h]	LIQC [bbl]	QLT <sub>out</sub> [bbl/day]
PL_2	-1.8	-1.9	-14.0	-	-	593	9,552
PL_1	<b>(H) 6.7</b>	<b>(H) 6.6</b>	-6.2	-	-	461	6,416
FL_01	-0.5	-0.7	-12.8	235.0	0.0	72	1,487
FL_02	<b>(H) 20.8</b>	<b>(H) 20.6</b>	<b>(H) 8.4</b>	1,551.7	535.3	296	1,596
FL_03	-0.1	-0.3	-12.4	360.0	0.0	112	2,220
FL_04	-25.0	-25.0	-37.9	0.0	0.0	23	3,219
FL_05	<b>(H) 1.1</b>	<b>(H) 0.8</b>	-11.3	239.8	0.0	52	1,115

## WC26\_60\_1.17''

Branch	QGST [MMscfd]	PT <sub>in</sub> [barg]	PT <sub>out</sub> [barg]	DP [barg]	TM <sub>in</sub> [°C]	TM <sub>out</sub> [°C]	Q2 [W/m <sup>2</sup> ·K]
PL_2	31.2	50.2	45.0	5.2	33.1	29.0	0.65
PL_1	20.2	51.7	50.3	1.5	28.7	25.9	0.65
FL_01	4.8	52.4	51.8	0.6	35.3	30.6	1.14
FL_02	4.8	53.5	51.8	1.7	37.2	20.1	1.14
FL_03	7.1	53.0	51.8	1.2	41.2	34.5	1.14
FL_04	10.9	51.0	50.3	0.7	47.7	46.3	1.14
FL_05	3.6	52.2	51.8	0.5	29.8	26.3	1.14

Branch	DTHYD <sub>out</sub> OP [°C]	DTHYD <sub>out</sub> EP [°C]	DTHYD <sub>out</sub> ES [°C]	QMeOH EP [kg/h]	QMeOH ES [kg/h]	LIQC [bbl]	QLT <sub>out</sub> [bbl/day]
PL_2	-12.9	-13.1	-25.1	-	-	548	9,297
PL_1	-9.1	-9.1	-22.0	-	-	422	6,167
FL_01	-13.6	-13.9	-26.0	0.0	0.0	69	1,440
FL_02	-3.1	-3.4	-15.6	68.1	0.0	271	1,496
FL_03	-17.5	-17.8	-29.9	0.0	0.0	106	2,129
FL_04	-29.5	-29.6	-42.5	0.0	0.0	22	3,188
FL_05	-9.3	-9.6	-21.7	0.0	0.0	51	1,086

## WC26\_60\_λ0

Branch	QGST [MMscfd]	PT <sub>in</sub> [barg]	PT <sub>out</sub> [barg]	DP [barg]	TM <sub>in</sub> [°C]	TM <sub>out</sub> [°C]	Q2 [W/m <sup>2</sup> ·K]
PL_2	31.2	50.5	45.0	5.5	40.5	39.2	0.00
PL_1	20.2	52.0	50.5	1.5	36.8	36.5	0.00
FL_01	4.8	52.6	52.0	0.6	35.4	35.3	0.00
FL_02	4.8	53.7	52.0	1.7	37.4	37.1	0.00
FL_03	7.1	53.2	52.0	1.2	41.3	41.1	0.00
FL_04	10.9	51.2	50.5	0.7	47.8	47.7	0.00
FL_05	3.6	52.5	52.0	0.5	30.0	29.9	0.00

Branch	DTHYD <sub>out</sub> OP [°C]	DTHYD <sub>out</sub> EP [°C]	DTHYD <sub>out</sub> ES [°C]	QMeOH EP [kg/h]	QMeOH ES [kg/h]	LIQC [bbl]	QLT <sub>out</sub> [bbl/day]
PL_2	-23.1	-23.2	-35.3	-	-	517	9,088
PL_1	-19.7	-19.8	-32.0	-	-	402	6,020
FL_01	-18.3	-18.6	-30.7	0.0	0.0	69	1,426
FL_02	-20.1	-20.3	-32.5	0.0	0.0	259	1,438
FL_03	-24.1	-24.4	-36.5	0.0	0.0	104	2,100
FL_04	-30.9	-31.0	-43.1	0.0	0.0	22	3,181
FL_05	-12.9	-13.2	-25.4	0.0	0.0	51	1,077

## WC26\_40\_0"

Branch	QGST [MMscfd]	PT <sub>in</sub> [barg]	PT <sub>out</sub> [barg]	DP [barg]	TM <sub>in</sub> [°C]	TM <sub>out</sub> [°C]	Q2 [W/m <sup>2</sup> ·K]
PL_2	21.2	47.8	45.0	2.8	(W) 12.4	(W) 9.5	0.65
PL_1	13.8	49.1	47.8	1.3	(W) 2.9	(W) 1.3	0.65
FL_01	3.2	49.8	49.1	0.6	23.8	(W) 6.5	24.17
FL_02	3.3	50.9	49.1	1.8	24.7	(W) -8.2	24.09
FL_03	4.9	50.1	49.1	1.0	32.9	(W) 7.2	24.44
FL_04	7.4	48.1	47.8	0.3	40.7	33.5	24.61
FL_05	2.4	49.6	49.1	0.5	(W) 17.5	(W) 5.1	23.96

Branch	DTHYD <sub>out</sub> OP [°C]	DTHYD <sub>out</sub> EP [°C]	DTHYD <sub>out</sub> ES [°C]	QMeOH EP [kg/h]	QMeOH ES [kg/h]	LIQC [bbbl]	QLT <sub>out</sub> [bbbl/day]
PL_2	(H) 6.6	(H) 6.5	-5.6	-	-	718	6,643
PL_1	(H) 15.1	(H) 14.6	(H) 2.5	-	-	510	4,466
FL_01	(H) 10.1	(H) 9.4	-2.6	539.0	95.1	81	1,030
FL_02	(H) 24.9	(H) 24.1	(H) 12.1	1,285.4	547.7	321	1,107
FL_03	(H) 9.5	(H) 8.8	-3.3	761.2	99.4	126	1,551
FL_04	-17.0	-17.6	-29.6	0.0	0.0	25	2,200
FL_05	(H) 11.5	(H) 10.8	-1.2	452.6	109.4	60	778

## WC26\_40\_1.17"

Branch	QGST [MMscfd]	PT <sub>in</sub> [barg]	PT <sub>out</sub> [barg]	DP [barg]	TM <sub>in</sub> [°C]	TM <sub>out</sub> [°C]	Q2 [W/m <sup>2</sup> ·K]
PL_2	21.2	47.8	45.0	2.8	23.5	19.5	0.65
PL_1	13.8	49.1	47.8	1.3	18.0	(W) 15.0	0.65
FL_01	3.2	49.7	49.1	0.6	24.4	19.3	1.14
FL_02	3.3	50.8	49.1	1.7	25.3	(W) 8.4	1.14
FL_03	4.9	50.1	49.1	1.0	33.3	25.4	1.14
FL_04	7.4	48.1	47.8	0.3	41.0	39.4	1.14
FL_05	2.4	49.6	49.1	0.5	18.2	(W) 14.6	1.14

Branch	DTHYD <sub>out</sub> OP [°C]	DTHYD <sub>out</sub> EP [°C]	DTHYD <sub>out</sub> ES [°C]	QMeOH EP [kg/h]	QMeOH ES [kg/h]	LIQC [bbbl]	QLT <sub>out</sub> [bbbl/day]
PL_2	-3.4	-3.6	-15.6	-	-	671	6,470
PL_1	(H) 1.4	(H) 0.9	-11.2	-	-	475	4,300
FL_01	-2.6	-3.3	-15.4	89.3	0.0	79	995
FL_02	(H) 8.2	(H) 7.5	-4.6	486.3	11.6	301	1,054
FL_03	-8.7	-9.4	-21.5	0.0	0.0	119	1,480
FL_04	-22.9	-23.4	-35.5	0.0	0.0	25	2,171
FL_05	(H) 2.0	(H) 1.3	-10.8	197.6	0.0	58	757

## WC26\_40\_1.75"

Branch	QGST [MMscfd]	PT <sub>in</sub> [barg]	PT <sub>out</sub> [barg]	DP [barg]	TM <sub>in</sub> [°C]	TM <sub>out</sub> [°C]	Q2 [W/m <sup>2</sup> ·K]
PL_2	21.2	47.8	45.0	2.8	24.7	20.6	0.65
PL_1	13.8	49.1	47.8	1.3	19.8	(W) 16.7	0.65
FL_01	3.2	49.7	49.1	0.6	24.4	20.4	0.82
FL_02	3.3	50.8	49.1	1.7	25.3	(W) 11.5	0.82
FL_03	4.9	50.1	49.1	1.0	33.4	27.1	0.82
FL_04	7.4	48.1	47.8	0.3	41.1	39.8	0.82
FL_05	2.4	49.6	49.1	0.5	18.3	(W) 15.5	0.82

Branch	DTHYD <sub>out</sub> OP [°C]	DTHYD <sub>out</sub> EP [°C]	DTHYD <sub>out</sub> ES [°C]	QMeOH EP [kg/h]	QMeOH ES [kg/h]	LIQC [bbbl]	QLT <sub>out</sub> [bbbl/day]
PL_2	-4.5	-4.7	-16.7	-	-	666	6,452
PL_1	-0.2	-0.7	-12.8	-	-	471	4,283
FL_01	-3.8	-4.5	-16.6	32.8	0.0	79	992
FL_02	(H) 5.1	(H) 4.4	-7.7	357.2	0.0	298	1,045
FL_03	-10.5	-11.2	-23.3	0.0	0.0	119	1,473
FL_04	-23.3	-23.8	-35.9	0.0	0.0	25	2,169
FL_05	(H) 1.2	(H) 0.5	-11.6	160.9	0.0	58	756

## WC26\_40\_2.43"

Branch	QGST [MMscfd]	PT <sub>in</sub> [barg]	PT <sub>out</sub> [barg]	DP [barg]	TM <sub>in</sub> [°C]	TM <sub>out</sub> [°C]	Q2 [W/m <sup>2</sup> ·K]
PL_2	21.2	47.8	45.0	2.8	25.5	21.3	0.65
PL_1	13.8	49.1	47.8	1.3	21.0	17.8	0.65
FL_01	3.2	49.8	49.1	0.6	24.4	21.2	0.64
FL_02	3.3	50.8	49.1	1.7	25.3	<b>(W) 13.8</b>	0.64
FL_03	4.9	50.1	49.1	1.0	33.4	28.3	0.64
FL_04	7.4	48.1	47.8	0.3	41.1	40.0	0.64
FL_05	2.4	49.6	49.1	0.5	18.3	<b>(W) 16.0</b>	0.64
Branch	DTHYD <sub>out</sub> OP [°C]	DTHYD <sub>out</sub> EP [°C]	DTHYD <sub>out</sub> ES [°C]	QMeOH EP [kg/h]	QMeOH ES [kg/h]	LIQC [bbl]	QLT <sub>out</sub> [bbl/day]
PL_2	-5.2	-5.4	-17.5	-	-	663	6,441
PL_1	-1.3	-1.8	-13.9	-	-	469	4,271
FL_01	-4.6	-5.3	-17.3	0.0	0.0	79	990
FL_02	<b>(H) 2.9</b>	<b>(H) 2.2</b>	-9.9	261.7	0.0	297	1,039
FL_03	-11.7	-12.4	-24.4	0.0	0.0	119	1,469
FL_04	-23.6	-24.1	-36.2	0.0	0.0	25	2,167
FL_05	<b>(H) 0.6</b>	-0.1	-12.1	135.6	0.0	58	754

## WC26\_40\_3.19"

Branch	QGST [MMscfd]	PT <sub>in</sub> [barg]	PT <sub>out</sub> [barg]	DP [barg]	TM <sub>in</sub> [°C]	TM <sub>out</sub> [°C]	Q2 [W/m <sup>2</sup> ·K]
PL_2	21.2	47.8	45.0	2.8	26.1	21.8	0.65
PL_1	13.8	49.1	47.8	1.3	21.8	18.5	0.65
FL_01	3.2	49.8	49.1	0.6	24.5	21.7	0.52
FL_02	3.3	50.8	49.1	1.7	25.4	<b>(W) 15.4</b>	0.52
FL_03	4.9	50.1	49.1	1.0	33.4	29.1	0.52
FL_04	7.4	48.1	47.8	0.3	41.1	40.2	0.52
FL_05	2.4	49.6	49.1	0.5	18.3	<b>(W) 16.4</b>	0.52
Branch	DTHYD <sub>out</sub> OP [°C]	DTHYD <sub>out</sub> EP [°C]	DTHYD <sub>out</sub> ES [°C]	QMeOH EP [kg/h]	QMeOH ES [kg/h]	LIQC [bbl]	QLT <sub>out</sub> [bbl/day]
PL_2	-5.8	-5.9	-18.0	-	-	661	6,433
PL_1	-2.1	-2.6	-14.7	-	-	467	4,262
FL_01	-5.1	-5.8	-17.8	0.0	0.0	78	989
FL_02	<b>(H) 1.3</b>	<b>(H) 0.6</b>	-11.5	201.2	0.0	295	1,035
FL_03	-12.5	-13.2	-25.2	0.0	0.0	118	1,467
FL_04	-23.7	-24.3	-36.3	0.0	0.0	25	2,166
FL_05	<b>(H) 0.3</b>	-0.5	-12.5	122.6	0.0	58	754

## WC26\_40\_λ0

Branch	QGST [MMscfd]	PT <sub>in</sub> [barg]	PT <sub>out</sub> [barg]	DP [barg]	TM <sub>in</sub> [°C]	TM <sub>out</sub> [°C]	Q2 [W/m <sup>2</sup> ·K]
PL_2	21.2	47.9	45.0	2.9	31.5	30.8	0.00
PL_1	13.8	49.1	47.9	1.3	26.6	26.4	0.00
FL_01	3.2	49.8	49.1	0.6	24.5	24.4	0.00
FL_02	3.3	50.8	49.1	1.7	25.4	25.1	0.00
FL_03	4.9	50.1	49.1	1.0	33.5	33.3	0.00

FL_04	7.4	48.2	47.9	0.3	41.1	41.1	0.00
FL_05	2.4	49.7	49.1	0.5	18.4	18.3	0.00
Branch	DTHYD <sub>out</sub> OP [°C]	DTHYD <sub>out</sub> EP [°C]	DTHYD <sub>out</sub> ES [°C]	QMeOH EP [kg/h]	QMeOH ES [kg/h]	LIQC [bbl]	QLT <sub>out</sub> [bbl/day]
PL_2	-14.7	-14.8	-26.9	-	-	632	6,300
PL_1	-9.9	-10.4	-22.5	-	-	453	4,182
FL_01	-7.7	-8.5	-20.5	0.0	0.0	78	982
FL_02	-8.5	-9.2	-21.2	0.0	0.0	289	1,010
FL_03	-16.6	-17.4	-29.4	0.0	0.0	117	1,453
FL_04	-24.6	-25.2	-37.2	0.0	0.0	25	2,162
FL_05	-1.6	-2.3	-14.4	70.9	0.0	58	750

Table H.8 – Pipeline parameters and methanol injection rates at design flowrate under different flowline insulation thicknesses and using 1D heat transfer

WC0_100_0"							
Branch	QGST [MMscfd]	PT <sub>in</sub> [barg]	PT <sub>out</sub> [barg]	DP [barg]	TM <sub>in</sub> [°C]	TM <sub>out</sub> [°C]	Q2 [W/m <sup>2</sup> ·K]
PL_2	52.2	55.5	45.0	10.5	(W) 13.4	(W) 7.3	0.56
PL_1	33.9	57.7	55.6	2.1	(W) 2.6	(W) -0.2	0.56
FL_01	8.0	58.3	57.7	0.6	32.8	(W) 11.6	3.86
FL_02	8.2	59.7	57.7	2.0	33.8	(W) -22.8	3.87
FL_03	11.9	59.8	57.7	2.2	39.4	(W) 10.8	3.87
FL_04	18.3	57.2	55.6	1.6	44.8	38.7	3.87
FL_05	5.8	58.1	57.7	0.4	27.1	(W) 9.7	3.87
Branch	DTHYD <sub>out</sub> OP [°C]	DTHYD <sub>out</sub> EP [°C]	DTHYD <sub>out</sub> ES [°C]	QMeOH EP [kg/h]	QMeOH ES [kg/h]	LIQC [bbl]	QLT <sub>out</sub> [bbl/day]
PL_2	(H) 8.8	(H) 8.6	-	-	-	489	13,342
PL_1	(H) 17.6	(H) 17.6	-	-	-	402	9,245
FL_01	(H) 6.1	(H) 5.8	-	17.4	-	56	2,108
FL_02	(H) 40.4	(H) 40.2	-	154.7	-	266	2,455
FL_03	(H) 6.8	(H) 6.6	-	29.0	-	89	3,153
FL_04	-21.2	-21.3	-	0.0	-	19	4,401
FL_05	(H) 8.0	(H) 7.7	-	14.5	-	42	1,540
WC0_100_1.17"							
Branch	QGST [MMscfd]	PT <sub>in</sub> [barg]	PT <sub>out</sub> [barg]	DP [barg]	TM <sub>in</sub> [°C]	TM <sub>out</sub> [°C]	Q2 [W/m <sup>2</sup> ·K]
PL_2	52.2	56.7	45.0	11.7	28.8	21.9	0.56
PL_1	33.9	59.1	56.7	2.4	24.7	20.9	0.56
FL_01	8.0	59.7	59.1	0.6	33.7	27.7	0.93
FL_02	8.2	61.3	59.1	2.2	34.7	(W) 12.6	0.93
FL_03	11.9	61.3	59.1	2.3	40.2	31.7	0.93
FL_04	18.3	58.3	56.7	1.6	45.3	43.5	0.93
FL_05	5.8	59.5	59.1	0.4	28.1	23.3	0.93
Branch	DTHYD <sub>out</sub> OP [°C]	DTHYD <sub>out</sub> EP [°C]	DTHYD <sub>out</sub> ES [°C]	QMeOH EP [kg/h]	QMeOH ES [kg/h]	LIQC [bbl]	QLT <sub>out</sub> [bbl/day]

PL_2	-5.8	-5.9	-	-	-	441	12,734
PL_1	-3.3	-3.5	-	-	-	344	8,635
FL_01	-9.9	-10.3	-	0.0	-	53	2,009
FL_02	<b>(H) 5.1</b>	<b>(H) 4.8</b>	-	16.0	-	223	2,152
FL_03	-13.9	-14.3	-	0.0	-	83	2,961
FL_04	-26.0	-26.1	-	0.0	-	19	4,353
FL_05	-5.5	-5.9	-	0.0	-	41	1,478

**WC0\_100\_1.75"**

Branch	QGST [MMscfd]	PT <sub>in</sub> [barg]	PT <sub>out</sub> [barg]	DP [barg]	TM <sub>in</sub> [°C]	TM <sub>out</sub> [°C]	Q2 [W/m <sup>2</sup> ·K]
PL_2	52.2	56.8	45.0	11.8	30.4	23.3	0.56
PL_1	33.9	59.2	56.8	2.4	27.0	23.0	0.56
FL_01	8.0	59.9	59.2	0.6	33.8	29.1	0.71
FL_02	8.2	61.4	59.2	2.2	34.8	<b>(W) 17.2</b>	0.71
FL_03	11.9	61.5	59.2	2.3	40.2	33.6	0.71
FL_04	18.3	58.4	56.9	1.6	45.4	43.9	0.71
FL_05	5.8	59.6	59.2	0.4	28.2	24.5	0.71

Branch	DTHYD <sub>out</sub> OP [°C]	DTHYD <sub>out</sub> EP [°C]	DTHYD <sub>out</sub> ES [°C]	QMeOH EP [kg/h]	QMeOH ES [kg/h]	LIQC [bbl]	QLT <sub>out</sub> [bbl/day]
PL_2	-7.2	-7.4	-	-	-	437	12,678
PL_1	-5.5	-5.6	-	-	-	339	8,579
FL_01	-11.3	-11.7	-	0.0	-	53	2,001
FL_02	<b>(H) 0.6</b>	<b>(H) 0.2</b>	-	8.7	-	219	2,121
FL_03	-15.8	-16.2	-	0.0	-	83	2,946
FL_04	-26.3	-26.5	-	0.0	-	19	4,350
FL_05	-6.6	-7.1	-	0.0	-	40	1,473

**WC0\_100\_2.43"**

Branch	QGST [MMscfd]	PT <sub>in</sub> [barg]	PT <sub>out</sub> [barg]	DP [barg]	TM <sub>in</sub> [°C]	TM <sub>out</sub> [°C]	Q2 [W/m <sup>2</sup> ·K]
PL_2	52.2	56.9	45.0	11.9	31.4	24.3	0.56
PL_1	33.9	59.3	56.9	2.4	28.5	24.5	0.56
FL_01	8.0	60.0	59.3	0.6	33.8	30.0	0.57
FL_02	8.2	61.5	59.3	2.2	34.8	20.2	0.57
FL_03	11.9	61.6	59.3	2.3	40.3	34.8	0.57
FL_04	18.3	58.5	56.9	1.6	45.4	44.1	0.57
FL_05	5.8	59.7	59.3	0.4	28.3	25.2	0.57

Branch	DTHYD <sub>out</sub> OP [°C]	DTHYD <sub>out</sub> EP [°C]	DTHYD <sub>out</sub> ES [°C]	QMeOH EP [kg/h]	QMeOH ES [kg/h]	LIQC [bbl]	QLT <sub>out</sub> [bbl/day]
PL_2	-8.2	-8.3	-	-	-	434	12,641
PL_1	-6.9	-7.1	-	-	-	336	8,543
FL_01	-12.2	-12.6	-	0.0	-	53	1,996
FL_02	-2.4	-2.8	-	3.6	-	217	2,100
FL_03	-17.0	-17.4	-	0.0	-	83	2,937
FL_04	-26.6	-26.7	-	0.0	-	19	4,348
FL_05	-7.4	-7.8	-	0.0	-	40	1,470

**WC26\_100\_0"**

Branch	QGST [MMscfd]	PT <sub>in</sub> [barg]	PT <sub>out</sub> [barg]	DP [barg]	TM <sub>in</sub> [°C]	TM <sub>out</sub> [°C]	Q2 [W/m <sup>2</sup> ·K]
PL_2	52.0	59.1	45.0	14.1	25.8	20.1	0.56
PL_1	33.6	61.7	59.2	2.5	<b>(W) 15.2</b>	<b>(W) 12.5</b>	0.56
FL_01	7.9	62.4	61.7	0.7	44.3	24.6	3.87
FL_02	8.0	64.1	61.7	2.4	45.0	<b>(W) -12.1</b>	3.87
FL_03	11.9	64.2	61.7	2.5	50.5	24.3	3.87
FL_04	18.4	61.2	59.2	2.0	55.4	50.1	3.87
FL_05	5.8	62.2	61.7	0.5	39.0	22.6	3.87
Branch	DTHYD <sub>out</sub> OP [°C]	DTHYD <sub>out</sub> EP [°C]	DTHYD <sub>out</sub> ES [°C]	QMeOH EP [kg/h]	QMeOH ES [kg/h]	LIQC [bbl]	QLT <sub>out</sub> [bbl/day]
PL_2	-4.0	-4.2	-16.2	-	-	547	15,844
PL_1	<b>(H) 5.3</b>	<b>(H) 4.9</b>	-7.4	-	-	458	10,839
FL_01	-6.5	-6.6	-19.4	0.0	0.0	65	2,489
FL_02	<b>(H) 30.1</b>	<b>(H) 30.1</b>	<b>(H) 17.2</b>	3925.4	1697.9	302	2,807
FL_03	-6.3	-6.3	-19.1	0.0	0.0	104	3,748
FL_04	-32.3	-32.7	-44.9	0.0	0.0	22	5,446
FL_05	-4.6	-4.7	-17.5	17.3	0.0	48	1,822
WC26_100_1.17"							
Branch	QGST [MMscfd]	PT <sub>in</sub> [barg]	PT <sub>out</sub> [barg]	DP [barg]	TM <sub>in</sub> [°C]	TM <sub>out</sub> [°C]	Q2 [W/m <sup>2</sup> ·K]
PL_2	52.0	60.3	45.0	15.3	40.8	34.4	0.56
PL_1	33.5	63.1	60.3	2.8	36.9	33.4	0.56
FL_01	7.9	63.9	63.1	0.7	45.0	39.6	0.93
FL_02	8.0	65.6	63.1	2.4	45.6	25.3	0.93
FL_03	11.9	65.7	63.1	2.6	51.0	43.6	0.93
FL_04	18.4	62.4	60.3	2.0	55.8	54.3	0.93
FL_05	5.8	63.6	63.1	0.5	39.8	35.4	0.93
Branch	DTHYD <sub>out</sub> OP [°C]	DTHYD <sub>out</sub> EP [°C]	DTHYD <sub>out</sub> ES [°C]	QMeOH EP [kg/h]	QMeOH ES [kg/h]	LIQC [bbl]	QLT <sub>out</sub> [bbl/day]
PL_2	-18.4	-18.5	-30.6	-	-	500	15,320
PL_1	-15.5	-16.0	-28.3	-	-	403	10,307
FL_01	-21.5	-21.7	-34.0	0.0	0.0	63	2,408
FL_02	-7.1	-7.3	-19.7	0.0	0.0	262	2,527
FL_03	-25.4	-25.7	-38.0	0.0	0.0	99	3,591
FL_04	-36.3	-36.9	-49.1	0.0	0.0	22	5,411
FL_05	-17.2	-17.4	-29.8	0.0	0.0	47	1,770

Table H.9 – Pipeline parameters and methanol injection rates after a six-hour shutdown under different flowline insulation thicknesses

WC0_100_1.17"					
Branch	PT <sub>DTHYD</sub> [barg]	TM <sub>DTHYD</sub> [°C]	PT <sub>avg</sub> [barg]	TM <sub>avg</sub> [°C]	Q2 [W/m <sup>2</sup> ·K]
PL_2	53.4	22.0	53.6	24.8	0.64
PL_1	53.3	19.8	53.4	22.2	0.64

FL_01	53.3	(W) 13.9	53.3	(W) 17.0	1.11
FL_02	53.3	(W) 9.2	53.0	(W) 14.6	1.11
FL_03	53.3	(W) 16.0	53.2	20.3	1.11
FL_04	53.5	19.3	53.5	24.8	1.11
FL_05	53.3	(W) 11.3	53.3	(W) 13.9	1.11

Branch	DTHYD <sub>max</sub> OP [°C]	DTHYD <sub>max</sub> EP [°C]	DTHYD <sub>max</sub> ES [°C]	QMeOH EP [kg/h]	QMeOH ES [kg/h]
PL_2	-4.8	-5.2	-	-	-
PL_1	-2.6	-3.0	-	-	-
FL_01	(H) 3.2	(H) 2.8	-	12.5	-
FL_02	(H) 8.0	(H) 7.6	-	20.1	-
FL_03	(H) 1.2	(H) 0.7	-	14.8	-
FL_04	-2.1	-2.6	-	10.0	-
FL_05	(H) 5.9	(H) 5.5	-	12.0	-

## WC0\_100\_1.75"

Branch	PT <sub>DTHYD</sub> [barg]	TM <sub>DTHYD</sub> [°C]	PT <sub>avg</sub> [barg]	TM <sub>avg</sub> [°C]	Q2 [W/m <sup>2</sup> ·K]
PL_2	53.6	22.8	53.8	25.6	0.64
PL_1	53.7	21.3	53.7	23.4	0.64
FL_01	53.7	(W) 17.4	53.7	20.0	0.80
FL_02	53.7	(W) 13.3	53.4	18.1	0.80
FL_03	53.7	19.2	53.6	23.9	0.80
FL_04	53.8	22.9	53.7	28.6	0.80
FL_05	53.7	(W) 14.4	53.7	(W) 16.6	0.80

Branch	DTHYD <sub>max</sub> OP [°C]	DTHYD <sub>max</sub> EP [°C]	DTHYD <sub>max</sub> ES [°C]	QMeOH EP [kg/h]	QMeOH ES [kg/h]
PL_2	-5.6	-6.0	-	-	-
PL_1	-4.1	-4.6	-	-	-
FL_01	-0.2	-0.7	-	7.0	-
FL_02	(H) 3.9	(H) 3.5	-	13.7	-
FL_03	-2.0	-2.4	-	6.7	-
FL_04	-5.7	-6.2	-	0.0	-
FL_05	(H) 2.9	(H) 2.4	-	8.4	-

## WC0\_100\_2.43"

Branch	PT <sub>DTHYD</sub> [barg]	TM <sub>DTHYD</sub> [°C]	PT <sub>avg</sub> [barg]	TM <sub>avg</sub> [°C]	Q2 [W/m <sup>2</sup> ·K]
PL_2	53.7	23.3	53.9	26.1	0.64
PL_1	54.0	22.5	54.0	24.3	0.64
FL_01	54.0	20.2	54.0	22.4	0.63
FL_02	54.0	(W) 16.5	53.8	20.8	0.63
FL_03	54.0	21.4	53.9	26.5	0.63
FL_04	53.9	25.7	53.9	31.4	0.63
FL_05	54.0	(W) 16.7	54.0	18.6	0.63

Branch	DTHYD <sub>max</sub> OP [°C]	DTHYD <sub>max</sub> EP [°C]	DTHYD <sub>max</sub> ES [°C]	QMeOH EP [kg/h]	QMeOH ES [kg/h]
PL_2	-6.0	-6.5	-	-	-
PL_1	-5.3	-5.8	-	-	-



FL_01	-2.9	-3.4	-	2.6	-
FL_02	<b>(H) 0.7</b>	<b>(H) 0.2</b>	-	8.6	-
FL_03	-4.2	-4.7	-	0.7	-
FL_04	-8.4	-8.9	-	0.0	-
FL_05	<b>(H) 0.5</b>	<b>(H) 0.0</b>	-	5.9	-

## WC0\_100\_3.19"

Branch	PT <sub>DTHYD</sub> [barg]	TM <sub>DTHYD</sub> [°C]	PT <sub>avg</sub> [barg]	TM <sub>avg</sub> [°C]	Q2 [W/m <sup>2</sup> ·K]
PL_2	53.8	23.6	54.0	26.5	0.64
PL_1	54.0	23.1	54.1	24.8	0.64
FL_01	54.2	22.0	54.2	24.0	0.51
FL_02	54.2	18.9	54.0	22.7	0.51
FL_03	54.2	22.7	54.1	28.4	0.51
FL_04	54.0	27.8	54.0	33.4	0.51
FL_05	54.2	18.4	54.2	20.0	0.51

Branch	DTHYD <sub>max</sub> OP [°C]	DTHYD <sub>max</sub> EP [°C]	DTHYD <sub>max</sub> ES [°C]	QMeOH EP [kg/h]	QMeOH ES [kg/h]
PL_2	-6.4	-6.9	-	-	-
PL_1	-5.8	-6.3	-	-	-
FL_01	-4.7	-5.3	-	0.0	-
FL_02	-1.6	-2.2	-	4.7	-
FL_03	-5.4	-5.9	-	0.0	-
FL_04	-10.5	-11.0	-	0.0	-
FL_05	-1.1	-1.7	-	3.9	-

## WC0\_80\_3.19"

Branch	PT <sub>DTHYD</sub> [barg]	TM <sub>DTHYD</sub> [°C]	PT <sub>avg</sub> [barg]	TM <sub>avg</sub> [°C]	Q2 [W/m <sup>2</sup> ·K]
PL_2	50.0	19.4	50.1	22.0	0.64
PL_1	50.2	17.8	50.3	19.5	0.64
FL_01	50.4	<b>(W) 17.2</b>	50.4	19.1	0.51
FL_02	50.4	<b>(W) 13.7</b>	50.3	<b>(W) 17.5</b>	0.51
FL_03	50.4	17.9	50.3	24.4	0.51
FL_04	50.2	24.2	50.2	30.1	0.51
FL_05	50.4	<b>(W) 13.0</b>	50.4	<b>(W) 14.7</b>	0.51

Branch	DTHYD <sub>max</sub> OP [°C]	DTHYD <sub>max</sub> EP [°C]	DTHYD <sub>max</sub> ES [°C]	QMeOH EP [kg/h]	QMeOH ES [kg/h]
PL_2	-2.7	-2.7	-	-	-
PL_1	-1.0	-1.1	-	-	-
FL_01	-0.4	-0.5	-	6.0	-
FL_02	<b>(H) 3.1</b>	<b>(H) 3.0</b>	-	10.6	-
FL_03	-1.1	-1.1	-	8.0	-
FL_04	-7.4	-7.4	-	0.0	-
FL_05	<b>(H) 3.8</b>	<b>(H) 3.7</b>	-	8.1	-

## WC26\_100\_1.17"

Branch	PT <sub>DTHYD</sub> [barg]	TM <sub>DTHYD</sub> [°C]	PT <sub>avg</sub> [barg]	TM <sub>avg</sub> [°C]	Q2 [W/m <sup>2</sup> ·K]
--------	-------------------------------	--------------------------	--------------------------	------------------------	--------------------------

PL_2	56.1	31.2	56.1	34.9	0.64
PL_1	55.7	28.6	55.9	32.4	0.64
FL_01	55.7	20.5	55.7	25.3	1.11
FL_02	55.7	<b>(W) 15.8</b>	55.4	22.8	1.11
FL_03	55.7	22.5	55.6	28.3	1.11
FL_04	56.1	25.2	56.0	32.6	1.11
FL_05	55.7	18.1	55.8	22.3	1.11
Branch	DTHYD <sub>max</sub> OP [°C]	DTHYD <sub>max</sub> EP [°C]	DTHYD <sub>max</sub> ES [°C]	QMeOH EP [kg/h]	QMeOH ES [kg/h]
PL_2	-13.8	-13.9	-26.7	-	-
PL_1	-11.2	-11.2	-24.1	-	-
FL_01	-3.0	-3.1	-15.9	134.7	0.0
FL_02	<b>(H) 1.7</b>	<b>(H) 1.6</b>	-11.2	506.3	0.0
FL_03	-5.1	-5.1	-17.9	0.0	0.0
FL_04	-7.7	-7.8	-20.6	0.0	0.0
FL_05	-0.6	-0.7	-13.5	233.8	0.0

## WC26\_100\_1.75"

Branch	PT <sub>DTHYD</sub> [barg]	TM <sub>DTHYD</sub> [°C]	PT <sub>avg</sub> [barg]	TM <sub>avg</sub> [°C]	Q2 [W/m <sup>2</sup> ·K]
PL_2	56.4	32.3	56.4	35.7	0.64
PL_1	56.2	30.3	56.3	33.6	0.64
FL_01	56.2	24.7	56.2	28.9	0.80
FL_02	56.2	20.8	55.9	26.9	0.80
FL_03	56.2	26.3	56.1	32.4	0.80
FL_04	56.4	29.3	56.4	36.8	0.80
FL_05	56.2	22.2	56.2	25.6	0.80

Branch	DTHYD <sub>max</sub> OP [°C]	DTHYD <sub>max</sub> EP [°C]	DTHYD <sub>max</sub> ES [°C]	QMeOH EP [kg/h]	QMeOH ES [kg/h]
PL_2	-14.8	-14.9	-27.1	-	-
PL_1	-12.8	-12.9	-25.1	-	-
FL_01	-7.3	-7.3	-19.6	0.0	0.0
FL_02	-3.4	-3.5	-15.7	108.8	0.0
FL_03	-8.8	-8.9	-21.2	0.0	0.0
FL_04	-11.8	-12.0	-24.2	0.0	0.0
FL_05	-4.7	-4.8	-17.1	7.8	0.0

## WC26\_80\_1.75"

Branch	PT <sub>DTHYD</sub> [barg]	TM <sub>DTHYD</sub> [°C]	PT <sub>avg</sub> [barg]	TM <sub>avg</sub> [°C]	Q2 [W/m <sup>2</sup> ·K]
PL_2	51.7	28.3	51.7	31.4	0.64
PL_1	51.6	26.1	51.7	28.8	0.64
FL_01	51.6	20.9	51.6	25.0	0.80
FL_02	51.6	<b>(W) 16.8</b>	51.4	23.0	0.80
FL_03	51.6	22.5	51.5	29.2	0.80
FL_04	51.7	26.1	51.7	34.1	0.80
FL_05	51.6	18.0	51.7	21.1	0.80

Branch	DTHYD <sub>max</sub> OP [°C]	DTHYD <sub>max</sub> EP [°C]	DTHYD <sub>max</sub> ES [°C]	QMeOH EP [kg/h]	QMeOH ES [kg/h]
--------	---------------------------------	---------------------------------	---------------------------------	--------------------	--------------------

PL_2	-11.3	-11.6	-23.7	-	-
PL_1	-9.1	-9.4	-21.5	-	-
FL_01	-4.0	-4.2	-16.4	42.8	0.0
FL_02	<b>(H) 0.1</b>	-0.1	-12.3	308.1	0.0
FL_03	-5.6	-5.8	-17.9	0.0	0.0
FL_04	-9.1	-9.4	-21.5	0.0	0.0
FL_05	-1.0	-1.3	-13.4	162.6	0.0

**WC26\_80\_2.43"**

Branch	PT <sub>DTHYD</sub> [barg]	TM <sub>DTHYD</sub> [°C]	PT <sub>avg</sub> [barg]	TM <sub>avg</sub> [°C]	Q2 [W/m <sup>2</sup> ·K]
PL_2	51.9	29.0	51.8	32.0	0.64
PL_1	51.9	27.4	51.9	29.7	0.64
FL_01	51.9	24.0	51.9	27.6	0.63
FL_02	51.9	20.5	51.8	25.8	0.63
FL_03	51.9	24.8	51.8	32.1	0.63
FL_04	51.9	29.4	51.8	37.0	0.63
FL_05	51.9	20.7	52.0	23.3	0.63

Branch	DTHYD <sub>max</sub> OP [°C]	DTHYD <sub>max</sub> EP [°C]	DTHYD <sub>max</sub> ES [°C]	QMeOH EP [kg/h]	QMeOH ES [kg/h]
PL_2	-12.0	-12.3	-24.4	-	-
PL_1	-10.4	-10.7	-22.8	-	-
FL_01	-7.0	-7.3	-19.5	0.0	0.0
FL_02	-3.5	-3.8	-15.9	70.3	0.0
FL_03	-7.8	-8.1	-20.3	0.0	0.0
FL_04	-12.5	-12.7	-24.9	0.0	0.0
FL_05	-3.8	-4.0	-16.2	39.7	0.0

**WC26\_60\_2.43"**

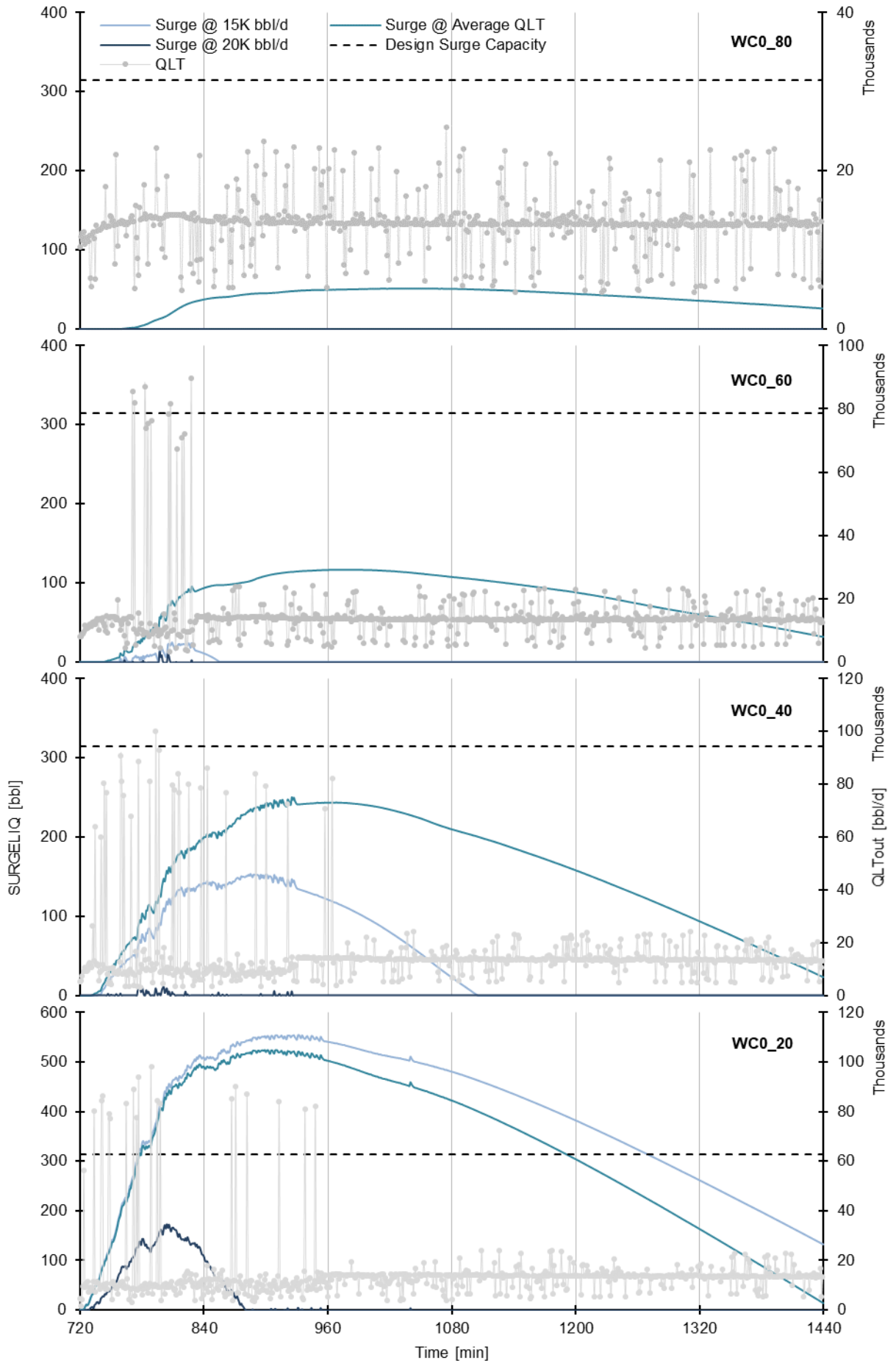
Branch	PT <sub>DTHYD</sub> [barg]	TM <sub>DTHYD</sub> [°C]	PT <sub>avg</sub> [barg]	TM <sub>avg</sub> [°C]	Q2 [W/m <sup>2</sup> ·K]
PL_2	47.9	23.9	48.2	26.6	0.64
PL_1	48.3	21.4	48.4	23.6	0.64
FL_01	48.5	18.8	48.5	22.5	0.63
FL_02	48.5	<b>(W) 14.4</b>	48.4	20.0	0.63
FL_03	48.5	19.6	48.4	27.6	0.63
FL_04	48.3	26.3	48.3	33.4	0.63
FL_05	48.5	<b>(W) 15.6</b>	48.5	18.1	0.63

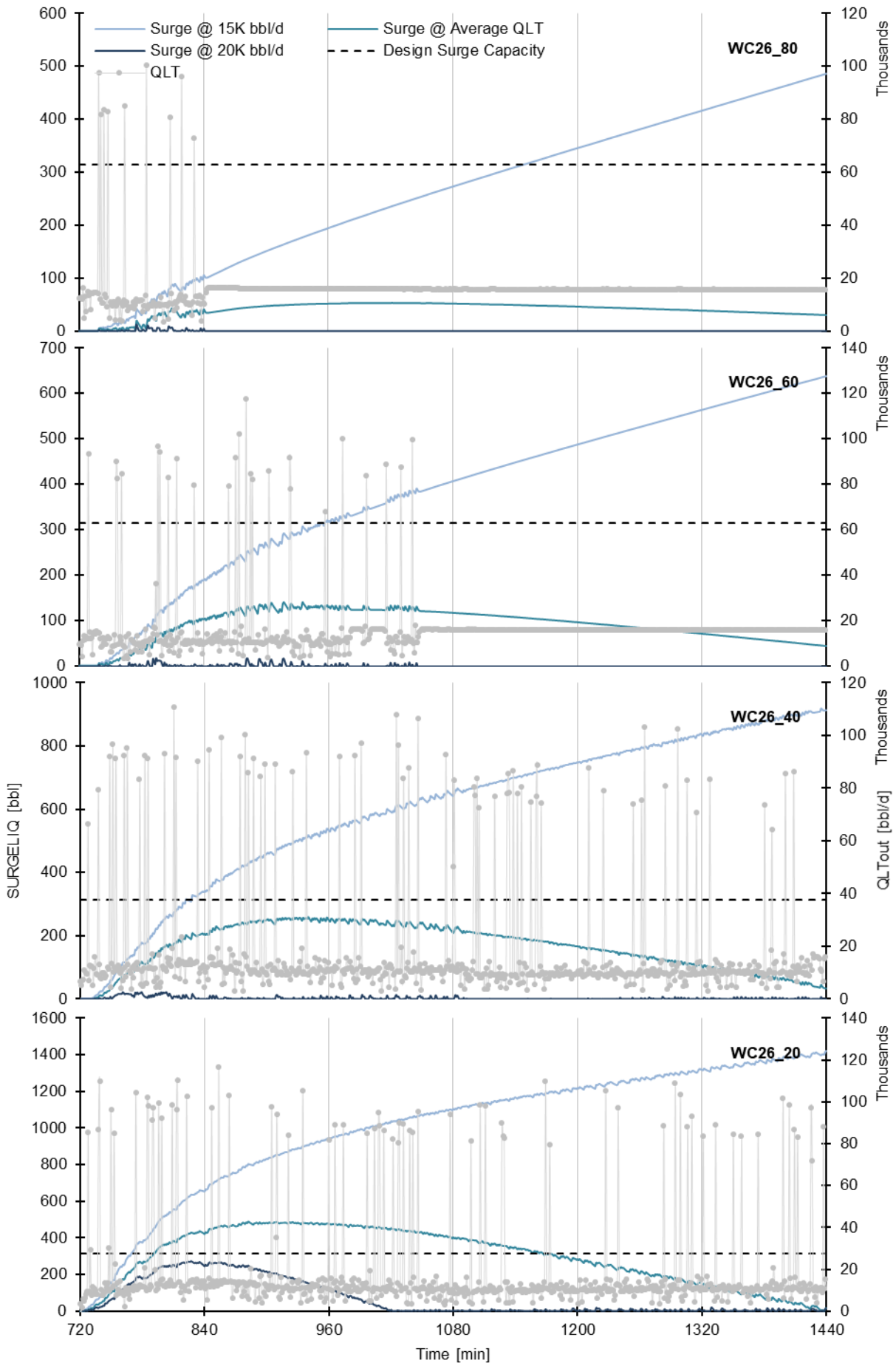
Branch	DTHYD <sub>max</sub> OP [°C]	DTHYD <sub>max</sub> EP [°C]	DTHYD <sub>max</sub> ES [°C]	QMeOH EP [kg/h]	QMeOH ES [kg/h]
PL_2	-7.4	-8.0	-20.0	-	-
PL_1	-4.9	-5.5	-17.6	-	-
FL_01	-2.2	-2.8	-14.9	111.8	0.0
FL_02	<b>(H) 2.1</b>	<b>(H) 1.5</b>	-10.6	321.2	0.0
FL_03	-3.1	-3.7	-15.7	98.3	0.0
FL_04	-9.8	-10.4	-22.4	0.0	0.0
FL_05	<b>(H) 0.9</b>	<b>(H) 0.3</b>	-11.7	199.7	0.0

**WC26\_60\_3.19"**

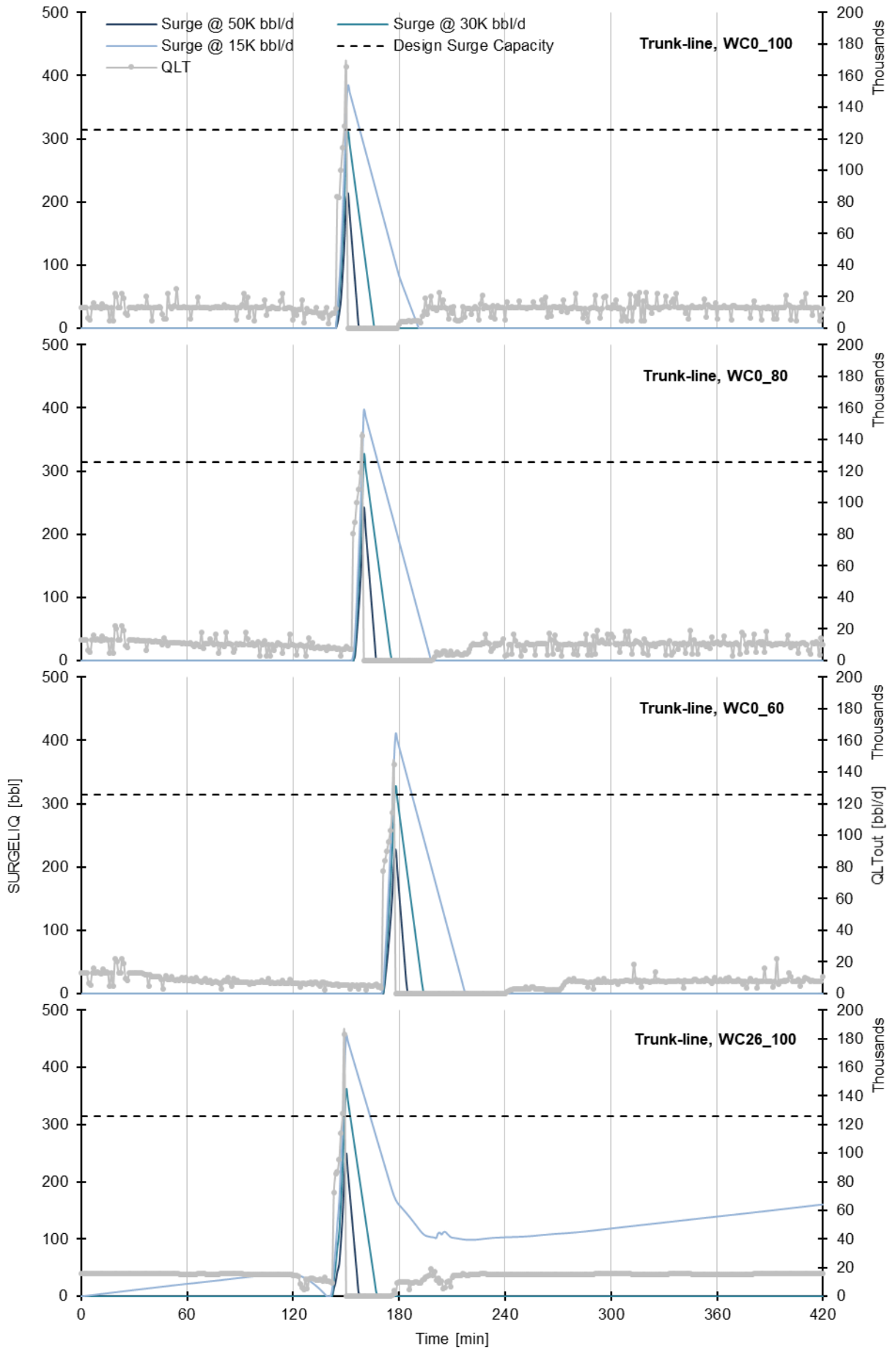
Branch	PT <sub>DTHYD</sub> [barg]	TM <sub>DTHYD</sub> [°C]	PT <sub>avg</sub> [barg]	TM <sub>avg</sub> [°C]	Q2 [W/m <sup>2</sup> ·K]
PL_2	47.9	24.3	48.2	27.1	0.64
PL_1	48.4	22.1	48.5	24.3	0.64
FL_01	48.6	20.7	48.6	24.1	0.51
FL_02	48.6	<b>(W) 16.9</b>	48.6	21.9	0.51
FL_03	48.6	21.7	48.5	29.6	0.51
FL_04	48.3	29.6	48.3	35.5	0.51
FL_05	48.6	<b>(W) 17.4</b>	48.6	19.5	0.51
Branch	DTHYD <sub>max</sub> OP [°C]	DTHYD <sub>max</sub> EP [°C]	DTHYD <sub>max</sub> ES [°C]	QMeOH EP [kg/h]	QMeOH ES [kg/h]
PL_2	-7.8	-8.4	-20.4	-	-
PL_1	-5.5	-6.2	-18.2	-	-
FL_01	-4.1	-4.8	-16.8	11.0	0.0
FL_02	-0.3	-1.0	-13.0	218.0	0.0
FL_03	-5.1	-5.8	-17.8	0.0	0.0
FL_04	-13.0	-13.7	-25.7	0.0	0.0
FL_05	-0.8	-1.5	-13.5	142.3	0.0

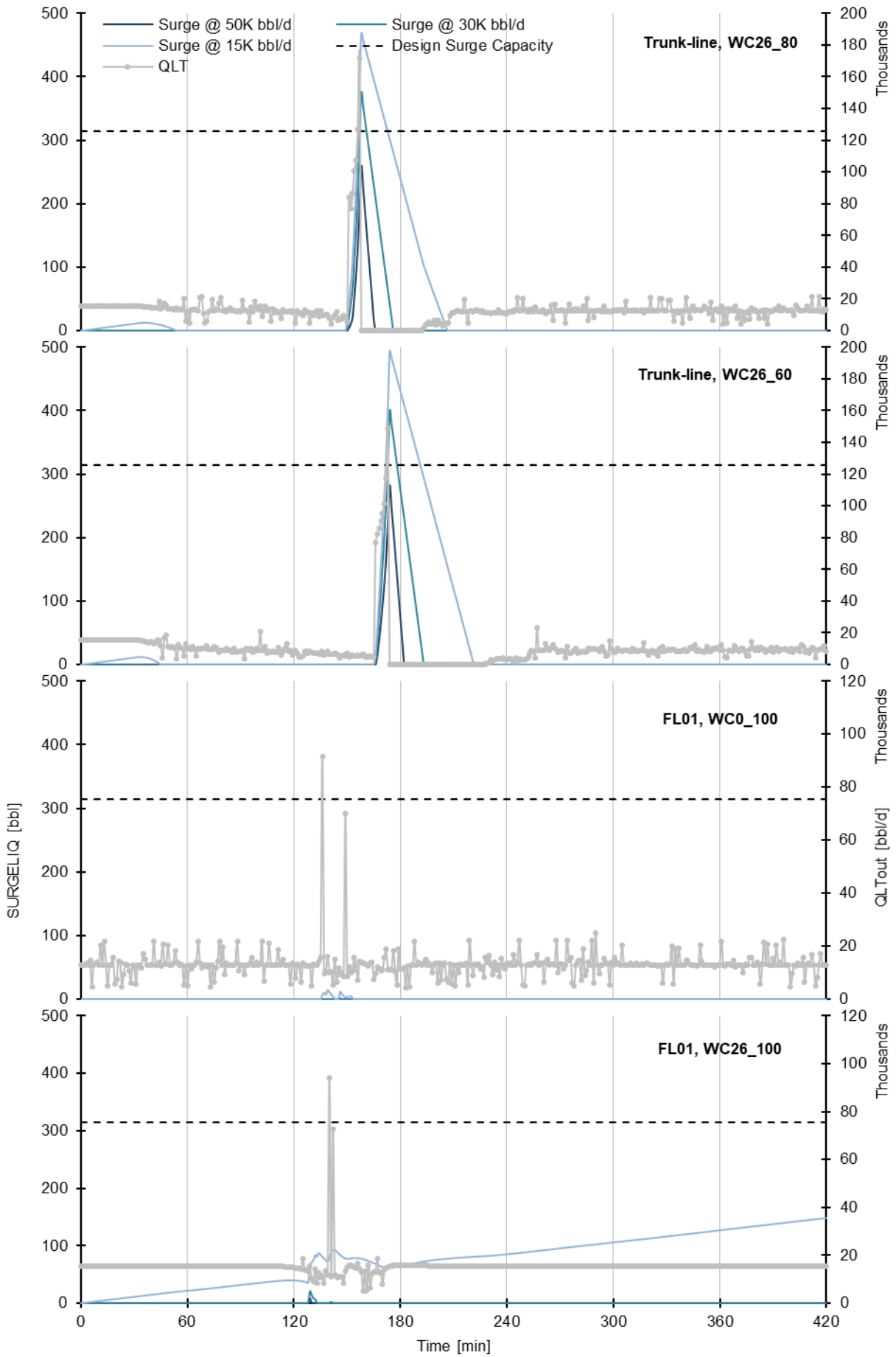
### I. Surge Volume during Ramp-up



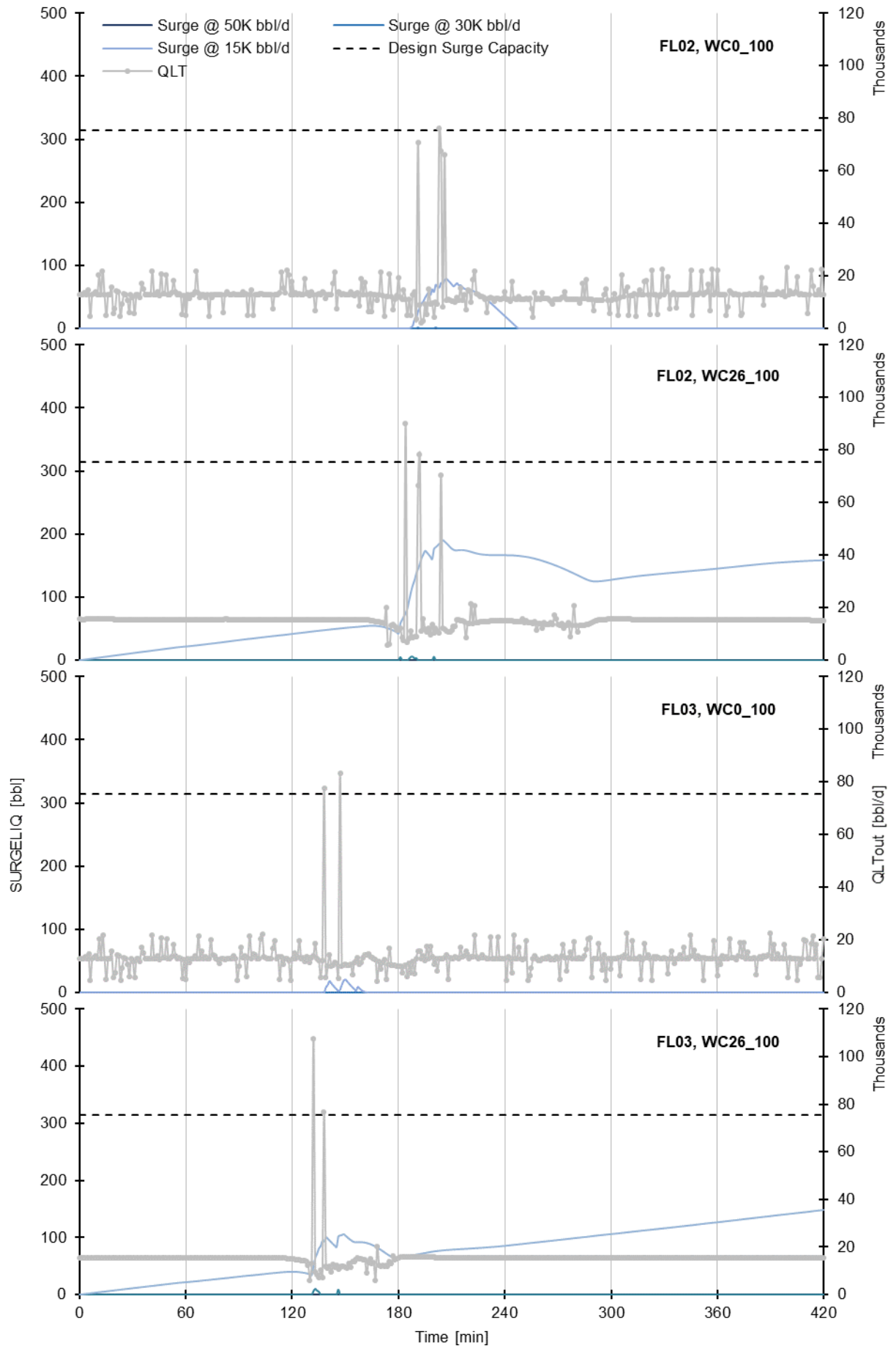


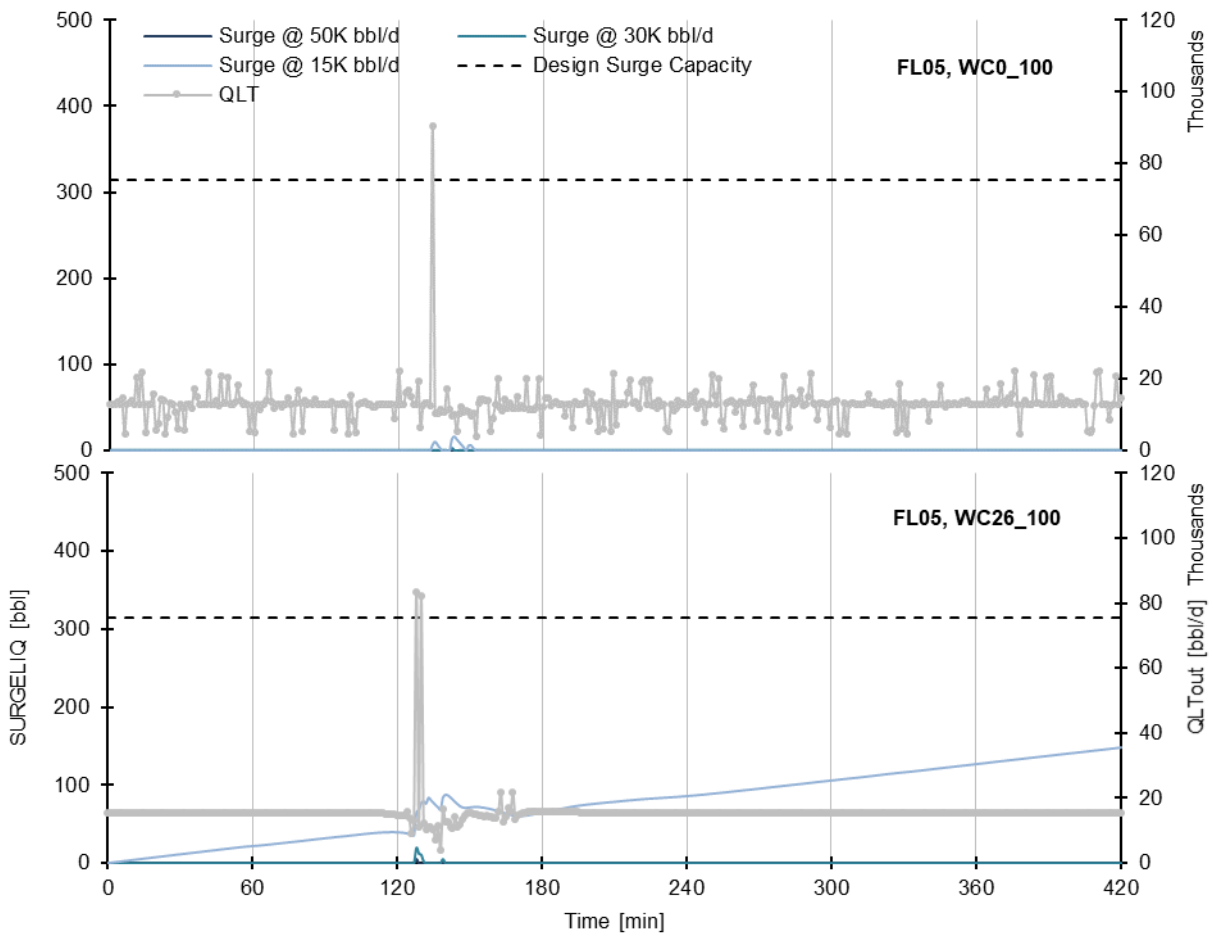
## J. Surge Volume during Pigging











## K. Cases Runtime

### Abbreviations

BO, CM	Black-oil, and Compositional Model
SS, TA, DY	Steady-state, Transient Analysis, and Dynamic (transient simulation for a steady-state flow)
FT, 1D	FEMTherm (two-dimensional heat transfer), and One-dimensional heat transfer
SA, WA, SD, WD	Summer Average, Winter Average, Summer Design, and Winter Design ambient conditions
FL, PL	Flowline, and Pipeline (trunk-line)
WC0, WC26	0%, and 26% Water-cut
F, S	Flowing, and Shutdown
MS	Mass Sources
0101, 0201, 0904, 1310, 1409, 2101	Dates in "yymm"
20, 40, 60, 80, 100	20%, 40%, 60%, 80%, and 100% turndowns
0, 1.17, 1.75, 2.43, 3.19, L0	0", 1.17", 1.75", 2.43", 3.19", and $\lambda=0$ insulations

### Runtime

Case	Total execution time [s] (hh:mm:ss)	Total CPU usage [%]	Simulation time [s]	Initialization time [s]
<b>Pipeline_Selection<sup>a</sup></b>				
CM_SS_FT_Size_FL01_SD_WC26	7.8	39 <sup>c</sup>	0.3	7.5
CM_SS_FT_Size_FL02_SD_WC26	8.8	40 <sup>c</sup>	0.5	8.2
CM_SS_FT_Size_FL03_SD_WC26	8.3	39 <sup>c</sup>	0.4	7.9
CM_SS_FT_Size_FL04_SD_WC26	5.1	36 <sup>c</sup>	0.2	4.9
CM_SS_FT_Size_FL05_SD_WC26	8.5	36 <sup>c</sup>	0.3	8.2
CM_SS_FT_Size_PL01_SD_WC26	7.6	35 <sup>c</sup>	0.3	7.3
CM_SS_FT_Size_PL02_SD_WC26	5.6	28 <sup>c</sup>	0.2	5.4
<b>Total</b>	<b>51.7</b>			
	<b>(00:00:52)</b>			
<b>Profiles<sup>a</sup></b>				
CM_DY_FT_0101_WA_WC0	5,798.6	82 <sup>d</sup>	5,416.7	381.9
CM_DY_FT_0201_WA_WC0	5,297.9	93 <sup>d</sup>	5,239.8	58.1
CM_DY_FT_0904_WA_WC0	6,074.9	81 <sup>d</sup>	5,756.2	318.7
CM_DY_FT_1310_WA_WC0	4,251.8	95 <sup>d</sup>	4,205.9	46.0
CM_DY_FT_1409_WA_WC0	4,251.8	95 <sup>d</sup>	4,205.9	46.0
CM_DY_FT_2101_WA_WC0	1,719.6	93 <sup>d</sup>	1,692.5	27.2
CM_DY_FT_0101_SA_WC0	5,143.8	91 <sup>d</sup>	5,072.7	71.1
CM_DY_FT_0201_SA_WC0	5,399.8	93 <sup>d</sup>	5,342.8	57.1
CM_DY_FT_0904_SA_WC0	5,105.1	93 <sup>d</sup>	5,060.2	44.9
CM_DY_FT_1310_SA_WC0	4,367.3	94 <sup>d</sup>	4,321.6	45.8
CM_DY_FT_1409_SA_WC0	3,833.4	95 <sup>d</sup>	3,792.9	40.5

Case	Total execution time [s] (hh:mm:ss)	Total CPU usage [%]	Simulation time [s]	Initialization time [s]
CM_DY_FT_2101_SA_WC0	1,805.1	93 <sup>d</sup>	1,778.0	27.0
CM_DY_FT_0201_WA_WC0_MS <sup>b</sup>	2,621.5	45 <sup>c</sup>	2,582.6	38.9
BO_DY_FT_0201_WA_WC0 <sup>b</sup>	3,727.5	48 <sup>c</sup>	3,573.4	154.1
<b>Total</b>	<b>59,398.2</b>			
	<b>(16:29:58)</b>			
<b>Turndown<sup>a</sup></b>				
CM_DY_FT_Turndown_WD_WC0_20	4,544.1	96 <sup>d</sup>	3,544.9	999.2
CM_DY_FT_Turndown_WD_WC0_40	4,644.3	95 <sup>d</sup>	4,553.2	91.1
CM_DY_FT_Turndown_WD_WC0_60	6,020.3	92 <sup>d</sup>	5,925.5	94.8
CM_DY_FT_Turndown_WD_WC0_80	7,591.2	91 <sup>d</sup>	7,534.9	56.3
CM_DY_FT_Turndown_WD_WC0_100	10,409.3	92 <sup>d</sup>	10,352.0	57.3
CM_DY_FT_Turndown_WD_WC26_20	5,332.2	96 <sup>d</sup>	4,474.4	857.8
CM_DY_FT_Turndown_WD_WC26_40	6,560.0	95 <sup>d</sup>	6,499.0	61.0
CM_DY_FT_Turndown_WD_WC26_60	8,300.9	92 <sup>d</sup>	8,164.2	136.7
CM_DY_FT_Turndown_WD_WC26_80	8,755.1	92 <sup>d</sup>	8,694.9	60.2
CM_DY_FT_Turndown_WD_WC26_100	10,344.8	91 <sup>d</sup>	10,285.0	59.7
<b>Total</b>	<b>72,502.1</b>			
	<b>(20:08:22)</b>			
<b>Shutdown</b>				
CM_TA_FT_Shutdown_WD_WC0_20	520.9	96 <sup>d</sup>	517.2	3.7
CM_TA_FT_Shutdown_WD_WC0_40	483.4	96 <sup>d</sup>	479.8	3.6
CM_TA_FT_Shutdown_WD_WC0_60	505.0	96 <sup>d</sup>	501.5	3.5
CM_TA_FT_Shutdown_WD_WC0_80	921.1	95 <sup>d</sup>	917.9	3.3
CM_TA_FT_Shutdown_WD_WC0_100	880.4	95 <sup>d</sup>	877.2	3.2
CM_TA_FT_Shutdown_WD_WC26_20	1,409.4	93 <sup>d</sup>	1,394.4	15.0
CM_TA_FT_Shutdown_WD_WC26_40	1,199.5	93 <sup>d</sup>	1,196.3	3.2
CM_TA_FT_Shutdown_WD_WC26_60	1,193.3	94 <sup>d</sup>	1,190.0	3.3
CM_TA_FT_Shutdown_WD_WC26_80	1,680.0	95 <sup>d</sup>	1,676.7	3.3
CM_TA_FT_Shutdown_WD_WC26_100	1,866.6	91 <sup>d</sup>	1,863.3	3.3
<b>Total</b>	<b>10,659.8</b>			
	<b>(02:57:40)</b>			
<b>Inhibitor_Flowing</b>				
CM_DY_FT_Methanol_F_WD_WC0_100	31,325.0	49 <sup>c</sup>	31,037.7	287.3
<b>Total</b>	<b>31,325.0</b>			
	<b>(08:42:05)</b>			
<b>Insulation_Flowing</b>				
CM_SS_FT_Insulation_F_WD_WC0_40_0	274.4	49 <sup>c</sup>	0.7	273.7
CM_SS_FT_Insulation_F_WD_WC0_40_L0	291.2	48 <sup>c</sup>	0.7	290.5
CM_SS_FT_Insulation_F_WD_WC0_60_0	271.7	47 <sup>c</sup>	0.6	271.0
CM_SS_FT_Insulation_F_WD_WC0_	277.9	47 <sup>c</sup>	0.7	277.2

<b>Case</b>	<b>Total execution time [s] (hh:mm:ss)</b>	<b>Total CPU usage [%]</b>	<b>Simulation time [s]</b>	<b>Initialization time [s]</b>
60_1.75				
CM_SS_FT_Insulation_F_WD_WC0_60_2.43	267.6	49°	0.7	266.9
CM_SS_FT_Insulation_F_WD_WC0_60_3.19	265.0	49°	0.7	264.3
CM_SS_FT_Insulation_F_WD_WC0_60_L0	281.2	47°	1.2	280.0
CM_SS_FT_Insulation_F_WD_WC0_80_0	182.7	47°	0.7	182.0
CM_SS_FT_Insulation_F_WD_WC0_80_1.17	189.3	45°	0.9	188.4
CM_SS_FT_Insulation_F_WD_WC0_80_1.75	175.6	47°	0.7	174.9
CM_SS_FT_Insulation_F_WD_WC0_80_2.43	175.3	46°	0.7	174.7
CM_SS_FT_Insulation_F_WD_WC0_80_L0	189.7	44°	0.7	189.0
CM_SS_FT_Insulation_F_WD_WC0_100_0	190.7	47°	0.8	189.9
CM_SS_FT_Insulation_F_WD_WC0_100_1.17	173.4	48°	0.6	172.7
CM_SS_FT_Insulation_F_WD_WC0_100_L0	168.9	49°	0.7	168.2
CM_SS_FT_Insulation_F_WD_WC26_40_0	515.3	49°	0.6	514.6
CM_SS_FT_Insulation_F_WD_WC26_40_1.17	693.6	41°	0.8	692.7
CM_SS_FT_Insulation_F_WD_WC26_40_1.75	475.5	49°	0.7	474.8
CM_SS_FT_Insulation_F_WD_WC26_40_2.43	523.1	49°	0.7	522.3
CM_SS_FT_Insulation_F_WD_WC26_40_3.19	456.6	49°	0.6	456.0
CM_SS_FT_Insulation_F_WD_WC26_40_L0	614.3	44°	0.6	613.6
CM_SS_FT_Insulation_F_WD_WC26_60_0	1,621.4	49°	0.7	1,620.6
CM_SS_FT_Insulation_F_WD_WC26_60_1.17	1,734.1	47°	0.7	1,733.4
CM_SS_FT_Insulation_F_WD_WC26_60_L0	552.1	95°	9.8	542.3
CM_SS_FT_Insulation_F_WD_WC26_80_0	198.4	45°	0.7	197.7

<b>Case</b>	<b>Total execution time [s] (hh:mm:ss)</b>	<b>Total CPU usage [%]</b>	<b>Simulation time [s]</b>	<b>Initialization time [s]</b>
CM_SS_FT_Insulation_F_WD_WC26_ 80_1.17	168.9	49 <sup>c</sup>	0.6	168.3
CM_SS_FT_Insulation_F_WD_WC26_ 80_L0	168.9	49 <sup>c</sup>	0.6	168.3
CM_SS_FT_Insulation_F_WD_WC26_ 100_0	188.9	48 <sup>c</sup>	0.8	188.1
CM_SS_FT_Insulation_F_WD_WC26_ 100_L0	444.2	49 <sup>c</sup>	0.6	443.6
CM_SS_1D_Insulation_F_WD_WC0_ 100_0	148.8	49 <sup>c</sup>	0.2	148.5
CM_SS_1D_Insulation_F_WD_WC0_ 100_1.17	187.7	46 <sup>c</sup>	0.3	187.4
CM_SS_1D_Insulation_F_WD_WC0_ 100_1.75	187.5	46 <sup>c</sup>	0.3	187.2
CM_SS_1D_Insulation_F_WD_WC0_ 100_2.43	204.6	43 <sup>c</sup>	0.3	204.4
CM_SS_1D_Insulation_F_WD_WC0_ 100_3.19	179.0	45 <sup>c</sup>	0.2	178.8
CM_SS_1D_Insulation_F_WD_WC0_ 100_L0	198.2	42 <sup>c</sup>	0.3	197.9
CM_SS_1D_Insulation_F_WD_WC26_ 100_0	197.7	37 <sup>c</sup>	0.2	197.5
CM_SS_1D_Insulation_F_WD_WC26_ 100_1.17	509.0	36 <sup>c</sup>	0.3	508.7
<b>Total</b>	<b>13,165.0</b>			
	<b>(03:39:25)</b>			
<b>Insulation_Shutdown</b>				
CM_TA_FT_Insulation_S_WD_WC0_ 80_3.19	879.9	95 <sup>d</sup>	822.3	57.7
CM_TA_FT_Insulation_S_WD_WC0_ 100_1.17	1,018.0	95 <sup>d</sup>	958.0	60.0
CM_TA_FT_Insulation_S_WD_WC0_ 100_1.75	960.2	95 <sup>d</sup>	903.1	57.1
CM_TA_FT_Insulation_S_WD_WC0_ 100_2.43	911.5	96 <sup>d</sup>	856.1	55.4
CM_TA_FT_Insulation_S_WD_WC0_ 100_3.19	895.2	96 <sup>d</sup>	838.5	56.7
CM_TA_FT_Insulation_S_WD_WC26_ 60_2.43	1,300.8	97 <sup>d</sup>	1,156.7	144.1
CM_TA_FT_Insulation_S_WD_WC26_ 60_3.19	1,181.7	96 <sup>d</sup>	1,039.0	142.6
CM_TA_FT_Insulation_S_WD_WC26_ 80_1.75	1,190.4	96 <sup>d</sup>	1,131.2	59.2

Case	Total execution time [s] (hh:mm:ss)	Total CPU usage [%]	Simulation time [s]	Initialization time [s]
CM_TA_FT_Insulation_S_WD_WC26_80_2.43	1,182.6	96 <sup>d</sup>	1,122.5	60.0
CM_TA_FT_Insulation_S_WD_WC26_100_1.17	1,403.5	93 <sup>d</sup>	1,192.6	210.9
CM_TA_FT_Insulation_S_WD_WC26_100_1.75	1,377.3	96 <sup>d</sup>	1,176.2	201.1
<b>Total</b>	<b>12,301.1</b>			
	<b>(03:25:01)</b>			
<b>Ramp-up</b>				
CM_TA_FT_Rampup_WD_WC0_20	26,357.2	80 <sup>d</sup>	26,353.5	3.7
CM_TA_FT_Rampup_WD_WC0_40	26,231.8	78 <sup>d</sup>	26,228.0	3.8
CM_TA_FT_Rampup_WD_WC0_60	20,966.3	93 <sup>d</sup>	20,962.6	3.7
CM_TA_FT_Rampup_WD_WC0_80	21,622.3	94 <sup>d</sup>	21,619.1	3.3
CM_TA_FT_Rampup_WD_WC26_20	24,244.0	92 <sup>d</sup>	24,228.5	15.4
CM_TA_FT_Rampup_WD_WC26_40	23,669.3	92 <sup>d</sup>	23,665.9	3.5
CM_TA_FT_Rampup_WD_WC26_60	21,242.6	92 <sup>d</sup>	21,239.2	3.4
CM_TA_FT_Rampup_WD_WC26_80	20,197.5	93 <sup>d</sup>	20,194.1	3.4
<b>Total</b>	<b>184,531.0</b>			
	<b>(51:15:31)</b>			
<b>Pigging</b>				
CM_TA_FT_Pig_FL01_WD_WC0_100	7,340.1	92 <sup>d</sup>	7,284.4	55.7
CM_TA_FT_Pig_FL01_WD_WC26_100	7,007.9	94 <sup>d</sup>	6,948.2	59.7
CM_TA_FT_Pig_FL02_WD_WC0_100	7,327.7	93 <sup>d</sup>	7,271.5	56.2
CM_TA_FT_Pig_FL02_WD_WC26_100	7,166.2	94 <sup>d</sup>	7,106.0	60.2
CM_TA_FT_Pig_FL03_WD_WC0_100	7,234.7	93 <sup>d</sup>	7,178.4	56.2
CM_TA_FT_Pig_FL03_WD_WC26_100	7,013.3	94 <sup>d</sup>	6,954.1	59.1
CM_TA_FT_Pig_FL05_WD_WC0_100	7,223.4	93 <sup>d</sup>	7,168.5	54.9
CM_TA_FT_Pig_FL05_WD_WC26_100	6,989.0	94 <sup>d</sup>	6,928.3	60.7
CM_TA_FT_Pig_PL_WD_WC0_60	7,166.2	94 <sup>d</sup>	7,106.0	60.2
CM_TA_FT_Pig_PL_WD_WC0_80	8,057.6	93 <sup>d</sup>	8,000.2	57.4
CM_TA_FT_Pig_PL_WD_WC0_100	7,343.7	93 <sup>d</sup>	7,285.9	57.8
CM_TA_FT_Pig_PL_WD_WC26_60	7,320.1	93 <sup>d</sup>	7,258.9	61.3
CM_TA_FT_Pig_PL_WD_WC26_80	11,913.7	68 <sup>d</sup>	11,852.5	61.2
CM_TA_FT_Pig_PL_WD_WC26_100	7,540.9	93 <sup>d</sup>	7,480.4	60.5
<b>Total</b>	<b>106,644.4</b>			
	<b>(29:37:24)</b>			
<b>Pipeline_Packing</b>				
CM_TA_FT_Packing_WD_WC0_20	1,937.7	96 <sup>d</sup>	1,933.9	3.7
CM_TA_FT_Packing_WD_WC0_40	1,156.5	96 <sup>d</sup>	1,152.9	3.6
CM_TA_FT_Packing_WD_WC0_60	1,734.3	96 <sup>d</sup>	1,730.7	3.6
CM_TA_FT_Packing_WD_WC0_80	1,821.1	95 <sup>d</sup>	1,817.7	3.3
CM_TA_FT_Packing_WD_WC0_100	1,767.4	95 <sup>d</sup>	1,764.0	3.3
CM_TA_FT_Packing_WD_WC26_20	2,103.0	95 <sup>d</sup>	2,088.0	15.0

<b>Case</b>	<b>Total execution time [s] (hh:mm:ss)</b>	<b>Total CPU usage [%]</b>	<b>Simulation time [s]</b>	<b>Initialization time [s]</b>
CM_TA_FT_Packing_WD_WC26_40	2,862.3	95 <sup>d</sup>	2,859.0	3.3
CM_TA_FT_Packing_WD_WC26_60	2,569.3	95 <sup>d</sup>	2,566.1	3.3
CM_TA_FT_Packing_WD_WC26_80	2,742.5	96 <sup>d</sup>	2,739.3	3.3
CM_TA_FT_Packing_WD_WC26_100	2,690.7	94 <sup>d</sup>	2,687.4	3.3
<b>Total</b>	<b>21,384.8</b>			
	<b>(05:56:25)</b>			

<sup>a</sup> Each case was run more than one time. Only the last run is reported.

<sup>b</sup> Case was run for 1 hr only.

<sup>c</sup> Case was run using an Intel Core i5-6200U Processor (2.30 GHz, up to 2.80 GHz, dual-core)

<sup>d</sup> Case was run using an Intel Core i5-7500 Processor (3.40 GHz, up to 3.80 GHz, quad-core)